CHARLES UNIVERISTY IN PRAGUE

2nd FACULTY OF MEDICINE

Iva Prajerová

Membrane properties of neural stem/progenitor cells during *in vitro* differentiation and after transplantation into the rat brain

Thesis

Prague 2010

ACKNOWLEDGEMENT

I would like to sincerely thank my supervisors, Dr. Alexandr Chvatal and Dr. Miroslava Anderova, for their guidance, experience and support during my PhD research and thesis writing. I would also like to thank all members of our research group and all those individuals who supported me in any respect during the completion of my doctoral studies. I would also like to thank Prof. E. Madarasz (Institute of Experimental Medicine, Hungarian Academy of Sciences, Hungary), for her kind gift of GFP/NE-4C cell line, Dr. Machon and Dr. Kozmik (Laboratory of Transcription Regulation, Institute of Molecular Genetics, v.v.i., Prague, Czech Republic) for their kind gift of transgenic D6-GFP mice and Prof. S. Krauss (Cellular and Genetic Therapy Research Group, Centre for Molecular Biology and Neuroscience and Institute of Medical Microbiology, Rikshospitalet, Oslo, Norway) for his kind gift of neonatal transduced neural stem/progenitor cells. Special thanks go to James Dutt for text corrections.

TABLE OF CONTENTS

1. LIST OF ABBREVIATIONS

4-AP: 4-aminopyridin

ACF: artificial cerebrospinal fluid

AMPA: α-amino-3-hydroxyl-5-methyl-4-isoxazole-propionate

AP: action potential

AP5: (2R)-amino-5-phosphonovaleric acid; (2R)-amino-5-phosphonopentanoate

APC: adenomatous poliposis coli

Ara-C: cytosine-β-D-arabinofuranoside

BDNF: brain derived neurotrophic factors

bFGF: basic fibroblast growth factor

BLBP: brain lipid binding protein

BMP: bone morphogenic protein

BrdU: 5-bromodeoxyuridine

CGE: caudal ganglionic eminence

CK1: casein kinase 1

C_m: membrane capacitance

CNQX: 6-cyano-7-nitroquinoxaline-2,3-dione

CNS: central nervous system

DAPI: 4', 6-diamidino-2-phenylindole

DCX: doublecortin

Disp: Dispatched

Dlx2: Distal less 2

DNA: deoxyribonucleic acid

Dvl: Dishevelled

E: embryonic day

EDTA: ethylenediaminetetraacetic acid

EGF: epidermal growth factor

EGFR: epidermal growth factor receptor

EGTA: ethyleneglycoltetraacetic acid

Emx1: Empty spiracles homeobox 1

ESCs: embryonic stem cells

FGF: fibroblast growth factor

Fz: Frizzled

GABA: gamma amino butyric acid

GAD65/67: glutamate decarboxylase 65/67

GAPDH: glyceraldehyde phosphate dehydrogenase

GAT-4: GABA transporter 4

GCL: granule cell layer

GDNF: glial cell line-derived neurotrophic factor

GFAP: glial fibrillary acidic protein

GFP: green fluorescent protein

g-GCS: g-glutamyl cysteine synthetase

GL: glomerular layer

GLAST: glutamate aspartate transporter

Gli1-3: Glioma-associated oncogene homolog 1-3

GLUK5: glutamate kainate receptor subunit 5

GluR: glutamate receptor

Grg/TLE: Groucho/transducin-like enhancer of split

Gsh2: Genomic screened homeobox

GSK3: glycogen synthase kinase 3

HEPES: 4-(2-hydroxyethyl)-1-piperazineethanesulfonic acid

Hes: Hairy and enhancer of split

Hh: Hedgehog

ICAT: inhibitor of β-catenin and TCF-4

IFT: intraflagelar transport

IR: input resistance

IRES: internal ribosome entry site

I/V: current/voltage

K_A current: fast activating and inactivating outwardly-rectifying K^+ current

KCC2: K^+ Cl^- co-transporter

K_{DR} current: delayed outwardly-rectifying K^+ current

Kif: Kinesin family member

K_{IR}: inwardly rectifying K^+ current

LeX: Lewis X

LGE: lateral ganglionic eminence

LRP5/6: low-density-lipoprotein receptor-related protein 5/6

LY: Lucifer yellow

Lhx6: Lim homeobox 6

LRP5/6: low-density lipoprotein receptor-related proteins 5 and 6

MAP-2: microtubule associated protein 2

Mash1: Mammalian achaete scute homolog 1

Math2: Meprin-associated Traf homology

MCAO: middle cerebral artery occlusion

MGE: medial ganglionic eminence

MOSP: myelin oligodendrocyte specific protein

NBXQ: 2, 3-dihydroxy-6-nitro-7-sulfamoyl-benzo[f]quinoxaline-2,3-dione

NE: neuroepithelial

NE-4C: neuroepithelial-clone 4

NF68: neurofilaments 68 kDa

NKCC1: Na^+- K^+-$2Cl^-$ co-transporter

Nkx2.1: NK2 homeobox 1

Nkx6.2: NK6 homeobox 2

NMDA: N-methyl-D-aspartate

NMDG: N-methyl D-gluconate

NPCs: neural progenitor cells

NS/PCs: neural stem/progenitor cells

NSCs: neural stem cells

OB: olfactory bulb

Olig2: Oligodendrocyte lineage transcription factor 2

Otx2: orthodenticle homolog 2

Pax6: Paired box 6

PB: phosphate buffer

PBS: phosphate-buffered saline

PCL: photochemical lesion

PDGF: platelet-derived growth factor

PDGFRα: platelet-derived growth factor receptor α

PKA: protein kinase A

PLL: poly-L-lysine

PSA-NCAM: polysialated-neural cell adhesion molecule

Ptc: Patched

RA: retinoic acid

RC1, 2: Radial Cell 1, 2

RIP: receptor interacting protein

RMS: rostral migratory stream

RT-PCR: real-time polymerase chain reaction

$SCF^{\beta TrCP}$: β transducing repeat containing Skp1–Cul1–F-box-protein

SDS: sodium dodecyl sulphate

S.E.M: standard error of the mean

sFRPs: Soluble Frizzled-Related Proteins

SGZ: subgranular zone

Shh: Sonic hedgehog

Smo: Smoothened

Sox: Sry-related high-mobility group box

SSEA-1: stage specific embryonic antigen 1

SVZ: subventricular zone

Tcf/Lef: T cell factor/lymphoid-enhancer binding factors

TEA: tetraethyl ammonium chloride

TGF-α: transforming growth factor α

TH: tyrosine hydroxylase

TTX: tetrodotoxin

TUNEL: terminal deoxynucleotidyl transferase dUTP nick end labelling

V_{rest}: resting membrane potential

V_{rev}: reversal potential

VZ: ventricular zone

2. INTRODUCTION

The number of people affected by stroke, neurodegenerative diseases or traumatic injuries increases every year. These neurological disorders cause severe disabilities, and there is currently no effective therapy available to repair the damaged tissue and to fully recover its lost functions. Regenerative medicine and neural stem cell research are therefore focused on finding suitable tools that would restore the affected nervous tissue and return patients back to their normal lives.

Neural stem/progenitor cells (NS/PCs) represent a promising tool in regenerative medicine. They are present in the embryonic as well as in the adult brain and are naturally predisposed to produce all cell types of the nervous system, most importantly neurons, astrocytes and oligodendrocytes. The principle of regeneration based on cell-replacement is to deliver transplantable cells to the site of injury. NS/PCs fulfil the basic criteria - the ability to survive under pathological conditions and to give rise to appropriate cell types that would replace the malfunctioning cells **(Fig. 1)**. Neural stem cell research is therefore aimed at exploring the properties of neural stem cells (NSCs), such as their proliferation, differentiation and potential to give rise to functional cells both *in vitro* and *in v*ivo, after transplantation into the nervous tissue.

Another approach involves the use of molecules such as morphogenes, growth factors and cytokines and components of the signalling pathways that control the processes of nervous system development and the continuous production of neurons in the adult brain. Since neurological disorders can transiently increase endogenous neurogenesis, the aim is to augment endogenous reparative mechanisms of the brain by delivering positive modulators of neurogenesis into the damaged tissue. It is therefore important to study the effects of these modulators on neural stem cell proliferation and differentiation *in vitro* and also on cell survival *in vivo*, using genetic manipulations of the NS/PCs or transgenic animal models **(Fig. 1)**.

An essential part of neural stem cell research is the study of the membrane properties of neural stem cells and their derivatives, including the functional expression of membrane receptors and ion channels, as only fully equipped and functional cells can represent a potent tool for regenerative medicine.

Fig. 1 Potential tools for regenerative medicine

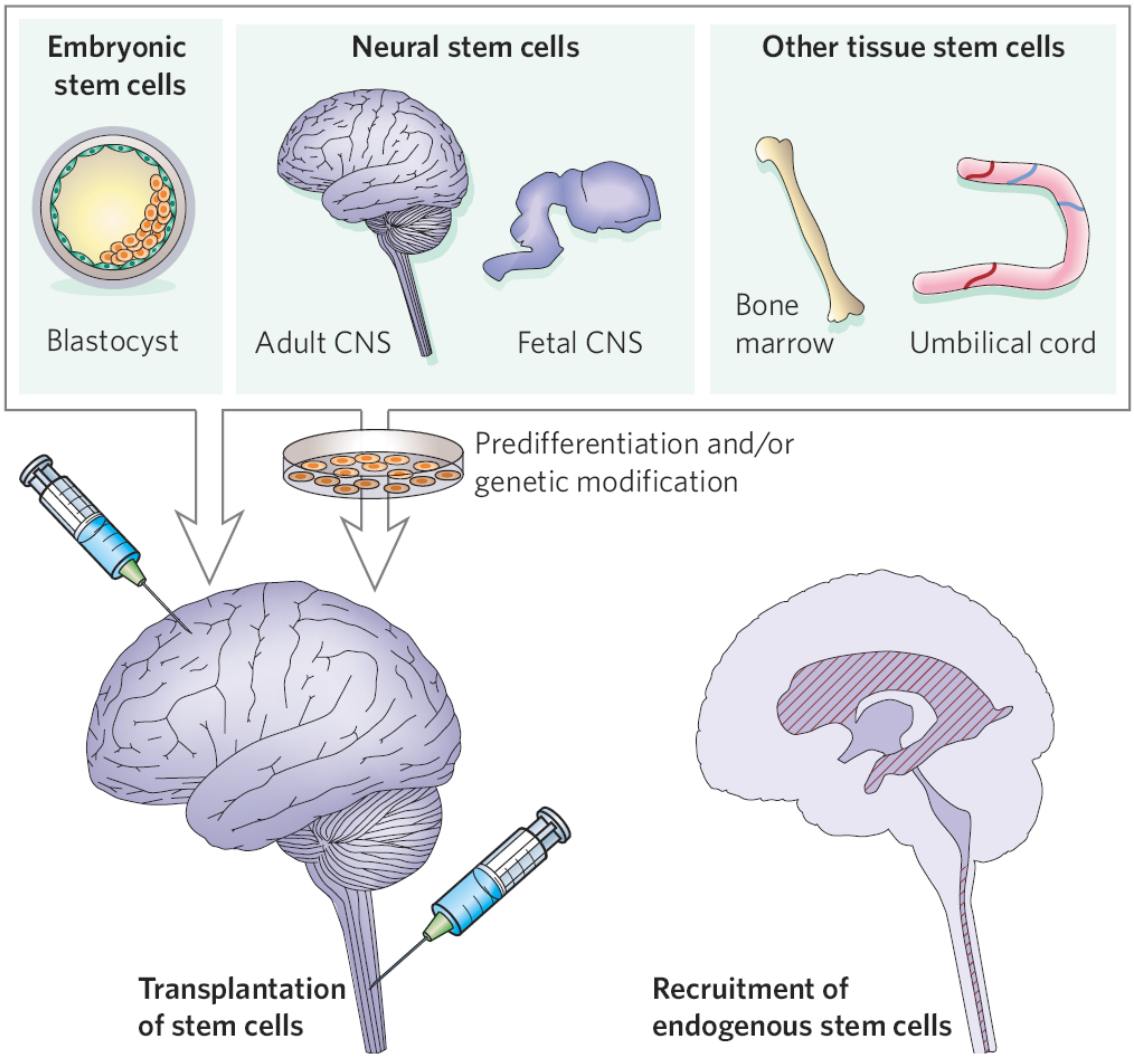

Methods for regenerative medicine involve the isolation and transplantation of stem cells into the damaged brain tissue, either directly or after pre-differentiation/genetic modification in culture to form specific types of neuron and glial cell, or cells producing neuroprotective molecules **(left)**. Another strategy is to enhance the recruitment of endogenous neural stem cells **(right,** Lindvall and Kokaia, 2006).

2.1 Embryonic neural stem cells as a tool for regenerative medicine

Stem cells are characterised by their ability to self-renew and to differentiate into many cell types. Embryonic stem cells (ESCs) are derived from the inner cell mass of the blastocyst, while embryonic germ cells are usually obtained from early stages of post-implantation embryos. Both of these represent pluripotent stem cells, which are able to give rise to various organs and tissues. Induced pluripotent cells, on the other hand, are adult somatic cells such as skin fibroblasts that were modified by the introduction of embryogenesis-related genes. Tissue-specific stem cells can be isolated from various

tissues at more advanced developmental stages (including postnatal tissues), such as hematopoietic stem cells, bone marrow mesenchymal stem cells, adipose tissue-derived stem cells, umbilical cord-derived stem cells and NS/PCs, as reviewed by Sanberg et al., (2005) and Kim and de Vellis (2009).

Generally, NS/PCs are mobile, relatively resistant to hypoxia and able to produce neurons, astrocytes and oligodendrocytes. They can be delivered to the site of interest either directly, by transplanting them into the site of a lesion (Buhnemann et al., 2006), or indirectly, using intravenous administration (Fujiwara et al., 2004). NS/PCs used for transplantation studies have been derived from both embryonic and adult rodent/human brains, and they have been successfully transplanted into animal models of neurodegenerative diseases such as Parkinson's disease (Sun et al., 2007, Wei et al., 2007), Huntington's disease (Vazey et al., 2006) and Alzheimer's disease (Xuan et al., 2009). They have also been used in models mimicking stroke (Buhnemann et al., 2006) or brain (Modo et al., 2002) and spinal cord injuries (Akesson et al., 2007, Mothe et al., 2008).

2.1.1 Different populations of NS/PCs in the developing brain

The population of NS/PCs in the embryonic brain is heterogeneous. The first identifiable NSCs are present in the neuroepithelium at the time of neural tube closure, at embryonic day (E) 8.5-9 in mice, and prior to the onset of neurogenesis (E9.5-10). All neurons and glia of the mammalian brain are therefore derived directly or indirectly from these neuroepithelial (NE) stem cells. They can be maintained in culture to undergo self-renewal, and they differentiate into neurons, astrocytes and oligodendrocytes (Mujtaba et al., 1999, Hitoshi et al., 2004).

Before neurogenesis starts, cells divide symmetrically to enlarge the pool of NE stem cells in the ventricular zone (VZ), which spans the entire wall of the developing telencephalon (Kosodo et al., 2004). With the onset of neurogenesis, NE stem cells also start to divide asymmetrically to produce the first neurons, which accumulate in the basal part of the VZ and form a preplate (**Fig. 2)**. During asymmetric cell divisions NE stem cells can also give rise to intermediate progenitors, called basal progenitors that migrate towards the basal surface, where they later divide symmetrically to give rise to two neurons (Haubensak et al., 2004). NE stem cells express nestin, a common marker of neural stem and progenitor cells, which is also expressed during brain development

by radial glia cells and, later on, also by reactive astrocytes and adult NSCs (Mignone et al., 2004). At the onset of neurogenesis, NE stem cells specifically express fibroblast growth factor receptor 4, Frizzled 9 (Fz9) and Sry-related homeobox related gene transcription factor 2 (Sox2). They are further characterised by the lack of epidermal growth factor receptor (EGFR) and platelet-derived growth factor receptor-alpha (PDGFRα, Cai et al., 2002). Proliferating cells of the developing telencephalon can be also identified by active Notch signalling, detected as early as E10.5 in a Hes5/green fluorescent protein (GFP) transgenic mouse. Hairy and enhancer of split (Hes) is a basic helix loop helix transcription factor and a downstream target of Notch signalling (Basak and Taylor, 2007). Shortly after the appearance of the first neurons, NE stem cells undergo a change in their characteristics; they give rise to more specific progenies called radial glia cells.

Fig. 2 Germinal cortical layers of the embryonic mouse cortex

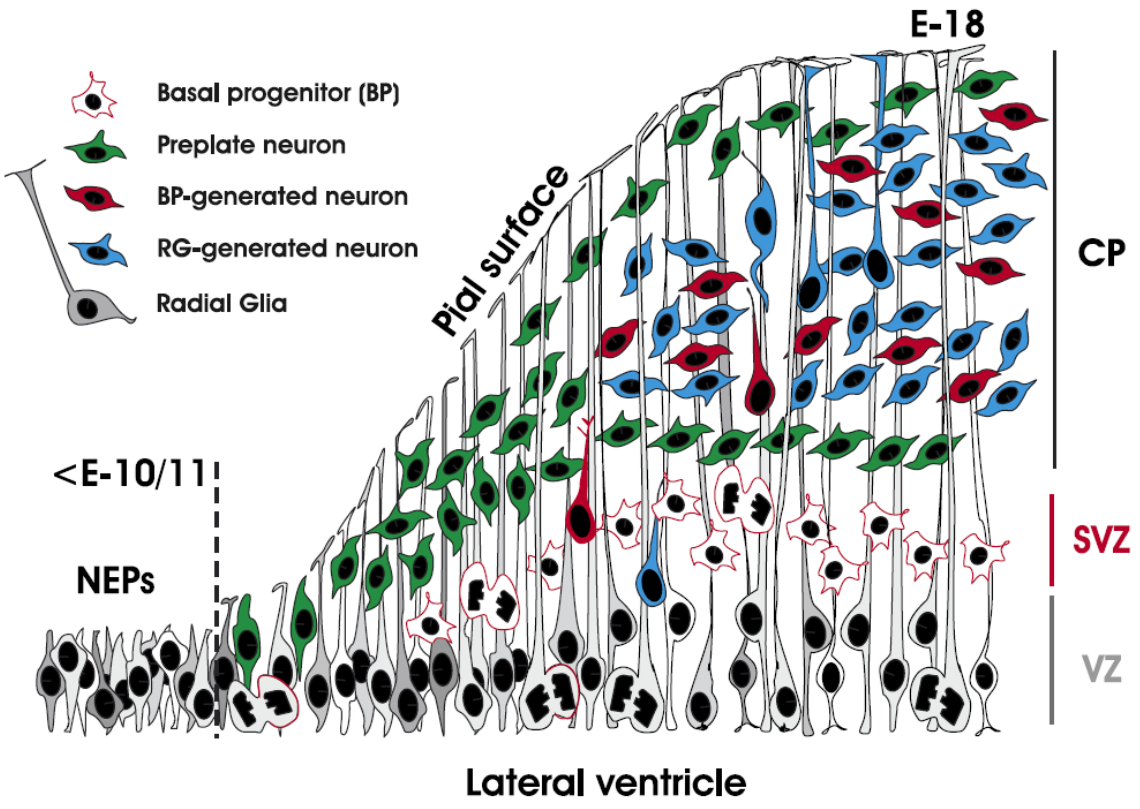

A schematic image, showing the transition of neuroepithelial cells to radial glia cells and the generation of the first neurons (Malatesta et al., 2008). **BP:** basal progenitor; **CP:** cortical plate; **RG:** radial glia; **SVZ:** subventricular zone; **VZ:** ventricular zone.

Radial glia cells represent more fate-restricted progenitors than are NE stem cells and successively replace the latter during embryonic development. They are present transiently in most brain regions. As a consequence, most of the neurons in the brain are derived directly or indirectly from radial glia cells (Anthony et al., 2004). Radial glia cells appear with the onset of neurogenesis (E10), and the neuroepithelium gradually transforms into a multi-layered tissue in which the VZ comprises only the layer that lines the ventricle, where the cell somata of radial glia reside **(Fig. 2)**.

Radial glia share several features with their ancestors, NE stem cells. They exhibit a bipolar morphology with one endfoot on the ventricular surface and a radial process that extends to the pia, an apico-basal polarity; and they also undergo interkinetic nuclear migration (Noctor et al., 2001). They are connected by gap junctions (Bittman et al., 1997), and the gap junction subunits connexin 26 and connexin 43 were shown to mediate the radial migration of newborn neurons in the neocortex (Elias et al., 2007). Both NE cells and radial glia express nestin as well as radial cell 1 and 2 (RC1 and 2); the expression of these markers starts as early as E9 (Hartfuss et al., 2001). However, only radial glia express glial markers, which can clearly distinguish them from NE cells, such as glutamate transporter (GLAST, Shibata et al., 1997, Malatesta et al., 2000), brain lipid binding protein (BLBP, Hartfuss *et al.*, 2001), glutamine synthetase (Akimoto et al., 1993), tenascin C (Yuasa, 2001) and vimentin (Elias et al., 2007). Glial fibrillary acidic protein (GFAP) is not endogenously expressed in rodent radial glia; however, the human promoter of the GFAP gene is transcriptionally active in murine radial glia (Brenner et al., 1994, Malatesta et al., 2000), and its expression co-localises with GLAST (Malatesta et al., 2000, Malatesta et al., 2003). GFP/GFAP transgenic mice are therefore used in genetic fate mapping studies as a tool for exploring radial glia cells *in vivo* (Zhuo et al., 1997, Malatesta et al., 2000, Hartfuss et al., 2001).

The transition from NE stem cells to radial glia is induced by Notch signalling (Gaiano et al., 2000) and mediated by Hes. Mice deficient for Hes1 and Hes5 have normal NE stem cells until E8.5, but the differentiation of radial glia is severely impaired after E9.5 (Hatakeyama et al., 2004). BLBP was also shown to be a direct target of Notch signalling, and its expression is diminished in the forebrain of mice deficient for both Notch1 and Notch3 (Anthony et al., 2005). Another candidate for regulating the transition from NE cells to radial glia is fibroblast growth factor 10

(FGF10), which acts through the FGF receptor (namely FGF-R2b). This receptor is expressed in the progenitors during the transition period, and its deletion was shown to decrease the pool of radial glia cells as well as their derivatives, basal progenitors and new neurons (Sahara and O'Leary, 2009).

In the dorsal telencephalon, radial glia cells of the VZ generate (between E14-E18) most of the pyramidal neurons in the neocortex (Tamamaki et al., 2001, Noctor et al., 2002, Malatesta et al., 2003, Wu et al., 2005) and the hippocampus (Nakahira and Yuasa, 2005). Neurons are generated from radial glia by asymmetric (neurogenic) division. It was shown that many cortical neurons inherit a pial process from proliferating radial glia cells. These pial-surface connected processes are RC2/nestin-positive and form a scaffold system for migrating young neurons together with other pial processes of proliferating radial glia (Miyata et al., 2001). Neurons arise from radial glia cells also indirectly, through intermediate progenitor cells (or basal progenitors), especially during later stages of neurogenesis, between E17-E19 (Noctor et al., 2004). The population of basal progenitors resides in a layer that is formed basally from the VZ and is called the subventricular zone (SVZ) and that is maintained by a continuous supply from asymmetric cell divisions of the radial glial cells of the VZ (Miyata et al., 2004). Basal progenitors divide once or twice before they migrate through the intermediate zone to finally differentiate into neurons of the cortical plate (**Fig. 2)**, a transient structure that subsequently gives rise to cortical layers (CA1-CA3 in the hippocampus and I-VI in the neocortex, Nakahira and Yuasa, 2005). Basal progenitors therefore represent a neuronally-committed transient population derived from radial glia cells (or NE cells, at early stages of neurogenesis). It was also suggested that basal progenitors are actually the major producers of neocortical neurons (Haubensak et al., 2004).

At the end of embryogenesis and early postnatally, the same radial glia that produced cortical neurons start to produce cortical astrocytes (Qian et al., 2000, Fan et al., 2005, Hatada et al., 2008). While these cells acquire the potential to produce astrocytes, they loose the potential to produce neurons, and neurogenesis is thus gradually replaced by gliogenesis. An *in vitro* study confirmed that progenitors isolated from E14 and E16 mouse embryos give rise to neurons predominantly, while those isolated at E18 give rise to astrocytes (Malatesta et al., 2000). The switch between neurogenesis and gliogenesis is probably mediated by DNA methylation in neural

progenitors (Fan et al., 2005). The change in their differentiation potential might also correlate with the change of their antigenic profile. In the radial glia of the dorsal telencephalon, the expression of individual radial glia markers is not uniform during the course of development. Hartfuss et al. (2001) explored the expression of radial glia using an hGFAP-GFP transgenic mouse. They isolated radial glia from E12-E18 mouse embryos, sorted them by fluorescence activated cell sorting and analysed them for the expression of a series of radial glia cell markers. They found that at E12, all radial glia of the developing cortex were RC2-positive, while 80% co-expressed GLAST and only 40% of RC2-positive cells were BLBP-positive. At E18, however, almost all cells were BLBP-positive and only half of the cells were RC2- or GLAST-positive (Hartfuss et al., 2001).

It was also suggested that already at the early stages of neurogenesis, before radial glia cells appear, NE stem cells are already restricted to becoming neuronal or glial progenitors. McCarthy et al. (2001) performed an *in vivo* clonal analysis of individual telencephalic precursors that were virally labelled at E9.5 and examined 3 weeks postnatally. They found that 34% of the clones contained only neurons, while 47% contained only glia, and 18% represented mixed clones containing both neurons and glia (McCarthy et al., 2001).

2.1.2 Isolation, cultivation and characterisation of NS/PCs *in vitro*

Primary cultures of NS/PCs used for transplantation studies are prepared from both embryonic and adult rodent brains; they can be propagated *in vitro* in the form of neurospheres or as adherent monolayers (Pollard et al., 2006).

Isolation protocols include mechanical trituration of the dissected tissue, which is usually sufficient for the isolation of embryonic NS/PCs (Machon et al., 2002, Carletti et al., 2004), or the use of various proteases (Hirsch et al., 2007, Yasuda et al., 2008). NS/PCs can be expanded under serum-free conditions, in medium supplemented with B27 (Machon et al., 2002) or N2 (Pollard et al., 2006) supplements and growth factors known to support proliferation of these cells: basic fibroblast growth factor (bFGF) and epidermal growth factor (EGF). These are used either alone or in combination, depending on the developmental stage and the responsiveness of the NS/PCs. NS/PCs derived from the neural tube and embryos at the early stages of neurogenesis (E9-E10) are able to form neurospheres in the presence of bFGF only

(Mujtaba et al., 1999, Qian et al., 2000). NS/PCs isolated from the embryo during the neurogenic phase (E13.5) are able to proliferate in the presence of bFGF or EGF alone; however, the combination of both yields increased proliferation (Parmar et al., 2002). Moreover, it was shown that cultivation of NS/PCs derived form E12.5 mouse forebrain in the presence of bFGF alone results in a more heterogeneous cell culture containing a greater number of dying cells. The addition of EGF into the culture medium results in a more homogenous cell population with a lower number of dying cells and no spontaneous differentiation. Interestingly, cells expanded in the presence of both EGF and bFGF can not be subsequently maintained in the presence of bFGF alone - they undergo differentiation - while using EGF only does not change their self-renewal or differentiation abilities (Pollard et al., 2006). Neural stem cells derived from the adult brain are able to self-renew in the presence of either bFGF (10 ng/ml) or EGF (20 ng/ml) alone (Pastrana et al., 2009), or in the presence of both (Babu et al., 2007).

Since the number of available NS/PCs might be limited, immortalised cell lines represent an almost inexhaustible source of cells for transplantation experiments. They represent homogenous cell populations and can be propagated indefinitely, thus they are studied as a potential source of cells for clinical applications. Nevertheless, there is an ongoing debate concerning their stability, safety and transformation-related changes, which might restrict their use in human patients. The cell lines are often prepared from foetal human tissue of different developmental stages and used in animal models of injury or degenerative diseases (Haas et al., 2007, Haas et al., 2008). However, rodent immortalised neural stem cell lines also exist. An example is the NE-4C/GFP cell line used in this study (Schlett et al., 1997). There are several methods of immortalisation used for both human and animal NSCs. These include non-transforming oncogene-mediated immortalisation using *v-myc* (Chu et al., 2004, Cacci et al., 2007), *c-myc* (De Filippis et al., 2008) or Simian virus 40 T antigen (Englund et al., 2002, Lundberg et al., 2002, Wang et al., 2008, Villa et al., 2009), which act by inactivating tumour suppressor genes. A novel method includes transfection with telomerase reverse transcription protein, which enables the maintenance of telomere length sufficient to avoid replicative senescence (Zhang et al., 2008). The NE-4C/GFP immortalised cell line was prepared from p53-deficient mouse embryos (Schlett et al., 1997). They are usually cultured under the same conditions as primary cultures, and they are cultivated as adherent monolayers (Cacci et al., 2007, Zhang et al., 2008, Villa et al., 2009).

The differentiation of NS/PCs *in vitro* is usually induced by the removal of growth factors and allowing the cells to attach to a surface coated with poly-L-lysine (PLL) or laminin. It was shown that transient treatment of cell cultures with bFGF can increase differentiation into neurons; however, prolonged application also stimulates proliferation. In the presence of EGF, cells tend to differentiate preferentially towards glial cells (Babu et al., 2007). Various growth factors and cytokines can further modulate the process of differentiation. Brain-derived neurotrophic factor (BDNF) promotes differentiation into neurons in both embryonic (Shetty, 2004) and adult progenitors cells (Babu et al., 2007). Neurotophin 3, Sonic hedgehog (Shh), vascular endothelial growth factor or endothelial cell growth factor also increase the production of new neurons. In contrast, bone morphogenic protein 2 (BMP2) and leukaemia inhibiting factor significantly reduce the number of cells that differentiate into neurons (Babu et al., 2007). Moreover, it was shown recently that the addition of growth factors into a cell culture might affect the membrane properties of differentiating cells. The continual presence of BDNF in a cell culture derived from the E15 rat hippocampus caused a change in the passive membrane properties of differentiated neurons as well as changes in the current densities of Na^+ and K^+ currents (Leng et al., 2009).

2.1.3 Transplantation studies using embryonic NS/PCs

Embryonic NS/PCs used for transplantation are usually isolated from mouse embryos between E12 and E18. The majority of studies so far have explored the properties of NS/PCs derived from the entire embryonic VZ. However, it was shown that radial glia of the developing telencephalon exhibit region-specific features; their fate is specified by a set of transcription factors.

During the neurogenic phase of telencephalic development (E14-E18), radial glia cells of the ventral telencephalon produce primarily striatal neurons. Those residing in the lateral ganglionic eminences (LGE) give rise to striatal projection neurons (DARPP-32-positive) and to somatostatin containing interneurons, while radial glia cells of the medial ganglionic eminences (MGE, another part of the ventral telencephalon) produce cholinergic interneurons (Olsson et al., 1998). However, distinct populations of radial glia cells within the LGE and MGE also contribute to the production of γ-amino butyric acid (GABA)-ergic inhibitory neurons of the cortex.

They migrate tangentially from the VZ of the ventral telencephalon to reach their final destination in the cortex (Tanaka et al., 2006). Genetic fate-mapping studies using transgenic animals revealed that the telencephalic VZ (dorsal and ventral) can be subdivided into regions defined by the expression of transcription factors, which produce distinct populations of cortical cells. For example, empty spiracles homeobox 1 (Emx1)-positive radial glia cells are located predominantly in the VZ of the dorsal telencephalon, and these progenitors were shown to produce glutamatergic projection neurons of the cortex, cortical astrocytes and also myelinating oligodendrocytes of the white matter structures - the corpus callosum, the fimbria of the hippocampus and also layer I of the neocortex (Gorski et al., 2002). NK2 homeobox1 (Nkx2.1) expression defines radial glia cells in the MGE of the ventral telencephalon that produce parvalbumin- and somatostatin-positive interneurons of the neocortex and hippocampus and, additionally, white and grey matter oligodendrocytes (Xu et al., 2008). The expression of Nkx2.1 and Lim homeobox 6 (Lhx6) defines a population that generates calbindin-, parvalbumin-, and somatostatin-expressing interneurons of the neocortex (Fogarty et al., 2007), The expression of Nkx2.1 in the MGE, which defines a subpopulation of cortical interneurons, is, at least partly, Shh-dependent, since the loss of Shh signalling in the MGE results in the reduction of these interneurons in the layer II-IV of the neocortex (Xu et al., 2005). NK6 homeobox 2 (Nkx6.2)-expressing radial glia produce a subgroup of Martinotti cells that co-express calretinin and somatostatin. Most of the neuropeptide Y-expressing cells and all bipolar calretinin-expressing interneurons of the cortex are generated from the germinal zones of the LGE and the caudal ganglionic eminence (CGE) expressing genomic screened homeobox 2 (Gsh2) (Fogarty et al., 2007). The production of GABA-ergic interneurons of the ventral telencephalon is regulated by Distal less 2 (Dlx2), which suppresses oligodendrocyte lineage transcription factor 2 (Olig2)-expressing oligodendrocyte progenitors. On the other hand, mouse achaete scute homolog 1 (Mash1) was shown to promote oligodendrocyte progenitors in the ventral telencephalon by suppressing Dlx-positive progenitors (Petryniak et al., 2007).

These findings are important for transplantation studies, since they might help to selectively choose a suitable NS/PC population to replace a subset of cells in the damaged brain. Several studies have explored the fate of radial glia cells after homotopic and heterotopic transplantations. They were shown to differentiate into

appropriate phenotypes when transplanted homotopically into the embryonic brain. Carletti et al. (2004) used neocortical progenitors isolated from the E12 dorsal telencephalon and transplanted them into various brain regions of later stage embryos (E16). They discovered that after transplantation, the cells differentiated into neurons and glia; however, their proportion differed according to the site of transplantation. While in the neocortex, hippocampus, olfactory bulb (OB) and striatum, these cells differentiated primarily into neurons, after transplantation into extra-telencephalic sites, these cells differentiated into glia (Carletti et al., 2004). Another study by Gaillard et al. (2003) showed that within the cortex, E12 progenitors are not committed to a specific fate upon heterotopic transplantation into a neonatal host. They isolated radial glia from the E12 rat brain, from the presumptive parietal and occipital cortices, and transplanted them into the ventrobasal complex of neonatal rats. Both types of progenitors were able to integrate into the host tissue and form barrel-like structures as well as connections with host cells (Gaillard et al., 2003). NS/PCs derived from the embryonic cerebellum and cortex were shown to differentiate into their respective phenotypes only after their homotopic transplantation into the neonatal brain (Klein et al., 2005). A later study by Kallur et al. (2006) used human NSCs derived from the embryonic cortex or striatum and explored their fate upon transplantation into the striatum of neonatal rats. While *in vitro* the NSCs differentiated into neurons with the appropriate phenotype with respect to the site of origin, upon transplantation, the cells exhibited similar survival, migration and differentiation (Kallur et al., 2006). Although these studies show that upon transplantation, embryonic NSCs respond to the local cues of the embryonic/neonatal CNS, the situation might be different upon transplantation into the adult/lesioned brain. Recently, the same scientific group described differences in the migration and differentiation of human foetal striatal and cortical NSCs after transplantation into the striatum after a stroke. While both NSC types survived to a similar extent (30% survival one month after transplantation), striatal NSCs migrated more and occupied a greater volume in the damaged striatum and produced a larger number of parvalbumin- and calretinin-positive neurons than the cortical NSCs (Darsalia et al., 2007). Interestingly, GFAP/GFP astrocytes isolated from the neonatal mouse cerebellum and grafted into the environment of the adult mouse SVZ displayed properties similar to cells originally residing in the SVZ. They were able to proliferate and produce migrating cells that entered the rostral migratory stream (RMS), and in the OB they differentiated into

appropriate interneurons. Also within the SVZ the grafted cells interacted with the chains of migrating cells. These findings suggest that astrocytes derived from non-neurogenic regions of the mouse brain are able to respond to the cues provided by neurogenic zones (Zheng et al., 2006). In our work, we used a subset of telencephalic NS/PCs, which specifically give rise to cortical projection neurons and to a subset of cortical astrocytes (Machon et al., 2002).

Immortalised neural stem cell lines have also been successfully used in animal models of neurological disorders. One of the well characterised human neural stem cell lines used for transplantation studies is HB1.F3. This cell line was derived from the human foetal telencephalon and was infected with amphotropic, replication incompetent retroviral vector-containing *v-myc*. The clone-derived HB1.F3 cell line expresses the normal human caryotype of 46 and is further characterised by the expression of neural stem cell markers, such as nestin and vimentin. After their systemic administration through the tail vein in rats, these cells were able to reach a damaged site in the brain. They neither disrupted the tissue of systemic organs nor were they observed to form tumors. Moreover, upon engraftment, these cells differentiated and down-regulated *v-myc* (Lee et al., 2006, Lee et al., 2007). Chu et al. (2004) used HB1.F3 NSCs for intravenous administration in a rat model of global ischemia. The cells migrated into various parts of the brain and gave rise to astrocytes and neurons (Chu et al., 2004). They were also used in rat models of Huntington's disease (Lee et al., 2006) and Parkinson's disease (Yasuhara et al., 2006), and in both cases the transplantation of HB1.F3 cells ameliorated the behavioural symptoms of the model disease. They were also used in a mouse model of intracerebral haemorrhage stroke, in which transplantation led to improved behavioural performance (rotarod and limb place tests) of the animals, two weeks after transplantation (Lee et al., 2007). Also, NE-4C immortalised neural stem cells were shown to integrate after transplantation into the neonatal or adult mouse brain, without any sign of tissue disruption or tumour formation. However, the fraction of differentiated cells was very low (Demeter et al., 2004).

2.2 Physiology of adult neurogenesis

After the termination of embryonic neurogenesis, two major germinal zones remain to produce neurons throughout the postnatal life in the adult mammalian brain: the SVZ of the lateral ventricles and the subgranular zone (SGZ) of the hippocampal dentate gyrus. Although their primary goal is to supply the adult brain with neurons, cells present in these neurogenic niches exhibit the properties of neural stem cells under certain conditions *in vitro* and also *in vivo*. Recent works have suggested that cells with a stem cell potential can also be isolated from regions that are primarily thought to be non-neurogenic, such as the cerebellum or spinal cord, and that under certain conditions *in vitro*, these cells are able to form neurospheres and differentiate into neurons, astrocytes and oligodendrocytes (Jiao and Chen, 2008). Thus, NS/PCs of the adult brain represent a potential tool for regenerative medicine.

2.2.1 Architecture and cellular characterisation of the adult rodent SVZ

The SVZ is localised in the lateral walls of the lateral ventricles facing the striatum **(Fig. 3)**. The medial wall facing the septum is largely devoid of the SVZ, with the exception of the most anterior part of the anterior horn. In rodents, due to the postnatal closure of the olfactory ventricle, only the middle/posterior part of the SVZ remains in contact with the ventricles. The anterior part forms a rostral extension called the RMS, through which newborn neurons migrate into the OB, where they differentiate into distinct interneuron subtypes (Peretto et al., 2005, Merkle et al., 2007). These newly-added interneurons are important for perceptual memory. It was shown that in mice, an odour-enriched environment increases the survival of adult-born granule neurons, which are then preferentially recruited in the process of learned odour discrimination (Moreno et al., 2009).

The cellular composition of the SVZ-RMS-OB system has been extensively described using morphological and immunohistochemical criteria in mice (Doetsch et al., 1997, Doetsch et al., 1999a, Mirzadeh et al., 2008) as well as in rats (Danilov et al., 2009) and humans (Quinones-Hinojosa et al., 2006, Kam et al., 2009). There are 4 types of cells in the rodent SVZ: neural stem cells (also called astrocytic neural stem cells, or type-B cells), transit-amplifying progenitors (type-C cells), migrating neuroblasts (newly born neurons, type-A cells) and ependymal cells (type-E cells, **Fig. 3A-B**).

Type-B cells (B1 and B2) are located in a thin layer close to the ventricular surface, separated from the ventricle by a single layer of ependymal cells. They express astrocytic markers, such as nestin, GFAP, BLBP and GLAST (Pastrana et al., 2009, Platel et al., 2009), and further Lewis X (LeX, also called SSEA-1, stage specific embryonic antigen), which is a marker of both embryonic and adult neural stem cells (Capela and Temple, 2002, 2006). Type-B1 cells extend their apical endings to contact the ventricle and a long basal process that contacts a blood vessel. The apical processes are nestin-, GFAP- and CD133-positive (Mirzadeh et al., 2008). Both type-B1 and B2 cells ensheath migrating neuroblasts.

Fig. 3 Neurogenesis in the adult mouse SVZ

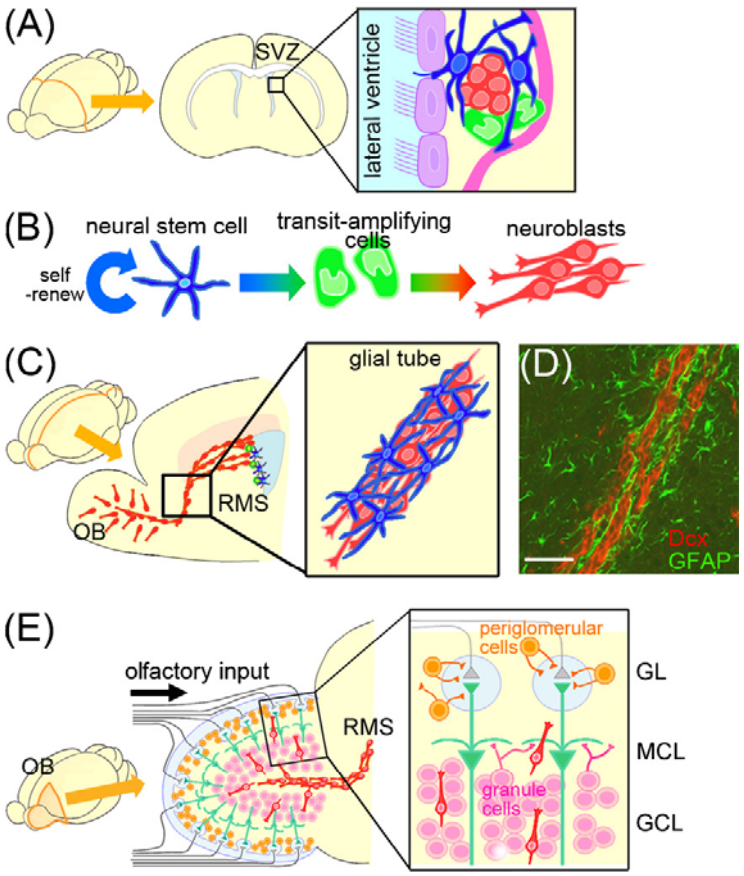

(A) The SVZ is located at the lateral wall of the lateral ventricle and consists of 4 types of cells: ependymal cells (purple), which line the surface of the lateral ventricle, astrocytic NSCs (blue); transit-amplifying cells (light green); and neuroblasts (red). The cells are embedded in a vascular niche (pink). **(B)** Astrocytic NSCs (blue) in the SVZ self-renew and produce transit-amplifying cells (green), which are fast-proliferating cells that produce migrating neuroblasts (red). **(C)** Newly generated neuroblasts migrate towards the OB through the RMS, in which they form chain-like clusters (red), which are surrounded by a glial tube formed by astrocytic NSCs (blue). **(D)** Immunohistochemistry of the RMS showing chains of DCX^+ neuroblasts surrounded by $GFAP^+$ NSCs. (Scale bar: 50 µm.) **(E)** In the OB, neuroblasts disperse radially from their chain and differentiate into olfactory interneurons - granule cells or periglomerular cells - which reside in the GCL or GL, respectively. **SVZ:** subventricular zone; **RMS:** rostral migratory stream; **GCL:** granule cell layer; **MCL:** mitral cell layer; **GL:** glomerular layer (Kaneko and Sawamoto, 2009).

Type-B1 cells separate the neuroblasts from the ependymal layer, while type-B2 cells separate them from the overlying striatum **(Fig. 3A)**. Type-B1 cells proliferate slowly and continuously to produce transit-amplifying cells (Doetsch et al., 1997, Pastrana et

al., 2009). They express EGFR (Doetsch et al., 2002), and in the presence of EGF they form neurospheres *in vitro* and give rise to neurons, astrocytes and oligodendrocytes (Haskell and LaMantia, 2005). Contacts between type-B1 cells are mediated by atypical adherens junctions and tight junctions; connexin 43 has also been detected, suggesting that these cells are also connected via gap junctions. In contrast to type-B1 cells, type-B2 cells represent non-proliferating GFAP-positive astrocytes with a multipolar morphology (Mirzadeh et al., 2008), which are unable to form neurospheres in the presence of various growth factors *in vitro* (Pastrana et al., 2009). A recent study revealed an interesting relationship between type-B1 and B2 cells. It was shown previously that after treatment with cytosine-β-D-arabinofuranoside (Ara-C), all proliferating cells are eliminated from the adult mouse SVZ and only non-proliferating type B2 astrocytes remain (Doetsch et al., 1999b). However, shortly after the termination of Ara-C treatment, these cells start to express EGFR, thus becoming 'activated' neural stem cells (type-B1), which are then able to regenerate the entire SVZ-OB niche (Pastrana et al., 2009). GFAP-positive cells with the ability to produce new OB neurons after Ara-C treatment were also identified in the mouse RMS (Alonso et al., 2008). Migrating neuroblasts derived from the RMS astrocytes appear 2 days after the termination of Ara-C treatment (Gritti et al., 2002), while in the SVZ, the first neuroblasts appear after 4 days (Doetsch et al., 1999b). However, SVZ astrocytes have a greater capacity to produce new neurons after Ara-C treatment than those residing in the RMS (Alonso et al., 2008). Permanent suppression of SVZ neurogenesis in adult rats by irradiation was also shown to induce a transient, but marked production of calretinin-positive interneurons in the OB, although this capacity is limited and declines dramatically beyond one year (Panagiotakos et al., 2007). Type-B cells of the adult SVZ were shown to be descendants of embryonic radial glia (Merkle et al., 2004). Based on the transcription factor expression known from the embryonic VZ, corresponding zones were also identified in the adult SVZ. Analysis showed that the embryonic LGE (marked by Gsh2 expression), MGE (marked by Nkx2.1 expression) and cortex (marked by Emx1 expression) contribute differently to the formation of the adult SVZ. Most of the proliferating NSCs are derived from the LGE, a minor fraction from the cortex and almost none from the MGE. They also contribute differently to the production of OB interneurons. NSCs derived from the embryonic cortex, despite being a minority, generate the majority of calretinin-positive interneurons but none of the

calbindin-positive interneurons in the olfactory glomerulus, which are exclusively produced by NSCs derived from the embryonic LGE. Tyrosine hydroxylase (TH)-positive interneurons are then produced by both subpopulations of adult neural stem cells (Young et al., 2007).

Type-C cells form small clusters and, unlike type-A cells, they are not isolated from the surrounding parenchyma by type-B cells. They are the most actively proliferating cells in the SVZ (Doetsch et al., 1997, Adachi et al., 2007). They express EGFR and respond to EGF by increased proliferation and decreased formation of type-A cells *in vivo*. In the presence of EGF *in vitro*, they are able to form neurospheres and are tripotent upon differentiation (Doetsch et al., 2002, Haskell and LaMantia, 2005). The majority of these nestin-positive cells are located in the SVZ, although they are also found in the RMS (Gritti et al., 2002, Alonso et al., 2008). They give rise to type-A cells from which they can be distinguished by immunocytochemical double staining, as Dlx2-positive/plysialated neural cell adhesion molecule (PSA-NCAM)-negative cells (in contrast to Dlx2-positive/PSA-NCAM-positive type-A cells (Doetsch et al., 2002). In the work of Aguirre *et al*., C-type cells were identified as LeX-positive/GFAP-negative cells expressing NG2 proteoglycan (Aguirre et al., 2004); however, recent studies have indicated that the population of type-C cells in the adult rodent SVZ is actually NG2-negative (Komitova et al., 2009) and that NG2-positive cells derived from the adult brain lack neurogenic potential (Buffo et al., 2008). C-type cells also express the transcription factors Mash1 (Parras et al., 2004), and Olig2 (Menn et al., 2006); however, these markers are not unique for this cell population. Olig2 is also expressed by a subset of type-B cells (Hack et al., 2005, Menn et al., 2006), and the Olig2-positive cell population of the adult SVZ was shown to give rise to NG2-positive oligodendrocyte progenitor cells that migrate out of the SVZ into the corpus callosum, neighbouring striatum, and fimbria fornix to differentiate into non-myelinating and myelinating oligodendrocytes. During their migration, they are not surrounded by astrocytes, and they are associated with myelinated and unmyelinated axons (Menn et al., 2006). Mash1 is also expressed by a subset of type-B cells (Pastrana et al., 2009), and its expression probably reflects the transition from a type-B to a type-C cell population (Platel et al., 2009). Additionally, Olig2 over-expression in the adult SVZ was shown to promote the proliferation of C-type cells, while neuroblasts were suppressed. Moreover, an increased number of cells left the RMS, and they reached the

corpus callosum to differentiate into adenomatous poliposis coli (APC)- and Sox10-positive oligodendrocytes (Hack et al., 2005).

Proliferating type-B cells as well as transit amplifying progenitors are located directly on blood vessels in places that lack astrocytic endfeet (marked by the lack of aquaporin 4, which is abundantly expressed in the endfeet of perivascular astrocytes) and pericyte coverage. Additionally, after Ara-C treatment that eliminates all rapidly dividing cells, the regeneration of the SVZ by type-B cells starts in the vicinity of blood vessels: newly appearing transit-amplifying cells are directly coupled to the vasculature and frequently localised at sites lacking aquaporin 4 (Tavazoie et al., 2008). Proliferating cells of the adult SVZ bind to the blood vessels via α6β1 integrin, a receptor for laminin. The adhesion is crucial for cell proliferation, as its disruption causes cell displacement from the blood vessels and decreases their proliferation (Shen et al., 2008).

Type-A cells were identified as neuroblasts that migrate in tangentially oriented chains (in parallel to the wall of the ventricle) through the RMS to the OB **(Fig. 3C)**. These cells co-express PSA-NCAM, Dlx2 (Doetsch et al., 2002), βIII tubulin (Pastrana et al., 2009) and doublecortin (DCX), but they are also nestin-positive (Platel et al., 2009). Unlike type-B and C cells, neuroblasts are committed to the neuronal linage, and a subset of these cells is able to proliferate, although to what extent is a matter of controversy (Pastrana et al., 2009, Platel et al., 2009). These cells also express CD24, similarly as ependymal cells. However, the expression of CD24 in neuroblasts is low, while it is high in ependymal cells, thus enabling an effective separation of these two cell populations (Pastrana et al., 2009). In the RMS the migrating neuroblasts exhibit a bipolar morphology (Young et al., 2007) and upon reaching the OB, they detach from the migratory chain, and the individual cells migrate radially into the granule cell layer (GCL) and the glomerular layer (GL), where they differentiate into two types of olfactory interneurons, the granule cells and periglomerular cells, respectively. Periglomerular cells can be further sub-divided into calretinin-, calbindin-expressing cells and TH-expressing dopaminergic neurons. Granular cells comprise deep, superficial and calretinin-positive cells (Merkle et al., 2007, Young et al., 2007). The population of the migrating neuroblasts is not uniform, and distinct regions of the SVZ contribute differently to the subpopulations of the OB interneurons **(Fig. 3D**; Merkle et al., 2007). Paired box 6 (Pax6) is a transcription factor expressed in neuroblasts along

the RMS, but later it is down-regulated during neuronal differentiation except in dopaminergic neurons of the periglomerular layer. The over-expression of Pax6 increases the differentiation of neuroblasts into TH-positive dopaminergic interneurons (Hack et al., 2005), and the over-expression of Dlx2 promotes neuroblast migration (Brill et al., 2008). New neurons are continuously added to the GL of the OB, reaching one-third of the total neuronal population within 9 months (starting in a 3-month-old mouse), while in the GCL, the number of newly generated neurons reaches a plateau within two months. These neurons represent a relatively minor contribution to the entire population of neurons; however, their numbers remain stable at this low proportion for many months (Ninkovic et al., 2007).

Apart from these major cell types, the SVZ also contains ependymal cells (E-type cells) that form a monolayer (ependymal layer) separating the SVZ from the ventricular cavity. The majority of ependymal cells are multiciliated (E1-type), while only 5% of ependymal cells have only one or two cilia and a large cell body (E2-type cells). While multiciliated ependymal cells participate in the flow of the cerebrospinal fluid, the role of E2-type cells is as yet unknown. E1- and E2-type cells are connected by tight junctions and symmetric adherens junctions and also express connexin 43, suggesting the presence of gap junctions. Both cell types are GFAP-negative and are CD24-, S100β- and vimentin-positive. They are organized in a pinwheel structure, and in its centre an apical process of a type-B1 cell contacts the lateral ventricle (Mirzadeh et al., 2008). Multiciliated ependymal cells also express CD133 (Coskun et al., 2008). It was proposed that multiciliated cells lining the ventricle in adult mice could act as slowly proliferating quiescent neural stem cells (Johansson et al., 1999, Coskun et al., 2008). Other studies showed that ependymal cells proliferate *in vitro* to form sphere-like structures; however, they do not have the ability to form secondary neurospheres after dissociation or to produce neurons. When plated under differentiation conditions in culture, they preferentially generate GFAP-positive cells (Chiasson et al., 1999, Doetsch et al., 2002). *In vivo*, they are Ki67-, 5-bromo-2-deoxyuridine (BrdU)- and PH3-negative (Mirzadeh et al., 2008), they do not incorporate 3H-thymidin and are generated from a subpopulation of embryonic radial glia, which terminally differentiate during the first postnatal week (Spassky et al., 2005). However, recent studies suggest that these cells might act as neural stem cells under certain conditions. They express Notch1 receptor, and it was suggested that the canonical Notch signalling pathway maintains

these cells in a quiescent state. Inhibition of this signalling pathway after a stroke enabled these cells to proliferate and to produce neurons of the OB (Carlen et al., 2009). Other recent studies on rats showed that in response to a combination of lesioning with 6-hydroxydopamine and the infusion of transforming growth factor α (TGFα, Gleason et al., 2008) or after Ara-C treatment (Coskun et al., 2008), these cells divide both symmetrically to self-renew and asymmetrically to transfer their progeny into the SVZ, where they further divide and produce new neurons. Therefore, these cells are not classified as true stem cells; however, they represent a unique reservoir of cells that can be recruited to neurogenesis under certain conditions after injury.

Although the SVZ is formed at the end of embryogenesis, it undergoes structural changes during the first three postnatal weeks, in both mice and rats, to gain the form described above (Peretto et al., 2005). In neonatal mice, GFAP/nestin/vimentin-positive cells are already present in the SVZ (Alves et al., 2002). However, they display distinct modes of migration. While in the adult SVZ cells migrate tangentially towards the OB to produce neurons, in the SVZ during the first postnatal week NSCs of the SVZ also migrate tangentially to produce astrocytes of the cortex (Suzuki and Goldman, 2003). Nevertheless, the antigenic profile of the cells within the SVZ-OB system is similar to that described in the adult SVZ. In the work of Cesetti et al., (2009), the authors used fluorescence activated cell sorting to separate distinct cell populations of the neonatal SVZ. They found that both NSCs (type-B cells) and transit amplifying cells (type-C cells) express EGFR, and they defined the NSCs as EGFR/GFAP/LeX-positive. However, unlike in the adult SVZ, they were also PSA-NCAM-positive. Transit-amplifying cells were defined as EGFR/Dlx2/PSA-NCAM-positive and neuroblasts as PSA-NCAM/DCX-positive cells (Cesetti et al., 2009).

2.2.2 Hippocampal dentate gyrus

Hippocampal neurogenesis is confined to the dentate gyrus, which is largely composed of granule neurons of the GCL. Granule cells receive inputs from the entorhinal cortex (perforant path) and subcortical regions, including the raphe nucleus and locus coeruleus. The granule cells project their axons (called mossy fibres) to the CA3 region, where they form synapses with pyramidal neurons (**Fig. 4,** Kaneko and Sawamoto, 2009). Continuous hippocampal neurogenesis is important for learning and memory. It was shown that in mice, newly generated neurons of the hippocampus are preferentially

recruited into the networks supporting spatial memory (Kee et al., 2007) and that the ablation of hippocampal neurogenesis leads to defects in the retention of spatial memories (Imayoshi et al., 2008).

Fig. 4 Neurogenesis and neuronal circuitry of the dentate gyrus in the hippocampus of the adult rodent brain

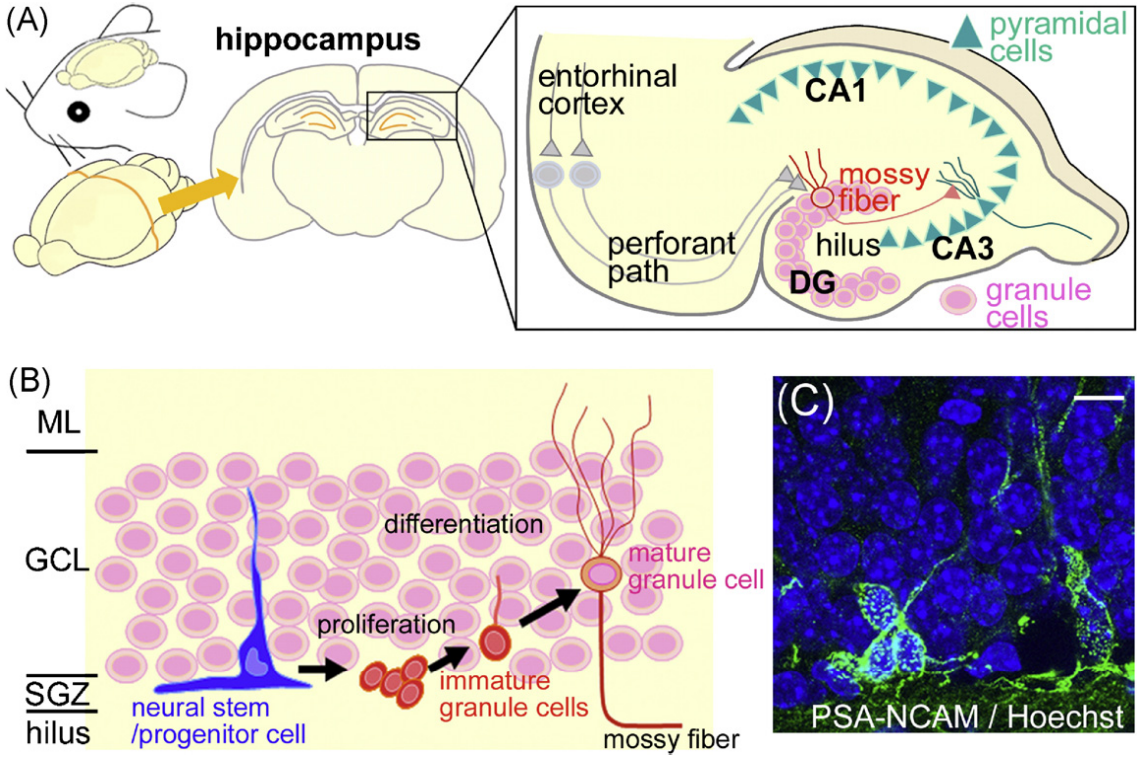

(A) The input to the hippocampus is mainly provided by the entorhinal cortex through the perforant path (grey) to the granule cells (pink) in the molecular layer of the dentate gyrus. Each granule cell projects an axon (called a mossy fibre, red line) to the CA3 region, where it forms synapses with pyramidal cells (blue-green). **(B)** NSCs reside in the SGZ (blue), proliferate, and generate transient progenitors that produce immature granule cells (red). The immature cells migrate into the GCL, where they differentiate into mature granule neurons (pink), which project their axons (mossy fibres) to the CA3 region. **(C)** Immunohistochemistry showing PSA-NCAM$^+$ immature granule cells having short, thin process, residing in the border between the SGZ and the GCL (Green - PSA-NCAM; blue - Hoechst; scale bar, 10 μm.) **DG:** dentate gyrus; **GCL**: granule cell layer; **SGZ:** subgranular zone; **ML:** molecular layer (Kaneko and Sawamoto, 2009).

Neural stem cells reside in the SGZ, a thin cell layer between the GCL and the dentate hilus (Seri et al., 2001). NSCs in the dentate gyrus comprise two populations of astrocytic NSCs with distinct morphologies, radial and non-radial, both of which express Sox2, Mushashi 1 (Suh et al., 2007) and vimentin (Seri et al., 2004). Radial astrocytes have a large cell body with a major radial process projecting through the GCL into the molecular layer (Filippov et al., 2003), and they have been identified as the stem cell population in the SGZ of the dentate gyrus (Seri et al., 2001, Seri et al.,

2004). They also express nestin and the radial glia markers BLBP and GFAP (Kronenberg et al., 2003, Anthony et al., 2005, Suh et al., 2007). Similarly to NSCs of the SVZ, they contact blood vessels via endfeet (Filippov et al., 2003). Several studies have suggested that radial astrocytes are not the only NSCs in this region and that non-radial Sox2-positive cells are actually the major proliferating population in the dentate gyrus, while radial Sox2-positive (Suh et al., 2007) or nestin-positive (Kronenberg et al., 2003) cells rarely divide under physiological conditions. Using retro-viral labelling, Suh et al. (2007) demonstrated that non-radial Sox2-positive cells represent the proliferating NSCs in the dentate gyrus and that these cells self-renew and give rise to radial Sox2-positive cells, which are quiescent and represent a reservoir of cells that can rarely divide. Non-radial Sox2-positive NSCs are able to proliferate both *in vitro,* where they have the ability to produce neurons, astrocytes and oligodendrocytes, as well as *in vivo*, where they produce predominantly neurons and a small portion of astrocytes, since the hippocampal niche promotes neurogenesis (Suh et al., 2007).

Similarly to the SVZ, dentate neurogenesis progresses through transient progenitor cells, also called type-D cells or type II progenitors (Seri et al., 2001, Fukuda et al., 2003). They form tight clusters and express PSA-NCAM, TUC-4, a protein related to axonal outgrowth, NeuroD, a transcription factor regulating neuronal differentiation, and prospero-related homeobox 1, which is expressed in dentate granule cells in the postnatal brain. Unlike neuroblasts in the SVZ, newly derived neurons of the dentate gyrus migrate only a short distance into the GCL, where they terminally differentiate into neurons. They extend dendrites towards the molecular layer and axons into the CA3 region (Seri et al., 2004). To evaluate the axonal maturation of newly born hippocampal neurons in detail, Ide *et al.*, (2008) labelled nestin-positive progenitors by injecting a GFP-Cre reporter adenovirus into Nestin-Cre mice and followed their development. They found that as early as one week after infection, new neurons received axosomatic cholinergic or GABA-ergic inputs and projected mossy fibres to the CA3 region to form glutamatergic synapses (marked by vesicular glutamate transporter 1) with hilar and CA3 interneurons as well as CA3 pyramidal cells (Ide et al., 2008).

A genetic fate mapping study in mice using a tamoxifen-inducible form of Cre recombinase (CreERT2) in the locus of GLAST revealed that the proportion of newly generated neurons in the hippocampal dentate gyrus is low and represents a relatively

minor contribution (about 14%) to the entire population of NeuN-positive neurons. It reaches a plateau within 2 months and remains stable at this low proportion for up to 9 months (Ninkovic et al., 2007). Another study using adult rats showed that newly-derived cells in the GCL are dying at a steady rate between 6 and 28 days after labelling, resulting in a 50% loss of BrdU-labelled cells over this 22-day period, before they can function as mature neurons (Dayer et al., 2003). Thus, neurogenesis in the adult hippocampus contributes only to a minor fraction of the entire neuronal network (Ninkovic et al., 2007).

2.2.3 Endogenous neurogenesis is increased by injury; its reparative capacity is, however, limited

The existence of neuron-producing NSCs in the adult brain raised the possibility that these cells participate in the processes of brain regeneration. Moreover, it was discovered that brain insults, such as Ara-C treatment or irradiation, can transiently stimulate endogenous neurogenesis. Also, in animal models of neurological disorders such as global ischemia, the number of proliferating cells in the neurogenic niches is increased early after an insult. An increased number of macrophages and microglia appear at the site of injury, and GFAP-positive astrocytes start to express nestin. Neurons and DCX-positive cells die, while the number of proliferating DCX-positive cells is not altered (Pforte et al., 2005). However, a recent study showed that microglia persist after ischemia and produce insulin-like growth factor 1, a factor promoting neurogenesis (Thored et al., 2009). Parent et al. (2002) showed that two weeks after middle cerebral artery occlusion (MCAO, a model of focal stroke) the production of new neuroblasts is increased in the adult SVZ and, additionally, that migrating neuroblasts can leave their normal route towards the OB, enter the peri-infarct area of the striatum damaged by MCAO and differentiate into appropriate neurons (Parent et al., 2002). However, the reparative capacity of endogenous NS/PCs is limited, since both physiological neurogenesis, as well as injury-induced neurogenesis, decline with age. Hattiangady et al., (2008) showed that the neurogenic potential of hippocampal NSCs is preserved during adulthood and aging; however, the number of proliferating cells and new neurons is decreased in middle-aged and aged rats (either intact or after injury, Hattiangady et al., 2008).

2.2.4 Modulators of endogenous and injury-induced neurogenesis

NS/PCs in the adult brain are located in a specific microenvironment, called the neurogenic niche, which is formed by cellular elements, the vascular system and, in the case of the SVZ, also by cerebrospinal fluid. All these components provide the cells in the niche with distinct molecular determinants that tightly regulate their proliferation, survival and fate determination. These include growth factors, molecules of signalling pathways and neurotransmitters. Many of these molecules also participate in the increased neurogenesis induced by neurological disorders or have neuroprotective effects. Therefore, by delivering these agents into the site of injury, endogenous neurogenesis might be augmented to provide a substantial pool for repairing the damaged tissue.

The effects of growth factors on adult and injury-induced neurogenesis are explored by infusing them intraventricularly or using genetic manipulations, such as the over-expression of a growth factor in a distinct cell population. It was also shown that intranasally applied growth factors (bFGF and heparin-binding EGF) can modulate neurogenesis in the SVZ, but not in the dentate gyrus (Jin et al., 2003). The infusion of bFGF into the lateral ventricle of rats with traumatic brain injury increased SVZ neurogenesis and also improved the cognitive recovery of the injured animals (Sun et al., 2009). The over-expression of vascular endothelial growth factor in transgenic mice led to improved spatial memory after permanent occlusion of the common carotid artery (Plaschke et al., 2008). The intravenous application of BDNF into post-stroke rats improved their sensorimotor functions and increased the number of DCX-positive progenitors in the striatum and NeuN-positive cells in the dentate gyrus of the hippocampus (Schabitz et al., 2007).

Several signalling cascades have been implicated in NS/PC maintenance and differentiation. Notch signalling maintains cell proliferation in the dentate gyrus, and its blockage increases cell differentiation into neurons (Breunig et al., 2007). This signalling pathway also mediates cell proliferation in NS/PCs isolated from the adult SVZ after stroke (Wang et al., 2009). BMP signalling is active in the SVZ in NSCs as well as in transit amplifying progenitors and plays an essential role in the neuronal fate determination of progenitor cells. Using transgenic mice lacking Smad 4, a transcription factor that mediates BMP signalling, it was shown that in these mice the number and self-renewal potential of the NSCs are not disrupted; however, the number of

Dlx2/DCX-positive neuroblasts is decreased, while transit amplifying progenitors up-regulate Olig2 and increase their migration into the corpus callosum, where they differentiate into PDGFR-α- and APC-positive oligodendrocytes (Colak et al., 2008). BMP signalling also participates in the regulation of hippocampal neurogenesis. The BMP inhibitor Noggin is expressed in the SGZ, and its over-expression *in vivo* increases the number of proliferating GFAP-positive cells and subsequently the number of transient progenitors (Bonaguidi et al., 2008). Shh and Wnt/β-catenin signalling pathways are major regulators of adult and injury-induced neurogenesis, and therefore their effects on neural stem cell proliferation and differentiation and their role in brain pathologies have been extensively studied. However, no data are available so far on how these morphogenes affect the membrane properties and the expression of ion channels and receptors of neural stem cells and their derivatives.

2.3 Sonic Hedgehog signalling pathway

The Shh signalling pathway **(Fig. 5)** plays a key role in regulating vertebrate organogenesis, including the central nervous system. It acts as a morphogene along the entire neuraxis; its expression is crucial for the patterning of the ventral spinal cord, telencephalon, midbrain and cerebellum. It also regulates the expression of the midbrain-hindbrain organizer FGF8. It is crucial for eye development, where it modulates the splitting of bilateral eye fields (reviewed in Fuccillo et al., 2006) and is involved in tumorigenesis (reviewed in Ruiz i Altaba et al., 2002). In the developing telencephalon, Shh affects the proliferation and differentiation of neural stem/progenitor cells. The loss of Shh signalling in conditional knock-out mice resulted in a prolonged cell-cycle of neural stem cells, decreased neuronal differentiation, increased neuronal death and also a disorganisation of the arising cortical structures (Komada et al., 2008). Shh signalling is also involved in adult and injury-induced neurogenesis.

2.3.1 Sonic Hedgehog production and modification

Shh is a glycoprotein and a member of the Hedgehog family (Hh) of signalling molecules that were identified by their homology to the Hedgehog protein discovered in *Drosophila*. In mammals, three homologues exist: Shh, Indian hedgehog and Desert hedgehog.

In mammals, Shh protein undergoes a set of post-translational processing reactions **(Fig. 5A)**. The ~45 kDa precursor protein is proteolytically auto-cleaved to produce a ~19 kDa N-terminal protein (N-Shh) that mediates all signalling activities and a ~25 kDa C-terminal protein (C-Shh), which contains the protease that catalyses the cleavage and also introduces a molecule of cholesterol to the C-terminal amino acid (Porter et al., 1996). N-Shh is further modified by the addition of a palmitoyl group to the N-terminal cysteine by Hedgehog acyltransferase (Buglino and Resh, 2008) and is released from the cell through the action of the membrane transporter protein Dispatched (Disp). In mammals two homologues of Disp exist - Disp1 and 2; however, only Dips1 is required to move Shh away from the site of synthesis (Caspary et al., 2002). Cholesterol modification enables the tethering of N-Shh to the cell membrane and is also crucial for long-range signalling (Lewis et al., 2001). N-Shh palmitoylation is also important for the long range activity of Shh, since it enables the morphogene to form multimeric complexes in which the hydrophobic moieties cluster together in an inner core, allowing their diffusion and long range signalling (Chen et al., 2004, Goetz et al., 2006).

2.3.2 Shh signalling cascade

In mammals, the Shh signalling cascade is initiated by binding Shh to Patched (Ptc), a twelve-pass transmembrane receptor found on a surface of a target cell **(Fig. 5B)**. In mammals, two isoforms of Ptc exist, Ptc1 and Ptc2; both of these bind to Shh and are able to form a complex with Smoothened (Smo), a seven-pass transmembrane G-protein-coupled receptor (Carpenter et al., 1998). Ptc1 is localised in the primary cilia and in the absence of Shh inhibits Smo by preventing its accumulation in the cilia. Binding Shh to Ptc1 eliminates Ptc1 from the cilia and, instead, Smo is sequestered to the primary cilia and the intracellular part of the signalling cascade is initiated (Corbit et al., 2005, Rohatgi et al., 2007). A further step in the signalling pathway is mediated by zinc finger transcription factors Glioma-associated oncogene homolog 1-3 (Gli1-3). Among the three Gli proteins, Gli1 does not contain a repressor domain and can not be proteolytically processed (Dai et al., 1999), while Gli2 and 3 contain both repressor and activator domains (Dai et al., 1999, Sasaki et al., 1999). In the absence of the Hh signal, Gli3 full-length protein (Gli3-190) is proteolytically processed to lose the C-terminal

activation domains and to form the Gli3 transcriptional repressor (Gli3-83). This process requires phosphorylation by protein kinase A (PKA), casein kinase 1 (CK1) and glycogen synthase kinase 3 (GSK3). Following the phosphorylation, Gli3-190 is ubiquitinated by the β transducing repeat containing protein ($SCF^{\beta TrCP}$) ubiquitin E3 ligase and is processed by proteasome (Tempe et al., 2006). Gli2 is processed in the same way resulting, however, in protein degradation (Pan et al., 2009). In the presence of the Hh signal, Gli2 acts as the major transcriptional activator, while Gli3 processing is inhibited and the full-length protein is activated. Gli1 activation is indirect, through the formation of Gli2/Gli3 activator proteins (Sasaki et al., 1999). Unprocessed Gli proteins are localised in the distal segment of the cilia, which provide the platform for transmitting the signal from the cell membrane to the nucleus. Intraflagellar transport (IFT) proteins are essential for cilia formation, and several IFT proteins were shown to be essential in Shh signalling transduction. Double mutants of IFT172 and IFT88 proteins were shown to abolish cilia formation and therefore block Shh signal transduction in the mouse *in vivo* (Huangfu et al., 2003). Both IFT proteins and IFT motor proteins, such as Kinesin family member 3a (Kif3a; Huangfu and Anderson, 2005) and Kif7 (Cheung et al., 2009), have been implicated in the modulation of Gli transcription factors. Biochemical analyses showed that they are required for both the generation of active Gli2 in response to Hedgehog ligand and also for the protein processing that generates the Gli3 repressor (Haycraft et al., 2005, Huangfu and Anderson, 2005, Liu et al., 2005a). The final output of the Shh signalling cascade is mediated by target genes such as Nkx2.2 (Vokes et al., 2007).

The Shh signalling pathway can be modulated at various steps **(Fig. 5B)**. Hedgehog interacting protein is a type I transmembrane protein that inhibits Shh signalling by binding Shh with an affinity similar to Ptc1 (Chuang and McMahon, 1999). Vitronectin, on the other hand, is an extracellular glycoprotein that enhances Shh activity, also by binding to it directly (Pons and Marti, 2000). Cyclopamine, an alkaloid produced by plants of the genus *Veratrum*, is known to inhibit Shh pathway activation by binding directly to Smo. This binding interaction is localised to the heptahelical bundle and probably influences the Smo protein by changing its conformation (Chen et al., 2002). Mouse Suppressor of Fused is an intracellular regulator of the Shh signalling cascade that interacts with Gli proteins and inhibits Gli-mediated transcriptional activation. Its activity is inhibited by Smo in a cilia-dependent manner, while the

inhibitory function of Suppressor of Fused does not require the presence of cilia (Jia et al., 2009).

Fig. 5 Sonic hedgehog signalling pathway

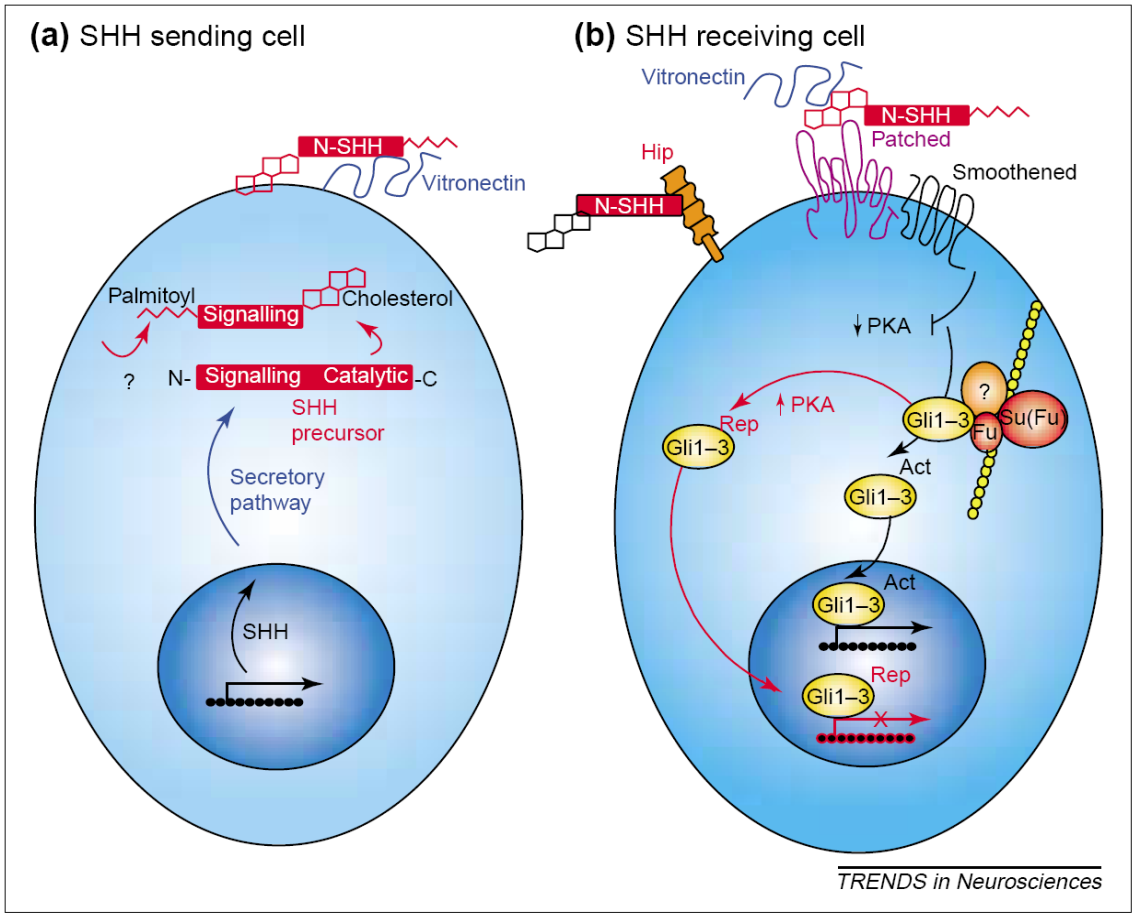

A schematic image showing the production of the Shh signalling molecule **(A)** and the Shh signalling pathway **(B)**. **Shh:** Sonic hedgehog; **Fu:** Fused; **Sufu:** Suppressor of Fused; **PKA:** protein kinase A; **Act:** activator; **Rep:** repressor; **Hip:** Hedgehog interacting protein, **Gli 1-3:** Glioma-associated oncogene homolog 1-3 (Marti and Bovolenta, 2002).

2.3.3 The role of Shh in adult and injury-induced neurogenesis

In the postnatal rodent brain the Shh receptor Ptc is expressed in the hippocampus, particularly within the hilus and in the pyramidal cells of CA1 through CA3. Viral injection with a vector carrying Shh cDNA increases cell proliferation and subsequently the production of new neurons in the dentate gyrus (Lai et al., 2003). Ahn and Joyner used mice that express a Cre-estrogen receptor fusion gene under the control of the Gli-1 promoter, restricting Cre-estrogen receptor expression to cells with Shh signalling. They discovered that Shh-responding cells (Gli1-positive) in the ventral SVZ and SGZ represent GFAP-positive neural stem cells, a subset of transient progenitors (identified

as Dlx2- and Olig2-positive) and PSA-NCAM-positive neuroblasts. However, no Gli1-positive cells were found within the RMS and OB, suggesting that only cells within the germinal zones are targets of Shh signalling. The Shh-responding neural stem/progenitor cells appeared at the time of SVZ and SGZ formation, at E15.5 and at E17.5, respectively. The initial small population expanded (due to its self-renewal capacity) and produced cells that colonized the RMS and OB and the granular zone of the dentate gyrus. Shh signalling is thus activated during late neurogenesis, with the sequential establishment of the neurogenic niches (Ahn and Joyner, 2005).

Machold *et al*. used a conditional loss-of-function approach. They specifically removed the Shh or Smo activity in nestin-positive precursors. In their $Shh^{n/c}$; $Nestin^{Cre}$ or $Smo^{n/c}$; $Nestin^{Cre}$ mice the patterning in the telencephalon appeared relatively normal as early as E12.5. The expression of markers such as Pax6, Neurogenin 2, Gsh2 and Dlx2 was indistinguishable from controls, and the only deficit was a decreased size of the MGE and the reduced production of early oligodendrocyte progenitors. The major effects appeared postnatally. The number of proliferating cells in the dentate gyrus and SVZ was markedly decreased in $Smo^{n/c}$; $Nestin^{Cre}$ animals. Additionally, the loss of Shh signalling resulted in SVZ cells undergoing programmed cell death (Machold et al., 2003). These results are in accordance with other studies using a pharmacological approach, where the blockade of the Shh signalling pathway by cyclopamine in adult and perinatal mice resulted in the diminished expression of Gli1 and deficits in SVZ cell proliferation *in vivo* (Palma et al., 2005) and also decreased cell proliferation in the hippocampal dentate gyrus (Lai et al., 2003). It was shown recently that the ablation of Sox2 in mice leads to the loss of Shh signalling and subsequently to the loss of proliferating cells in the postnatal germinal zones. Shh administration partly averted the effects, resulting in moderate defects in the size of the hippocampal dentate gyrus and a smaller reduction of the proliferating stem cell population. By ablating Sox2 in adult mice using the Cre-ERT2 system, it was also shown that the population of proliferating GFAP/Sox2/nestin-positive cells in the hippocampus is diminished and subsequently, that the production of new neurons is impaired. Moreover, the data suggest that Sox2 acts directly via Shh (Favaro et al., 2009).

Two recent studies using $Nestin^{Cre/+}$;$Smo^{c/c}$ mutants confirmed that type-B cells and Mash1-positive type-C cells are Hh responsive and that Hh signalling is required for their maintenance and proliferation in the SVZ stem cell niche. The loss of Hh

signalling led to a gradual depletion (due to increased cell death) of both type-B and subsequently type-C cells. Migrating type-A cells did not respond to Hh signalling (they were LacZ- negative in Gli1^{lacZ} mice), and they were massively over-produced in the mutant mice at P8. However, they failed to migrate, accumulated in the striatocortical angle and underwent cell death. The authors suggested that Slit homolog 1, a non-autonomous signal important for proper cell migration, might be involved, as the inability to migrate correlated with its decreased expression in the mutant mice. Type-E cells (S100β and mCD24-positive) did not respond to the Hh signal nor were they affected by its loss when compared to controls (Balordi and Fishell, 2007b). After Ara-C treatment, the stem cell niches in the SVZ and SGL are quickly replenished by Shh-responding, slowly dividing, quiescent neural stem cells, which responded to this insult by increased proliferation and the production of transit-amplifying cells; this ability is Shh-dependent (Balordi and Fishell, 2007a). It was also suggested that in the dentate gyrus the effects of Shh on neural progenitors require Kif3a, an essential motor for assembling primary cilia. Its conditional removal in hippocampal progenitors resulted in defective Shh signalling and subsequently impaired proliferation of neural progenitors (Han et al., 2008). Shh was also shown to play an essential role in the increased neurogenesis after electroconvulsive seizures; a blockade of Shh signalling abolished the enhanced proliferation of progenitors in the hippocampal dentate gyrus mediated by the seizures (Banerjee et al., 2005). It was shown recently that reactive astrocytes, which appear after mechanical brain injury, are the source of Shh and that its production increases the number of proliferating Olig2-positive cells. The production of Shh by reactive astrocytes is induced by inflammatory stimuli released by CD11b-positive cells, which participate in the post-injury processes in the damaged tissue (Amankulor et al., 2009).

The effect of Shh on the proliferation and differentiation of neural stem cells was also explored *in vitro.* It was shown that the addition of Shh to cell cultures promotes their proliferation (Dahmane et al., 2001) and increases the number of neurons generated by cells derived from the adult SVZ (Palma et al., 2005) and the hippocampal dentate gyrus (Lai et al., 2003). The effect on proliferation is synergic with low concentrations of EGF (Palma et al., 2005), and the effect of Shh is abolished by the application of cyclopamine (Lai et al., 2003, Palma et al., 2005). Another *in vitro* study demonstrated that carbamylated erythropoietin promotes proliferation and selectively

enhances the differentiation of progenitor cells derived from the adult SVZ into neurons. This effect was averted by treating the cell cultures with cyclopamine or si-mRNA cassettes for Mash1 and Gli1. It was also shown that Shh acts as an intermediate signal in regulating neuronal differentiation between carbamylated erythropoietin and Mash1 (Wang et al., 2007a).

2.4 Wnt/β-catenin signalling pathway

Wnt signalling is involved in virtually every aspect of embryonic development including that of the central nervous system (Toledo et al., 2008). It also controls homeostatic self-renewal in many adult tissues, such as the gut, hair follicles, bone, and hematopoietic stem cells. It is also involved in cancers of the above-mentioned tissues (reviewed in Clevers, 2006). In the central nervous system disruptions of Wnt signalling are associated with pathologies such as autism, schizophrenia and Alzheimer's disease (reviewed in De Ferrari and Moon, 2006). During the embryonic development of the nervous system, Wnt signalling controls the proliferation and differentiation of neural stem cells (Hirabayashi et al., 2004), and therefore the role of this signalling pathway has also been studied in the context of adult neurogenesis.

2.4.1 Wnt family of glycoproteins

The Wnt family of secreted glycoproteins is encoded by 7 genes in *Drosophila* and 19 genes in the mouse (Kemp *et al.*, 2005). The first member of the Wnt family was identified as a preferential site for the integration of the mouse mammary tumour virus (Int-1) in virally induced breast tumours (Nusse and Varmus, 1982). Later it was found that Int-1 is an orthologue of the *Drosophila* gene wingless, which plays a role in segment polarity (Rijsewijk et al., 1987), and the current name (Wnt-1) was created. The size of the proteins varies between 39-112 kDa, and they show 20-85% identity in amino acids within the family. They are further characterised by a high number of conserved cysteine residues (Miller, 2002). Post-translational modifications of Wnt proteins include glycosylation by acyltransferase porcupine, which in turn stimulates palmitoylation (Komekado et al., 2007). This modification takes place at the conserved C-terminal cysteine residue (Cys77 in Wnt-3a) of the signalling protein (Willert et al., 2003). Murine Wnt-3a is also palmitoylated at a conserved serine residue (Ser 209),

which was shown to be crucial for the transport of Wnt proteins from the endoplasmic reticulum and its subsequent secretion (Komekado et al., 2007). Both palmitoylation and glycosylation are crucial for protein secretion and activity (Willert et al., 2003, Komekado et al., 2007), and palmitoylation is the reason for the decreased solubility of Wnt proteins and their association with cell membranes (Willert et al., 2003).

2.4.2 Wnt/β-catenin signalling pathway

Three major Wnt signalling pathways have been identified, all of which are thought to signal via Fz receptors:

1. Wnt/β-catenin pathway, in which β-catenin, a *Drosophila* armadillo-related protein, is crucially involved
2. Planar cell polarity pathway
3. Wnt/Ca^{2+} pathway

The Wnt/β-catenin pathway is also called the canonical signalling pathway, and is best understood **(Fig. 6)**. It is the major signalling pathway implicated in adult neurogenesis. The latter two pathways transduce the signal independently of β-catenin and are therefore referred to as non-canonical pathways.

The key component of the Wnt/β-catenin signalling pathway is β-catenin. In the absence of a Wnt signal **(Fig. 6, left)**, low levels of free cytoplasmic β-catenin are maintained by a large multiprotein complex consisting of Axin, APC, CK1 and a serine/threonine kinase (glycogen synthase kinase 3β, GSK3β; Hinoi et al., 2000, Liu et al., 2002). Axin acts as a scaffolding protein that binds other components of the destruction complex. The primary function of this complex is to enable the phosphorylation of β-catenin (by CK1 and GSK3β), thus creating a binding site for the βTrCP component of the E3 ubiquitin ligase complex; β-catenin is then conjugated with ubiquitin and subsequently degraded in proteasomes. The role of APC in this process is to associate with β-catenin (after its phosphorylation by GSK3) and to protect the binding site for βTrCP ubiquitin ligase. In the absence of APC, β-catenin is dephosphorylated, thus the binding site for βTrCP ubiquitin ligase disappears and β-catenin can not be degraded (Su et al., 2008).

Fig.6 Wnt/β-catenin signalling pathway

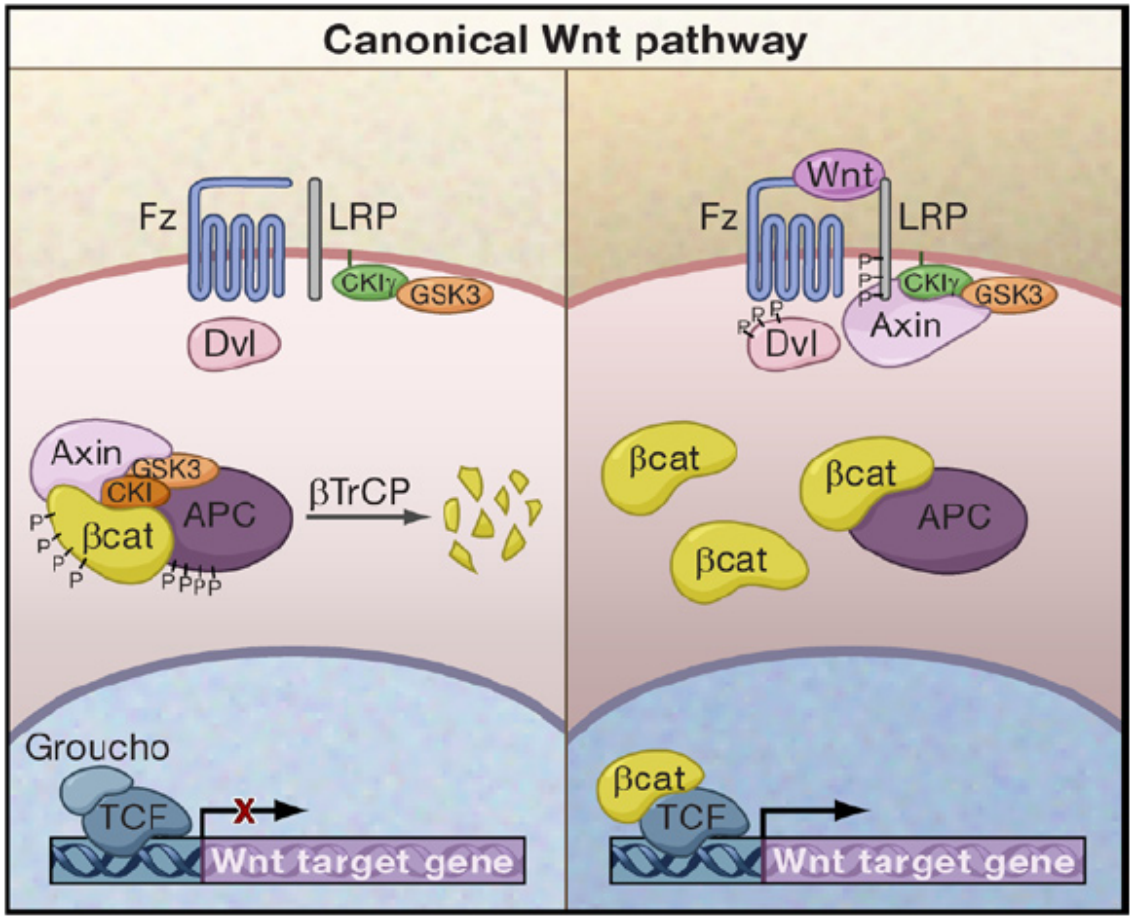

A schematic image showing the canonical Wnt/β-catenin signalling pathway in the absence **(left)** and in the presence of the Wnt signal **(right). Fz:** Frizzled; **LRP:** low-density lipoprotein; **Dvl:** Dishevelled; **CK-γ**: casein kinase γ; **GSK3:** glycogen synthase kinase 3; **β-cat:** β-catenin; **APC:** adenomatous poliposis coli; **TCF:** T cell factor (Clevers, 2006).

Extracellular Wnt molecules bind to Fz seven-pass transmembrane receptors, which contain an extracellular N-terminal cysteine-rich domain with the binding site for Wnt proteins **(Fig. 6, right;** Dann et al., 2001). The binding of Wnt to Fz prevents the degradation of β-catenin by GSK3β. The exact mechanism is not yet fully understood; most of the studies have been performed in *Drosophila*; however, the suggested mechanism is the following: Binding of the Wnt molecule to Fz induces the phosphorylation of Dishevelled (Dvl), which in turn activates the phosphorylation of low-density lipoprotein receptor-related proteins 5 and 6 (LRP5/6) by GSK3 and CK1-γ. This phosphorylation provides the docking sites for the scaffolding protein Axin, which is then removed from the destruction complex; as a result, β-catenin can not be phosphorylated and its cytoplasmic level rises (Zeng et al., 2005, Zeng et al., 2008). It was also suggested that Dvl phosphorylation leads to the activation of GSK3 binding

proteins, which displace GSK3 from the destruction complex, thus disabling the phosphorylation of APC which subsequently loses its affinity for β-catenin (Salic et al., 2000). Accumulated β-catenin is then translocated into the nucleus in a concentration-dependent manner and interacts with the high-mobility group box of transcription factors, predominantly from the family of T cell factor/lymphoid-enhancer binding factors (Tcf/Lef). In the absence of β-catenin, Tcf/Lefs form a complex with Groucho, a member of the Groucho/transducin-like enhancer of split (Grg/TLE) family and act as repressors (Brantjes et al., 2001). When β-catenin enters the nucleus, it replaces Groucho in its bond to Tcf/Lefs and activates the Wnt target genes (Daniels and Weis, 2005).

Secreted Dickkopf proteins inhibit Wnt signalling directly by binding to LRP5/6 (Bafico et al., 2001). Soluble Frizzled-Related Proteins (sFRPs) are a large family of proteins binding directly to Wnts and preventing them from interacting with Fz receptors. They contain a cystein rich domain similar to that found in Fz proteins, and this domain is crucial for their inhibitory activity (Bhat et al., 2007). Two members of the sFRP family, Frzb and Crescent, were recently shown to act as extracellular transporters of Wnt ligands, facilitating their diffusion in the extracellular space and suggesting an alternate role in the regulation of Wnt signalling (Mii and Taira, 2009). Inhibitor of β-catenin and Tcf-4 (ICAT) antagonizes Wnt signalling by preventing the complex formation between β-catenin and Tcf-4 (Tago et al., 2000).

2.4.3 The role of the Wnt/β-catenin signalling pathway in adult and injury-induced neurogenesis

In the adult SVZ, β-catenin signalling is activated in B- and C-type cells, and it was shown that the retrovirus-mediated expression of a stabilized β-catenin or the inhibition of GSK3β increases the number of proliferating Mash1-positive transit amplifying progenitors in the SVZ, which subsequently leads to an increase in the number of newly generated NeuN-positive neurons in the OB (Adachi et al., 2007). Also, hippocampal neurogenesis is under the control of Wnt/β-catenin signalling. Wnt-3 is expressed in the hippocampal astrocytes, which also express all major components of the β-catenin signalling cascade. Blocking β-catenin signalling in the rat hippocampus by injecting a

lentivirus carrying a dominant-negative mutation of Wnt protein led to a decrease in the population of proliferating neuroblasts as well as in the number of new DCX-positive neurons. In contrast, the over-expression of Wnt-3 in the adult rat hippocampus increased the number of proliferating progenitors as well as the production of new neurons (Lie et al., 2005). NeuroD1 is expressed in the transient progenitors of the hippocampus as well as in the immature granule neurons. Its expression is important for the differentiation of granule neurons as well as for their survival (Gao et al., 2009). NeuroD1 is a target gene of Wnt/β-catenin signalling, and a new binding motif was discovered recently, formed by an overlapping sequence of binding sites for Sox2 and Tcf/Lef. Wnt-3a activates NeuroD1 through this sequence, and a deletion of β-catenin in mice leads to the loss of NeuroD1-positive progenitors as well as neurons in the hippocampus (Kuwabara et al., 2009).

The Wnt/β-catenin signalling pathway is also crucial for neurogenesis induced by injury. It was demonstrated that inhibition of β-catenin by siRNA cassettes decreases the neurogenesis induced by MCAO. In this study, the stroke-induced infract volume was enlarged and SVZ expansion was reduced. Also, the number of proliferating cells and newborn neurons was decreased (Lei et al., 2008). Another study in gerbils and adult rats showed that after transient global cerebral ischemia, which eliminates CA1 and later also CA2 neurons, Dickkopf expression increased in the damaged parts of the hippocampus. The neuronal loss in the CA1 region was averted by the intraperitoneal administration of lithium ions (which rescue the Wnt/β-catenin signalling by acting downstream of the Dickkopf 1 blockade, by inhibiting GSK3β) or by the intracerebroventricular administration of Dickkopf antisense oligonucleotides, suggesting that Dickkopf is responsible for the neuronal death in ischemia (Cappuccio et al., 2005).

In vitro studies have explored the effect of Wnts on NS/PC proliferation and differentiation. Progenitors isolated from the adult hippocampus differentiate into neurons when co-cultured with hippocampal astrocytes, which provide the cell culture with Wnt-3a. In the presence of sFRP2/3, the production of new DCX-positive neurons is decreased, as is the number of maturing MAP-2-positive neurons. Similar results were obtained when the cell culture of hippocampal progenitors was electroporated with a construct carrying a dominant-negative form of Lef1 (a mutant form of Tcf/Lef that lacks the ability to bind β-catenin), thus blocking the β-catenin mediated transcriptional

activation. In contrast, transfecting the cell cultures with Wnt3 led to a five-fold increase in the number of new neurons, while differentiation into astrocytes and oligodendrocytes was not affected (Lie et al., 2005). The transfection of neural progenitor cells (NPCs) isolated from the adult SVZ with plasmids carrying Wnt-3a or Wnt-5a increased β-catenin expression in these cells, the formation of neurospheres and, under the differentiation conditions, the number of MAP-2 positive cells, while the number of GFAP-positive cells was decreased (Yu et al., 2006). Another study confirmed that NPCs isolated from neonatal mice are fully equipped to respond to Wnt stimulation. RT-PCR analysis revealed that they express mRNA for the Wnt receptors Fzs, key components of the destruction complex (APC1, Axin1, 2, and GSK3β) as well as other components of the Wnt pathway such as Dvl1, 2, 3 and β-catenin. They also transcribe TCF1, 3 and 4 and all six co-repressors of the Grg/TLE family of genes and express genes for wnt3, 4, 5a, 7a and 7b. However, only a subset of these neonatal NPCs actually responded to the Wnt stimulus, when added to the primary culture. Under differentiation conditions, Wnt-3a did not affect the number of GFAP-positive cells, but the number of βIII tubulin expressing cells nearly doubled, while the number of nestin-positive progenitors decreased. During the course of differentiation, levels of Hes1 and 5 decreased, suggesting that in these cells Wnt acts via interaction with Notch signalling (Hirsch et al., 2007). Another recent study explored the proliferation and differentiation of mouse NS/PCs transduced with various Wnt/β-catenin signalling pathway agonists/antagonists (Dickkopf 1, sFRP5 and Wnt-7a). While they had no effect on neurosphere formation, they influenced the cell fate during differentiation. The over-expression of Wnt-7a led to an increase of MAP-2-positive cells, while GFAP-positive cells were suppressed. In contrast, both Dickkopf 1 and sFRP5 significantly increased the proportion of glial cells in the cell culture (Kunke et al., 2009). All these studies were based on the exogenous activation or inhibition of the Wnt/β-catenin signalling pathway. Recently, a study exploring endogenous Wnt/β-catenin signalling in neural progenitors isolated from the adult rat hippocampus appeared. Interestingly, the authors found that the endogenous Wnt/β-catenin signalling pathway exerts different effects on progenitors. Its inhibition up-regulated genes involved in neuronal differentiation and down-regulated those involved in maintaining the progenitor stage (Wexler et al., 2009).

2.5 Neural stem cells can act as carriers for delivering factors to the injured brain

A new genetic strategy in cell replacement therapy appeared recently. Cells engineered to produce growth factors or other signalling molecules can influence not only their own fate upon transplantation, but may also affect the surrounding damaged tissue. C17.2 is a clonal multipotent progenitor cell line derived from the neonatal mouse cerebellar external granular layer and immortalised using the avian *v-myc* oncogene. This line was subsequently transfected with glial cell line-derived neurotrophic factor (GDNF), and the cells showed increased survival, migration and differentiation into NeuN-positive neurons 6 weeks after transplantation (Bakshi et al., 2006). The HB1.F3 cell line was transfected with Olig2, thus the cells gained a new profile. They expressed (in contrast to the non-transfected cell line) Nkx2.2, a transcription factor that directly regulates the differentiation and maturation of oligodendrocytes. Immunocytochemical analysis detected oligodendrocyte lineage markers, such as O4, GalC or myelin basic protein. Olig2 transduction also increased their proliferative capacity *in vitro*. After their transplantation into the contused spinal cord (a model of spinal cord injury), a greater number of Olig2-transduced cells was detected in grafts seven weeks after transplantation, and the cells increasingly migrated towards the white matter and differentiated into oligodendrocytes (APC-positive cells). Additionally, the volume of the cavity after contusion was significantly decreased and the animal showed an improvement in the quality of their hind limb locomotion (Bakshi et al., 2006). To increase the survival of stem cells after transplantation, the same cell line (HB1.F3) was also transduced with B-cell lymphoma X_L, an anti-apoptotic gene, and used in the same model of spinal cord injury. The major effect of this transduction was the increased survival of the cells, with cell numbers being stable several weeks after transplantation (Lee et al., 2009).

2.6 Membrane properties of neural stem/progenitor cells and their derivatives *in vitro* and *in vivo*

The membrane properties of neural stem cells have been described *in vitro*, as well as *in situ*, in slices prepared from the neonatal (Cesetti et al., 2009) and adult brain (Liu et al., 2006).

Immature neural precursor cells isolated from the E15 rat SVZ and recorded *in vitro* were shown to have a resting membrane potential (V_{rest}) around -46 mV and low membrane capacitance (C_m, ~9 pF). They displayed two different voltage-gated K^+ currents: a fast activating and inactivating outwardly-rectifying K^+ (K_A) current and a delayed outwardly-rectifying K^+ (K_{DR}) current. While the K_{DR} current was sensitive to the application of 10 μM 4-aminopyridine (4-AP, 52% reduction), the K_A current was not (Smith et al., 2008).

Neural stem/progenitor cells were also recorded in the early postnatal brain. In the work of Cesetti et al., (2009), the authors recorded cells from the neonatal SVZ *in situ*. They found that the membrane properties of neural stem and transit amplifying cells (called precursors in this study) were significantly different to those in neuroblasts. The precursor cells were dye-coupled, similarly as in the adult SVZ, and they displayed more negative values of V_{rest}, (~-54 mV), higher values of C_m (~24 pF) and lower input resistance (IR, ~870 MΩ) than those recorded in neuroblasts (V_{rest}~-33 mV; C_m~4 pF and IR~1.8 GΩ). There were also differences in the current densities of the tetraethyl ammonium chloride (TEA)-sensitive K^+ currents. Current injection did not evoke action potentials in precursors or in neuroblasts, and the precursors lacked functional voltage-dependent Ca^{2+} channels (Cesetti et al., 2009).

Similarly, neural stem cells in the adult SVZ (GFAP-positive cells) are dye-coupled (usually to 4-10 other cells) and display even more negative V_{rest} (~-85 mV) and lower IR (~300 pF). They show time- and voltage-independent currents and approximately 80% of these currents are Ba^{2+}-sensitive. The remaining outward current is then sensitive to TEA. They do not express functional α-amino-3-hydroxyl-5-methyl-4-isoxazole-propionate (AMPA) receptors, but they possess functional glutamate transporter-1 and GLAST (Liu et al., 2006).

Upon differentiation, NS/PCs give rise to neurons with variable functional characteristics. NSCs derived from the embryonic E16 brain were shown to give rise to neurons with immature characteristics within one week of *in vitro* cultivation. They displayed a depolarised V_{rest}, high input resistance and overshooting action potentials (APs) sensitive to tetrodotoxin (TTX). About 25% of these neurons displayed repetitive APs, however, with a decreasing spike amplitude and rise time. They displayed 4-AP-sensitive K^+ outward currents and responded to GABA application and to a certain extent also to AMPA (Pagani et al., 2006). Also, adult NSCs were shown to develop

into firing neurons *in vitro*. Stem cells isolated from the adult human brain were cultured as neurospheres, and differentiation was induced by the addition of foetal calf serum and mitogen removal. The cells developed mature APs after 16 days of differentiation. They also exhibited outwardly-rectifying currents sensitive to the application of 4-AP and TEA (Westerlund et al., 2003). NSCs from the adult rodent brain are also able to differentiate into neurons after long-term cultivation (68 passages). In this experiment, the concentration of bFGF was gradually decreased, while the concentration of BDNF was gradually increased during the course of differentiation. With this optimized protocol, the authors obtained neurons with negligible TTX-sensitive currents after 7 days of culture; however, after 22 days, these cells were able to fire overshooting APs. The cells responded to the application of GABA (57%), kainite (84%), AMPA (30%) and N-methyl-D-aspartate (NMDA, 2%, Goffredo et al., 2008). The ability to generate neurons with mature characteristics was shown to decline with age. Ahlenius et al. (2009) compared proliferation, differentiation and membrane properties of NSCs isolated from embryonic, adult and aged mouse brain. They showed that upon differentiation, NSCs derived from the aged brain produced a higher number of neurons which were unable to fire APs than NSCs derived from embryonic and adult brain (Ahlenius et al., 2009).

Functional neurons can also be obtained from ESCs. It was shown that human ESCs, initially transformed into NE cells, differentiate into neurons (Kozubenko et al., 2009). One week after the differentiation of ESC-derived NE cells, 50% of the neurons were able to generate an AP, and the proportion increased to 83% after 4 weeks of cultivation. The neurons displayed a 4-AP-sensitive K_A current and a TEA-sensitive K_{DR} current (Johnson et al., 2007). Another study explored the functional development of motoneurons in a co-culture system. The authors used motoneurons derived from ESCs, which were treated with RA and Shh-Ag and co-cultured with a monolayer of differentiated myotubes. Differentiated neurons displayed characteristics typical of motoneurons: GABA and glycine evoked an inward current in these cells and cell hyperpolarisation, while the application of glutamate elicited an inward current and cell depolarisation and also excitatory post-synaptic currents, which were abolished by the application of TTX. They displayed TEA- and 4-AP-sensitive K^+ currents and also Ca_v1-type Ca^{2+} channels. They were able to form functional synapses with the myotubes represented by post-synaptic potentials, which were elicited by the

application of glutamate and abolished by the application of TTX (Miles et al., 2004).

2.7 Exploring the membrane properties of transplanted cells

Since only cells that possess functional ion channels and receptors can effectively replace the lost elements in damaged neural tissue, data concerning the membrane properties of transplanted cells are essential for developing successful transplantation strategies. However, only a limited number of transplantation studies have investigated the membrane properties of single cells after their transplantation into the damaged brain.

It was shown that NS/PCs derived from ESCs are able to incorporate successfully into hippocampal slices prepared from 9-day-old rats. This system represents a transition between *in vitro* cell cultures and transplantation into living animals. Using electrophysiological methods, the authors found that the transplanted cells developed into neurons displaying TTX-sensitive Na^+ currents and also post-synaptic spontaneous currents mediated by GABA (recorded in the presence of 6-cyano-7-nitroquinoxaline-2,3-dione,CNQX; and (2R)-amino-5-phosphonovaleric acid, AP5, to block the AMPA/kainate- and NMDA-specific responses) and AMPA/kainate receptors (recorded in the presence of bicuculline to block the GABA-specific responses and AP5), while the contribution of NMDA receptors (responses recorded in the presence of bicuculline and CNQX) to these currents was negligible. These cells were also able to receive inputs from host neurons, thus being effectively integrated in the host tissue (Benninger et al., 2003). NSCs were also transplanted into neonatal rats, as shown in the work of Englund and colleagues (2002). They used the RN33B cell line labelled with GFP derived from the foetal rat brain to show that after transplantation into the neonatal cortex and hippocampus, these cells are able to differentiate into pyramidal neurons, and by means of retrograde labelling they showed that RN33B-derived neurons are able to establish axonal projections with the ventral thalamic nuclei (cortical neurons) and contralateral CA3 region (hippocampal neurons), which are the two major targets of intrinsic pyramidal cells. Electrophysiological analysis revealed that the transplanted cells are able to fire APs after depolarising current pulses and receive excitatory synaptic inputs from the host cells. The excitatory post-synaptic currents were blocked by AP5 and 2, 3-dihydroxy-6-nitro-7-sulfamoyl-

benzo[f]quinoxaline-2, 3-dione (NBXQ, a selective non-NMDA receptor antagonist). In the presence of NBQX and AP5, inhibitory post-synaptic currents sensitive to picrotoxin were recorded; showing that the cells also receive inhibitory GABA-ergic inputs (Englund et al., 2002). Buhnemann et al. (2006) investigated the membrane properties of ES cell-derived NS/PCs after transplantation into endothelin-induced MCAO. Four and seven weeks after transplantation, they detected TTX-sensitive Na^+ currents in neuronal cells and outward K^+ currents sensitive to the application of 10 mM TEA; their blockage disabled the generation of the APs in differentiated cells. They were also able to detect spontaneous excitatory post-synaptic currents (Buhnemann et al., 2006).

In summary, the major goal of neural stem cell research is to characterise different populations of NS/PCs derived from the embryonic as well as the adult brain and to test their potential to survive and differentiate after transplantation *in vivo*, using animal models of injury and neurodegenerative diseases. Another goal is to develop tools, such as genetic manipulations, for enhancing cell survival and promoting cell differentiation towards a desired fate. It is of paramount importance to explore the functional properties of *in vitro* differentiated or transplanted cells, since only cells that are fully equipped to integrate into the host tissue and to re-establish functional connections can help the host to regain lost cognitive or motor function.

3. THE AIMS

The aim of this work was to explore the differentiation of neural stem/progenitor cells (NS/PCs) *in vitro* and their survival and differentiation *in vivo*, after transplantation into the injured adult rat brain.

The major goals of this study are summarised below:

1. To investigate the differentiation potential and membrane properties of NS/PCs *in vitro*;
2. To explore the survival and differentiation of NS/PCs after transplantation into the non-injured (intact) adult rat brain and to compare the results with those obtained after transplantation into the site of a photochemical lesion, a model of ischemic brain injury;
3. To investigate and to compare the membrane properties of NS/PCs differentiated in the intact/injured brain;
4. To explore the effect of Shh and Wnt-7a on the proliferation and *in vitro* differentiation of neonatal NS/PCs;
5. To elucidate the effect of Shh and Wnt-7a on the production of neurons and their further development;
6. To clarify the effect of Shh and Wnt-7a on the membrane properties of differentiated cells.

The following NS/PCs were used:

A) Immortalised GFP/NE-4C NSC line cloned from primary neuroepithelial cell cultures derived from p53-deficient mouse embryos (at E9) and labelled with GFP;

B) Primary cell cultures of embryonic NS/PCs isolated from the dorsal telencephalons of transgenic D6-GFP mice. In these mice GFP is expressed under the control of D6, a promoter of the *mDach1* gene;

C) Neonatal NS/PCs that were genetically manipulated to produce Shh or Wnt-7a, morphogenes know to be involved in neurogenesis.

4. MATERIALS AND METHODS

All procedures involving the use of animals were approved by the local ethical review committee and were in agreement with European Communities Council Directive (86/609/EEC).

4.1 Cell cultures of NS/PCs and their *in vitro* differentiation

4.1.1 Culture of the GFP/NE-4C immortalised cell line

The NE-4C/GFP immortalised neural stem cell line was kindly provided by Prof. E. Madarasz (Institute of Experimental Medicine, Hungarian Academy of Sciences, Hungary). The neuroepithelial-clone 4 (NE-4C) cell line was cloned from primary neuroectodermal cultures established from the forebrain vesicles of transgenic mice lacking the p53 gene ($p53^{-/-}$), at E9 (Schlett and Madarasz, 1997) and labelled with GFP (GFP/NE-4C, Demeter et al., 2004). Cell aliquots were stored at -130°C in liquid nitrogen. Cells were defrosted and cultured as a monolayer on PLL- (Sigma Aldrich, St. Luis, MO, USA) coated Petri dishes, in a humidified atmosphere with 5% CO_2 at 37ºC in minimum essential medium (Sigma-Aldrich), supplemented with 10% foetal calf serum (Invitrogen, Carlsbad, CA, USA), 4 mM glutamine, 40 μg/ml gentamycine, and 400 μg/ml Geneticine (Sigma-Aldrich). Sub-confluent cultures were split by trypsinisation with 0.05% trypsin in phosphate-buffered saline (PBS) and replated at a cell density of 10^4 cells/cm^2. After one or two passages, neural differentiation was induced. GFP/NE-4C cells were trypsinised, plated at a density of 2.5 x 10^4 cells/cm^2 onto PLL-coated cover slips, and cultured in minimum essential medium supplemented with 5% foetal calf serum and retinoic acid (RA, 10^{-7}M). After 48 hours the medium was removed and replaced by medium devoid of RA or the cells were used for transplantation into the intact or lesioned rat cortex. Ten days after the induction of differentiation, the cells were analysed for the expression of K^+-and Na^+-channels using the patch-clamp technique; after fixation, the cells were analysed for the expression of glia and neuron specific markers.

4.1.2 Primary culture of D6-GFP embryonic NS/PCs

D6-GFP NS/PCs were harvested from the dorsal telencephalons of D6-GFP mouse embryos at E12. In these transgenic mice (kindly provided by Dr. Machon and Dr. Kozmik, Laboratory of Transcription Regulation, Institute of Molecular Genetics, v.v.i., Prague, Czech Republic), GFP is expressed under the D6 promoter/enhancer of the *mDach1* gene. The expression is first activated at E10.5 in the cortical anlage of the mouse telencephalon (Machon et al., 2002). At E12.5 D6-GFP activity expands throughout the dorsal telencephalon, where dividing cortical progenitors and early-born postmitotic neurons in the outer layer (the preplate) are labelled by GFP (Machon et al., 2002). The embryos were taken by caesarean section from deeply anaesthetised D6-GFP mice. The GFP-fluorescent tissue of the telencephalons was visualised and dissected using aseptic technique under a fluorescent microscope **(Fig. 7)**. The collected tissue was then mechanically dissociated, and the resulting single-cell suspension was cultured as floating neurospheres in a humidified atmosphere with 5% CO_2 at 37ºC. NS/PCs were maintained in Neurobasal-A medium supplemented with B27-supplement, penicillin/streptomycin (all from Invitrogen), 4 mM glutamine (Sigma-Aldrich, further referred to as basal medium), 10 ng/ml bFGF and 20 ng/ml EGF (both from R&D Systems, Minneapolis, MN, USA). After 1 week of cultivation the neurospheres were trypsinised (0.05% trypsin + 0.02% ethylenediaminetetraacetic acid, EDTA; Sigma-Aldrich) and used for *in vitro* experiments or for transplantation into the intact or lesioned cortex of adult rats.

For *in vitro* experiments cells were trypsinised and plated on PLL-coated Petri dishes or cover slips at a cell density of 6 x 10^4 cells/cm^2 and cultured in basal medium supplemented with 20 ng/ml bFGF. One week after the onset of differentiation, the cells were analysed for the expression of K^+- and Na^+-channels using the patch-clamp technique; cell lysates of differentiated cells were used for Western blot analysis. After fixation, the cells were analysed for the expression of glia and neuron specific markers using immunocytochemistry.

4.1.3 Cell culture of neonatal NS/PCs transduced with Shh and Wnt-7a

The neonatal NS/PCs were kindly provided by Prof. S. Krauss (Cellular and Genetic Therapy Research Group, Centre for Molecular Biology and Neuroscience and Institute

of Medical Microbiology, Rikshospitalet, Oslo, Norway). Briefly, the cells were prepared as follows: forebrains of neonatal C57BL/6 mice were dissected and mechanically dissociated in basal medium containing 10 ng/ml bFGF and 20 ng/ml EGF. Cells were cultured as neurospheres in a humidified atmosphere with 5% CO_2 at 37ºC and sub-cultured using trypsinisation (0.05%). Early passages (2-5) were then used for retroviral transduction (Rappa et al., 2004). Briefly, a 1923-bp NotI fragment of the human full-length catalytic subunit of g-glutamyl cysteine synthetase (g-GCS) heavy cDNA was obtained by subjecting pSF91GCS-MRP to the polymerase chain reaction.

Fig. 7 The telencephalic region of an E12 D6-GFP mouse embryo used for the isolation of NS/PCs

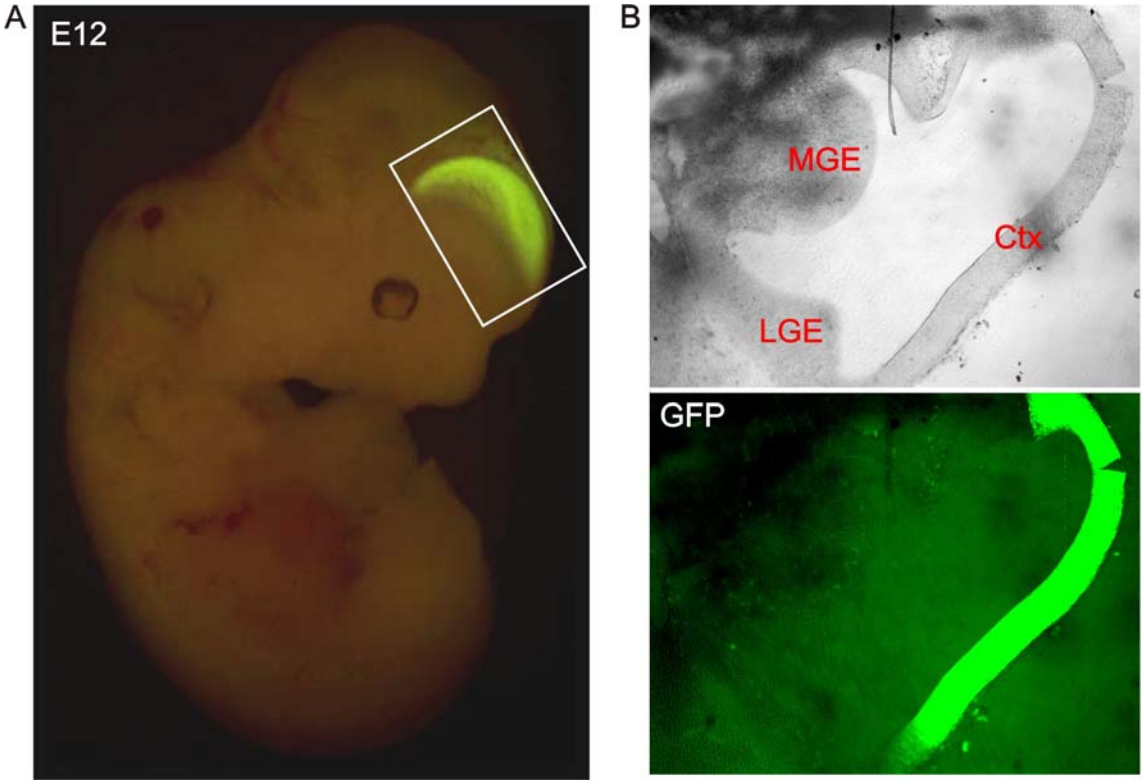

(A) GFP fluorescence in the telencephalon of an E12 D6-GFP mouse embryo. **(B)** Enlarged sagittal view of the telencephalic region imaged by a live digital camera (objective 5x) visualising the structure **(top)** and fluorescence **(bottom)**, showing clearly the area used for cell culture. Note that the fluorescence spans the entire wall of the dorsal telencephalon (future cortex), while the ganglionic eminences (future striatum) are completely devoid of the GFP signal. **LGE:** lateral ganglionic eminence; **MGE:** medial ganglionic eminence; **Ctx:** cortex.

The primer sequences were: 5′ATA-AGA-ATG-CGG-CCG-CCA-TGG-GGC-TGC-TGT-CCC-AG-3′ and 5′-ATA-GTT-TAG-CGG-CCG-CTA-GTT-GGA-TGA-GTC-AGT-TTT-AC-3′. The fidelity of the g-GCS sequence was confirmed by DNA

sequence analysis. pSF91-GCSh-I-EGFP-WPRE (pSF91-GCSh [heavy GCS]-EGFP) was cloned by introducing the 1923-bp g-GCSh cDNA fragment into the NotI site of pSF91-I-EGFP-WPRE, a derivative of pSF91 containing EGFP cDNA under the control of the poliovirus internal ribosome entry site (IRES, Rappa et al., 2004).

This subcloning strategy was used for the following rRV vectors: IRES (controls), shh (Shh/EGFP cells) and wnt-7a (Wnt-7a/EGFP cells). In the plasmid pSF91-GCSh-EGFP gene coding for gGCS was deleted by NotI and either self-ligated - IRES-gfp or an NotI fragment containing the appropriate gene was ligated (a 1909-bp fragment for mShh or a 1771-bp fragment for mWnt7a (Kunke et al., 2009). Cells over-expressing Shh or Wnt-7a were further termed Shh- and Wnt-7a-expressing cells; cells expressing only EGFP were termed controls and used as such **(Fig. 8)**. The cell aliquots were stored at -130 °C in liquid nitrogen.

Fig. 8 Viral transduction of neonatal NS/PCs and the subsequent Western blot analysis of the Shh and Wnt/ β-catenin pathway components

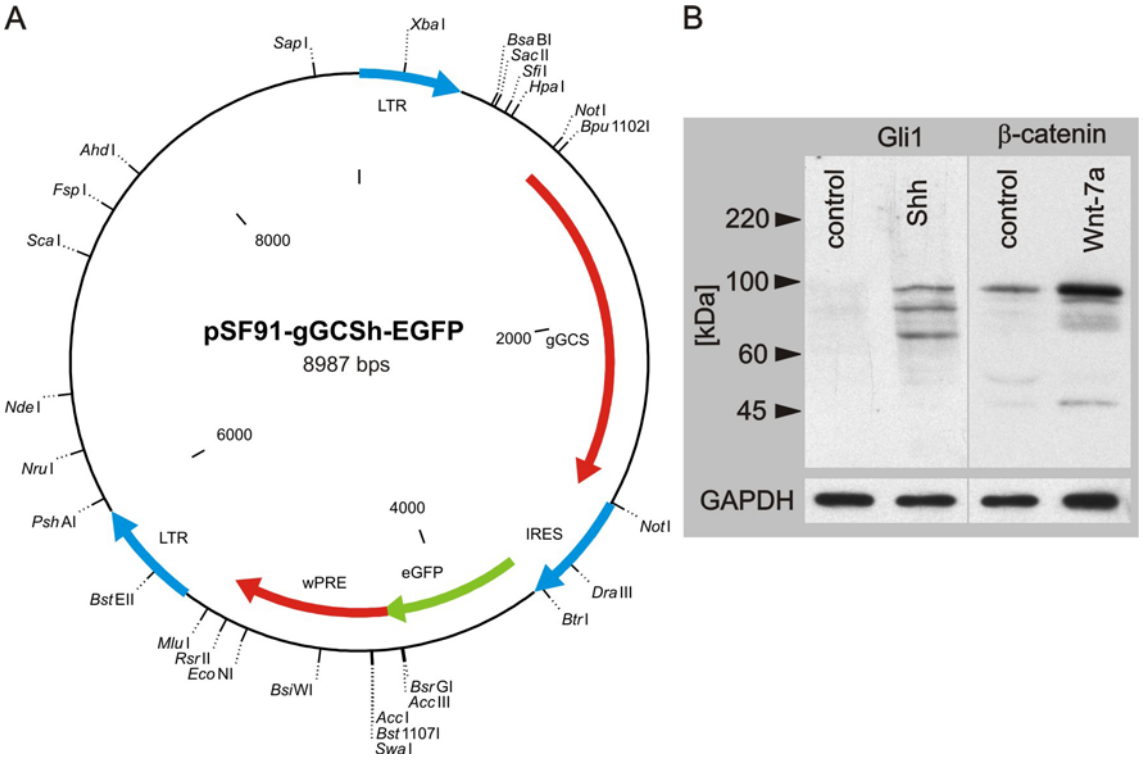

(A) A scheme of the retroviral vector used for the transduction of neonatal NS/PCs (provided by Dr. O. Kunke). **(B)** The activation of the Shh and Wnt/β-catenin signalling pathways was confirmed by Western blotting for the pathway components Gli1 and β-catenin. Note their increased expression when compared to control cells.

Control, Shh- and Wnt-7a-expressing cells were defrosted and cultured as floating neurospheres (4 x 10^4 cells/ml) in a humidified atmosphere with 5% CO_2 at 37ºC and maintained in basal medium supplemented with 10 ng/ml bFGF and 20 ng/ml EGF. The cells were sub-cultured once or twice a week by trypsinisation (0.05 trypsin + 0.02 EDTA) and then used for *in vitro* experiments.

For *in vitro* differentiation control, Shh- and Wnt-7a-expressing neurospheres were trypsinised and plated on PLL-coated Petri dishes or cover slips at a cell density of 6 x 10^4 cells/cm^2 and cultured in basal medium supplemented with 20 ng/ml bFGF and 10^{-6} M RA. After 24 hours, the medium was replaced by basal medium supplemented with 20 ng/ml bFGF only. Eight days after the onset of differentiation, the cells were analysed for the expression of K^+- and Na^+- channels using the patch-clamp technique; as well as for the expression of glia and neuron specific markers using immunocytochemical and Western blot analyses. Quantitative analysis of neuronal marker expression was performed and the number of proliferating cells was determined using anti-BrdU staining. The number of apoptotic cells was determined by using the TUNEL assay.

4.2 Photochemical lesion

A photochemical lesion, a model of thrombotic stroke leading to cerebral infarction, was chosen as a model of cortical injury suitable for transplantation studies (Comelli et al., 1993). Rose Bengal (Sigma-Aldrich), a potent photosensitizing dye, was injected intravenously into the femoral vein (8 mg/100 g) of 5-6-week-old Wistar male rats (150-200 g) anaesthetised with 2% isoflurane in air (Forane, Abbott Laboratories Ltd., Great Britain). The scalp was incised to expose the skull surface, and the area of the skull above the right somatosensory cortex (from bregma: caudally 2 mm and laterally 2.5 mm) was exposed to a condensed beam of cold light for 10 min. The skin overlying the cranium was then sutured. The area of the infarct extended to approximately 1.0-1.5 mm in diameter.

4.3 Cell transplantation

Cells diluted to their final concentration (1-2 x 10^5/μl) in culture medium were immediately used for transplantation into intact and lesioned cortex. The transplantation

was carried out 7 days after the induction of the photochemical lesion. Rats were anaesthetised with isoflurane and mounted in a stereotactic frame. Using aseptic technique, a small hole was drilled into the skull above the lesion or the intact cortex (from bregma - caudally 2 mm, laterally 2.5 mm) and 3 µl of a cell suspension were slowly injected over a 10-min period into the lesion (or the intact cortex) using a Hamilton syringe. For immunosuppression, methylprednisolone (Depo-Medrol, Pfizer, New York, NY, USA) was administered at a single dose of 2 mg once a week and cyclosporine (Sandimmun, Novartis, Basel, Switzerland) was injected intraperitoneally, daily at a dose of 10 mg/100 g body weight. One to four weeks after transplantation, brain slices were prepared and used for patch-clamp experiments *in situ*, or the brains were used for immunohistochemical analysis.

4.4 Preparation of acute brain slices

For patch-clamp recording the animals transplanted with D6/GFP NS/PCs were sacrificed one week and the animals transplanted with GFP/NE-4C cells were sacrificed 3-4 weeks after transplantation. The rats were anaesthetised with pentobarbital (100 mg/kg, Sigma-Aldrich), and transcardial perfusion was carried out using NMDG solution containing (in mM): N-methyl-D-glucamine (NMDG) 110.0, KCl 2.5, $NaHCO_3$ 24.5, Na_2HPO_4 1.25, $CaCl_2$ 0.5, $MgCl_2$ 7.0 and D-glucose 20.0. The pH was adjusted to 7.4 with HCl, and the osmolarity was 300 ± 5 mmol/kg. After perfusion the rat was decapitated, and the brain was quickly dissected and placed into artificial cerebrospinal fluid (ACF) at 6-8°C. The brain was hemisected and glued with tissue adhesive (3M Vetbond, World Precision Instruments, Sarasota, FL, USA) to a teflon plate. Transverse 200 µm thick slices were made using an automatic vibrating tissue slicer (Microm HM 650V, Thermo Fisher Scientific, Waldorf, Germany). The slices were kept at 22-25°C for up to 6 hours in ACF containing (in mM): NaCl 122.0, KCl 3.0, $CaCl_2$ 1.5, $MgCl_2$ 1.3, Na_2HPO_4 1.25, $NaHCO_3$ 28.0 and D-Glucose 10.0. Osmolarity was 300 ± 5 mmol/kg. The solution was continuously gassed with a mixture of 95% O_2 and 5% CO_2 to maintain a final pH of 7.4. The osmolarity of solutions was measured using a vapour pressure osmometer (Vapro 5520, Wescor Inc., Logan, UT, USA).

4.5 Patch-clamp recordings

Cell membrane currents were recorded with the patch-clamp technique in the whole-cell configuration (Hamill et al., 1981). Recording pipettes with a tip resistance of 6-8 MΩ were made from standard wall borosilicate capillaries with filament (0.86 ID, Sutter Instruments Company, Novato, CA, USA) using a Brown-Flaming micropipette puller (P-97, Sutter Instruments). Electrodes for recording *in vitro* or *in situ* were filled with a solution containing (in mM): KCl 130.0, $CaCl_2$ 0.5, $MgCl_2$ 2.0, ethylene glycol tetraacetic acid (EGTA) 5.0, 4-(2-hydroxyethyl)-1-piperazineethanesulfonic acid (HEPES) 10.0. The pH was adjusted with KOH to 7.2. To visualise the recorded cells within the GFP-positive cell population, the cells were filled with Lucifer Yellow (LY, Sigma-Aldrich) by dialyzing the cytoplasm with the patch pipette solution. The morphology of cells imaged by LY was used for subsequent immunocytochemical/immunohistochemical identification using a confocal microscope. The recordings were made either in brain slices or cultured cells attached to PLL-coated cover slips perfused with ACF at a temperature of 22-25°C. The brain slices or cultured cells were placed into a chamber mounted on the stage of a fluorescence microscope (Axioskop2 FS plus, Zeiss, Oberkochen, Germany). Slices were fixed using a U-shaped platinum wire with a grid of nylon threads. The cells were approached by the patch electrode using an INFRAPATCH system (Luigs & Neumann, Ratingen, Germany). The cells and the recording electrodes were imaged with a digital camera (Axiocam HRc, Zeiss, Oberkochen, Germany). Current signals were amplified with an EPC-9 or EPC-10 amplifiers (HEKA Elektronik, Lambrecht/Pfalz, Germany), lowpass-filtered at 3 kHz and sampled at 5 kHz by an interface connected to an AT-compatible computer system, which also served as a stimulus generator. Data acquisition, storage and analysis were performed with either TIDA software (in the study using the GFP/NE-4C cell line) or PATCHMASTER/FITMASTER softwares (HEKA Elektronik, Lambrecht/Pfalz, Germany). Recorded membrane potentials were corrected for the liquid junction potential using JPCALCW software (Barry, 1994).

4.6 Electrophysiological measurements and protocols

V_{rest} was measured by switching the EPC-9 or EPC-10 amplifiers to the current-clamp mode. C_m was determined either from the time constant (τ) of current transients elicited

by a 10-mV test pulse depolarising the cell membrane from -70 to -60 mV (with TIDA) or automatically during acquisition by PATCHMASTER. R_{series} was compensated automatically by the recording software (50% compensation with TIDA and 60% compensation with PATCHMASTER). *Input resistance* (IR) was determined from the currents elicited by a 10-mV test pulse depolarising the cell membrane from a holding potential of -70 mV to -60 mV, 40 ms after the onset of the depolarising pulse.

To study the time- and voltage-independent currents (also termed passive currents/conductance), a 50 mM K^+-solution was used, containing (in mM): NaCl 75.0, KCl 50.0, $NaHCO_3$ 28.0, Na_2HPO_4 1.25, D-glucose 10.0, $CaCl_2$ 1.5 and $MgCl_2$ 3.0, osmolarity 300 ± 5 mmol/kg. The solution was continuously gassed with a mixture of 95% O_2 and 5% CO_2 to maintain a final pH of 7.4. To block these currents, 10 mM $BaCl_2$ was used. To determine changes in *reversal potential* (V_{rev}) during the application of 50 mM K^+ and 10 mM $BaCl_2$ cell membrane was clamped to different potentials by rectangular voltage steps (250 ms duration) from a holding potential of -70 mV to potentials of -150, -130, -110, -90, -50, -30, -10, +10, and +30 mV.

Current patterns were obtained by clamping the cell membrane from a holding potential of -70 mV to values ranging from -160 mV to +20 mV, at intervals of 10 mV. Pulse duration was 50 ms. In order to isolate the K_{DR} current component; a voltage step from -70 to -60 mV was used to subtract time- and voltage-independent currents. To activate the K_{DR} current only, the cells were held at -50 mV, and the cell membrane was clamped to values ranging from -140 mV to +40 mV. The amplitude of the K_{DR} current was measured at +40 mV at the end of the pulse. To activate the K_A current component, a hyperpolarisation prepulse to -110 mV was applied. The K_A current component was then isolated by subtracting the current traces clamped at -110 mV from those clamped at -50 mV, and its amplitude was measured at the peak value. TEA (10 mM) and 4-AP (5 mM) were used to block the K_A and K_{DR} current components. The inwardly rectifying K^+ (K_{IR}) current component was isolated by subtracting the current traces measured in 1 mM CsCl-containing solution from those measured under control conditions. K_{IR} current amplitudes were measured at the end of the pulse. TTX (Alomone Labs, Jerusalem, Israel)- sensitive Na^+ currents were isolated by subtracting the current traces recorded in 1 μM TTX-containing solution from those recorded under control conditions. Na^+ current amplitudes were measured at the peak value.

Action potential (AP) generation was carried out by switching the EPC-10 amplifier to the current-clamp mode and injecting currents in 10 pA increments. The duration of each step was 500 ms. The AP amplitude was measured from the threshold to the peak of the voltage deflection. The AP half-width duration was measured as the duration of the AP at half of the maximum amplitude (Johnson et al., 2007). The AP amplitude and the AP half-width duration were analysed using a trace corresponding to ~50 pA current injection. To study the functional properties of glutamate or $GABA_A$ receptors, 100 μM glutamate and 100 μM GABA and bicuculline (100 μM) were used. All ion channel blockers/activators were diluted in ACF and applied to cells using a pressurized 8-channel-perfusion system (AutoMate Scientific, Inc. Berkeley, CA, USA). All chemicals were purchased from Sigma-Aldrich.

4.7 Preparation of cell cultures and tissue for immunocytochemistry and immunohistochemistry

Neurospheres and cell differentiated in vitro: neurospheres or cells attached to PLL-coated cover slips were fixed in 4% paraformaldehyde solution (in 0.2 M phosphate buffer - PB, pH 7.4) for 15 minutes, washed twice and kept in 0.01 M PBS at 4ºC for further processing.

Brain slices: The animals transplanted with D6/GFP NS/PCs were sacrificed one week and the animals transplanted with GFP/NE-4C cells were sacrificed 3-4 weeks after transplantation. The animals were anaesthetised (100 mg/kg sodium pentobarbital, Sigma-Aldrich) and perfused transcardially with 70 ml of 0.9% saline with heparin (2500 IU /100 ml, Zentiva, Prague, Czech Republic), followed by 70 ml of 4% paraformaldehyde solution. Brains were dissected and post-fixed in 4% paraformaldehyde solution at 4°C overnight, then placed into a gradient of sucrose ranging from 10-30% sucrose in 0.2 M PB and allowed to sink for cryoprotection. Coronal slices, 30 μm thick, were prepared using a microtome (HM 400, Thermo Fisher Scientific, Waldorf, Germany). For evaluation of the transplanted cells the entire grafts (in the intact or photochemically lesioned brains) were used for immunohistochemical analysis, corresponding to the coordinates (caudally from bregma) from 1.5 to 2.5 mm for grafts in a photochemical lesion and from 1.8 to 2.2 mm for cells transplanted into

the intact cortex. The same set of immunohistochemical stainings was used in serial sections in each transplanted animal.

4.8 Immunocytochemical/immunohistochemical protocols

The immunocytochemical/immunohistochemical stainings were performed at 4ºC in a blocking solution containing 5% Chemiblocker (Millipore) and 0.5% Triton X-100 (Sigma-Aldrich) in 0.01 M PBS. The procedure was as follows: brain slices or cultured cells attached to PLL-coated cover slips were incubated in the blocking solution for two hours, followed by overnight incubation with the primary antibody and subsequent incubation with the appropriate species/subclass-specific secondary antibody for two hours. To visualise the cell nuclei the brain slices or cultured cells were mounted using Vectashield mounting medium with 4',6-diamidino-2-phenylindole (DAPI, Vector Laboratories, Burlingame, CA, USA), and were then examined using an LSM 5 DUO spectral confocal microscope (Zeiss, Oberkochen, Germany) equipped with an Ar/HeNe laser. All primary and secondary antibodies, their dilutions and manufacturers are listed in **Table 1**.

Table 1 Primary and secondary antibodies used for immunohistochemistry and immunocytochemistry

antigen	dilution	isotype	manufacturer	secondary antibody
astrocytic/radial glia				
GFAP	1:800	mouse IgG	Sigma-Aldrich	Cy3-conjugated
S100β	1:200	mouse IgG	Sigma-Aldrich	GAM 594/660
nestin	1:1000	mouse IgG	Millipore	GAM 594/660
RC2	1:100	mouse IgM	Millipore	IgM Cy3
BLBP	1:500	rabbit IgG	Millipore	GAR 594/660
GFAP-δ	1:500	rabbit IgG	Millipore	GAR 594/660
neuronal				
MAP-2	1:800	mouse IgG	Millipore	GAM 594/660
βIII tubulin	1:800	mouse IgG	Sigma-Aldrich	GAM 594/660
DCX	1:500	goat IgG	Santa-Cruz	DAG 594/660
NeuN	1:100	mouse IgG	Millipore	GAM 594/660
NF68	1:200	mouse IgG	Sigma-Aldrich	GAM 594/660
oligodendrocytes/progenitors				
Olig2	1:1000	rabbit IgG	Abcam	GAR 594/660
Dlx2	1:500	rabbit IgG	Sigma	GAR 594/660
MOSP	1:1000	mouse IgM	Millipore	IgM Cy3
NG2	1:400	rabbit IgG	Millipore	GAR 594/660
RIP	1:2000	mouse IgG	Millipore	GAM 594/660
O1	1:000	mouse IgG	Millipore	GAM 594/660
O4	1:000	mouse IgG	Millipore	GAM 594/660
Sox10	1:1000	rabbit IgG	Abcam	GAM 594/660
APC	1:200	mouse IgG	Millipore	GAM 594
microglia				
CD11b	1:200	mouse IgG	Millipore	GAM 594
other				
GABA	1:1000	mouse IgG	Sigma-Aldrich	GAM 594
glutamate	1:1000	mouse IgG	Sigma-Aldrich	GAM 594
synaptophysin	1:1000	mouse IgG	Millipore	GAM 594
GAD 65/67	1:200	rabbit IgG	Calbiochem	GAR 594

GAR 594/660: goat anti-rabbit IgG conjugated with Alexa Fluor 594 or 660; **GAM 594/660:** goat anti-mouse IgG conjugated with Alexa Fluor 594 or 660; **DAG 594/660:** donkey anti-goat IgG conjugated with Alexa Fluor 594 or 660 (all from Invitrogen); **IgM Cy3:** goat anti-mouse IgM conjugated with Cy3 (Millipore); **GFAP:** glial fibrillary acidic protein; **GFAP Cy3:** mouse glial fibrillary acidic protein conjugated with Cy3; **RC2:** radial glia cell 2; **BLBP:** brain lipid binding protein; **MAP-2:** microtubule associated protein 2; **DCX:** doublecortin; **NF68:** neurofilaments 68 kDa; **Olig2:** Oligodendrocyte lineage transcription factor 2; **Dlx2:** Distal less 2; **MOSP:** myelin oligodendrocyte specific protein; **RIP:** receptor interacting protein; **Sox 10:** Sry-related high-mobility group box 10; **APC:** adenomatous poliposis coli;
GABA: γ-aminobutyric acid; **GAD65/67:** glutamate decarboxylase 65/67.

4.9 Immunocytochemical analyses

4.9.1 Quantitative immunocytochemistry of neuronal marker expression in the cultures of neonatal NS/PCs

The effect of morphogenes on neuronal marker expression is presented as the percentage of MAP-2-, βIII tubulin-, or DCX-positive cells or as the average area of cell-specific marker immunoreactivity per a single, positively stained cell. The analysis was performed in 3 independent cultures. Five zones (900 x 900 μm) were imaged in each cover slip using a fluorescent microscope (Axioskop, 2 plus, Zeiss) connected to a digital camera (Axiocam HRc, Zeiss).

To determine the proportion of cells that expressed specific neuronal markers, the total number of cells (based on DAPI staining) and the number of MAP-2-, βIII tubulin-, or DCX-positive cells were determined in each zone using GSA Image Analyzer v3.0.5 (GSA, Rostock, Germany). To obtain the average area corresponding to neuronal marker immunoreactivity in a single positively stained cell, the image processing and area calculation were performed using the CellAnalyst program, developed in the Laboratory of Neurobiology, Institute of Experimental Medicine (Prague, Czech Republic; Chvatal et al., 2007). The entire procedure consisted of three steps: filtering, setting a threshold and calculating the area. A constant threshold of 60% was used in each zone. The area corresponding to the neuronal marker immunoreactivity was determined using an edge-detecting algorithm and recalculated to real values in square micrometers **(Fig. 9)**.

4.9.2 TUNEL and BrdU incorporation assays

Apoptotic cells were detected by using an ApopTag Red *in situ* apoptosis Detection Kit (TUNEL, Millipore), 8 days after the onset of *in vitro* differentiation.

Proliferating cells were identified as BrdU-positive cells, 3 and 8 days after the onset of *in vitro* differentiation. 10 μM BrdU (Sigma-Aldrich) in culture medium was added two and seven days after the onset of differentiation. After 24 hours the cover slips with cells were fixed in 4% paraformaldehyde for 15 minutes at room temperature, treated with 2N HCl at 37°C for 30 minutes and washed subsequently with PBS. The cover slips were then treated with blocking solution for 2 hours and incubated overnight with rat anti-BrdU conjugated to FITC (Abcam, Cambridge, UK).

Fig. 9 The quantitative analysis of neuronal marker expression in transduced neonatal NS/PCs, 8 days after the onset of *in vitro* differentiation

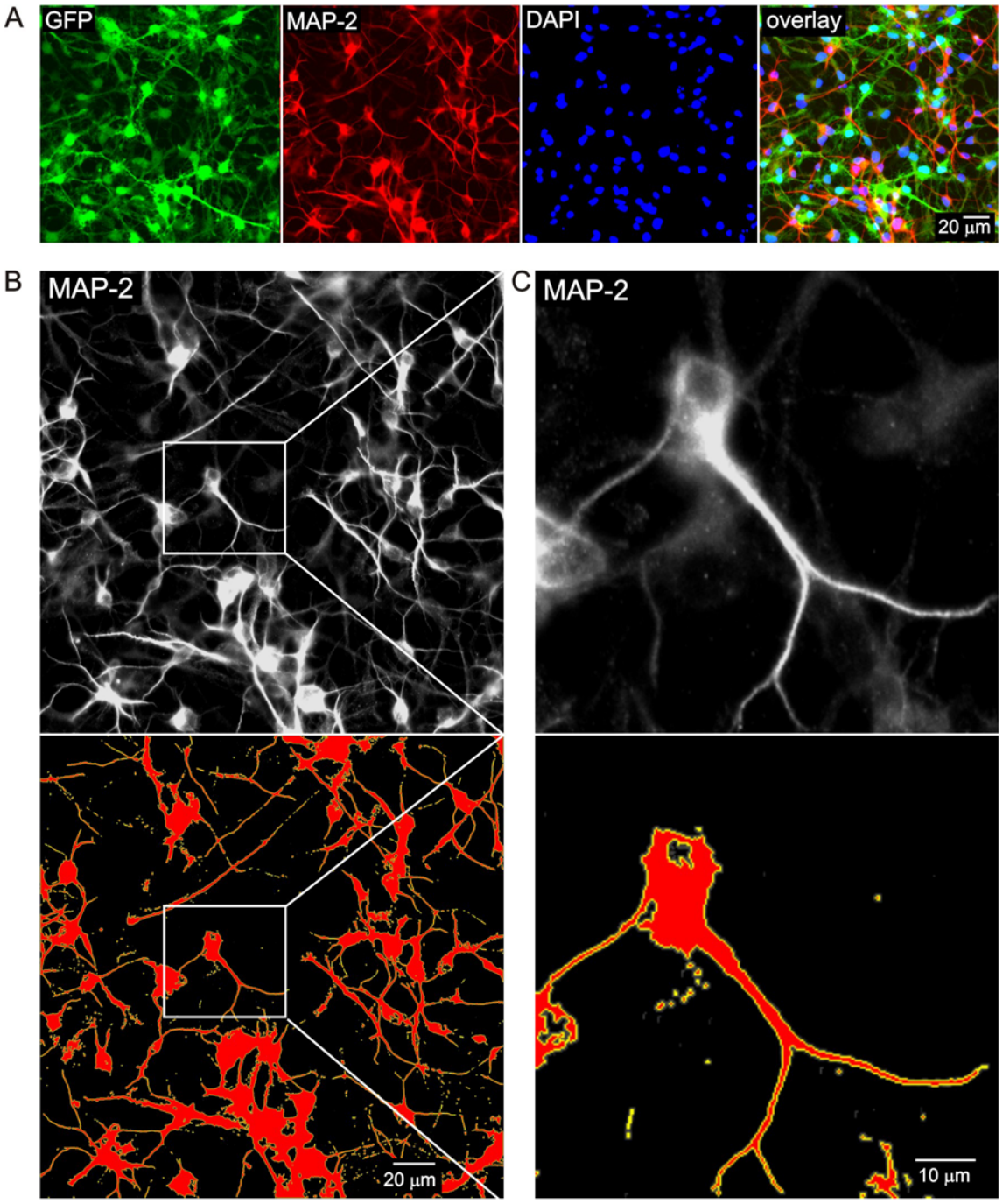

(A) Image of a Shh-expressing cell culture immunostained for MAP-2 and DAPI, 8 days after the onset of *in vitro* differentiation **(B)** MAP-2 immunoreactivity imaged using a fluorescent microscope before **(top)** and after **(bottom)** digital filtering and setting the threshold to 60%. The edge between the MAP-2 immunoreactivity (red) and the background (black) is indicated by the yellow colour. Pixels forming this edge were used for calculating the surface area, based on the pixel dimension (length). **(C)** Enlarged images shown in B.

The total number of cells was determined using DAPI staining. Quantification was performed in 3 independent cultures, and 3 zones (450 x 450 µm) were analysed in

each cover slip using a GSA Image Analyser (GSA, Rostock, Germany). The results were expressed as the proportion of TUNEL- or BrdU-positive cells.

4.9.3 Neurosphere size analysis

Cells were cultured under proliferating conditions for 1 week, and then non-dissociated neurospheres were fixed with 4% paraformaldehyde and visualised using DAPI staining. Under low magnification (10x, area 900 x 900 μm), ~50 spheres were scanned in 3 independent cell cultures and their size measured using LSM Image Browser Tools (Zeiss, Oberkochen, Germany). The size was expressed as the average diameter (A+B/2) measured along two orthogonal axes (A and B).

4.10 Western blot analysis

Cells from embryonic tissue were harvested by mechanical dissociation, neurospheres were harvested by trypsinisation and differentiated cells grown on PLL-coated Petri dishes were harvested mechanically using a cell scraper. The single-cell suspension was lysed in 1 M Tris buffer (pH=6.8) containing 10% glycerol and 1% sodium dodecyl sulfate (SDS) and sonicated twice for 5 seconds. The protein concentration was quantified using a Micro BCA^{TM} Protein Assay Kit (Thermo Fisher Scientific, Waldorf, Germany). Equal amounts of protein were loaded on a 6-12% SDS gel, correspondingly to the expected size of the analysed protein. After separation by electrophoresis, the proteins were transferred to nitrocellulose membranes, which were then saturated for 1 hour with PBS containing 0.05% Tween and 5% non-fat dry milk. The incubation with the primary antibodies diluted in PBS containing 0.05% Tween, 0.1% NaN_3 and 1% non-fat dry milk was performed at 4°C overnight, followed by goat-anti-rabbit IgG or goat anti-mouse IgG conjugated to horseradish peroxidase (Sigma-Aldrich). The bands were visualized by SuperSignal West Pico Chemiluminiscent Substrate (Thermo Fisher Scientific, Waldorf, Germany). Normalisation of the results was ensured by running parallel Western blots with anti-GAPDH (1:35 000, Sigma-Aldrich) antibody. All primary antibodies, their dilutions and manufacturers are listed in **Table 2**.

Table 2 Primary antibodies used for Western blot analysis

antigen	host	dilution	manufacturer
Gli1	rabbit	1:1000	Millipore
β-catenin	rabbit	1:200	Santa Cruz
GFAP	rabbit	1:600	Sigma-Aldrich
BLBP	rabbit	1:500	Millipore
Mash1	rabbit	1:500	Abcam
Olig2	rabbit	1:1000	Abcam
DCX	rabbit	1:200	Santa Cruz
MAP-2	mouse	1:5000	Millipore
βIII tubulin	mouse	1:600	Sigma-Aldrich
K_{IR} 4.1	rabbit	1:400	Alomone Labs
anti-$GABA_A$ R α1-6	rabbit	1:200	Santa Cruz
anti-GluR 1-4	rabbit	1:200	Santa Cruz

Gli1: Glioma-associated oncogene homolog 1; **GFAP:** glial fibrillary acidic protein; **BLBP:** brain lipid binding protein; **Mash1:** Mammalian achaete scute homolog 1; **Olig2:** Oligodendrocyte lineage transcription factor 2; **DCX:** doublecortin; **MAP-2:** microtubule associated protein 2; **Kir4.1:** inwardly rectifying K^+ channel 4.1; **$GABA_AR$:** γ-aminobutyric acid receptor subunit A; **GluR1-4:** glutamate recptor subunit 1-4.

3.11 Statistical analysis

The results are expressed as the mean ± S.E.M. Statistical analysis of the differences between groups was evaluated using either Student's t-test or ANOVA. Values of $p<0.05$ were considered significant, values of $p<0.01$ were considered very significant and values of $p<0.001$ were considered extremely significant.

5. RESULTS

5.1 Differentiation potential of immortalised neuroectodermal progenitor cells after transplantation into the site of a photochemical lesion

5.1.1 Membrane properties of GFP/NE-4C-derived neuronal cells 8 days after the induction of differentiation *in vitro*

Within two days after plating, non-differentiated GFP/NE-4C cells adhered to the PLL substrate and started to form extensions. From day 3 on, neuronal cells could be identified by the expression of βIII tubulin **(Fig. 10A)**. These cells developed on the top of apparently non-differentiated cells and showed a clear neuronal phenotype, with a small cell body (<20 μm) and long thin processes that made contact with other neuronal cells. Using the patch-clamp technique in the whole-cell configuration, we found that from day 6 on, these cells displayed outwardly rectifying K^+ currents: K_A and K_{DR} currents **(Fig. 10B)**, and moreover they expressed TTX-sensitive Na^+ currents **(Fig. 10C)**. The following membrane parameters are summarised in **Table 3**: V_{rest}, IR, C_m, and K_{DR}, K_A, and Na^+ current densities. In 16 GFP/βIII tubulin-positive cells (out of 35), the application of 100 μM GABA elicited a bicuculline-sensitive inward current **(Fig. 11)**, the average current density of GABA responses was 22.9 ± 3.0 pA/pF (n=16). No response to 100 μM glutamate was observed. Besides GFP/βIII tubulin-positive cells, we also found GFP-positive cells displaying passive, symmetrical non-decaying as well as decaying currents, as shown by (Jelitai et al., 2007), however, we were not able to identify them either as astrocytes or oligodendrocytes based on GFAP- or MOSP-positive staining.

These data demonstrate that 6 to 10 days after the induction of differentiation *in vitro*, GFP/NE-4C derived neuronal cells display K_A, K_{DR}, and Na^+ currents and that ~50% of these cells express functional $GABA_A$ receptors. No astrocytes or oligodendrocytes were identified.

Fig. 10 GFP/NE-4C cells express a neuronal current pattern 8 days after the induction of differentiation by RA *in vitro*

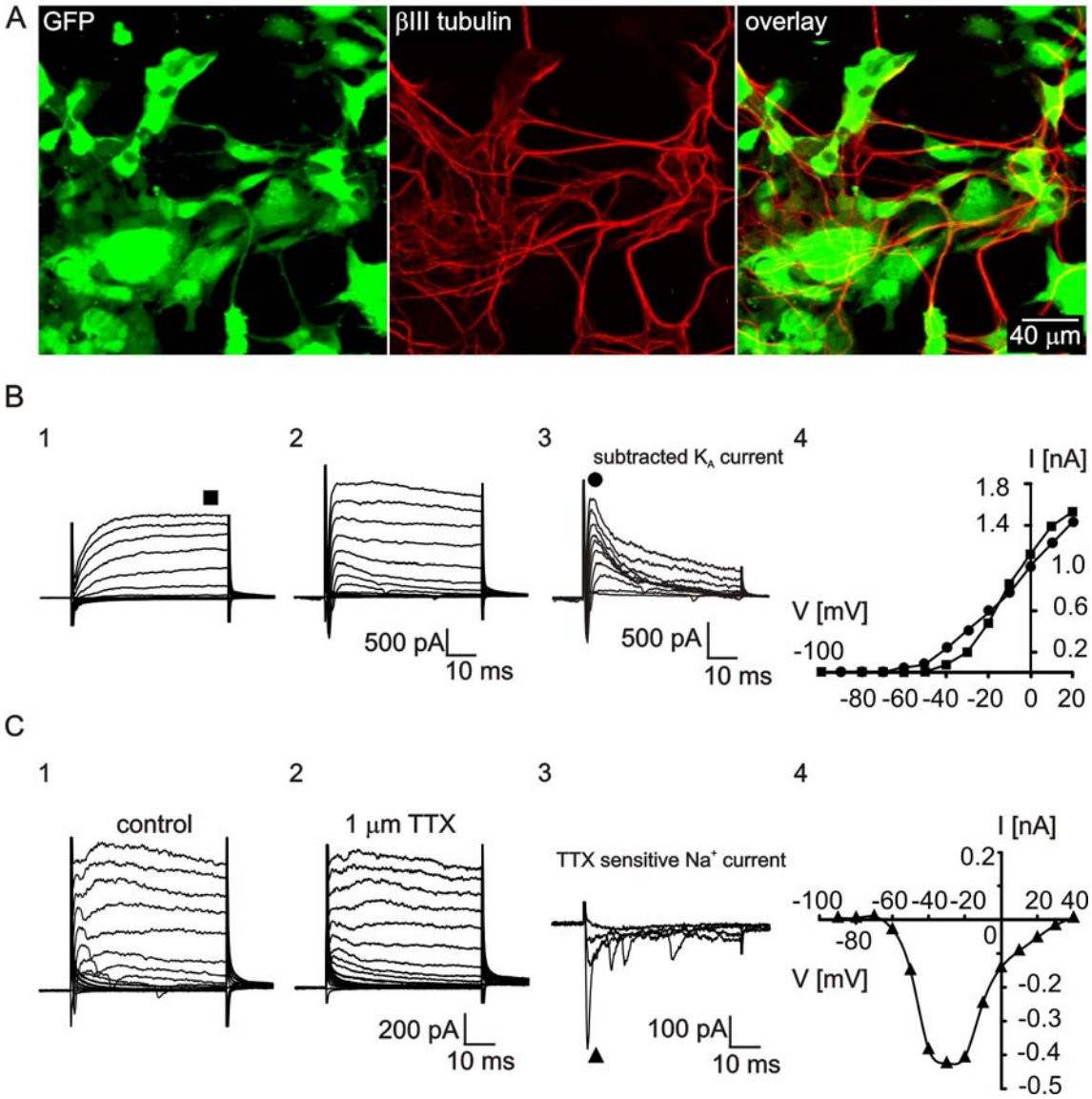

(A) Images of GFP-labelled cells **(left)**, after 8 days of differentiation *in vitro*, immunostained for βIII tubulin **(middle)**. Yellow colour indicates similar patterns in the overlay **(right)**. **(B)** Typical current profiles obtained by hyper- and depolarising the cell membrane from a holding potential of -50 mV to potentials ranging from -140 to +40 mV **(B1)** and those obtained by hyper- and depolarising the cell membrane from a holding potential of -50 mV to potentials ranging from -140 to +40 mV, after a hyperpolarising prepulse to -110 mV **(B2)**. The fast activating K_A current shown in **(B3)** was isolated by subtracting the current traces in B1 from those shown in B2. The resulting current/voltage (I/V) relationships for the K_{DR} current (obtained by passive current subtraction, filled squares) and K_A current (filled circles) are shown in **(B4)**. **(C)** The membrane current pattern of GFP/βIII tubulin-positive cells prior to (control, **C1)** and after the application of 1 µM TTX **(C2)**. The TTX-sensitive current was obtained by subtracting the currents after TTX application from control currents **(C3)**. The resulting I/V relationship for the TTX-sensitive current is shown in **(C4**, filled triangles).

Table 3 Membrane properties of GFP/βIII tubulin-positive cells 8 days after the induction of differentiation *in vitro* and 4 weeks after transplantation into the intact cortex or into the site of a photochemical lesion (PCL)

	in vitro	intact cortex	PCL
V_{rest} (mV)	-40.6 ± 1.6	-51.6 ± 5.6*	-61.6 ± 4.0***
C_m (pF)	55.7 ± 3.9	22.5 ± 5.2**	35.1 ± 6.9*
IR (MΩ)	812.1 ± 47.2	435.4 ± 65.7**	460.6 ± 38.1***
K_{DR}/C_m (pA/pF)	12.7 ± 3.7	39.6 ± 9.6*	35.8 ± 7.2**
K_A/C_m (pA/pF)	12.8 ± 3.5	46.5 ± 13.2*	46.2 ± 10.6***
Na^+/C_m (pA/pF)	17.2 ± 2.9	53.9 ± 18.5***	50.9 ± 10.1***
n	5	8	18

V_{rest}: resting membrane potential; **C_m:** membrane capacitance; **IR:** input resistance; **K_{DR}/C_m, K_A/C_m, Na^+/C_m:** K_{DR}, K_A, and Na^+ current densities; **n:** number of cells. Asterisks indicate significant differences between neuronal cells differentiated *in vitro* and those differentiated in the intact cortex or in PCL. Note that there were no significant differences between GFP/βIII tubulin-positive cells differentiated in the intact and lesioned cortex. * $p < 0.05$; ** $p < 0.01$; *** $p < 0.001$.

Fig. 11 *In vitro* derived GFP/NE-4C neuronal cells respond to the application of 100 μM GABA

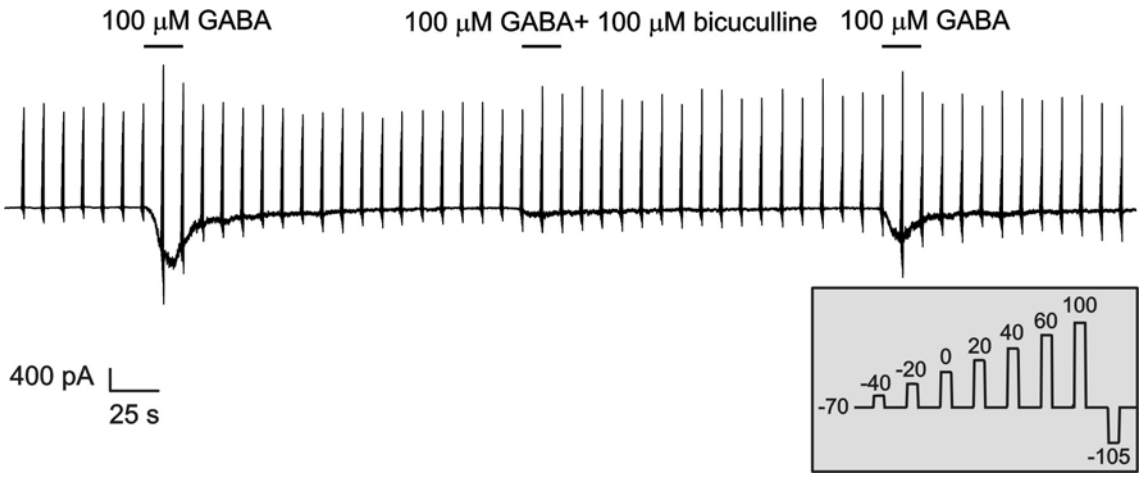

A typical inward current evoked by the application of 100 μM GABA was sensitive to 100 μM bicuculline and re-appeared after washout. The currents shown were obtained by clamping the cell membrane potential to different values, by rectangular voltage steps, from a holding potential of -70 mV to potentials ranging from -105 mV to +100 mV (see the inset).

5.1.2 Transplantation of GFP/NE-4C cells into the non-lesioned cortex

The survival and differentiation of GFP/NE-4C cells were first studied in cortical tissue that was not subjected to photochemical lesioning (further termed intact cortex). Immunohistochemical analysis of the transplants was performed in a total of 7 rats. The animals were sacrificed 4 weeks after transplantation. A large number of GFP-positive cells survived, and they filled the entire track produced by the injection **(Fig. 12A)**. The injection site was surrounded by endogenous reactive astrocytes and filled partly with GFP/GFAP- and GFP/S100β-positive cells **(Fig. 12A, B)**, which displayed morphology typical of reactive astrocytes **(Fig. 12B).** GFP/NE-4C-derived neuronal cells could be identified by NeuN-, βIII tubulin-, MAP-2- and NF68-positive staining **(Fig. 13)**, their morphology was characterised by a round cell body with a diameter of ~15-20 μm and one or two short processes **(Fig. 13)**.

Fig. 12 GFP/NE-4C immortalised cells give rise to astrocytes and oligodendrocytes, 4 weeks after transplantation into the intact cortex

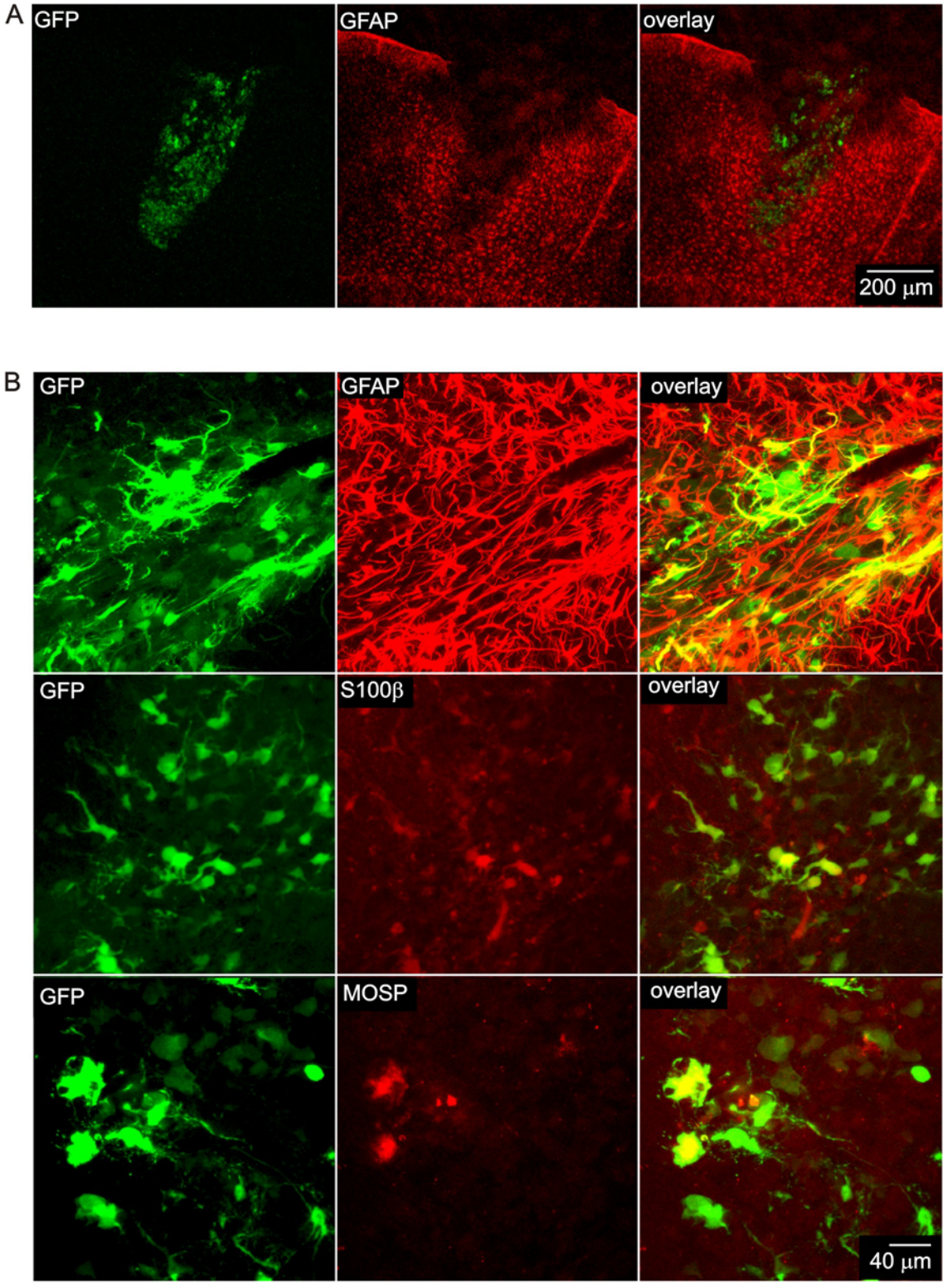

(A) Coronal section of an adult rat cortex showing the injection site filled with GFP/NE-4C cells immunostained for GFAP, 4 weeks after transplantation. **(B)** Higher magnification images of GFP/NE-4C cells showing their immunoreactivity for the astrocyte markers GFAP **(top)** and S100β **(middle)**, and the oligodendrocyte marker MOSP **(bottom)**.

Fig. 13 Four weeks after transplantation into the intact cortex GFP/NE-4C immortalised cells express a range of neuronal markers

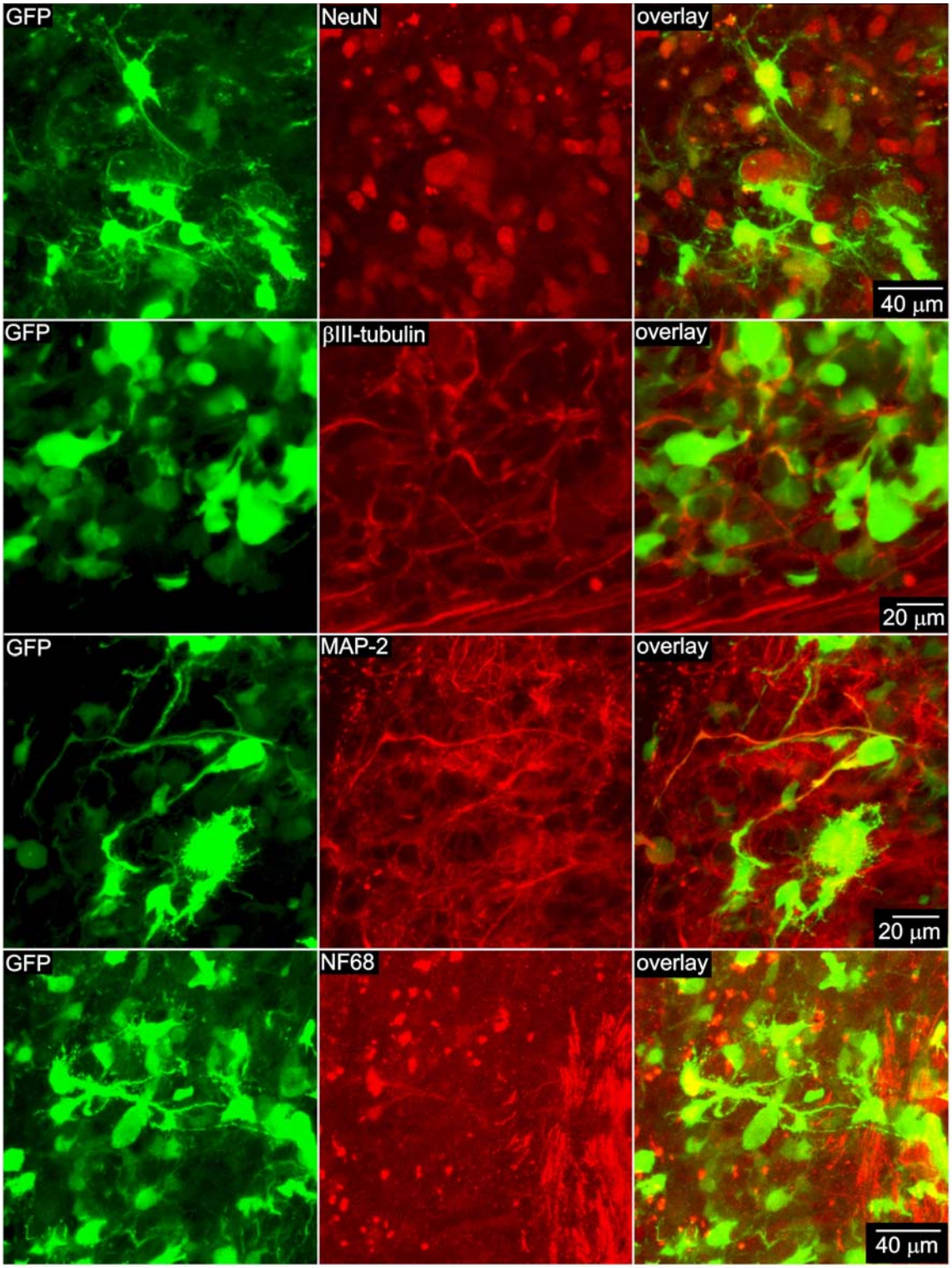

Images showing NE-4C/GFP cells immunostained for the neuronal markers NeuN, βIII tubulin, MAP-2 and NF68. Yellow colour indicates double-stained cells.

The electrophysiological analysis showed that GFP/GFAP-positive cells displayed time- and voltage-independent K^+ currents, and additionally they displayed either K_A and K_{DR} currents (further termed A1 astrocytes, n= 7) or K_{DR} currents only (A2 astrocytes, n =6, **Fig. 14A**). Their membrane properties are summarised in **Table 4**.

Table 4 Membrane properties of GFP/GFAP-positive cells 4 weeks after transplantation into the intact cortex or into the site of a photochemical lesion (PCL)

	A1 astrocytes		A2 astrocytes	
	intact cortex	PCL	intact cortex	PCL
V_{rest} [mV]	-72.4 ± 5.5	-70.3 ± 3.9	-62.8 ± 5.6	-73.5 ± 3.5
C_m [pF]	38.9 ± 4.3	57.8 ± 6.3*	59.7 ± 13.4	71.6 ± 10.8
IR [MΩ]	239.3 ± 43.7	156.8 ± 19.7	146.2 ± 24.0	130.8 ± 18.4
K_{DR}/C_m [pA/pF]	12.9 ± 2.9	2.8 ± 0.6**	3.8 ± 0.6	5.2 ± 3.2
K_A/C_m [pA/pF]	19.3 ± 6.4	3.9 ± 0.4**	---	---
K_{IR}/C_m [pA/pF]	---	0.9 ± 0.2*	---	---
n	7	12	6	11

V_{rest}: resting membrane potential; **C_m:** membrane capacitance; **IR:** input resistance; **K_{DR}/C_m, K_A/C_m:** K_{DR} and K_A current densities; **n:** number of cells. A1 astrocytes displayed large time- and voltage-independent K^+ currents, but additionally they displayed K_A, K_{DR}, and K_{IR} currents that became most apparent following passive-current subtraction; A2 astrocytes displayed K_{DR} currents in addition to time- and voltage-independent K^+ currents. Asterisks indicate significant differences between GFP/GFAP-positive cells in control and those derived in lesioned cortex. *p < 0.05, **p < 0.01, ***p < 0.001.

GFP-positive cells expressing neuronal markers displayed a typical neuronal current pattern: K_A and K_{DR} currents **(Table 3)** and TTX-sensitive Na^+ currents induced by depolarising pulse or by 20 mM K^+ application **(Fig. 14B, C)**. A small number of GFP/ NE-4C cells differentiated into oligodendrocytes based on MOSP-positive staining **(Fig. 12B).** However, no GFP/O1- or GFP/RIP-positive cells were identified. Additionally, no GFP-positive cells were identified post-recording as oligodendrocytes.

In conclusion, our data show that 4 weeks after transplantation into the intact rat cortex GFP/NE-4C immortalised cells survive and differentiate into neuronal cells, two distinct groups of astrocytes and a limited number of oligodendrocytes.

Fig. 14 Membrane properties of GFP/NE-4C cells, 4 weeks after transplantation into the intact rat cortex

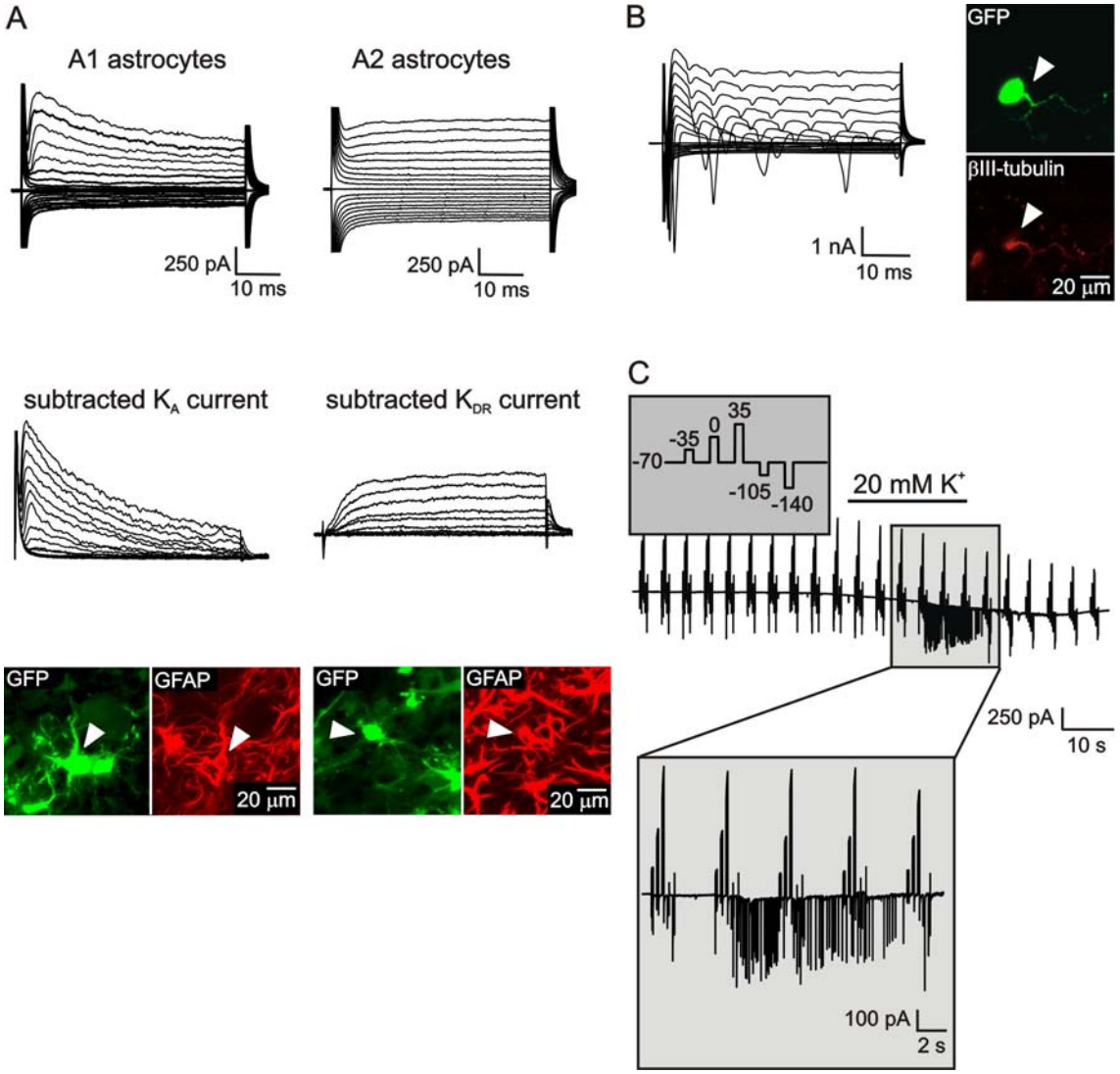

(A) The membrane current patterns of GFP/GFAP-positive A1 and A2 astrocytes obtained by hyper- and depolarising the cell membrane from a holding potential of -70 mV to potentials ranging from -160 to +20 mV **(top)**; the K_A current was isolated by subtracting the current traces obtained by hyper- and depolarising the cell membrane from a holding potential of -50 mV to potentials ranging from -140 to +40 mV from those obtained by hyper- and depolarising the cell membrane from a holding potential of -50 mV to potentials ranging from -140 to +40 mV, after a hyperpolarising prepulse to -110 mV; the K_{DR} current was isolated by passive-current subtraction **(middle)**; the morphology and immunohistochemical identification of the recorded A1 and A2 astrocytes (indicated by arrowheads) showing positive staining for GFAP **(bottom)**. **(B)** The current pattern **(left)** of a βIII tubulin/GFP-positive cell obtained as described in (A) and the morphology and immunohistochemical identification of the recorded cell (indicated by arrowheads) showing positive staining for βIII tubulin **(right). (C)** Typical current pattern evoked in a GFP/βIII tubulin-positive cell by the application of 20 mM K^+ at a holding potential of -70 mV. The membrane currents were obtained by clamping the cell membrane potential to different values, by rectangular voltage steps, from the holding potential of -70 mV to potentials rating from -140 mV to +35 mV (see the inset).

5.1.3 Fate of GFP/NE-4C cells after transplantation into the site of a photochemical lesion

The development of a photochemical lesion without subsequent cell transplantation over the same time course as transplanted photochemical lesions was studied in the cortex of 4 rats (controls). We found that there is no significant endogenous neuro- or gliogenesis in the cortex that could replace damaged cells, 4 to 5 weeks after the lesion induction **(Fig. 15)**. The fate of GFP/NE-4C cells transplanted into the site of a photochemical lesion was studied in 11 rats, using immunohistochemical and electrophysiological analyses. These animals were subjected to a photochemical lesion, and 1 week after they were transplanted with RA induced GFP/NE-4C cells. Subsequently, they were sacrificed 3 to 4 weeks after transplantation, and the results were compared with those obtained from grafts into the intact cortex and from control animals.

Fig. 15 Immunohistochemical analysis of a photochemical lesion, 4 weeks after its induction

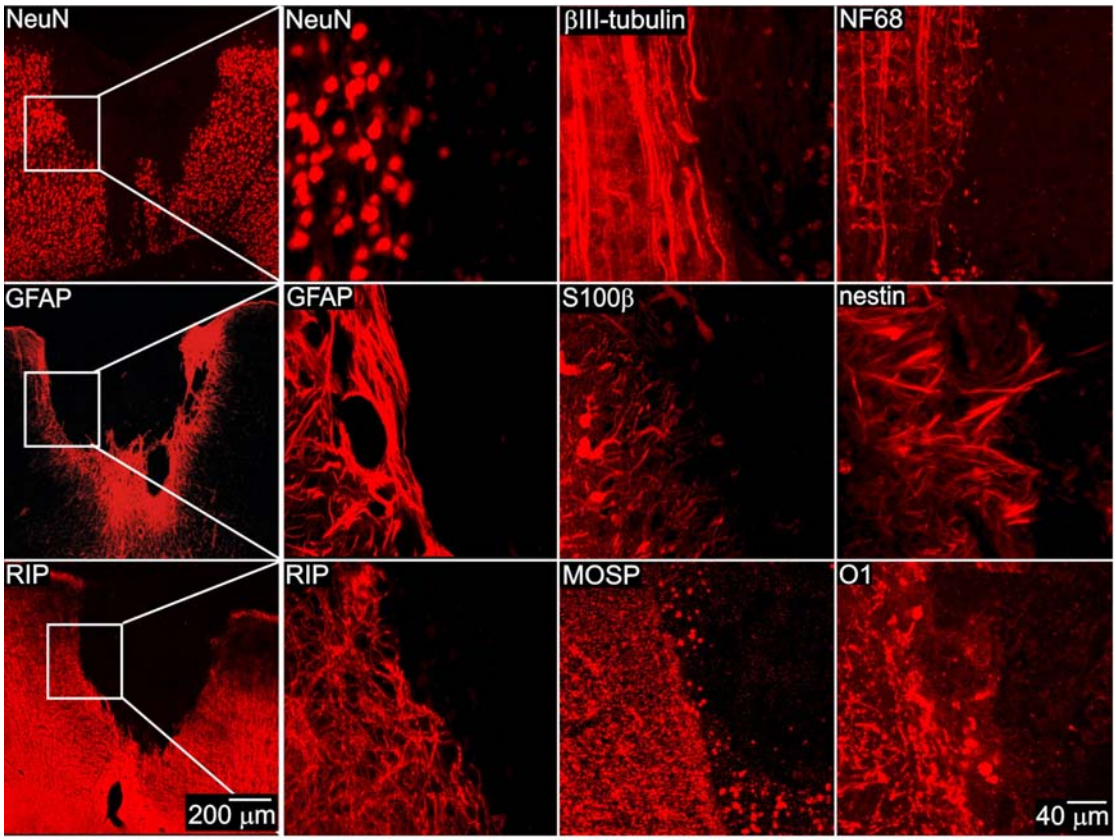

Coronal sections showing an overview of a non-transplanted photochemical lesion **(left column)** and higher magnification images **(right)** showing in detail the interface between normal and lesioned cortex, 4 weeks after lesion induction, immunostained for neuronal **(top)**, astrocyte **(middle)** and oligodendrocyte **(bottom)** markers.

Neuronal cells

In control rats, close to the photochemical lesion the cortex showed typical staining for NeuN, βIII tubulin and NF68. At the site of the photochemical lesion, there was a cavity partially filled with necrotic tissue, and no positive staining for NeuN, βIII tubulin, or NF68 was observed inside the photochemical lesion **(Fig. 15)**. Four weeks after cell transplantation, a large number of GFP-positive cells survived, and they filled the entire photochemical lesion **(Fig. 16A)**. No migration of GFP-positive cells outside of the photochemical lesion was observed. GFP-positive cells were identified as neuronal according to their positive staining for NeuN, βIII tubulin, or NF68 **(Fig. 16B)**. These cells were characterised by a round cell body with a diameter of ~15-20 μm and by one or two, occasionally more, short processes. Surprisingly, there was a larger number of NeuN-positive cells inside of the lesion compared to the number of GFP-positive cells **(Fig. 16B)**. Patch-clamp recording revealed that GFP/βIII tubulin- or GFP/NF68-positive cells displayed a typical neuronal current pattern represented by the expression of K_{DR} and K_A currents, and TTX-sensitive Na^+ currents induced by depolarising pulse or by the application of 20 mM K^+ **(Fig. 17)**. The average V_{rest} and IR were -61.6 ± 4.0 mV and 460.6 ± 38.1 MΩ (n =18), respectively, and their values were, together with values of K_{DR} K_A and Na^+ current densities, comparable to those recorded in neuronal cell in the intact cortex **(see Table 3)**. To show that NE-4C-derived neuronal cells start to form synaptic connections, we used an antibody against synaptophysin **(Fig. 18)**. No synaptophysin-positive staining was observed inside of the photochemical lesions of control rats **(Fig. 18A)**. However, the lesions in rats transplanted with GFP/NE-4C cells showed synaptophysin-positive staining in the areas that were occupied by transplanted cells **(Fig. 18B)**.

Fig. 16 Four weeks after transplantation into the site of a photochemical lesion (PCL), GFP/NE-4C immortalised cells express a range of neuronal markers

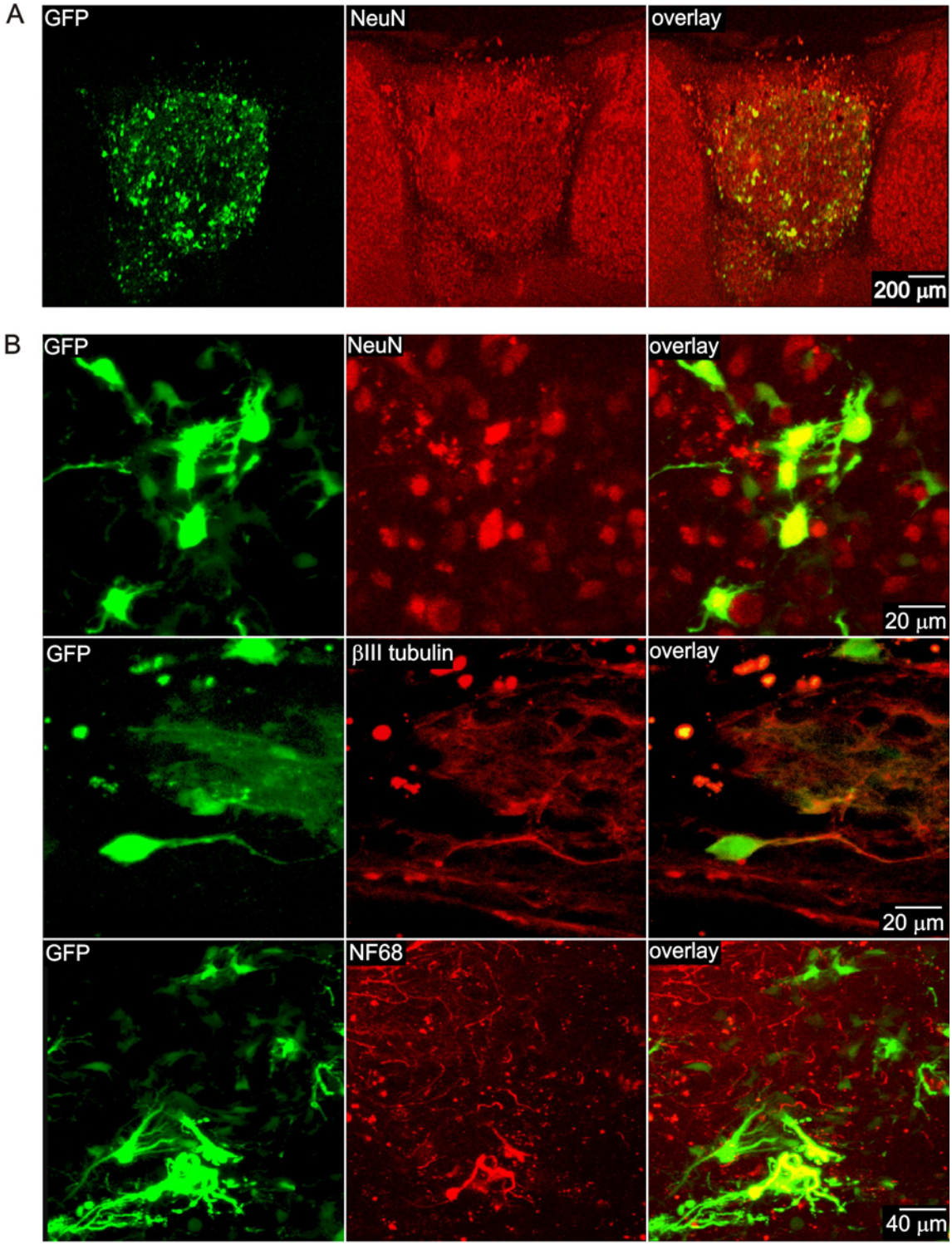

(A) Coronal section of adult rat cortex showing a PCL filled with transplanted GFP/NE-4C cells immunostained for NeuN. **(B)** Higher magnification images of the interior of the lesion showing details of GFP/NE-4C cells immunostained for NeuN **(top)**, βIII tubulin **(middle)**, and NF68 **(bottom)** inside the lesion. Yellow colour indicates double stained cells.

Fig. 17 GFP/βIII tubulin- and NF68-positive cells express a neuronal current pattern, 4 weeks after transplantation into the site of a photochemical lesion

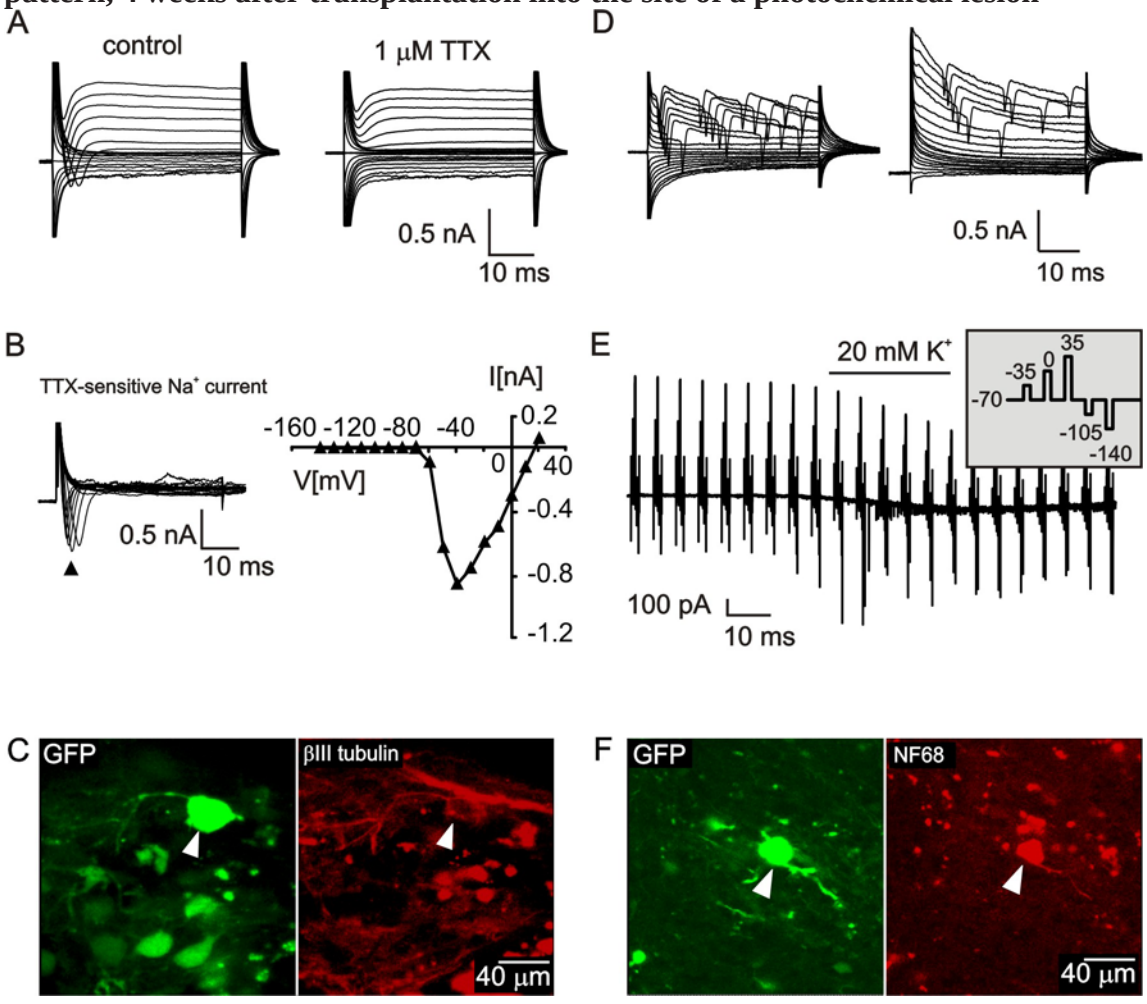

A typical membrane current pattern of a GFP/βIII tubulin-positive cell prior to **(left)** and after **(right)** the application of 1 µM TTX, obtained by hyper- and depolarising the cell membrane from a holding potential of -70 mV to potentials ranging from -160 mV to +20 mV. **(B)** The TTX-sensitive current obtained by subtracting the currents recorded after TTX application from those recorded in ACF (control, **left)**, and the resulting I/V relationship for the TTX-sensitive Na^+ current **(right)**. **(C)** The morphology **(left)** and immunohistochemical identification **(right)** of a recorded GFP/NE-4C cell (indicated by arrowhead) showing positive staining for βIII tubulin. **(D)** The membrane current pattern of a GFP/NF68-positive cell **(left)** was obtained as described in (A), and the current traces in **(D, right)** show the activation of a K_A current in response to a hyperpolarising prepulse to -110 mV. **(E)** Currents evoked by the application of 20 mM K^+ at a holding potential of -70 mV. The membrane currents were obtained by clamping the cell membrane potential to different values, by rectangular voltage steps, from the holding potential to potentials ranging from -140 to +35 mV (see the inset). **(F)** The morphology **(left)** and immunohistochemical identification **(right)** of a recorded GFP/NE-4C cell (indicated by arrowhead) showing positive staining for NF68.

Fig. 18 Synaptophysin is expressed inside a photochemical lesion 4 weeks after the transplantation of GFP/NE-4C cells

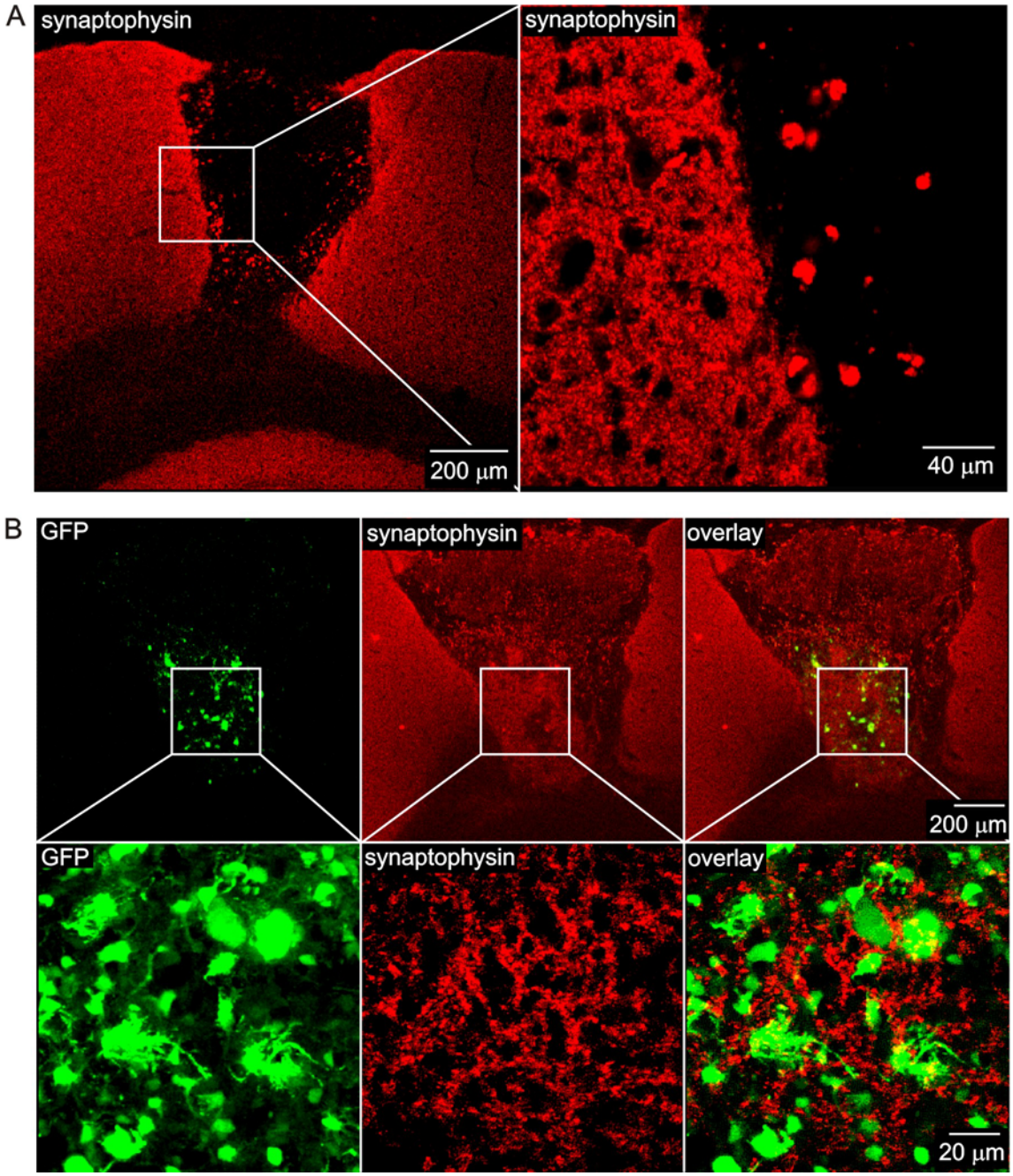

(A) Coronal sections of adult rat cortex showing an overview of a non-transplanted photochemical lesion with the inner space devoid of synaptophysin **(left)** and a detail showing the interface between the normal and lesioned tissue **(right)**. **(B)** Coronal sections of adult rat cortex showing an overview of a photochemical lesion transplanted with GFP/NE-4C cells, immunostained for synaptophysin 4 weeks after transplantation **(top)** and higher magnification images showing in detail that synaptophysin expression co-localises with the GFP signal of transplanted cells **(bottom)**.

Astrocytes

In controls as well as in animals grafted with NE-4C cells, immunohistochemical analysis of the photochemical lesions showed increased GFAP, S100β, and nestin staining in the vicinity of the lesion, a typical feature of astrogliosis **(Fig. 15 and 19A)**. No GFAP-, S100β-, or nestin-positive cells were found inside the lesion of control rats **(Fig. 15)**, while in grafted animals GFP cells that were GFAP- or S100β- or nestin-positive were identified inside the lesion **(Fig. 19B)**. GFP-positive astrocytes showed the morphology of either reactive or normal astrocytes. Patch-clamp analysis revealed two electrophysiologically different types of GFP/GFAP-positive cells and their membrane properties were comparable with those recorded after transplantation into the intact tissue **(see Table 4)**. A1 astrocytes (12 cells out of 23) displayed large time- and voltage-independent K^{+} currents, together with K_A and K_{DR} currents **(Fig. 20A, B, D)**. In contrast to A1 astrocytes recorded in the intact cortex, they also displayed K_{IR} currents that became most apparent following passive-current subtraction **(Table 4**). A2 astrocytes displayed K_{DR} currents in addition to time- and voltage-independent K^{+} currents (11 cells out of 23 **Fig. 20C, D**), similarly to A2 astrocytes recorded in the intact cortex. No voltage-dependent Na^{+}currents were detected in these cells. Despite the fact that two electrophysiologically distinct types of astrocytes were found, their passive membrane properties were not significantly different **(Table 4)**.

Fig. 19 The GFP/NE-4C cell line gives rise to astrocytes 4 weeks after transplantation into the site of a photochemical lesion

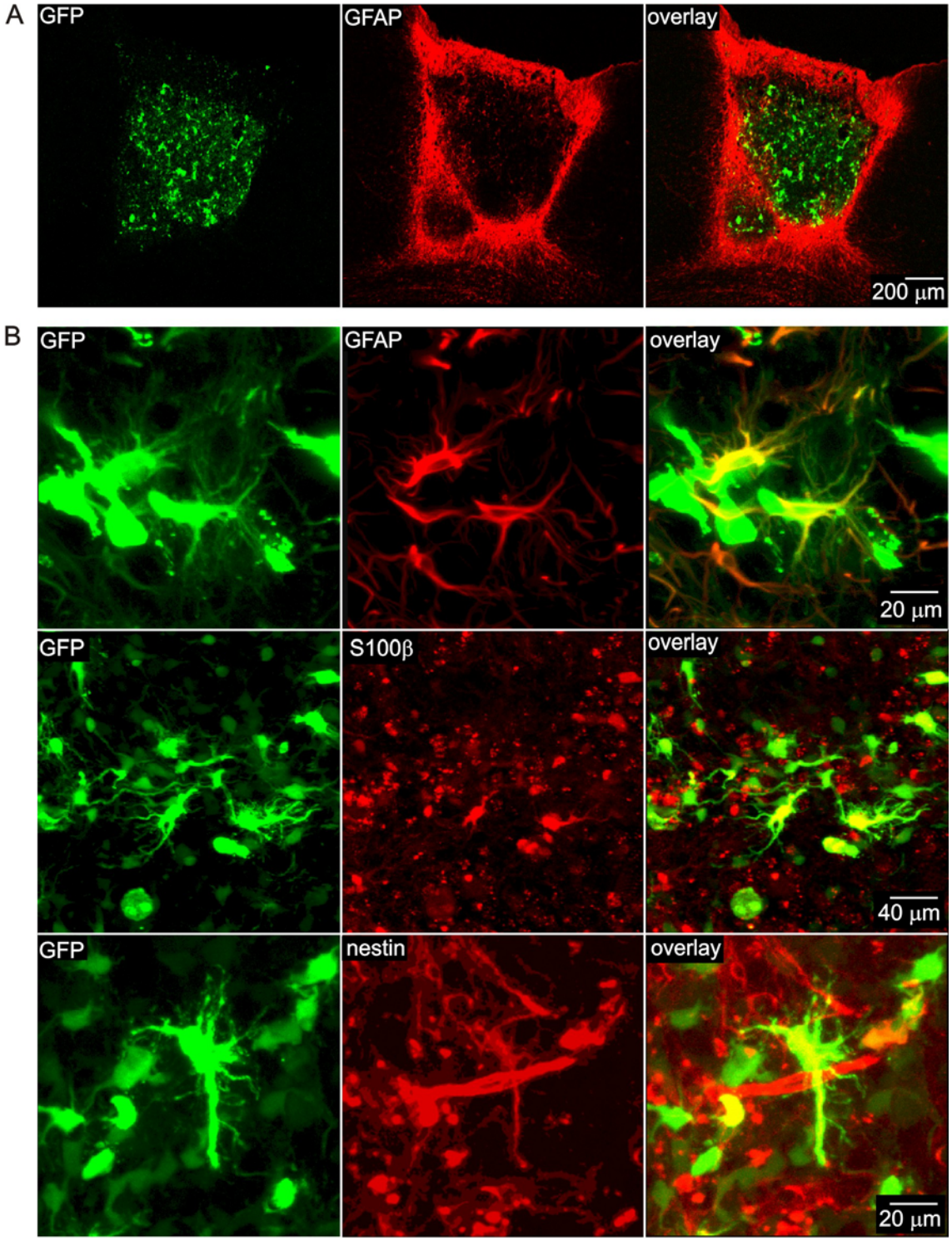

(A) Coronal section of adult rat cortex with a photochemical lesion transplanted with GFP/NE-4C cells immunostained for GFAP 4 weeks after transplantation. **(B)** Higher magnification images illustrating details of GFP/NE-4C cell immunoreactivity for GFAP **(top)**, S100β **(middle)** and nestin **(bottom)** inside the lesion. Yellow colour indicates double stained cells.

Fig. 20 The membrane current patterns of GFP/GFAP-positive cells in the rat cortex 4 weeks after transplantation

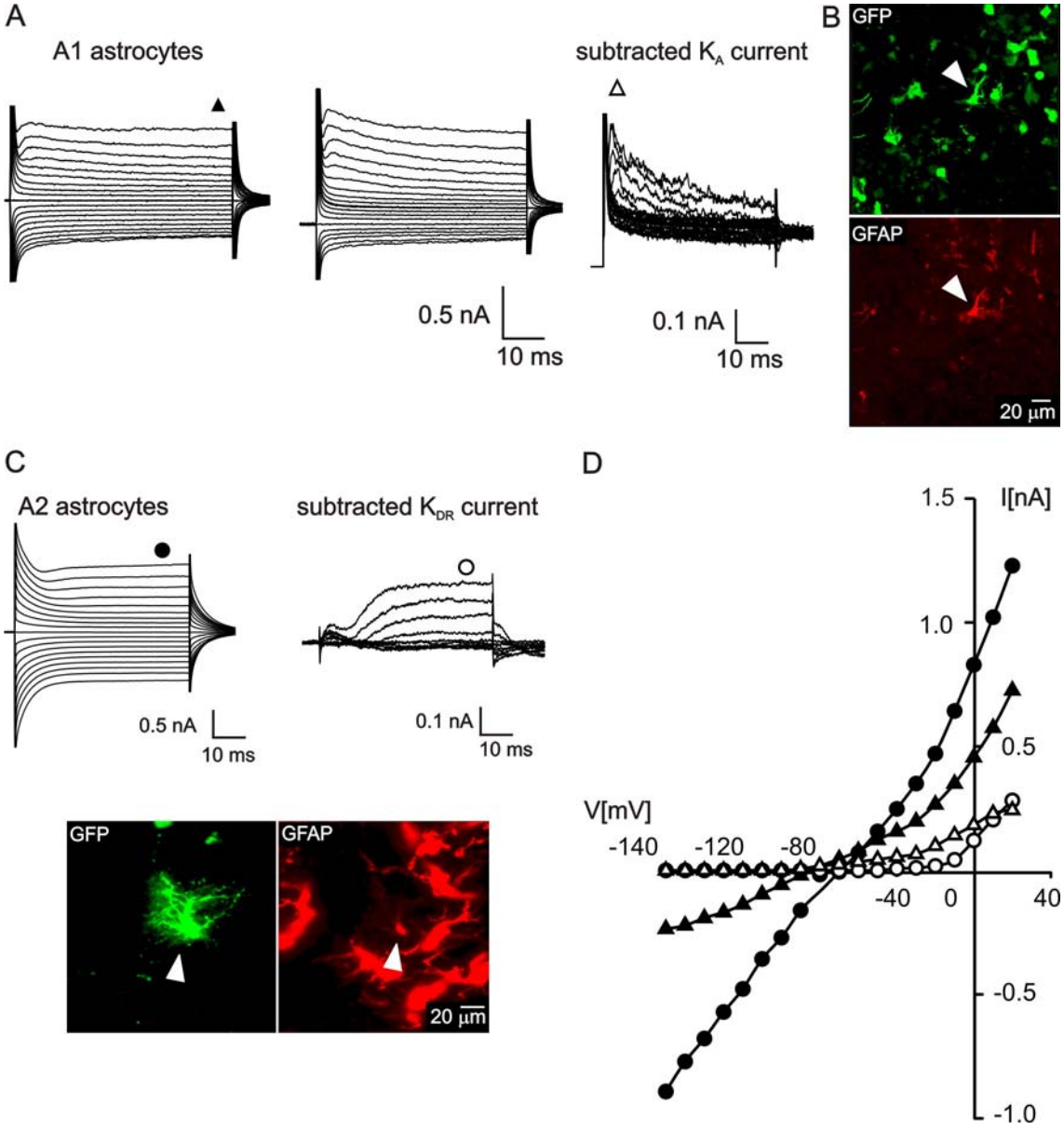

(A) Typical current pattern of a GFP/GFAP-positive A1 astrocyte obtained by hyper- and depolarising the cell from a holding potential of -50 mV to potentials ranging from -140 mV to +40 mV **(left)** and after a hyperpolarising prepulse to -110 mV **(middle)**, and the isolated K_A current **(right)** obtained by subtracting the currents shown in (left) from those shown in (middle). **(B)** The morphology (**top)** and immunohistochemical identification **(bottom)** of a recorded A1 astrocyte derived from GFP/NE-4C cells showing positive staining for GFAP. **(C)** Typical current pattern of a GFP/GFAP-positive A2 astrocyte obtained by hyper- and depolarising the cell from a holding potential of -50 mV to potentials ranging from -140 mV to +40 mV and the isolated K_{DR} current, obtained by passive currents subtraction **(top)** and immunohistochemical identification of the recorded cell showing positive staining for GFAP. **(D)** The resulting I/V relationship for the current traces shown in (A left; filled triangles) and in (C, left; filled circles) and for the isolated K_A (empty triangles) and K_{DR} (empty circles) currents.

Oligodendrocytes

Similarly to the astrocytic and neuronal markers, no positive staining for the oligodendrocyte markers MOSP, RIP, or O1 **(Fig. 15)** was observed inside the photochemical lesion of control rats. Similarly to the intact cortex, we found a small number of GFP/MOSP-positive cells, and additionally, RIP- or O1-positive cells were identified in the lesion **(Fig. 21)**. While GFP/MOSP-positive cells displayed the morphology of oligodendrocyte precursors with small cell bodies and short processes, GFP/RIP- and O1-positive cells showed a few parallel processes, reflecting the morphology of more mature oligodendrocytes. Only one GFP-positive cell was identified post-recording as MOSP-positive. This cell expressed decaying passive K^+ currents and large K_{DR} currents, the current pattern being similar to that shown by astrocytes **(Fig. 20C)**. The V_{rest} and IR were -68 mV and 128 MΩ, respectively.

In summary, our results indicate that GFP-labelled NE-4C neural stem cells transplanted into the site of a photochemical lesion survive, and they give rise to neuronal cells and astrocytes with membranes properties similar to those transplanted into the intact cortex.

Fig. 21 The GFP/NE-4C cell line gives rise to oligodendrocytes 4 weeks after transplantation into the site of a photochemical lesion

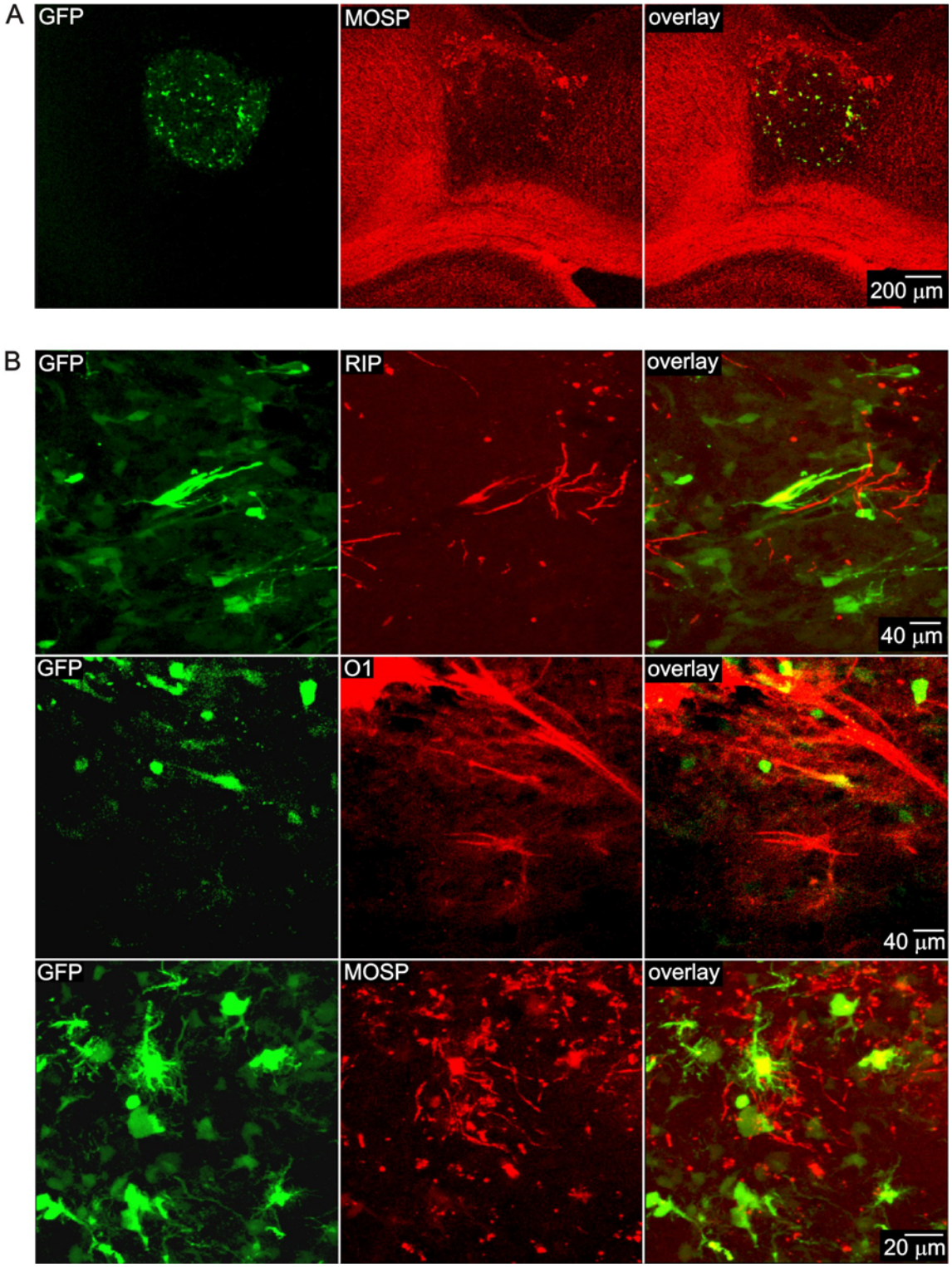

(A) Coronal section of rat cortex showing an overview of a photochemical lesion transplanted with GFP/ NE-4C cells, immunostained for MOSP 4 weeks after transplantation. **(B)** Higher magnification images illustrating details of the GFP/NE-4C cell immunoreactivity for RIP **(top)**, O1 **(middle)**, and MOSP **(bottom)** inside the lesion. Yellow colour indicates double stained cells.

5.2 Neural stem/progenitor cells derived from the embryonic dorsal telencephalon of D6-GFP mice differentiate primarily into neuronal cells after transplantation into a cortical lesion

5.2.1. One week after the onset of *in vitro* differentiation D6-GFP NS/PCs give rise to neuronal cells and GFAP-positive cells

In the D6-GFP mouse embryo (E12), GFP was expressed throughout the entire wall of the developing dorsal telencephalon, which contains predominantly NS/PCs **(Fig. 22A and 23).** In the adult brain GFP-positive cells were detected in the cortex as well as in the hippocampus and were positive for neuronal markers such as NeuN and MAP-2; moreover, GFAP-positive astrocytes were found in the hippocampus and also in the mantle zone of the cortex **(Fig. 24)**. Our findings are in agreement with previously published data, showing that D6/GFP NS/PCs generate cortical and hippocampal CA1 neurons and a subset of cortical and hippocampal astrocytes with sustained *mDach1* gene expression and can therefore be visualised by GFP expression in the adult mouse brain (Machon et al., 2002). NS/PCs isolated from E12 embryos were cultured under proliferating conditions to form neurospheres, after one week, most of the neurospheres expressed GFP. After dissociation, these cells were able to form secondary neurospheres; however, the number of GFP-positive neurospheres was decreased. These data show that the unique character of these cells might be lost with an increasing number of passages, as suggested previously (Hack et al., 2004, Machon et al., 2005). Therefore, only neurospheres that were cultured for 1 week without further passages were used for all experiments. The isolated embryonic tissue and the derived neurospheres were analysed using Western blotting **(Fig. 22A)** and immunocytochemistry **(Fig. 23)**.

Fig. 22 Characterisation of D6-GFP-derived NS/PCs in the embryonic telencephalon and in the neurospheres

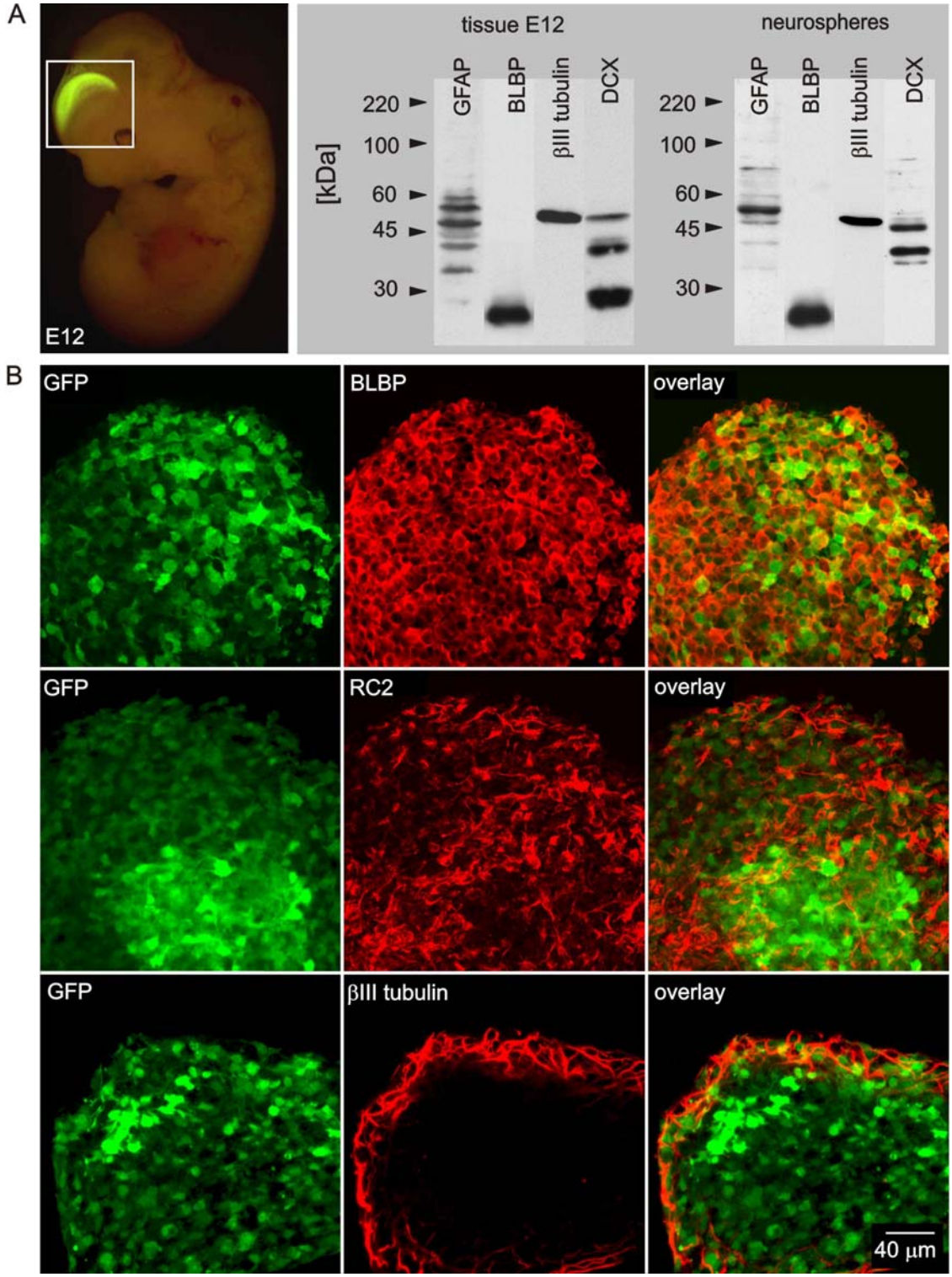

(A) Sagittal view of a D6-GFP E12 embryo showing fluorescence in the dorsal part of the developing cortex **(left)**. Western blot analysis of isolated tissue and derived neurospheres, harvested 1 week after cultivation, showing GFAP, BLBP, βIII tubulin and DCX in both samples **(right)**. **(B)** Immunocytochemical analysis of neurospheres showing the expression of radial glia markers BLBP **(top)** and RC2 **(middle)** and the neuronal marker βIII tubulin **(bottom)**.

Fig. 23 Immunohistochemical characterisation of the embryonic dorsal telencephalon of a D6-GFP transgenic mouse

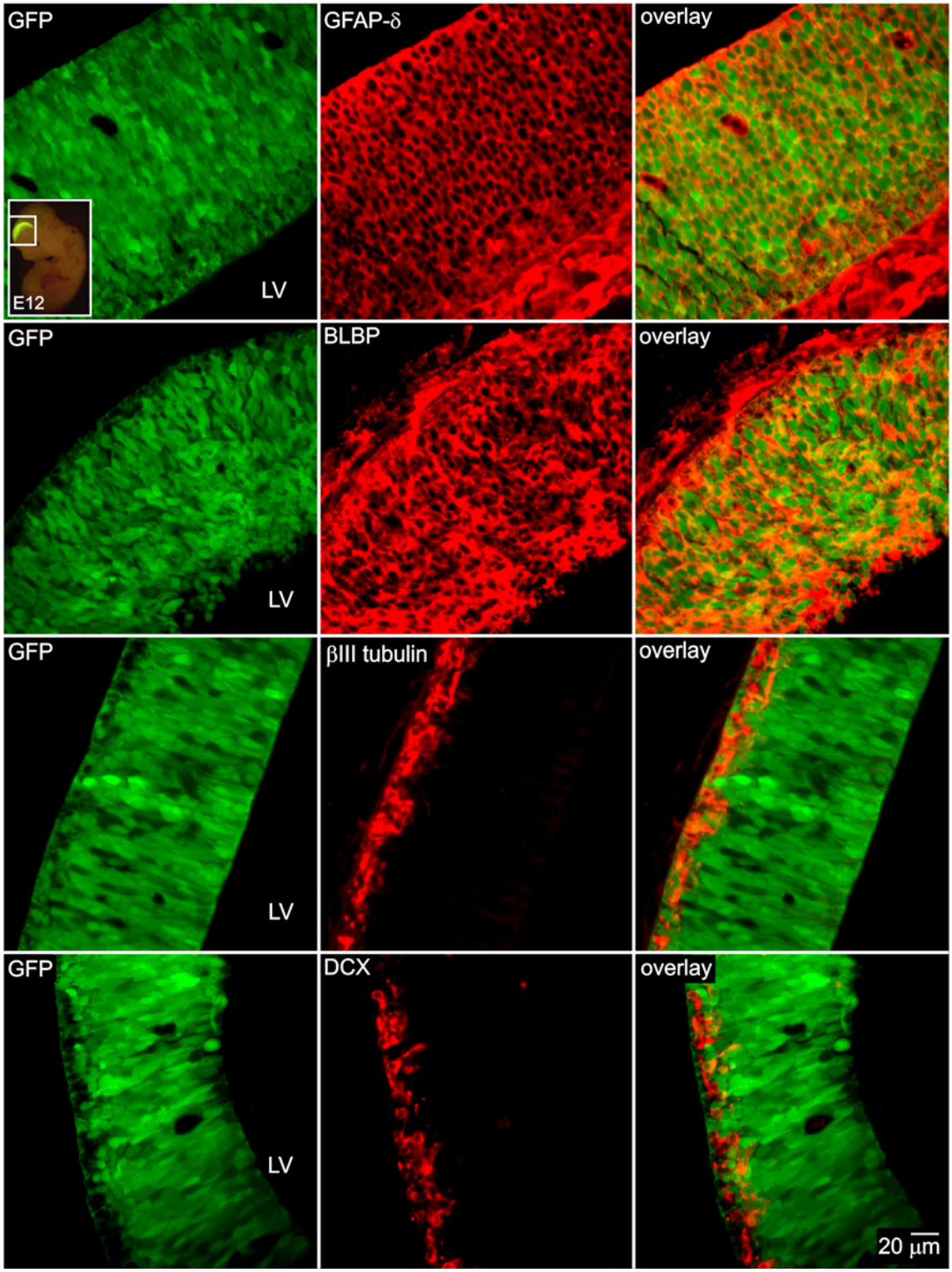

Sagittal sections of the developing dorsal telencephalon (see the inset) showing the co-localisation of GFP and GFAP-δ, BLBP, βIII tubulin and DCX at E12; **LV:** lateral ventricle.

Fig. 24 Immunohistochemical analysis of the adult cortex in a D6-GFP transgenic mouse

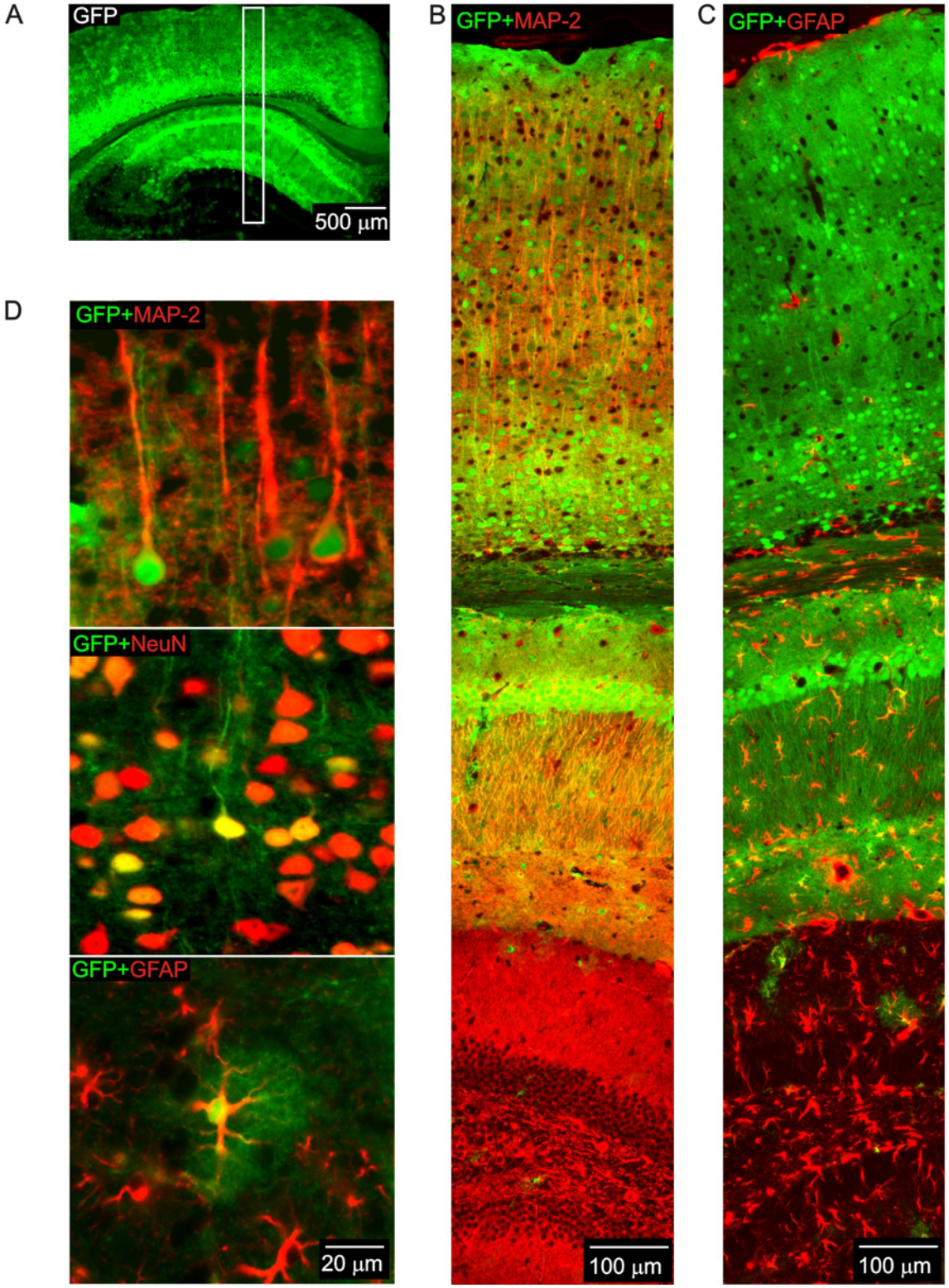

(A) Overview of the adult cortex in a D6-GFP transgenic mouse **(B)** Enlargement of the brain section shown in (A) illustrating the immunoreactivity of GFP-positive cells for the neuronal marker MAP-2 and the astrocytic marker GFAP. **(C)** Details of GFP-positive cells in the cortex stained for MAP-2 **(top)**, NeuN **(middle)** and GFAP **(bottom)**.

Western blot analysis revealed that isolated tissue as well as neurospheres expressed markers of radial glia: BLBP (~15 kDa) and GFAP. While in the embryonic tissue 4 bands immunoreactive for GFAP were detected (~40, 45, 55, 60 kDa), only 2 main bands (~50 and 55 kDa) were found in neurospheres. Additionally, the neuronal markers DCX and βIII tubulin were detected in the neurospheres as well as in the embryonic tissue. Interestingly, besides the typical 40 kDa band of DCX, another two bands immunoreactive for DCX appeared in embryonic tissue (~28 and 45 kDa), while in neurospheres only one additional band (~45 kDa) was detected. Immunocytochemical analysis revealed that GFAP-δ and BLBP were expressed in most of the GFP-positive cells of the dorsal telencephalon and that neuronal markers βIII tubulin and DCX were localised in the GFP-positive cells of the outer layer of the developing cortex **(Fig. 23)**.

Similarly, immunocytochemical analysis demonstrated that all the neurospheres expressed the radial glia marker BLBP, and most of the neurospheres expressed RC2, another marker of radial glia cells **(Fig. 22B)**. Also βIII tubulin-positive cells were detected in the neurospheres and were localised on the surface of the neurospheres **(Fig. 22B)**.

One week after the onset of *in vitro* differentiation, D6-GFP neural stem/progenitor cells gave rise to two morphologically distinct cell populations. Large flat cells that formed an underlying layer expressed nestin and GFAP **(Fig. 25A)**. The proportion of GFAP-positive cells in the cell culture was 27.5 ± 1.8% (n=9, 9 zones and 1693 cells were analysed in total). Some of these cells were also RC2-positive **(Fig. 25A)**. Quantification was performed in 3 independent cultures, and 3 zones (225 x 225 μm) were analyzed in each cover slip; the total cell number was determined based on DAPI staining. However, the majority of cells displayed a neuronal morphology, a small round body and one or several, often very long, processes. These cells were detected individually or in clusters, positioned on the top of the nestin/GFAP-positive cells, and expressed DCX, a marker of newly-derived neurons, MAP-2 and NeuN, markers of mature neurons **(Fig. 26)**. Quantification revealed that 65.0 ± 2.7% of cells (n=9, 9 zones and 1441 cells were analysed in total) expressed βIII tubulin, a marker expressed in immature and mature neurons. To identify oligodendrocytes or their progenitors, the cells were stained with specific antibodies directed against O4, Olig2

and MOSP. MOSP- and O4-positive cells were not detected; however, we detected Olig2-positive cells in cell culture **(Fig. 25B)**.

These findings suggest that D6-GFP NS/PCs are able to form neurospheres that express markers of radial glia and that 1 week after the onset of *in vitro* differentiation they give rise predominantly to neuronal cells and to GFAP-positive cells.

Fig. 25 One week after the onset of *in vitro* differentiation, D6-GFP NS/PCs express glial cell markers

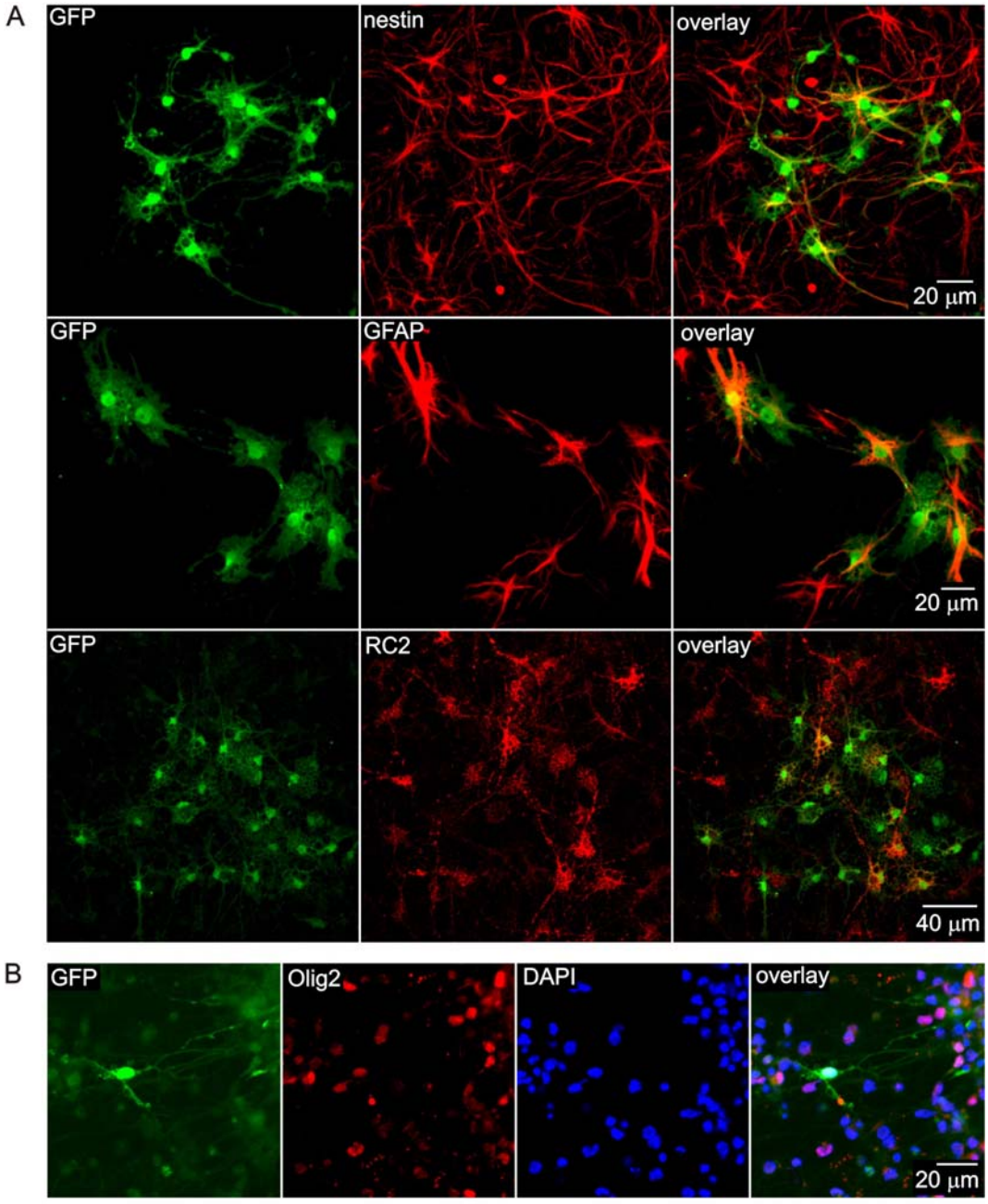

(A) Large flat cells of the underlying layer positive for nestin **(top)**, GFAP **(middle)** and RC2 **(bottom)**. **(B)** A detailed image of a GFP-positive cell stained for Olig2. Yellow colour indicates double-stained cells.

Fig. 26 One week after the onset of *in vitro* differentiation, D6-GFP NS/PCs express a range of neuronal markers

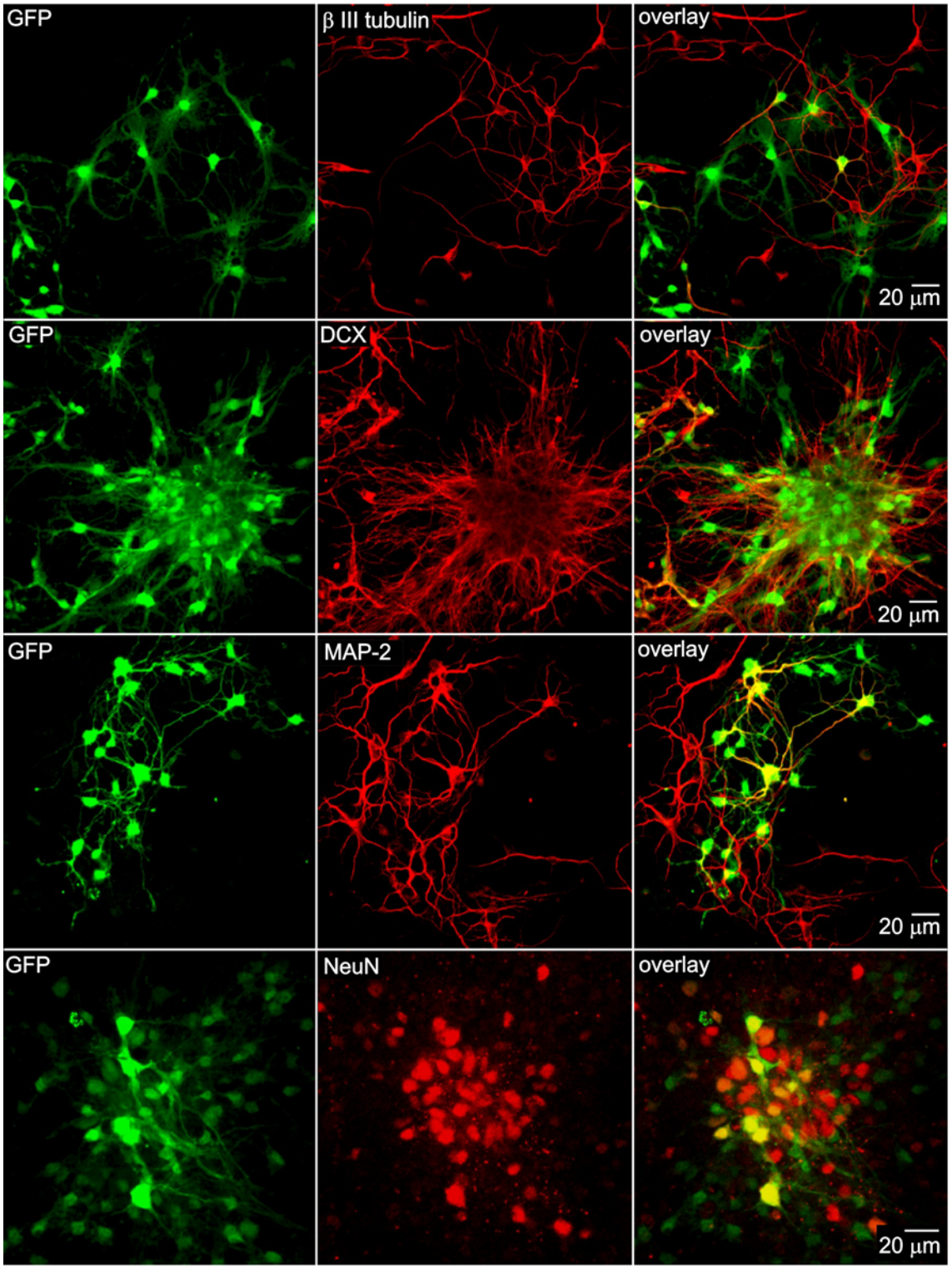

Clusters of D6-GFP cells with neuronal morphology were positively stained for the neuronal markers βIII tubulin, DCX, MAP-2 and NeuN. Yellow colour indicates double-stained cells.

5.2.2 D6-GFP cells display either a passive or a neuronal current pattern one week after the onset of *in vitro* differentiation

Using the patch-clamp technique in the whole-cell configuration, two cell populations with distinct passive and active membrane properties were detected, correlating with the morphological and immunohistochemical features described above.

Large flat cells of the underlying layer expressed symmetrical, time- and voltage- independent passive currents **(Fig. 27A, B)**, hyperpolarised V_{rest} (-81.7 ± 1.9 mV, n=39), low IR (81.8 ± 5.8 MΩ, n=39) and high C_m (47.1 ± 5.7 pF, n=39). These cells were further termed "passive cells". All these cells were identified post-recording as GFAP-positive **(Fig. 27A)**. To characterise the ionic components of the passive currents, a 50 mM K^+ solution was applied to the passive cells, as described previously (Jelitai et al., 2007). During the application of the K^+ solution, the average V_{rev} shifted from -90.1 ± 2.8 to -29.6 ± 5.5 mV (n=5, **Fig. 27D)**, a value close to the theoretical value calculated from the Nernst equation (-24.5 mV). Therefore, the major components carried by the passive currents are K^+ ions. In addition to passive conductance, in two cells a K_{DR} current was detected. The application of 5 mM 4-AP decreased the amplitude of the K_{DR} current in these two cells by 67.3% and 68.8%; the addition of 1 mM TEA further decreased the amplitude, resulting in 97.6% and 93.1% blockage of the K_{DR} current. Furthermore, the application of 1 mM CsCl (in 6 cells out of 8) revealed a K_{IR} current **(Fig. 27B, C)**. Further pharmacological analysis showed that in 56.3% of passive cells (9 out of 16), 100 μM GABA evoked an inward current that was completely blocked by 100 μM bicuculline **(Fig. 27E)**. The average current density of the GABA-evoked current was 3.9 ± 0.6 pA/pF (n=9). No cells with a passive current pattern responded to the application of glutamate.

Fig. 27 Electrophysiological characterisation of D6-GFP-derived passive cells, 1 week after the onset of *in vitro* differentiation

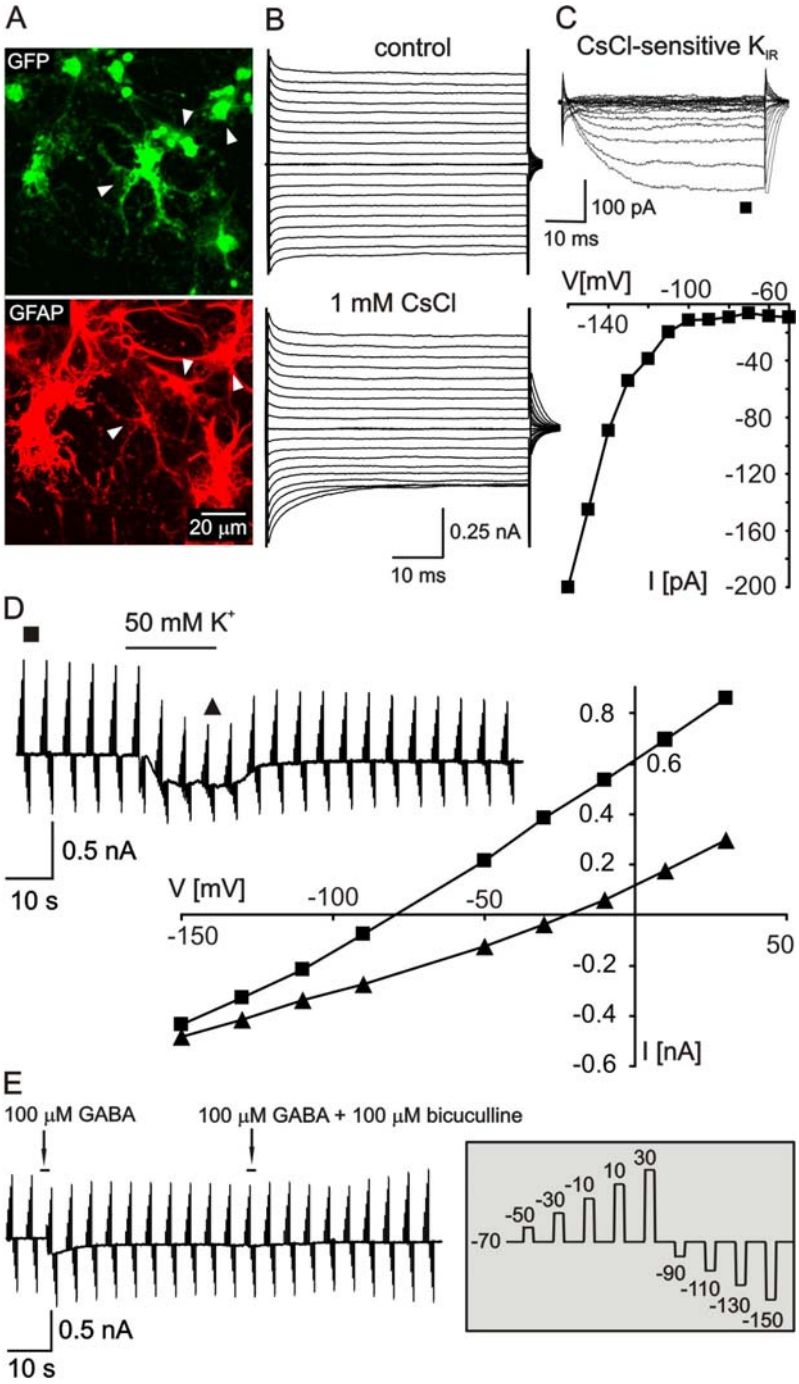

(A) Immunocytochemical identification of recorded cells (indicated by arrowheads, **top)**, showing positive staining for GFAP **(bottom)**. **(B)** Typical current pattern of a large flat D6-GFP-derived cell obtained by hyper- and depolarising the cell from a holding potential of -70 mV to potentials ranging from -160 to +20 mV, recorded in ACF (control, **top)** and after the application of 1 mM CsCl **(bottom). (C)** The subtracted CsCl-sensitive K_{IR} current **(top)** and the resulting I/V plot of the CsCl-sensitive current **(bottom)**. **(D)** A typical inward current and depolarisation evoked by the application of a 50 mM K^+-solution **(left)** and the resulting I/V plot **(right)** for traces recorded in ACF (filled squares) and 50 mM K^+ solution (filled triangles), showing the shift of V_{rev}. **(E)** A typical inward current evoked by the application of 100 µM GABA and completely blocked by the application of 100 µM bicuculline. The currents shown in (D, E) were obtained by clamping the cell membrane potential to different values, by rectangular voltage steps, from a holding potential of -70 mV to potentials ranging from -150 mV to +30 mV (see the inset in E).

Cells with a neuronal morphology displayed membrane properties and current patterns significantly different from those of the passive cells. They were characterised by high IR, depolarised V_{rest} and large amplitudes of outwardly rectifying K^+ currents, specifically K_{DR} and K_A currents **(Fig. 28A, B, Table 5)**. Post-recording identification

confirmed the expression of the neuronal markers βIII tubulin **(Fig. 28C)**, MAP-2 and DCX. Therefore, these cells were further termed "neuronal cells", though only 38.6% (37/95) of these cells expressed TTX-sensitive Na^+ currents **(Fig. 28A, B)**. Five cells out of 15 (33.3%) were able to fire an AP with a clear threshold of activation, at the beginning of the current injection. The average AP amplitude was 14.5 ± 2.6 mV and the AP half-width duration was 1.6 ± 0.2 ms. Pharmacological analysis revealed that in 74.1% (40/54) of neuronal cells, the application of 100 μm GABA evoked an inward current **(Fig. 28D)**. Interestingly, the average GABA/C_m was significantly higher than in cells expressing passive currents (46.7 ± 8.2 pA/pF, n=40 compared to 3.9 ± 0.6 pA/pF, n=9; and 30.1 ± 2.8 mV, n=40 compared to 17.2 ± 1.5 mV, n=9). Neither GABA-responsive nor GABA-non-responsive cells reacted to the application of glutamate, although glutamate receptors (GluR 1-4) were detected in cell cultures by Western blotting, together with $GABA_A$ receptors **(Fig. 29A)**. Further immunocytochemistry revealed that a number of D6-GFP cells differentiated *in vitro* contained GABA and also glutamate decarboxylase (GAD) 65/67 **(Fig. 29B)**. Outwardly rectifying K^+ currents were sensitive to 5 mM 4-AP. The K_A and K_{DR} current amplitudes decreased by 46.1 ± 7.3% and 57.7 ± 6.8% (n=19), respectively **(Fig. 30)**, following 5 mM 4-AP application. The additional application of 10 mM TEA did not cause a further decrease in the current amplitudes. The membrane and pharmacological properties of the neuronal cells are summarised in **Table 5**.

Together, these data show that 1 week after the onset of *in vitro* differentiation, D6-GFP NS/PCs give rise to cells with distinct membrane properties: cells expressing glial markers display passive K^+ currents, while cells expressing neuronal markers display the current patterns of immature neurons.

Fig. 28 Membrane properties of D6-GFP-derived neuronal cells, 1 week after the onset of *in vitro* differentiation

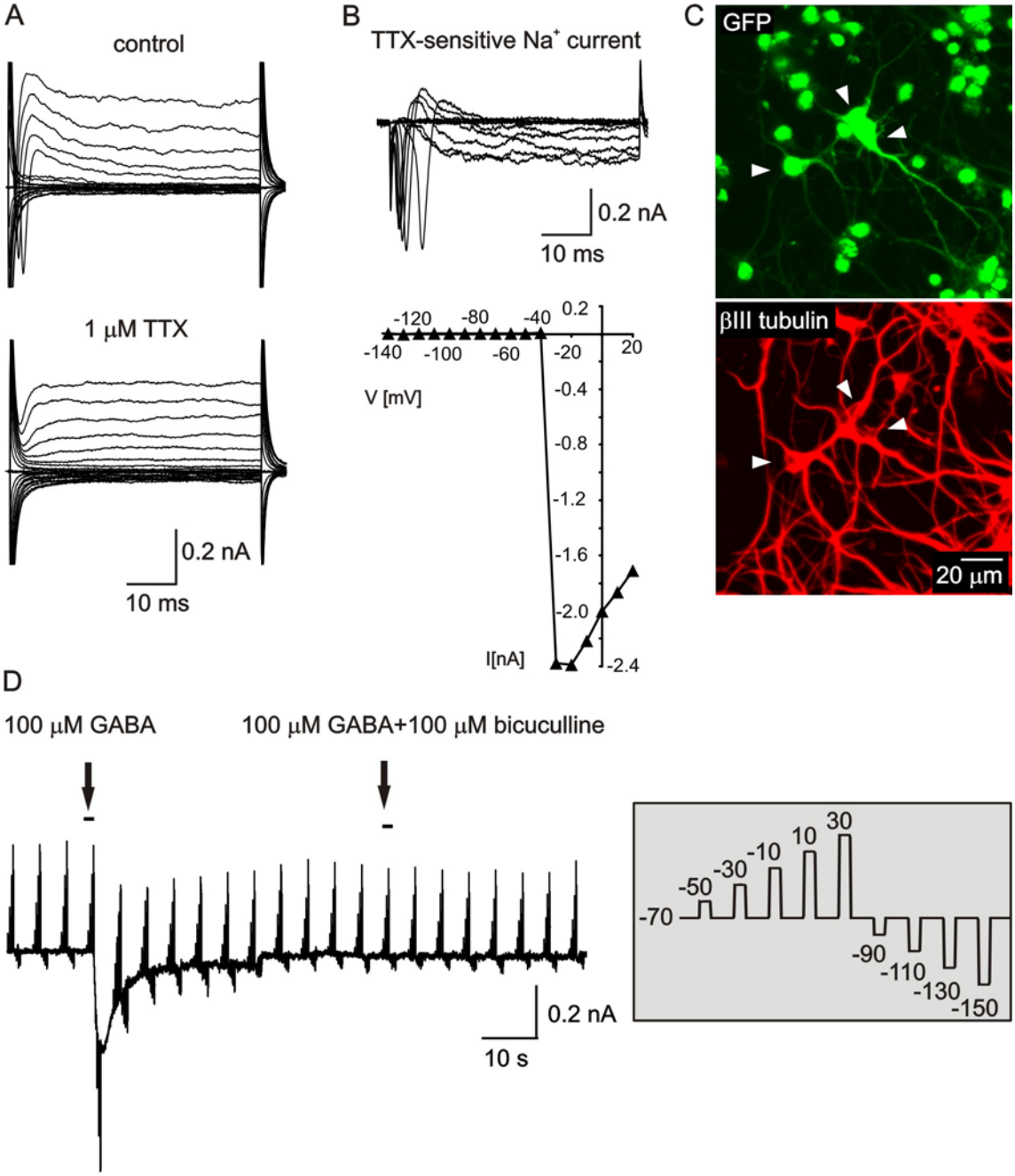

(A) A typical membrane current pattern of a GFP/βIII tubulin-positive cell prior to **(top)** and after **(bottom)** the application of 1 μM TTX, obtained by hyper- and depolarising the cell membrane from a holding potential of -70 mV to potentials ranging from -160 mV to +20 mV. **(B)** The TTX-sensitive current was obtained by subtracting the currents recorded after TTX application from those recorded prior to the TTX application (control). The resulting I/V relationship for the TTX-sensitive current is shown below. **(C)** The morphology and immunocytochemical identification of a recorded neuronal cell (indicated by an arrowhead, **top)** showing positive staining for βIII tubulin **(bottom)**. **(D)** A typical inward current evoked by the application of 100 μM GABA and blocked by 100 μM bicuculline. The currents were obtained by clamping the cell membrane potential to different values, by rectangular voltage steps, from a holding potential of -70 mV to potentials ranging from -150 mV to +30 mV (see the inset).

Table 5 Membrane and pharmacological properties of D6-GFP-derived neuronal cells one week after the onset of *in vitro* differentiation or one week after transplantation into the intact cortex or into the site of a photochemical lesion (PCL)

neuronal cells		*in vitro*	intact cortex	PCL
V_{rest}	[mV]	-57.8 ± 1.6	-56.4 ± 1.9	-50.3 ± 3.3
IR	[MΩ]	2515.2 ± 183.6	1944.1 ± 208.9	1494.2 ± 211.5
C_m	[pF]	8.7 ± 0.3	9.5 ± 0.9	7.5 ± 1.2
K_A/C_m	[pA/pF]	106.0 ± 10.0	50.0 ± 7.0***	40 ± 6.2*
K_{DR}/C_m	[pA/pF]	69.4 ± 4.0	47.2 ± 4.1**	48.7 ± 8.6
n		95	42	15
Na^+/C_m	[pA/pF]	22.6 ± 2.8	74.8 ± 8.8***	101.5 ± 17.1***
n		37	35	11
K_A + 4-AP	[%]	46.1 ± 7.3	69.7 ± 7.4	76.6 ± 11.8
K_A + 4-AP + TEA	[%]	57.7 ± 6.8	76.9 ± 6.3	76.6 ± 11.8
K_{DR} + 4-AP	[%]	43.4 ± 5.5	54.7 ± 5.4	62.0 ± 8.6
K_{DR} + 4-AP + TEA	[%]	56.7 ± 4.7	55.8 ± 5.5	62.0 ± 8.6
n		19	9	3
$GABA/C_m$	[pA/pF]	46.7 ± 8.2	65.6 ± 10.3	103.1 ± 43.9
n		40	13	3

V_{rest}: resting membrane potential; **C_m:** membrane capacitance; **IR:** input resistance; **K_A/C_m, K_{DR}/C_m, Na^+/C_m, $GABA/C_m$:** K_A, K_{DR}, Na^+ and GABA current densities; **n:** number of cells; **K_A + 4-AP, K_A + 4AP + TEA, K_{DR} + 4-AP, K_{DR} + 4-AP + TEA:** relative amplitude decrease after the application of 4-AP (4-aminopyridine) or 4-AP in combination with TEA (tetraethylamonium chloride). Asterisks indicate significant differences between neuronal cells derived *in vitro* and those differentiated after transplantation into the intact brain or into the site of a photochemical lesion. * $p< 0.05$; ** $p< 0.01$, *** $p< 0.001$.

Fig. 29 GABA and glutamate in D6-GFP cells during *in vitro* differentiation

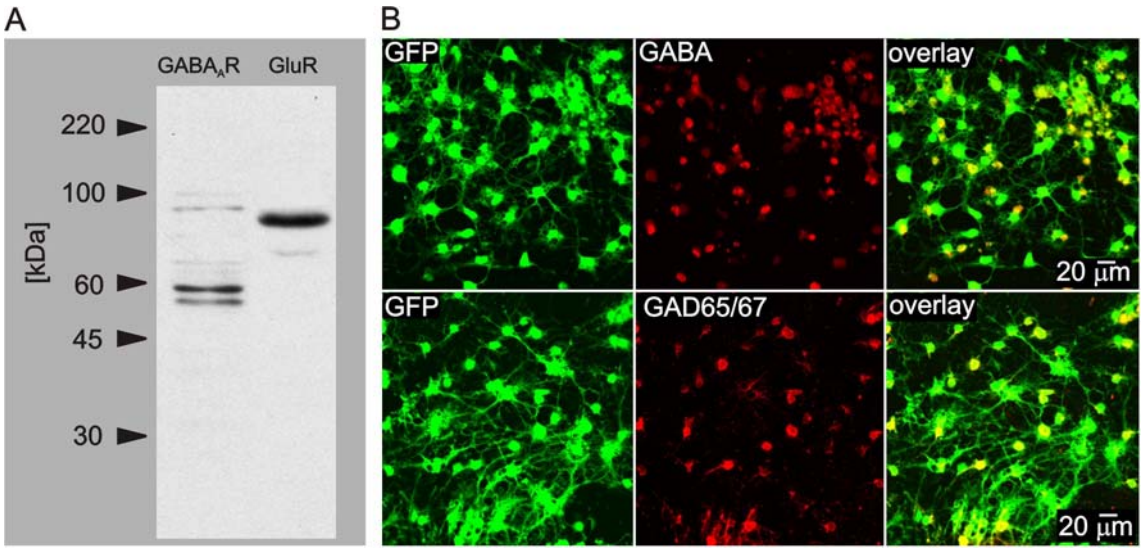

(A) Western blot analysis showing the expression of $GABA_A$ and glutamate receptors in the lysates obtained from D6-GFP cell culture. **(B)** GABA immunoreactivity (red) in D6-GFP cells (green, **top)** and GAD65/67 immunoreactivity (red) in D6-GFP cells (green), 1 week after the onset of *in vitro* differentiation. Yellow colour indicates double-stained cells.

Fig. 30 Voltage-dependent K^+ currents of D6-GFP-derived neuronal cells and their pharmacological properties, 1 week after the onset of *in vitro* differentiation

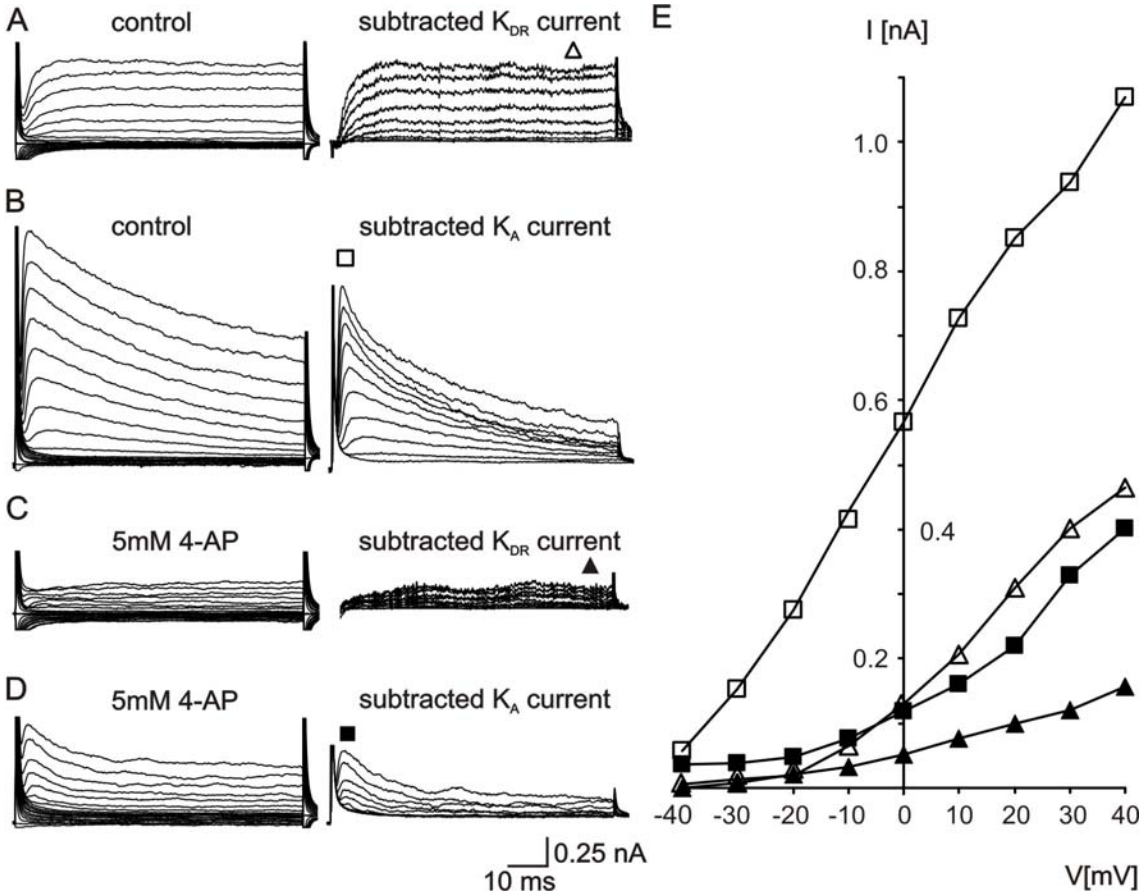

(A) Current patterns obtained by hyper- and depolarising the cell membrane from a holding potential of -50 mV to potentials ranging from -140 mV to +40 mV **(left)** and the isolated K_{DR} current, obtained by passive-current subtraction **(right)**. **(B)** Current patterns obtained by hyper- and depolarising the cell membrane from a holding potential of -50 mV to potentials ranging from -140 mV to +40 mV, after a hyperpolarising prepulse to -110 mV **(left)**, and the isolated K_A current **(right)** obtained by subtracting the currents shown in (A, left) from those shown in (B, left). **(C)** Current pattern shown in (A) after the application of 5 mM 4-AP **(left)** and the isolated K_{DR} current **(right)**. **(D)** Current pattern shown in (B) after the application of 5 mM 4-AP (left) and the isolated K_A current (right). **(E)** I/V relationships for the subtracted K_A and K_{DR} currents recorded in ACF (empty squares and triangles) and after the application of 5 mM 4-AP (filled squares and triangles).

5.2.3. *In vivo* differentiated D6-GFP cells express predominantly neuronal markers

The immunohistochemical properties of D6-GFP-derived NS/PCs were first studied after their transplantation into the intact rat cortex of 16 animals **(Fig. 31A)**. The analysis was performed 1 week after transplantation. GFP-positive cells filled the track **(Fig. 31B)** that extended through the entire cortex, and in some animals the cells reached the corpus callosum and started to migrate. Immunohistochemical analysis revealed that GFP-positive cells expressed the neuronal marker βIII tubulin, but also more mature markers such as MAP-2, NeuN or NF68 **(Fig. 31C)**. Only a few GFP/GFAP cells were detected, and they displayed an immature morphology – a small round cell body and several thin processes **(Fig. 31C)**. We did not detect any GFP/NG2- or GFP/MOSP- positive cells.

Fig. 31 One week after transplantation into the intact rat cortex D6-GFP NS/PCs cells survive and express predominantly neuronal markers

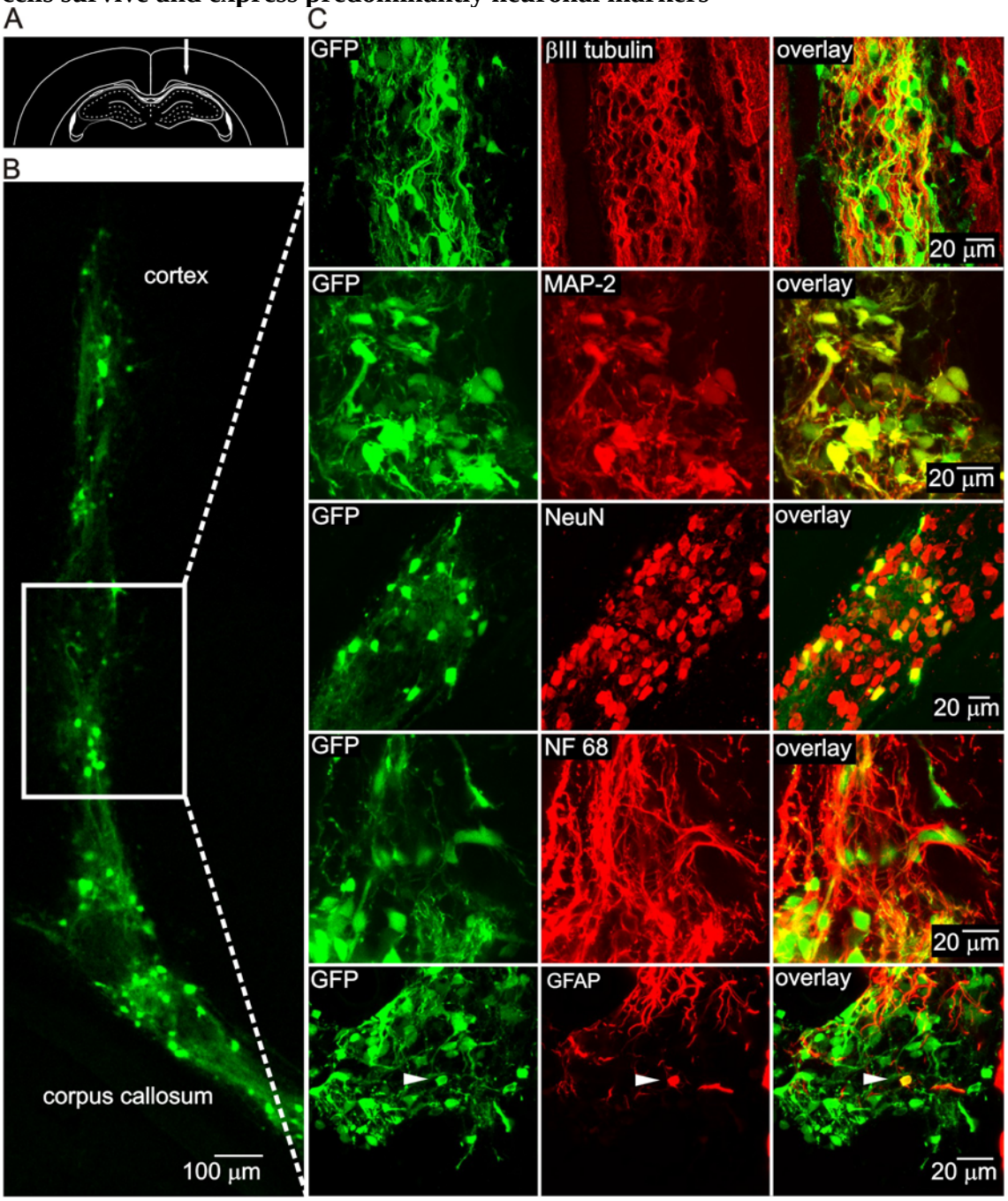

(A) A schematic image of the injection site in the cortex. **(B)** Coronal section of an adult rat cortex and corpus callosum showing the injection site filled with D6-GFP cells, 1 week after transplantation. **(C)** Higher magnification images of the injection site showing GFP-positive cells immunostained for the neuronal markers βIII tubulin, MAP-2, NeuN and NF68. Note that D6-GFP cells surviving in the brain were positive predominantly for neuronal markers, while GFP/GFAP double stained cells were rare (an example is indicated by the arrowhead) and displayed an undifferentiated morphology. Yellow colour indicates double-stained cells.

Subsequently, cells were transplanted into the site of a photochemical lesion. At first, the photochemical lesion was examined for evidence of surviving cells or endogenous neurogenesis in non-transplanted animals (control) over the same time course as in transplanted animals. Two weeks after the induction of the photochemical lesion (equivalent to 1 week after transplantation into the site of the photochemical lesion), the lesion was typically surrounded by a glial scar, formed by GFAP- and NG2-positive cells. The inner space of the lesion was devoid of any surviving neuronal cells, as shown by the lack of MAP-2 staining; MAP-2 was, however, normally distributed in the surrounding cortex, and the staining clearly delineated the damaged tissue **(Fig. 32)**. The lesion was also immunostained for DCX, a marker of newly born neurons that is rarely expressed under physiological conditions in the adult cortex. There was no DCX-positive staining inside the lesion, suggesting that there was no endogenous neurogenesis or NS/PC migration from neurogenic regions into the injured cortex. The inside of the lesion was filled with CD11b-positive activated microglia, with a typical amoeboid morphology that differed from the quiescent microglia in the tissue surrounding the lesion **(Fig. 32B)**.

D6-GFP NS/PCs were transplanted into 7 animals. One week after transplantation, GFP-positive cells were dispersed within the entire inner space of the lesion **(Fig. 33)**. They displayed the morphology of more mature neurons: small round bodies of ~20 μm in diameter with one or more branched and very well developed cell processes. All these cells were immunopositive for neuronal markers, including DCX, MAP-2 and NeuN **(Fig. 33A-D)**. We also identified GFP-negative cells expressing NeuN inside the lesion **(Fig. 33D)**. Additionally, synaptophysin was also detected within the lesion and co-localised with the GFP signal, suggesting that D6-GFP-derived neuronal cells are able to form synapses **(Fig. 34)**. No GFAP-, MOSP- or NG2-positive cells were detected inside the lesion.

In summary, these data show that after their transplantation into the intact or lesioned rat cortex, D6-GFP NS/PCs give rise primarily to neuronal cells. The persisting GFP signal of the transplanted cells suggests that the cells are able to maintain their cortical character following transplantation into the adult rat cortex.

Fig. 32 Immunohistochemical analysis of a photochemical lesion, 2 weeks after its induction

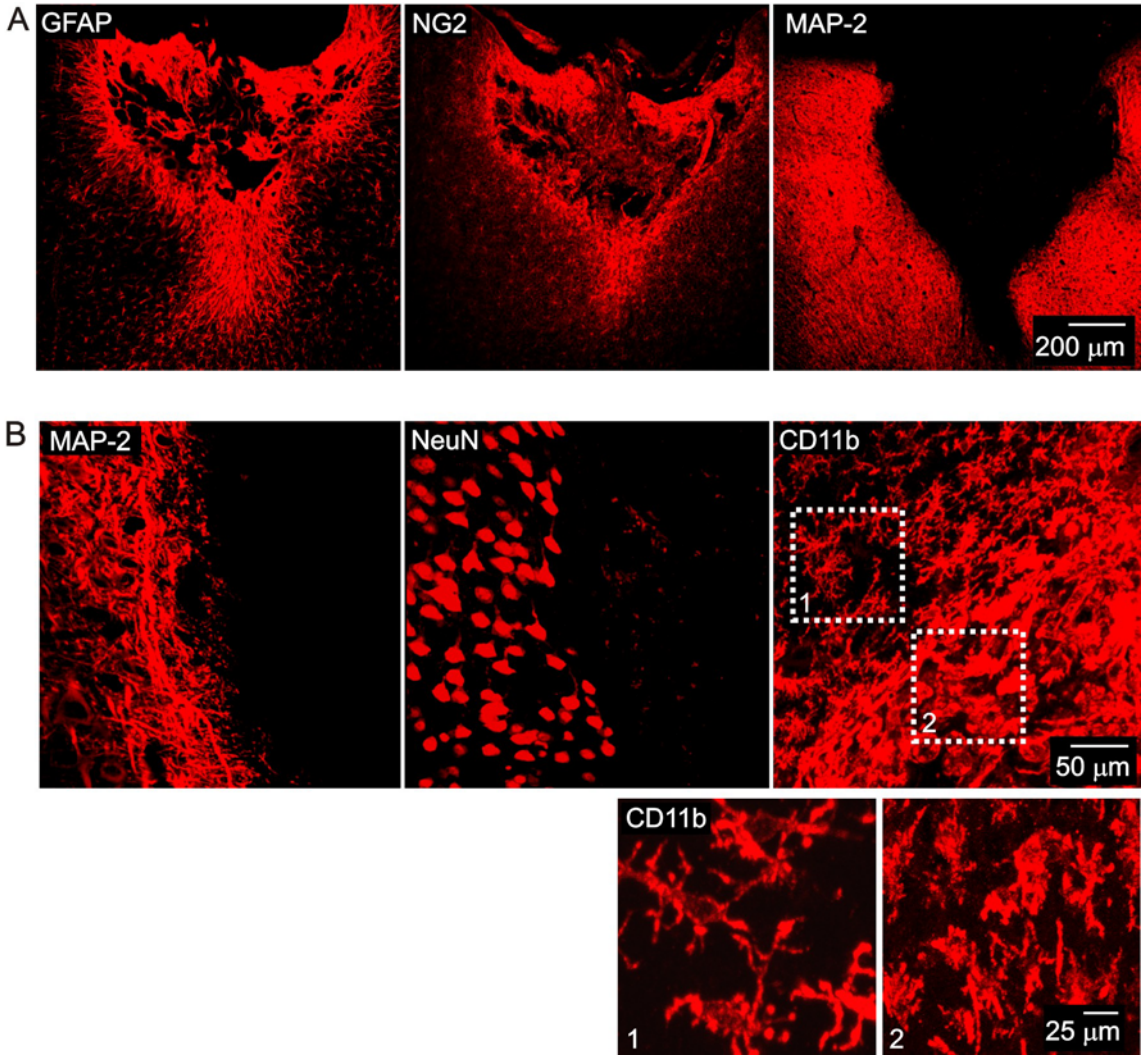

(A) Coronal sections of a non-transplanted photochemical lesion, 2 weeks after its induction, that were immunostained for GFAP, NG2 and MAP-2. **(B)** Higher magnification images of the interface between normal and lesioned tissue, immunostained for neuronal markers and CD11b. Note the difference in the morphology of CD11b-positive microglia in the surrounding tissue **(inset 1)** and inside the photochemical lesion **(inset 2)**.

Fig. 33 One week after transplantation into the site of a photochemical lesion D6-GFP NS/PCs express a range of neuronal markers

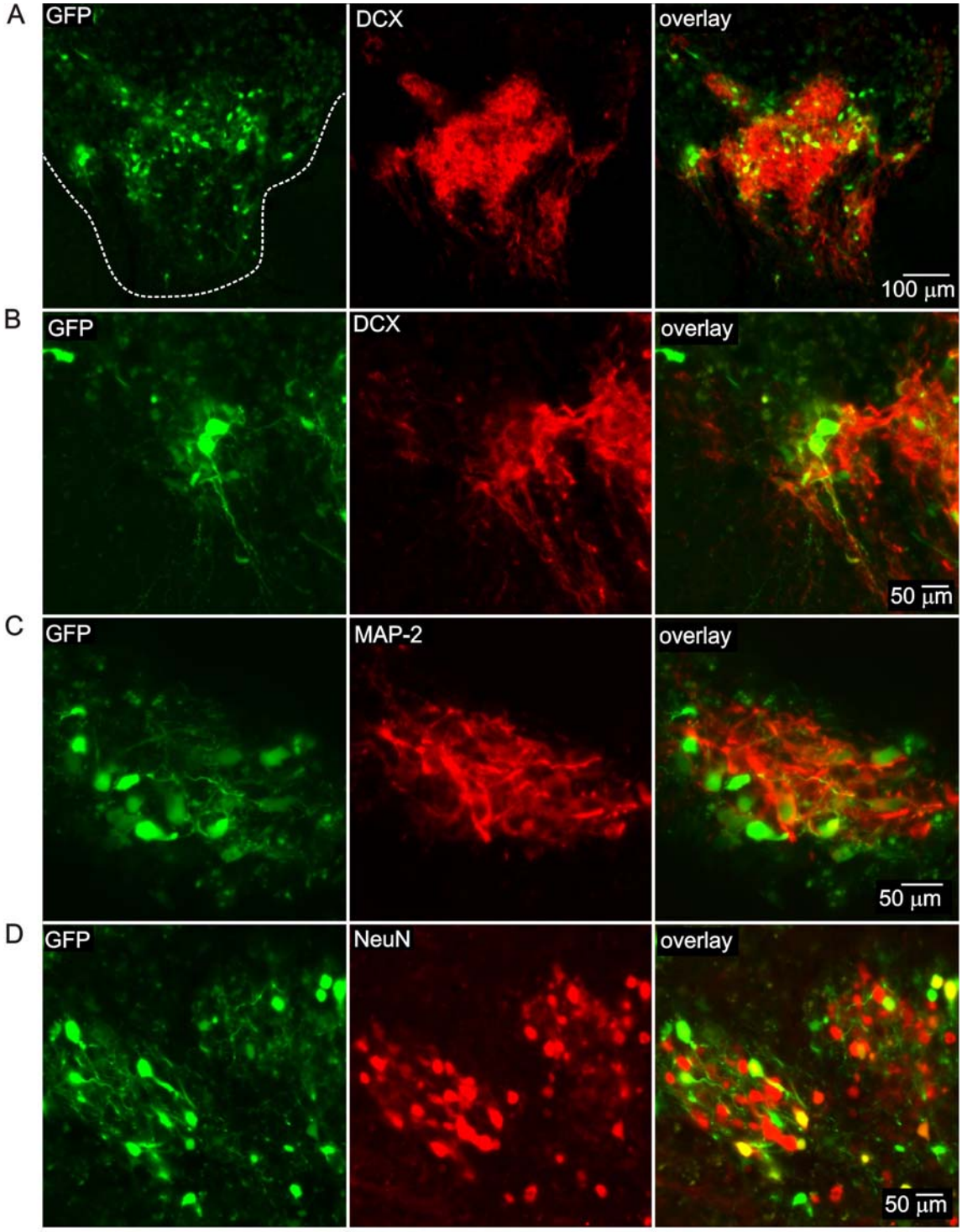

(A) Overview of a photochemical lesion filled with GFP-positive cells 1 week after transplantation and immunostained for DCX. **(B-E)** Higher magnification images showing the interior of the lesion filled with GFP-positive cells immunostained for DCX **(B)**, MAP-2 **(C)** and NeuN. **(D)** Yellow colour indicates double-stained cells.

Fig. 34 Synaptophysin is expressed inside a photochemical lesion one week after transplantation of D6-GFP NS/PCs

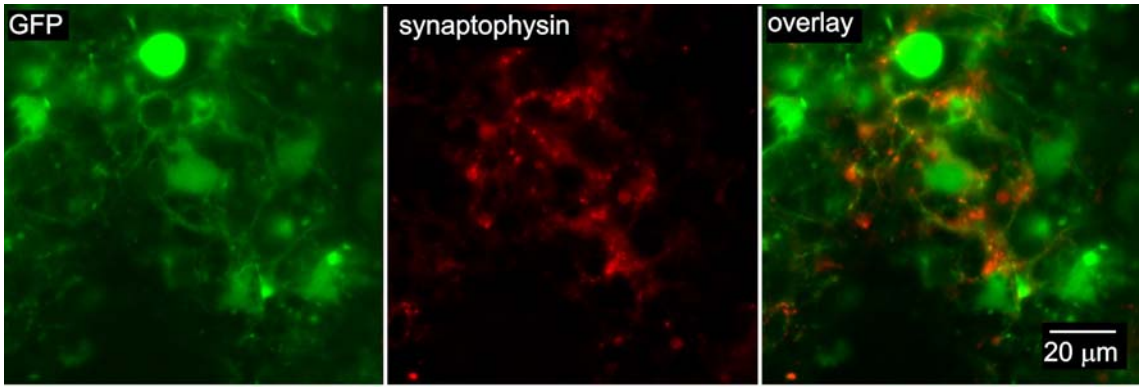

A detailed image showing the synaptophysin immunoreactivity inside the lesion, in the vicinity of D6-GFP-derived neuronal cells, one week after the transplantation of D6-GFP NS/PCs. Yellow colour indicates double-stained cells.

5.2.4 Membrane properties of D6-GFP-derived neuronal cells *in situ*

The electrophysiological properties of D6-GFP-derived NS/PCs were studied in acute brain slices, 1 week after their transplantation into the intact or injured rat cortex, using the patch-clamp technique in the whole-cell configuration **(Fig. 35)**. Cells were chosen for recording based on their GFP signal and post-recording identification confirmed the expression of the neuronal markers NeuN **(Fig. 35B)**, βIII tubulin and MAP-2. In the intact brain, 42 cells were recorded in total. All these cells displayed the membrane properties of early neurons or their precursors, with high IR and a depolarised V_{rest} **(Table 5)**. In 83.3% of recorded cells (35/42), a TTX-sensitive Na^+ current was detected **(Fig. 35A)**; 82.4% of the cells (28/34) were able to fire an AP after injecting currents in 10 pA increments (see the inset in **Fig. 35A)**. Moreover, 53.6% (15/28) of recorded cells were able to fire more than once, without a decrease in the AP amplitude. 86.7% (13/15) of tested cells responded to GABA application with an inward current which was bicuculline-sensitive **(Fig. 36A)**. No tested cell responded to the application of 100 μM glutamate. Interestingly, immunohistochemical analysis revealed only one GABA/GFP-positive cell, while the majority of GABA-positive cells in the graft were GFP-negative **(Fig. 36B)**. Additional immunohistochemical analysis revealed that no D6-GFP cells transplanted into the intact cortex or into the photochemical lesion expressed GAD 65/67, a marker of interneurons (Deng et al., 2007). Similarly, we found that in the transgenic D6-GFP mouse, GAD65/67 did not co-localise with the GFP signal **(Fig. 36B)**, demonstrating that the *mDach1* gene is not active in

interneurons, as was shown by Machon *et al*., for calretinin- and calbindin-positive cells (Machon et al., 2005).

Fig. 35 Membrane properties of D6-GFP-derived neuronal cells *in situ*, one week after transplantation into the intact or injured rat brain

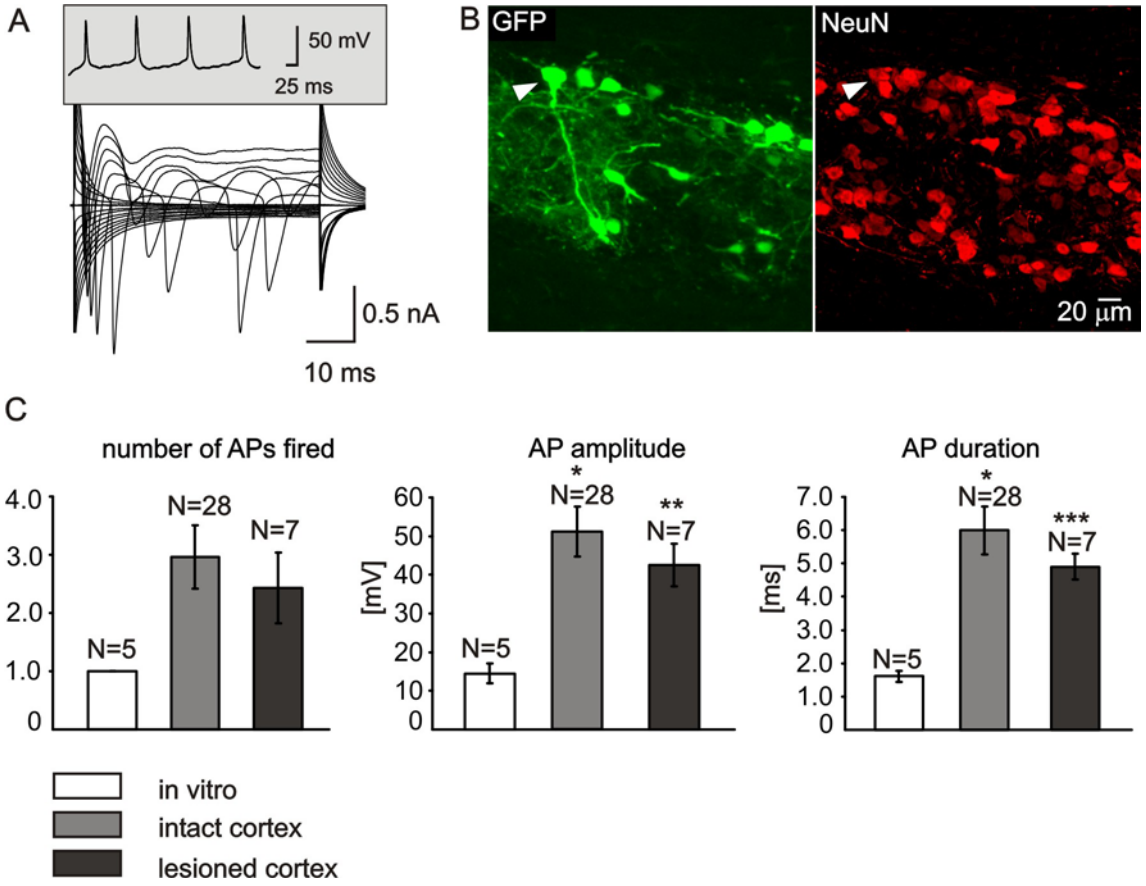

(A) A typical membrane current pattern of an *in vivo* D6-GFP-derived neuronal cell obtained by hyper- and depolarising the cell membrane from a holding potential of -70 mV to potentials ranging from -160 mV to +20 mV. Note the repetitive firing of APs during a 500 ms current injection of ~50 pA (see the inset). **(B)** The morphology and immunohistochemical identification of a recorded D6-GFP-derived neuronal cell (indicated by an arrowhead, **top)**, 1 week after transplantation into the intact rat cortex, showing positive staining for NeuN **(bottom)**. **(C)** The characteristics of the APs in D6-GFP-derived neuronal cells differentiated *in vitro* and after transplantation into the intact and injured rat brain, demonstrating that during a ~50 pA current injection, cells differentiated *in vivo* showed a higher number of APs, an increased AP amplitude and AP duration. Asterisks indicate significant differences between cells differentiated *in vitro* and cells differentiated *in vivo*. * $p < 0.05$; ** $p < 0.01$, *** $p < 0.001$

Fig. 36 One week after transplantation into the intact or injured rat brain, D6-GFP-derived neuronal cells respond to GABA

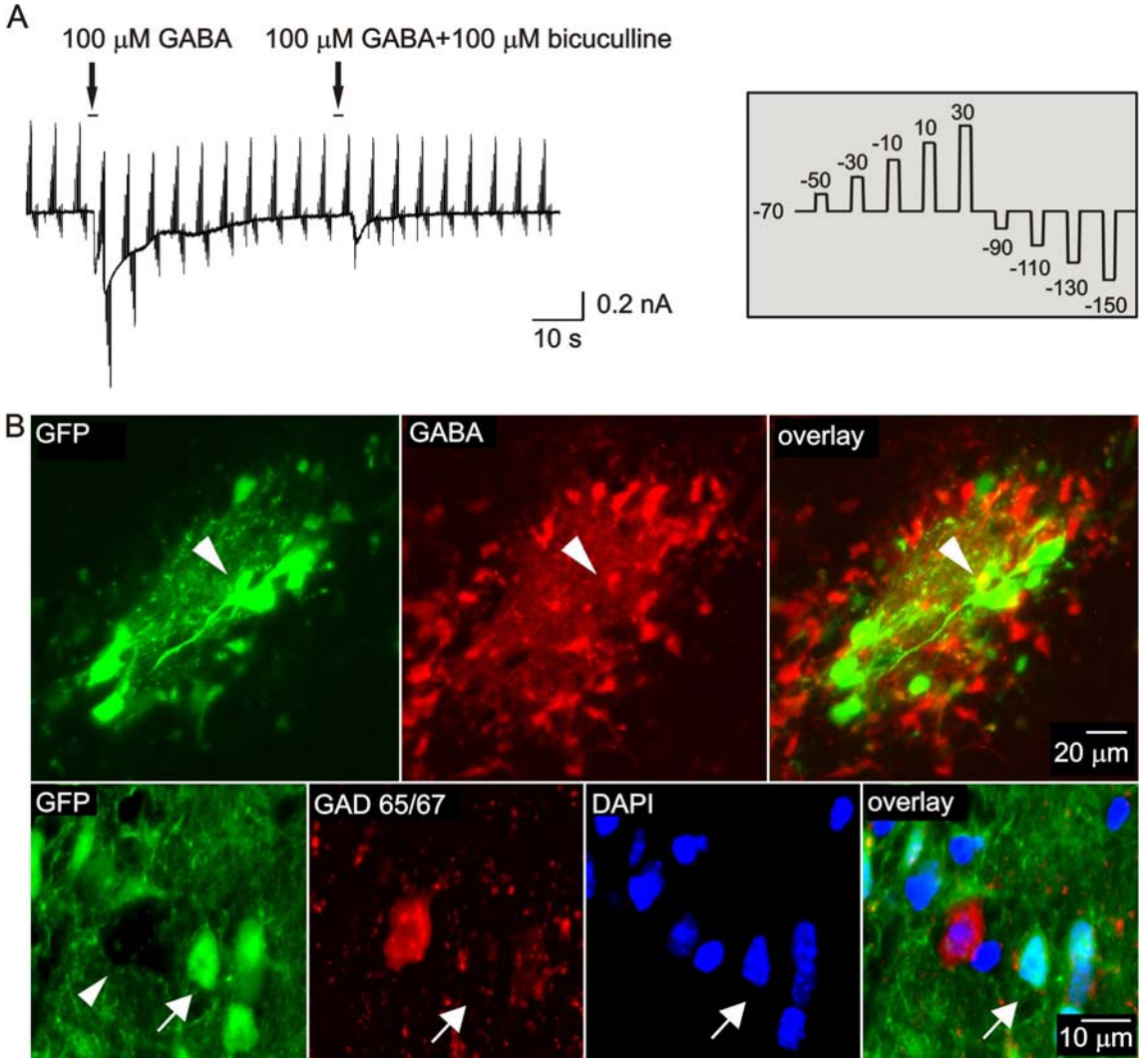

(A) A typical inward current evoked by the application of 100 μM GABA and blocked by 100 μM bicuculline. The currents were obtained by clamping the cell membrane potential to different values, by rectangular voltage steps, from a holding potential of -70 mV to potentials ranging from -150 mV to +30 mV (see the inset). **(B)** Images showing GABA immunoreactivity (red) in D6-GFP cells (green), 1 week after transplantation into the intact brain **(top)** and images showing GAD65/67 immunoreactivity (red) in D6-GFP cells (green) in the adult brain of a D6-GFP transgenic mouse **(bottom)**. Note that the majority of GABA-positive cells are GFP-negative and that unlike in D6-GFP cells differentiated *in vitro* (for comparison see Fig. 24), GAD65/67 immunoreactivity does not overlap with GFP signal.

D6-GFP-derived neuronal cells also displayed K_A and K_{DR} currents sensitive to 4-AP. The application of 4-AP resulted in a 69.7 ± 7.4% and a 54.7 ± 5.4% (n=9) decrease in K_A and K_{DR} currents, respectively. The additional application of TEA caused no further decrease in the K_A or K_{DR} current amplitudes. Interestingly, several cells, displaying similar passive membrane properties as D6-GFP-derived neuronal cells, showed a

different expression of voltage-gated ion channels. Three cells expressed Na^+ and K_{DR} currents, but lacked a K_A current, and 6 cells expressed only a K_{DR} current.

The passive membrane properties and current patterns of D6-GFP-cells transplanted into the photochemical lesion (n=15) were comparable to those recorded after transplantation into the intact rat cortex. In 73.3% (11/15) of the cells, a TTX-sensitive Na^+ current was detected, while 77.7% (7/9) of the cells were able to fire an AP after current injection and 4 out of 7 fired more than once. The membrane properties of cells recorded *in situ* are summarised in **Table 5** and compared to the properties of cells differentiated *in vitro*. AP characteristics, such as AP amplitude, AP duration and the number of APs per trace, were also compared between cells differentiated *in vitro* and *in vivo*. After transplantation into a photochemical lesion or into the intact cortex, D6-GFP-derived neuronal cells were able to fire a comparable number of APs per trace; also, the AP amplitude and duration were similar. However, the AP characteristics of *in vivo* derived neuronal cells were significantly different from those derived *in vitro*. D6-GFP *in vivo* derived neuronal cells displayed a higher number of APs per trace with higher amplitudes, though, surprisingly, with a longer duration, when compared to *in vitro* derived neuronal cells **(Fig. 35C)**.

In conclusion, these data suggest that D6-GFP NS/PCs transplanted into the lesioned rat brain give rise to neuronal cells displaying functional properties comparable to those of cells transplanted into the intact brain.

5.3 Diverse effects of Sonic hedgehog and Wnt-7a on the differentiation of neonatal neural stem/progenitor cells *in vitro*

5.3.1 Wnt-7a suppresses the incidence of GFAP-positive cells in neurospheres

Control, Shh- and Wnt-7a-expressing neonatal NS/PCs were defrosted and cultured under proliferating conditions and neurospheres after 2-4 passages were used for further experiments. Within this range all neurospheres consistently expressed GFP, and Western blot analysis confirmed the up-regulation of Wnt/β-catenin and Shh signalling pathways. Compared to control cells, Shh-expressing cells showed an increased expression of Gli1 and Wnt-7a-expressing cells a higher level of β-catenin (see **Fig. 8B** in Materials and Methods).

To explore the effect of both morphogenes on the expression of NS/PC markers, the neurospheres were analyzed using immunocytochemistry and Western blotting. The following markers were used: nestin, GFAP, BLBP, NG2 proteoglycan, Mash1, Olig2, Dlx2 and DCX. The immunocytochemical analysis revealed that all neurospheres ubiquitously expressed nestin **(Fig. 37A)**. They further expressed GFAP and NG2 **(Fig. 37C, 38A)**. In contrast to control and Shh-expressing neurospheres, Wnt-7a-expressing neurospheres contained a significantly lower number of GFAP-positive cells **(Fig. 37C, 35A)**, while the majority of cells expressed NG2. Since GFAP and NG2 immunoreactivity did not overlap (see details in **Fig. 38A)**, we can conclude that neonatal neurospheres are formed by two separate cell populations and that in Wnt-7a-expressing neurospheres, the population of GFAP-positive cells is markedly reduced.

Western blot analysis confirmed the marked down-regulation of GFAP (~50 kDa band) in Wnt-7a- expressing neurospheres when compared to controls **(Fig. 38B)**, and it further showed that the ~50 kDa band was also down-regulated in Shh-expressing neurospheres. Further, 3 additional bands (a ~40 kDa band and two bands of ~60 kDa) were detected in control neurospheres, probably corresponding to the existence of various GFAP isoforms (Roelofs et al., 2005). In Shh- and Wnt-7a-expressing neurospheres these additional bands were not detected (see the intensity profiles in **Fig. 38B)**. Western blot analysis further showed that control, Shh- and Wnt-7a- expressing neurospheres expressed to a similar extent BLBP, Olig2 and Mash1 **(Fig. 38C)**.

Fig. 37 Immunocytochemical analysis of neonatal control, Shh- and Wnt-7a-expressing neurospheres

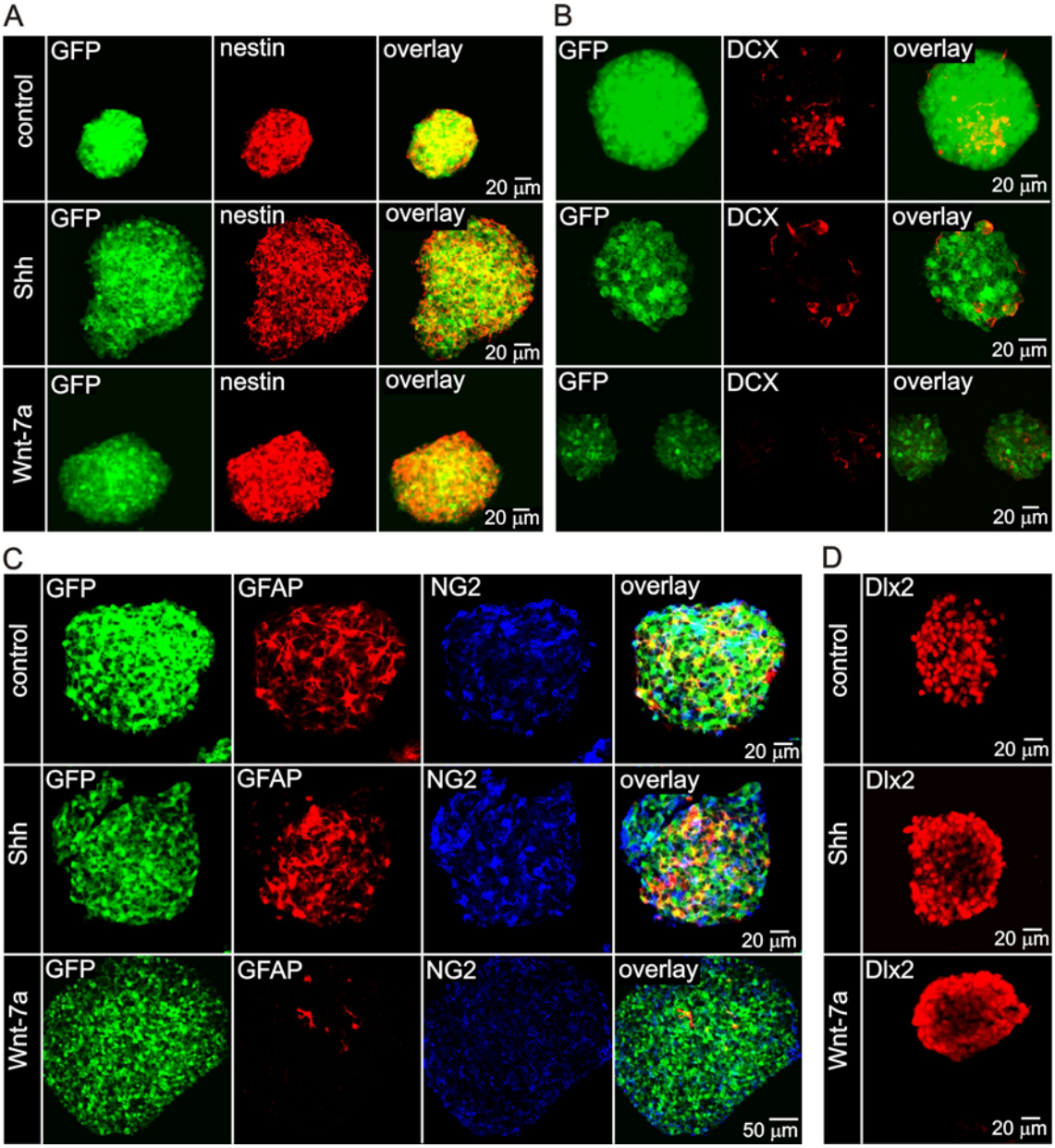

Images showing the expression of nestin **(A)**, DCX **(B)**, GFAP and NG2 **(C)** and Dlx2 **(D)** in control, Shh- and Wnt-7a-expressing neurospheres. Note the reduction in GFAP immunoreactivity in the Wnt-7a-expressing neurospheres.

Additionally, DCX was detected in control as well as in morphogene-expressing neurospheres **(Fig. 37B)**. However, Western blotting showed, that in both Shh- and Wnt-7a-expressing neurospheres, the ~40 kDa band corresponding to DCX was reduced, suggesting that the incidence of neuroblasts in these neurospheres is suppressed **(Fig. 38B)**.

Fig. 38 Detailed immunocytochemical analysis and Western blotting of control, Shh- and Wnt-7a-expressing neurospheres

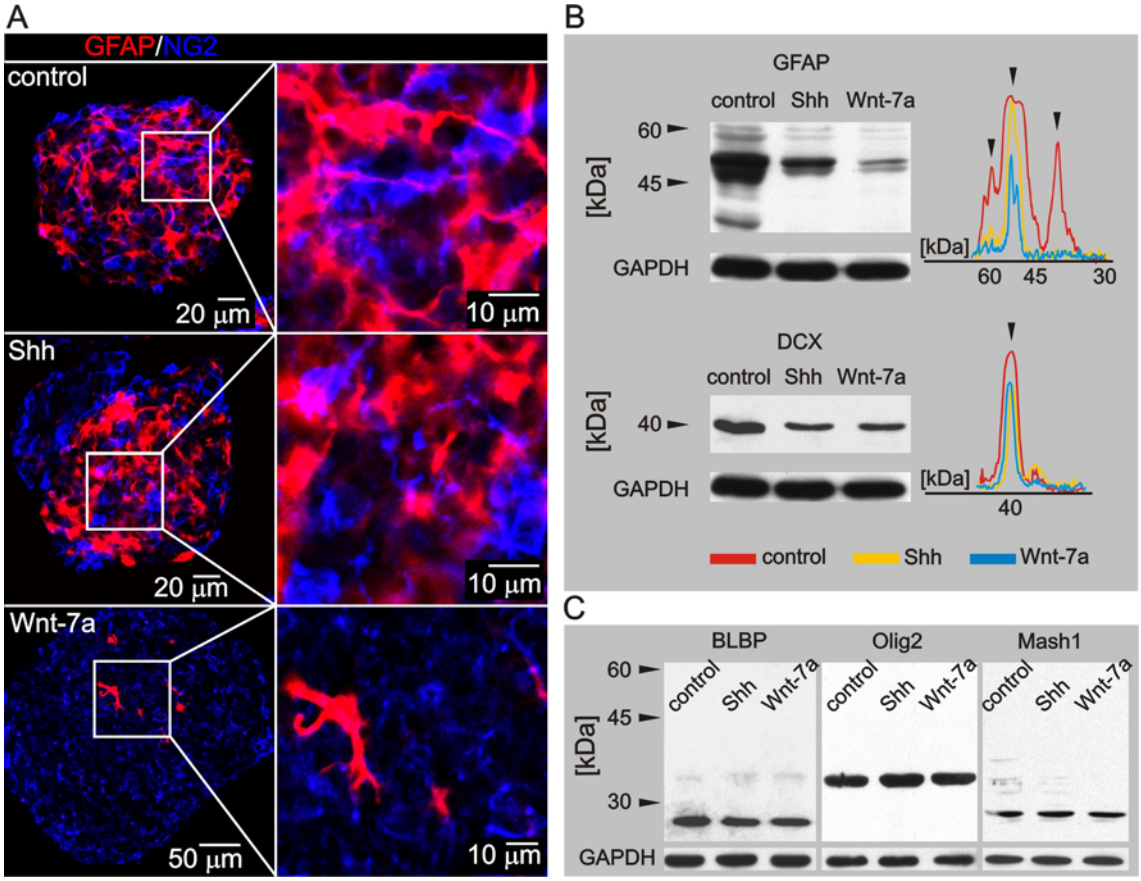

(A) Immunocytochemical analysis of neurospheres showing double staining for GFAP (red) and NG2 (blue) in the entire neurosphere **(left)** and in a detail **(right)**. Note that Wnt-7a-expressing neurospheres contain a negligible number of GFAP-positive cells, while the majority of cells express NG2. **(B)** Western blot analysis of cell lysates from neurospheres showing the differences in GFAP and DCX expression **(left)** and intensity profiles representing the number and size of the respective bands marked by arrowheads **(right)**. **(C)** Western blot analysis showing similar levels of BLBP, Olig2 and Mash1 expression in lysates from control, Shh- and Wnt-7a-expressing neurospheres.

Since it was shown that Shh and Wnt/β-catenin signalling might affect NS/PC proliferation, we investigated the effect of these morphogenes on neurosphere size. The analysis revealed that both Shh- and Wnt-7a-expressing cells formed significantly larger neurospheres than did control cells **(Fig. 39)**. The average diameter of neurospheres was 132.9 ± 4.0 µm (n=175) in control, 192.1 ± 7.8 µm (n=150) in Shh- and 191.6 ± 4.8 µm (n=152) in Wnt-7a-expressing cells.

Together, our data show that neurospheres derived from the neonatal forebrain contain neural stem as well as progenitor cells and that Wnt-7a expression leads to a marked reduction of GFAP-positive neural stem cells.

Fig. 39 Shh and Wnt-7a increase the size of neurospheres

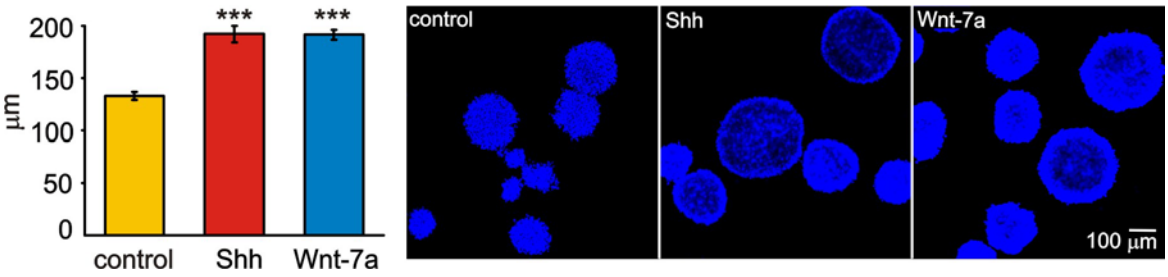

Graph showing the size of neurospheres after one week of *in vitro* cultivation **(left)** demonstrating that both Shh- and Wnt-7a-expressing NS/PCs produced significantly larger neurospheres than did control cells **(right)**. Asterisks indicate significant differences between Shh- or Wnt-7a-expressing neurospheres and control neurospheres; * $p < 0.05$; ** $p < 0.01$, *** $p < 0.001$.

5.3.2 Shh and Wnt-7a increase the expression of neuronal markers 8 days after the onset of *in vitro* differentiation

Eight days after the onset of *in vitro* differentiation, control, Shh- and Wnt-7a-expressing NS/PCs gave rise to 3 morphologically distinct cell populations. Large flat cells with a cell body diameter of ~30-40 µm formed an underlying layer and expressed GFAP and nestin **(Fig. 40A)**, and were Dlx2-negative **(Fig. 40D, E)**. The second population of cells with a triangular cell body (diameter of ~20 µm) expressed predominantly NG2-proteoglycan **(Fig. 40B)** and were weakly Dlx2-positive **(Fig. 40E)**, while the third population comprised cells with a cell body diameter of ~10 µm. These cells were βIII tubulin-, DCX- or MAP-2-positive and additionally they were strongly Dlx2-positive **(Fig. 40C-E)**. Further analysis of these cells revealed that in many of them, NG2 co-localised with neuronal markers **(Fig. 41A)**. No cells were positive for oligodendrocyte precursor markers, such as O4, or markers of mature oligodendrocytes, such as MOSP or APC. Western blot analysis showed, however, that all cultures expressed Olig2 to a similar extent **(Fig. 42A)**.

Fig. 40 Morphology and immunocytochemical analysis of cells in controls, 8 days after the onset of *in vitro* differentiation

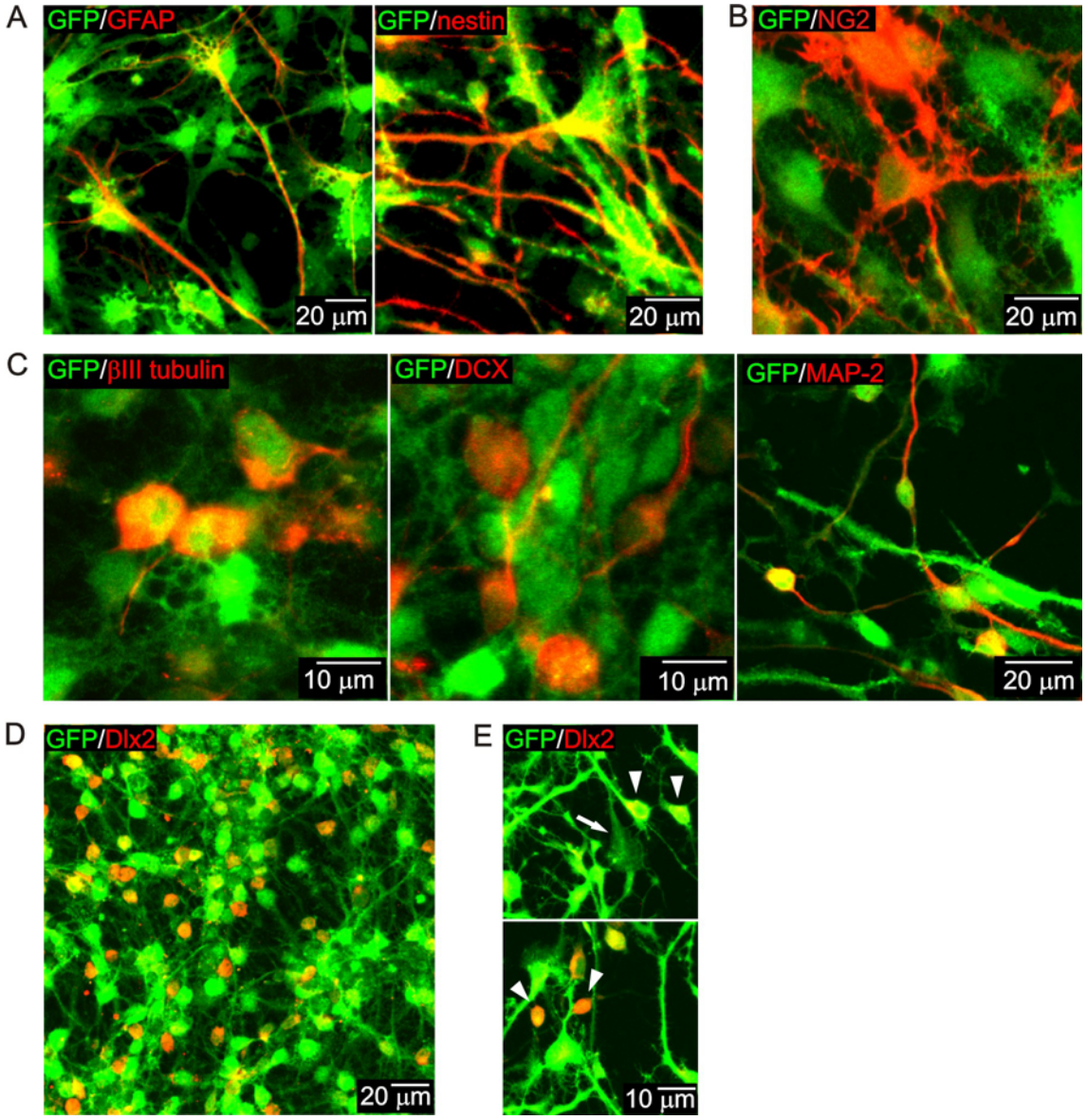

(A) Large flat cells expressed GFAP and nestin. **(B)** Cells with a triangular body expressed NG2. **(C)** Cells with a small round body and one or several cell processes were βIII-, DCX- or MAP-2-positive. **(D)** An image showing Dlx2 staining. **(E)** Detailed images showing Dlx2-negative large flat cells (top, arrow), triangular cells with moderate expression of Dlx2 (top, arrowheads) and small round cells with strong expression of Dlx2 (bottom, arrowheads).

Fig. 41 Immunocytochemical analysis of control, Shh- and Wnt-7a-expressing cell cultures, 8 days after the onset of *in vitro* differentiation

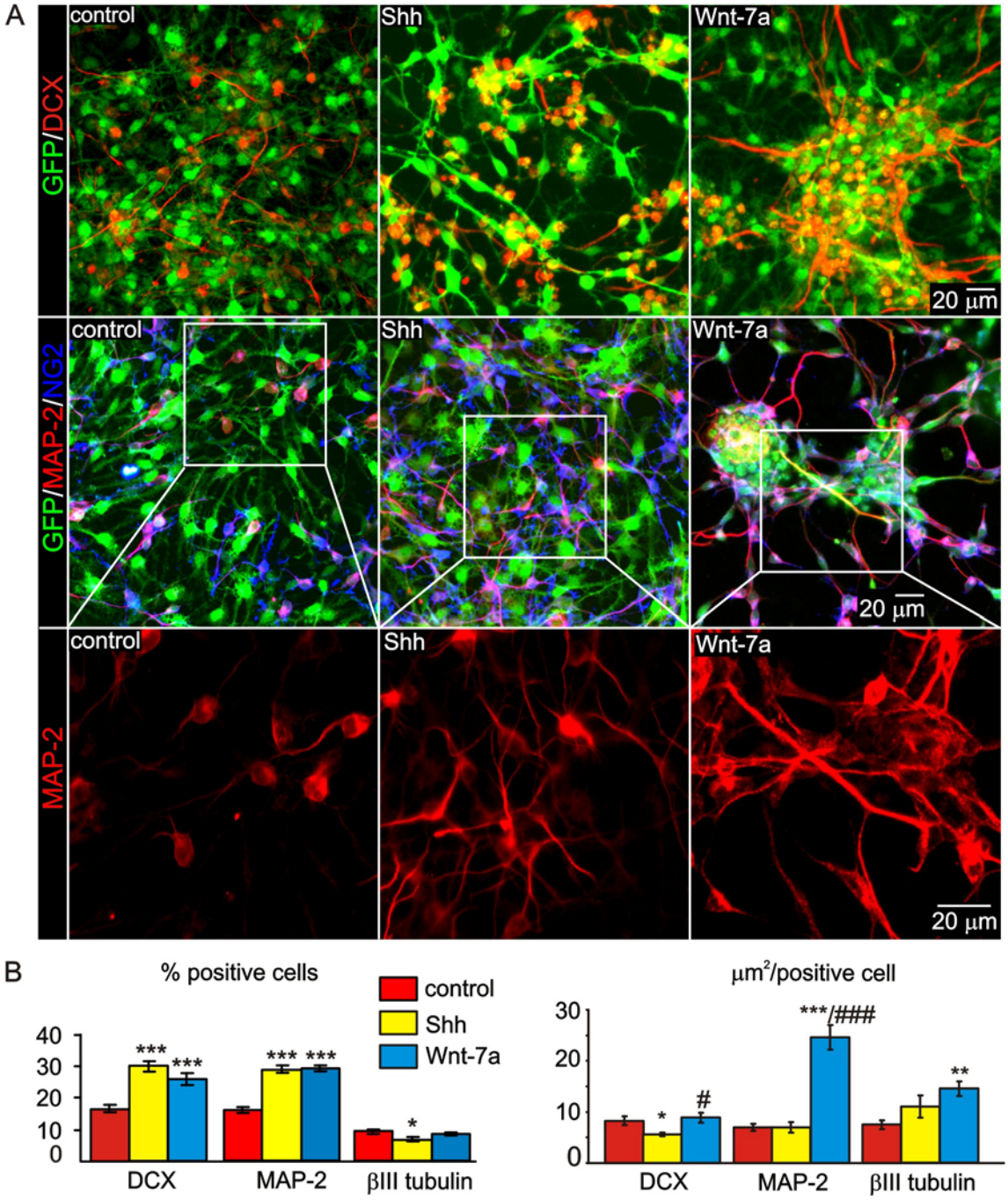

(A) Representative images of DCX **(top)** and MAP-2/NG2 **(middle)** stainings and detailed images showing MAP-2 staining for each cell culture **(bottom)**. **(B)** Quantitative analysis of DCX, MAP-2 and βIII tubulin expression showing the proportion of positively-stained cells in the respective cell culture **(left)** and the mean area of neuronal marker immunoreactivity found on a single positive cell **(right)**; n=15 (number of zones used for analysis). Asterisks indicate significant differences between Shh- or Wnt-7a-expressing cell cultures and controls; crosshatches indicate significant differences between Shh- and Wnt-7a-expressing cell cultures; */# p< 0.05; **/## p< 0.01, ***/### p< 0.001.

Fig. 42 Western blot analysis of glial marker levels in control, Shh-expressing and Wnt-7a-expressing differentiated cell cultures

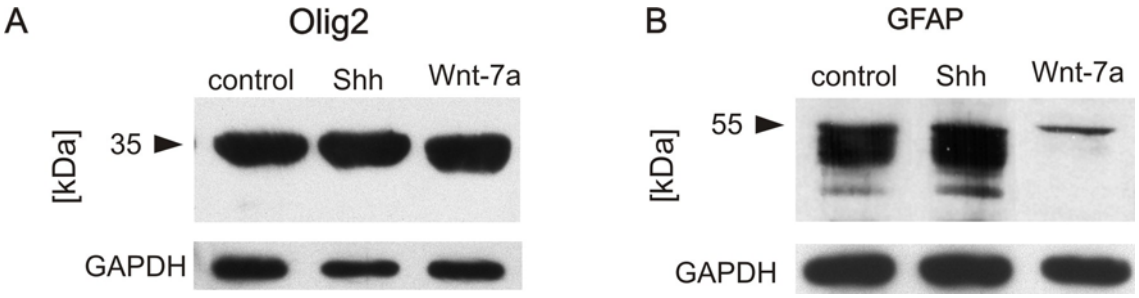

(A) Western blot analysis showing similar expression of the transcription factor Olig2 in control, Shh- and Wnt-7a-expressing cell cultures. **(B)** Decreased expression of GFAP in Wnt-7a expressing cell cultures, 8 days after the onset of *in vitro* differentiation.

To study the effects of Shh and Wnt-7a on the generation and morphological development of neuronal cells, quantitative analysis of neuronal marker expression was performed. First, the numbers of DCX-, MAP-2- and βIII tubulin-positive cells were determined and expressed as percentages of total cell numbers. To follow cell development in more detail, the mean area of neuronal marker immunoreactivity found on a single positive cell was determined **(Fig. 41, 43)**. Quantitative analysis revealed that both Shh and Wnt-7a increased the number of newly derived DCX-positive cells **(Fig. 41B)**; however, DCX expression in individual cells differed. In both control and Wnt-7a-expressing cells, DCX was expressed in the cell soma as well as in the majority of cell processes, while in Shh-expressing cells DCX expression was limited mainly to the cell soma **(Fig. 41A, B)**. Quantifying DCX immunoreactivity confirmed that in control and Wnt-7a-expressing cell cultures the average areas of DCX immunoreactivity in a single cell were comparable (8.3 ± 0.9 and 8.9 ± 0.9 μm^2; n=15), while in Shh-expressing cell cultures the average area was decreased (5.6 ± 0.4 μm^2, n=15; **Fig. 41B)**. Also, the number of maturing MAP-2-positive cells was significantly increased by both Shh and Wnt-7a; however, only Wnt-7a increased the expression of MAP-2 in individual cells **(Fig. 41A)**. Quantification of the area that corresponded to MAP-2 immunoreactivity in single cells revealed comparable values in controls and Shh-expressing cell cultures (6.9 ± 0.6 and 7.0 ± 1.0 μm^2, n=15), while in Wnt-7a-expressing cells the average area of MAP-2 immunoreactivity markedly increased (24.6 ± 2.4 μm^2, n=15; **Fig. 41B)**. Finally, Shh decreased the number of differentiating βIII tubulin-positive cells, while Wnt-7a did not affect their numbers. Further, only Wnt-7a increased the area of βIII tubulin staining in individual cells to 14.5 ± 1.5 μm^2 compared

to 7.5 ± 0.9 μm^2 in controls and 11.0 ± 2.2 μm^2 in Shh-expressing cell cultures (n=15; **Fig. 41B)**. The increase in DCX and MAP-2 expression caused by Shh and Wnt-7a was confirmed by Western blot analysis **(Fig. 44)**.

Fig. 43 Images used for the quantitative analysis of the immunocytochemistry

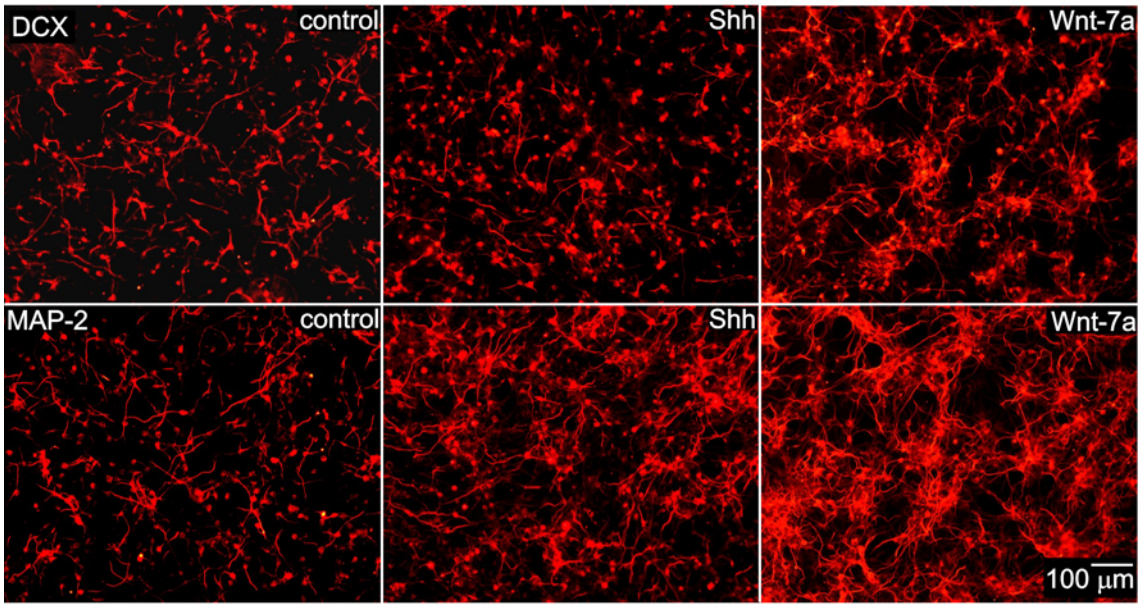

Images of DCX **(top)** and MAP-2 **(bottom)** immunoreactivity, which were used for the quantitative analysis of neuronal marker expression, 8 days after the onset of *in vitro* differentiation.

Additionally, both Shh and Wnt-7a increased the expression of Mash1, a known downstream target of the Shh signalling pathway **(Fig. 44,** Wang et al., 2007b). Similarly to neurospheres, GFAP levels were markedly down-regulated in Wnt-7a-expressing cell cultures **(Fig. 42)**.

Together, the immunocytochemical and Western blot analyses show that both morphogenes promote neuronal generation *in vitro*; however, only Wnt-7a increases the expression of neuronal markers in differentiating and maturing cells.

Fig. 44 Western blot analysis of the lysates of differentiated cells harvested 8 days after the onset of *in vitro* differentiation

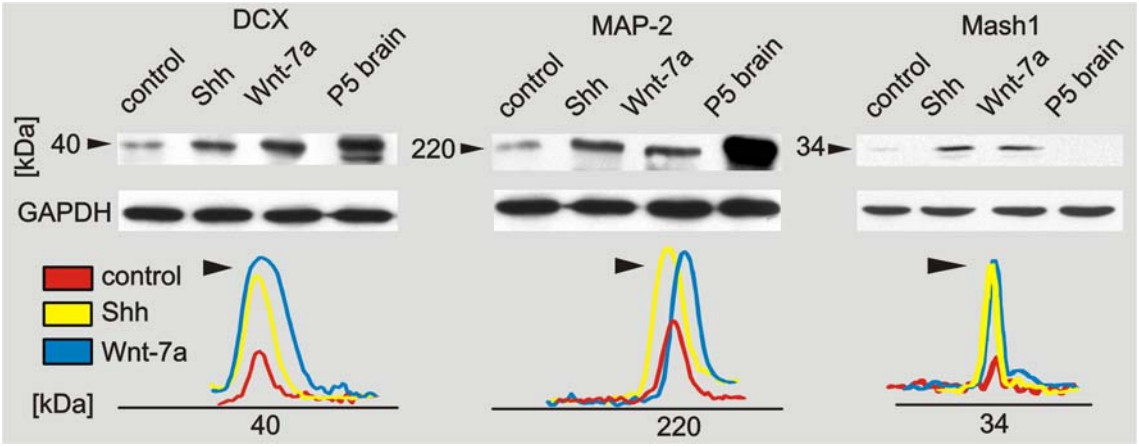

Eight days after the onset of *in vitro* differentiation, Shh- and Wnt-7a-expressing cell cultures show increased expression of Mash1, DCX and MAP-2 **(top)** and the intensity profiles representing the size of the respective bands marked by arrowheads **(bottom)**.

5.3.3 Shh and Wnt-7a affect cell proliferation during *in vitro* differentiation

Since the number of cells increased during the course of differentiation, presumably due to the presence of bFGF, the proliferation of NS/PCs was followed. The cells were loaded with 10 μM BrdU for 24 hours, two or seven days after the onset of *in vitro* differentiation. The analysis revealed that 3 days after the onset of *in vitro* differentiation, the number of proliferating BrdU-positive cells was significantly increased in both Shh- and Wnt-7a-expressing cultures (53.9 ± 1.8% and 68.1 ± 2.5%, respectively), when compared to controls (45.4 ± 3.0%, n=15; **Fig. 45A)**. However, after 8 days only Shh-expressing cell cultures showed increased proliferation (37.5 ± 3.0%) when compared to controls (26.1 ± 1.8%) and Wnt-7a-expressing cell cultures (28.0 ± 1.5%, n=15; **Fig. 45B)**. Most of the proliferating cells were NG2-positive. In addition, DCX/BrdU-positive cells in close apposition and with no cell processes were detected, suggesting that these cells also proliferate **(Fig. 45C)**.

In addition, a TUNEL assay was performed to investigate the possible effect of the morphogenes on ongoing apoptosis during differentiation and to exclude the possibility that the higher number of BrdU-positive cells might correlate with apoptotic cells as shown by Kuan et al., (2004) and Bauer and Patterson, (2005). The results showed that 8 days after the onset of *in vitro* differentiation, there was no significant difference in the number of TUNEL-positive cells among the cell cultures (2.5 ± 0.4% in controls, 1.8 ± 0.4% in Shh- and 1.6 ± 0.4% in Wnt-7a-expressing cell cultures, n=9).

Together, these data show that under our experimental conditions, both morphogenes support proliferation at the onset of *in vitro* differentiation, while later on, only Shh significantly increases the number of proliferating cells.

Fig. 45 Proliferation rate in control, Shh- and Wnt-7a-expressing cell cultures during *in vitro* differentiation

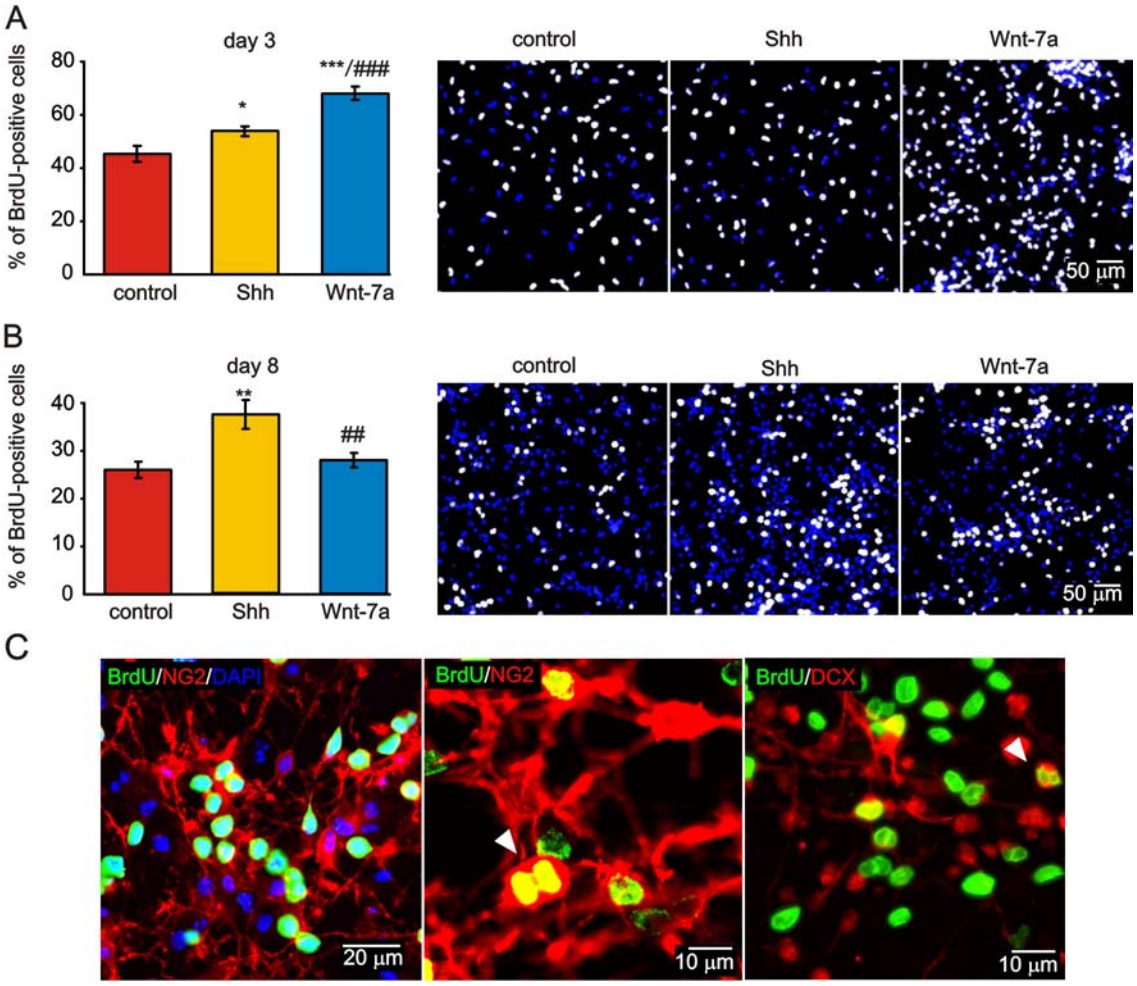

(A) The proportion of BrdU-positive cells at day 3 of *in vitro* differentiation **(left)** and representative images of BrdU (white) and DAPI (blue) staining **(right)**. **(B)** The proportion of BrdU-positive cells at day 8 of *in vitro* differentiation **(left)** and representative images of BrdU (white) and DAPI (blue) staining **(right)**; n=15 (number of zones used for the analysis shown in A and B). **(C)** Images of BrdU-positive cells (green) immunostained for NG2 and DCX (red), 8 days after the onset of *in vitro* differentiation. DAPI (blue) was used to visualize the cell nuclei. Yellow colour indicates the overlay of the red and green signals. White colour indicates the overlay of all three signals. Asterisks indicate significant differences between Shh- or Wnt-7a-expressing cell cultures and controls; crosshatches indicate significant differences between Shh- and Wnt-7a-expressing cell cultures; */# $p < 0.05$; **/## $p < 0.01$, ***/### $p < 0.001$.

5.3.4 Shh and Wnt-7a expression affects the membrane properties of NS/PCs 8 days after the onset of *in vitro* differentiation

Using the patch-clamp technique in the whole-cell configuration, 3 distinct current patterns were detected 8 days after the induction of differentiation in controls as well as in cell cultures expressing the morphogenes: a passive current pattern represented by symmetrical, time- and voltage-independent passive currents, a complex current pattern represented by inwardly- and outwardly rectifying K^+ currents, and a neuron-like current pattern represented by outwardly rectifying K^+ currents and TTX-sensitive Na^+ currents. To follow the current pattern distribution within each cell culture, 10-15 cells were recorded in each field imaged by a digital camera, in 5 independent experiments **(Fig. 46)**.

Fig. 46 Current pattern distribution in control, Shh- and Wnt-7a-expressing cell cultures, eight days after the onset of *in vitro* differentiation

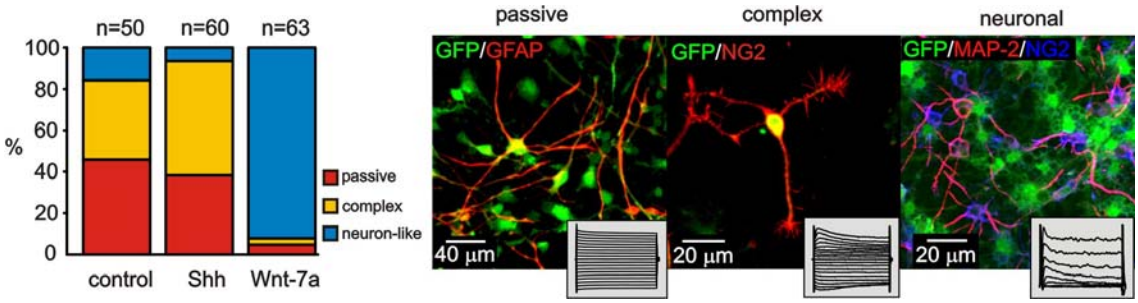

The proportion of individual current patterns in control, Shh- and Wnt-7a-expressing cell cultures, eight days after the onset of *in vitro* differentiation, demonstrating a reduced incidence of passive and complex current patterns in Wnt-7a-expressing cell cultures and an increased number of cells displaying a complex current pattern in Shh-expressing cell cultures when compared to the current pattern distribution in controls **(left)**; representative images showing the typical morphology and immunocytochemical identification of cells with the respective current patterns **(right)**.

5.3.5 Wnt-7a expression decreases the incidence of cells with a passive current pattern and affects their membrane properties

In controls, large flat cells of the underlying layer expressed symmetrical, time- and voltage-independent passive currents, a hyperpolarised resting membrane potential (V_{rest}, -86.4 ± 1.5 mV), low input resistance (IR, 70.7 ± 8.2 MΩ) and high membrane capacitance (C_m, 33.9 ± 5.5 pF, n=21; see **Table 6)**. These cells were further termed "passive cells", and they represented 46 % of the initially recorded cells (23 cells out of

50, **Fig. 46)**. All these cells were identified post-recording as GFAP-positive **(Fig. 46, 47A)**. Further pharmacological analysis showed the presence of a K_{IR} current (in 8 cells out of 12), which was revealed by the application of 1 mM CsCl **(Fig. 47B, C)**. The K_{IR} current densities are shown in **Table 6**. To characterise the main ionic components of the passive currents, a 50 mM K^+ solution was applied to the passive cells, as described previously (Jelitai et al., 2007). The elevated extracellular K^+ shifted the average V_{rev} from -81.2 ± 1.8 mV to -27.7 ± 1.3 mV (ΔV_{rev}= 54.2 ± 1.3, n=6, Fig. **47D, 48A)**, a value comparable with the theoretical value of V_{rev} calculated from the Nernst equation (-24.5 mV). Therefore, the major components carried by the passive currents are K^+ ions. The application of 10 mM $BaCl_2$ reduced the passive currents by 86.1 ± 2.8% **(Fig. 48B)** and revealed an outward current, presumably a K_{DR} current (in 13 cells out of 13; **Fig. 47E, F)**. It also shifted the V_{rev} from -86.4 ± 1.0 mV to -60.0 ± 2.7 mV (ΔV_{rev}=25.8 ± 2.9; n=13; **Fig. 48C)**. The application of 5 mM 4-AP decreased the amplitude of the K_{DR} current in these cells by 34.9 ± 4.5%, while the subsequent addition of 10 mM TEA further diminished the current amplitude **(Fig. 48E, F)** resulting in a 55.5 ± 5.7% blockage of the K_{DR} current (n=13, **Table 6)**.

Since GABA plays an important role in neurogenesis (Nakamichi et al., 2009), the functional expression of ionotropic $GABA_A$ receptors was investigated. However, a 1s application of 100 μM GABA evoked no response in passive cells (13 cells out of 13; data not shown).

Table 6 Membrane properties of passive cells 8 days after the onset of *in vitro* differentiation

passive		control	Shh	Wnt-7a
V_{rest}	[mV]	-86.4 ± 1.5	-84.8 ± 3.2	-64.7 ± 1.6***/###
C_m	[pF]	33.9 ± 5.5	39.8 ± 6.9	18.2 ± 2.0**/##
IR	[MΩ]	70.7 ± 8.2	55.3 ± 5.3	130.7 ± 13.8**/###
n		21	14	31
K_{DR}/C_m	[pA/pF]	13.1 ± 2.1	9.3 ± 1.4	30.3 ± 4.0***/##
n		13	7	16
K_{IR}/C_m	[pA/pF]	31.9 ± 5.8	27.1 ± 7.3	(12.5; 6.1)[a]
n		8	8	2
K_{DR} + 4-AP	[%]	34.9 ± 4.5	52.4 ± 7.5	38.7 ± 7.2
K_{DR} + 4-AP + TEA	[%]	55.5 ± 5.7	56.9 ± 7.2	51.0 ± 9.6
n		13	7	5
GABA/C_m	[pA/pF]	---	3.2 ± 1.2	13.6 ± 3.1□□□###
n		---	5	5

V_{rest}: resting membrane potential; **C_m:** membrane capacitance; **IR:** input resistance; **K_{DR}/C_m, K_{IR}/C_m, GABA/C_m:** K_{DR}, K_{IR} and GABA current densities; **n**: number of cells; **K_{DR} + 4-AP, K_{DR} + 4-AP + TEA:** relative amplitude decrease after the application of 4-AP (4-aminopyridine) or 4-AP in combination with TEA (tetraethylamonium chloride). Asterisks indicate significant differences between Shh- or Wnt-7a-expressing passive cells and control passive cells; crosshatches indicate significant differences between Shh- and Wnt-7a-expresssing passive cells; */# $p < 0.05$; **/## $p < 0.01$, ***/### $p < 0.001$. [a] values of individual cells.

Fig. 47 Electrophysiological characterisation of passive cells, 8 days after the onset of *in vitro* differentiation

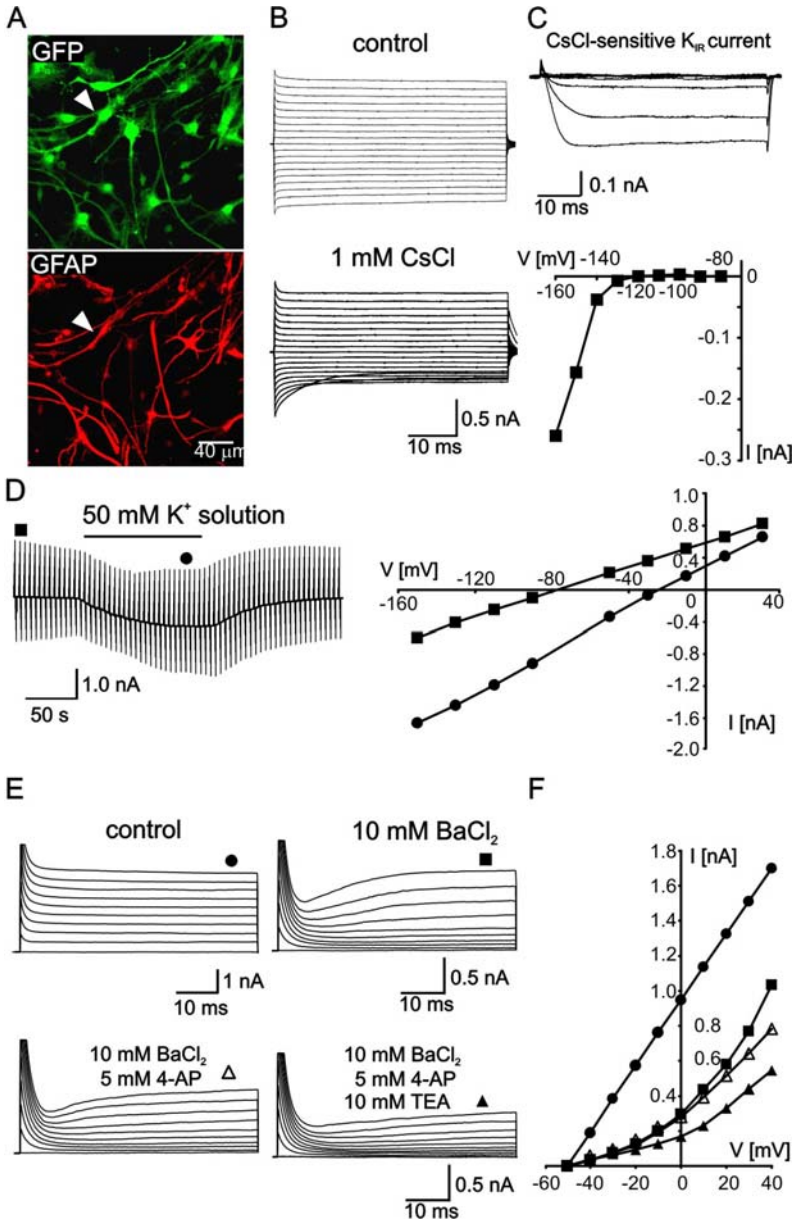

(A) Immunocytochemical identification of a recorded cell (indicated by arrowhead, **top)**, showing positive staining for GFAP **(bottom)**. **(B)** Typical current pattern of a large flat passive cell in control culture obtained by hyper- and depolarising the cell membrane from a holding potential of -70 mV to potentials ranging from -160 mV to +20 mV, prior to **(top)** and after the application of 1 mM CsCl **(bottom)**. **(C)** The subtracted CsCl-sensitive K_{IR} current **(top)** and its I/V relationship **(bottom)**. **(D)** A typical inward current and membrane depolarisation evoked by a 2-min application of a 50 mM K^+-solution **(left)** and the resulting I/V relationship **(right)** for traces recorded in ACF (filled squares) and 50 mM K^+ solution (filled circles), showing the shift of V_{rev}. **(E)** Typical current pattern of a large flat passive cell obtained by depolarising the cell membrane from a holding potential of -70 mV to potentials ranging from -160 mV to +20 mV, prior to and after the application of 10 mM $BaCl_2$ **(top)**, revealing a K_{DR} current sensitive to the application of 5 mM 4-AP and a subsequent application of 10 mM TEA **(bottom)**. **(F)** I/V relationships for the passive current pattern recorded in ACF (control, filled circles), after the application of 10 mM $BaCl_2$ (filled squares), 5 mM 4-AP (empty triangles) and 10 mM TEA (filled triangles).

Fig. 48 The effect of Shh and Wnt-7a on the pharmacological properties of passive currents

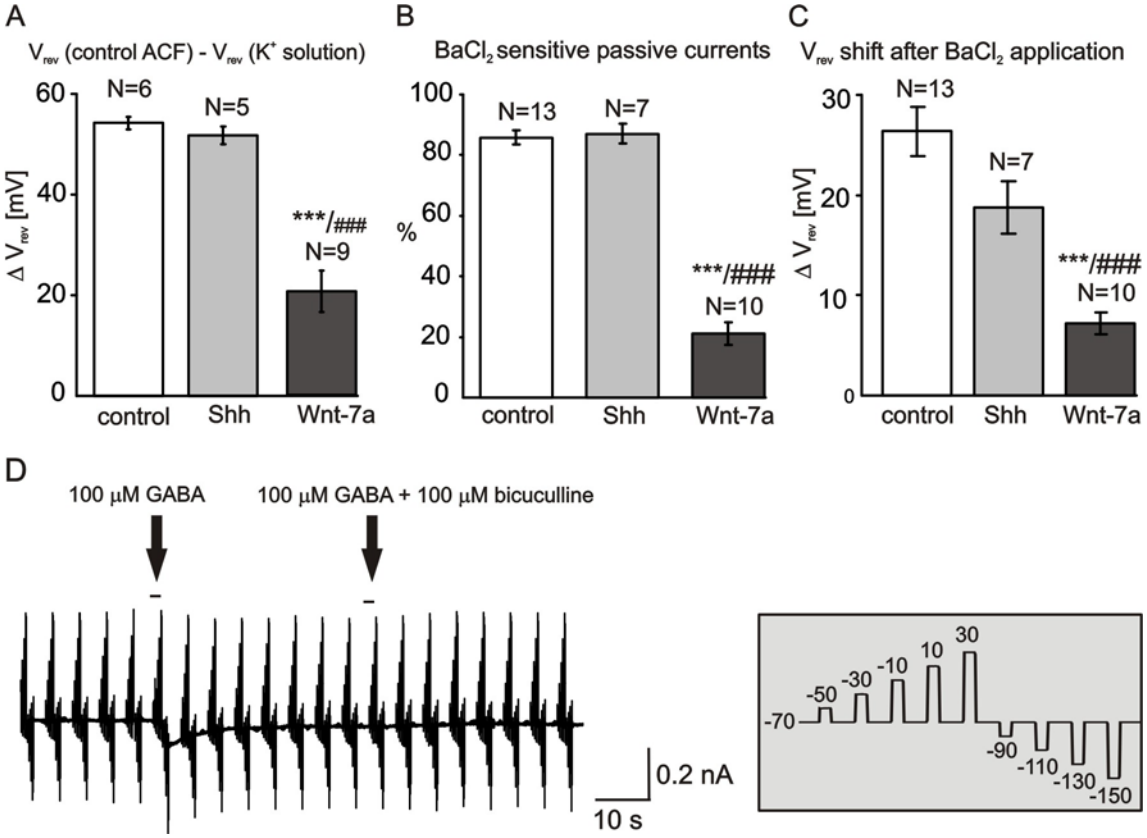

(A) The V_{rev} shift during the application of 50 mM K^+ solution showing a significantly smaller V_{rev} shift in Wnt-7a-expressing passive cells. **(B)** The proportion of $BaCl_2$-sensitive K^+ passive currents showing that Wnt-7a-expressing passive cells contained only ~20 % of $BaCl_2$-sensitive K^+ passive currents. **(C)** The V_{rev} shift in passive cells during the application of 10 mM $BaCl_2$, showing a significantly smaller V_{rev} decrease in Wnt-7a-expressing passive cells. **(D)** A typical inward current evoked by the application of 100 μM GABA in Shh-expressing cells that was completely blocked by the application of 100 μM bicuculline. The currents were obtained by clamping the cell membrane potential to different values, by rectangular voltage steps, from a holding potential of -70 mV to potentials ranging from -150 mV to +30 mV (see the inset). Asterisks indicate significant differences between Shh- or Wnt-7a-expressing passive cells and control passive cells; crosshatches indicate significant differences between Shh- and Wnt-7a-expresssing passive cells; */# $p< 0.05$; **/## $p< 0.01$, ***/### $p< 0.001$.

Cells displaying a passive current pattern were also detected in Shh-expressing cell cultures and represented 38.3% of the initially recorded cells (23 cells out of 60, **Fig. 46)**. Their morphology and membrane properties were similar to those recorded in controls **(Table 6)**. The application of 1 mM CsCl revealed a K_{IR} current in all tested cells (n=8, **Table 6)**. During the application of a 50 mM K^+ solution, the average V_{rev} shifted from -83.0 ± 2.1 mV to -31.2 ± 2.4 mV, resulting in a similar V_{rev} shift as observed in controls (ΔV_{rev}= 51.7 ± 1.7, n=5; **Fig. 48A)**. The application of 10 mM $BaCl_2$ reduced the passive currents by 87.0 ± 3.2% **(Fig. 48B)**, shifted the V_{rev} from -

83.1 ± 2.0 mV to -64.3 ± 1.7 mV (ΔV_{rev}=18.7 ± 2.6, n=7; **Fig. 48C)** and revealed a K_{DR} current in 7 cells out of 7. The sensitivity of the K_{DR} current to 4-AP and 4-AP in combination with TEA was not significantly different from that observed in controls **(Table 6)**. Interestingly, in 5 out of 11 passive cells, the application of 100 μM GABA evoked a bicuculline-sensitive inward current **(Fig. 48D)**.

In contrast, the incidence of cells with a passive current pattern in Wnt-7a-expressing cell cultures was reduced; such cells represented only 4.8% of the initially recorded cells (3 cells out of 63, **Fig. 46)**. Moreover, Wnt-7a had a significant effect on their membrane properties. These cells displayed a smaller C_m, more depolarised V_{rest} and higher IR, when compared to both control and Shh-expressing passive cells **(Table 6)**. The application of 1 mM CsCl revealed a K_{IR} current only in 2 out of 10 cells, and during the application of a 50 mM K^+ solution the V_{rev} shifted from -61.3 ± 2.0 mV to -41.0 ± 4.4 mV, resulting in a smaller V_{rev} shift when compared to Shh-expressing and control passive cells (ΔV_{rev}=20.6 ± 4.1, n=9, **Fig. 48A)**. Furthermore, the passive currents also showed a decreased sensitivity to the application of 10 mM $BaCl_2$ (21.5 ± 4.2 %, n=10; **Fig. 48B)**, and the V_{rev} shifted less when compared to control and Shh-expressing passive cells (from -65.7 ± 2.1 mV to -58.5 ± 2.9 mV, ΔV_{rev}=7.2 ± 2.3, n=10, **Fig. 48C)**. Interestingly, the K_{DR} current in these cells was detected prior to $BaCl_2$ application, and its current density was significantly higher when compared to the K_{DR}/C_m in control and Shh-expressing passive cells **(Table 6)**. In 5 out of 14 passive cells, the application of 100 μM GABA evoked a bicuculline-sensitive inward current and the GABA/C_m was significantly higher than that recorded in Shh-expressing passive cells **(Table 6)**.

Taken together, these results show that Wnt-7a-expression decreases the incidence of passive cells within the differentiated cell cultures and moreover, it affects their membrane properties. Additionally, both Shh and Wnt-7a expression lead to the appearance of functional $GABA_A$ receptors in passive cells.

5.3.6 The incidence of a complex current pattern is suppressed in Wnt-7a-expressing cell cultures

In controls, cells with a triangular cell body (about 20 μm in diameter) and one or several processes **(Fig. 46, 49A)** displayed a complex current pattern represented by a

CsCl-sensitive K_{IR} current **(Fig. 49B)** and outwardly rectifying K^+ currents, specifically K_{DR} and K_A currents **(Fig. 49C, D)**. These cells represented 38 % (19 cells out of 50) of initially recorded cells **(Fig. 46)**. Our post-recording identification revealed that these cells were NG2-positive **(Fig. 49A)**. A complex current pattern was also identified in small, round MAP-2-positive cells, but the MAP-2 expression was mainly limited to the cell soma, while NG2 was expressed on the entire surface of the cell **(Fig. 49A)**. Cells displaying a complex current pattern had a hyperpolarised V_{rest} (-91.6 ± 1.5 mV), but a higher IR (288.2 ± 17.7 MΩ) and a lower C_m (11.2 ± 0.7 pF) than passive cells (n=40, **Table 7)**. Outwardly rectifying K^+ currents were sensitive to 5 mM 4-AP: the K_A and K_{DR} current amplitudes decreased by 33.5 ± 8.8% and 55.1 ± 4.2% (n=10), respectively. The additional application of 10 mM TEA did not cause a further decrease in the current amplitudes **(Table 7)**. No cells with a complex current pattern responded to the application of 100 μM GABA (7 cells out of 7).

Cells displaying a complex current pattern appeared more frequently in Shh-expressing cell cultures than in controls (55% versus 38%, **Fig. 46)**; however, Shh had no effect on their membrane properties **(Table 7)**. Interestingly, pharmacological analysis revealed that the K_A currents in Shh-expressing cells were more sensitive to the application of 5 mM 4-AP than the K_A current recorded in complex cells of control cultures **(Table 7)**. The subsequent application of 10 mM TEA caused no further decrease in the amplitudes of the K_A and K_{DR} currents. The application of 100 μM GABA evoked an inward current sensitive to 100 μM bicuculline (in 7 cells out of 19, **Table 7)**.

Conversely, the incidence of cells with a complex current pattern was decreased in the Wnt-7a-expressing cell cultures (3.2%, **Fig. 46)** and moreover, their membrane properties were affected. These cells displayed a more depolarised V_{rest} and a lower K_{IR}/C_m when compared to complex cells of control and Shh-expressing cell cultures **(Table 7)**. Western blotting confirmed that the K_{IR} channel expression (namely K_{IR} 4.1) was markedly reduced in the cell lysates obtained from differentiated Wnt-7a-expressing cell cultures **(Fig. 49B)**. Similarly to Shh-expressing cells, pharmacological analysis revealed that the K_A currents were more sensitive to 5 mM 4-AP than those recorded in complex cells of control cultures. The subsequent application of 10 mM TEA did not further decrease the amplitude of the outwardly rectifying currents. Due to

the overall low presence of these cells, a GABA-evoked current was recorded only in 1 cell out of 4 **(Table 7)**.

Collectively, Wnt-7a significantly decreases the incidence of cells with a complex current pattern and markedly decreases the expression of K_{IR} channels in differentiated cells. Conversely, Shh over-expression leads to an increased incidence of a complex current pattern in differentiated cells.

Fig. 49 Membrane properties of cells displaying a complex current pattern, eight days after the onset of *in vitro* differentiation

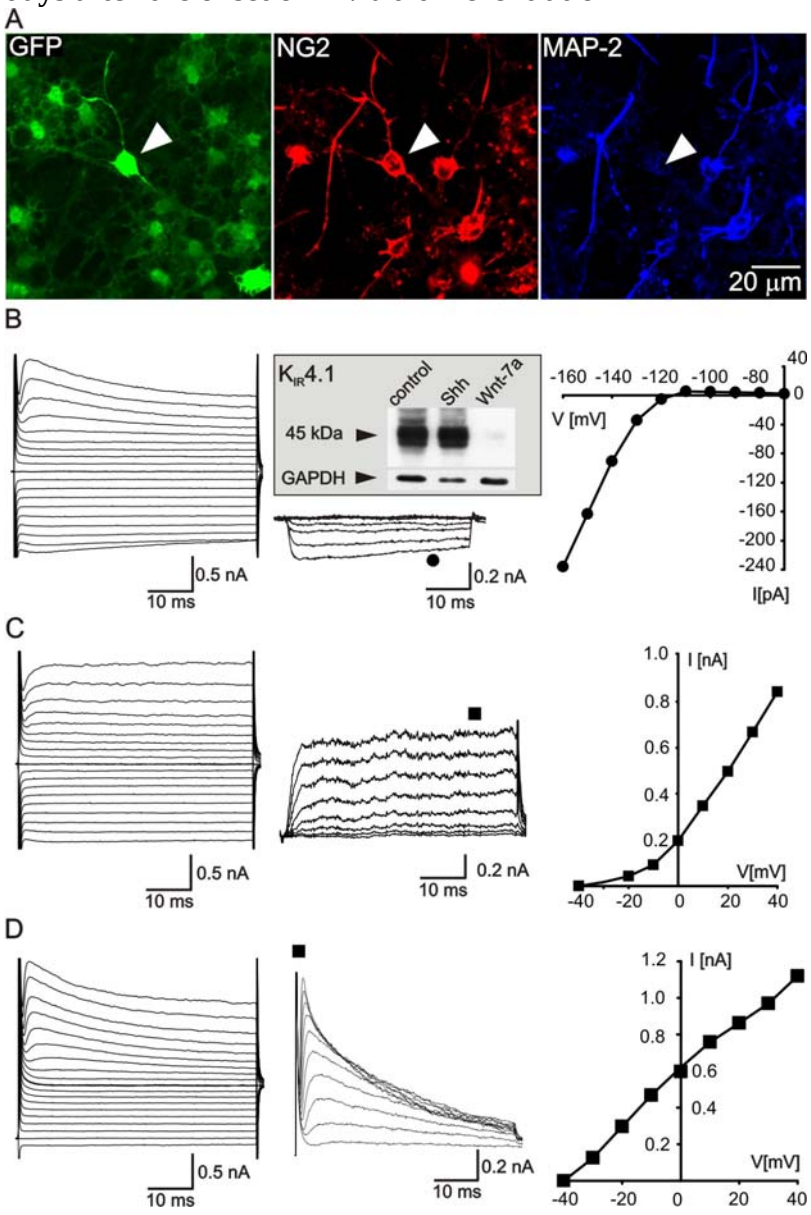

(A) Immunocytochemical identification of a recorded cell (indicated by arrowhead, **left)**, showing positive staining for NG2 **(middle)** and a very weak staining for MAP-2 **(right)**. **(B)** Typical current pattern of an NG2-positive cell in control culture obtained by hyper- and depolarising the cell membrane from a holding potential of -70 mV to potentials ranging from -160 mV to +20 mV **(left)**, the subtracted CsCl-sensitive K_{IR} current **(middle)** together with the Western blot analysis showing a reduced K_{IR} 4.1 channel expression in Wnt-7a-expressing cells **(inset)** and the I/V relationship of CsCl-sensitive K_{IR} current **(right)**. **(C)** Current patterns obtained by hyper- and depolarising the cell from a holding potential of -50 mV to potentials ranging from -140 mV to +40 mV **(left)** and the isolated K_{DR} current, obtained by passive-current subtraction **(middle)** and its I/V relationship **(right)**. **(D)** Current patterns obtained by hyper- and depolarising the cell from a holding potential of -50 mV to potentials ranging from -140 mV to +40 mV, after a hyperpolarising prepulse to -110 mV **(left)**, and the isolated K_A current **(middle)** obtained by subtracting the currents shown in (C, left) from those shown in (D, left) and the I/V relationship of the subtracted K_A current **(right)**.

Table 7 Membrane properties of complex cells 8 days after the onset of *in vitro* differentiation

complex		control	Shh	Wnt-7a
V_{rest}	[mV]	-91.6 ± 1.5	-88.1 ± 1.3	-62.5 ± 3.4***
C_m	[pF]	11.2 ± 0.7	11.4 ± 0.7	9.3 ± 1.3
IR	[MΩ]	288.2 ± 17.7	242.3 ± 19.0	346.8 ± 59.5
K_A/C_m	[pA/pF]	47.5 ± 5.0	51.3 ± 5.0	74.6 ± 10.6
K_{DR}/C_m	[pA/pF]	36.3 ± 4.2	50.4 ± 5.7	85.3 ± 12.3
K_{IR}/Cm	[pA/pF]	10.7 ± 1.0	13.8 ± 1.8	2.9 ± 0.9
n		40	61	9
K_A + 4-AP	[%]	33.5 ± 8.8	72.0 ± 7.8**	83.6 ± 8.1**
K_A + 4-AP + TEA	[%]	33.1 ± 8.7	74.3 ± 7.6**	84.6 ± 7.6**
n		10	12	4
K_{DR} + 4-AP	[%]	55.1 ± 4.2	66.3 ± 8.5	85.2 ± 5.1
K_{DR} + 4-AP + TEA	[%]	62.0 ± 4.1	77.1 ± 7.2	92.0 ± 2.8
n		10	12	4
GABA/C_m	[pA/pF]	---	23.9 ± 8.5	(35.5)a
n		---	7	1

V_{rest}: resting membrane potential; **C_m:** membrane capacitance; **IR:** input resistance; **K_A/C_m, K_{DR}/C_m, K_{IR}/C_m, GABA/C_m:** K_A, K_{DR} K_{IR} and GABA current densities; **n:** number of cells; **K_A + 4-AP, K_A + 4AP + TEA, K_{DR} + 4-AP, K_{DR} + 4-AP + TEA:** relative amplitude decrease after the application of 4-AP (4-aminopyridine) or 4-AP in combination with TEA (tetraethylamonium chloride). Asterisks indicate significant differences between Shh- or Wnt-7a-expressing complex cells and control complex cells; crosshatches indicate significant differences between Shh- and Wnt-7a-expresssing complex cells; */ p< 0.05; **/ p< 0.01, ***/ p< 0.001; [a] value of an individual cell.

5.3.7 A neuron-like current pattern prevails in Wnt-7a expressing cells 8 days after the onset of *in vitro* differentiation

In control cultures, small round cells with a cell body diameter of 10-15 µm and multiple processes displayed a high IR (1205.0 ± 149.1 MΩ), a V_{rest} of -78.8 ± 3.6 mV, and a low C_m (7.3 ± 0.6 pF, n=19, **Table 8)**. These cells were identified as MAP-2-positive **(Fig. 50A)** and were further termed "neuron-like cells". They represented 16% of the initially recorded cells (8 cells out of 50, **Fig. 46)**. These cells displayed large K_A

and K_{DR} current amplitudes **(Fig. 50C, D)**, and 5 out of 19 cells expressed TTX-sensitive Na^+ currents **(Fig. 50B)**. The application of 5 mM 4-AP decreased the amplitude of the K_A and K_{DR} currents in these cells by 26.6 ± 9.2% and 42.1 ± 6.8% (n=6), respectively. The additional application of 10 mM TEA did not cause a further decrease in the current amplitudes **(Table 8)**. Interestingly, no neuron-like cells reacted to the application of 100 μM GABA (9 cells out 9).

Shh-expressing cell cultures showed a lower incidence of a neuron-like current pattern (6.7 % versus 16 % in controls, **Fig. 46)** and a lower incidence of TTX-sensitive Na^+ currents (2 cells out of 20). Other membrane properties were not significantly different from those observed in controls **(Table 8)**. Pharmacological analysis revealed that the K_{DR} currents were more sensitive to the application of 5 mM 4-AP than those recorded in neuron-like cells of controls. The subsequent application of 10 mM TEA caused no further blockage of the K_A and K_{DR} currents. The application of 100 μM GABA evoked a bicuculline-sensitive inward current in 5 cells out of 15 **(Fig. 50E)**.

Surprisingly, in Wnt-7a-expressing cell cultures the incidence of a neuron-like current pattern markedly increased to 92.1% **(Fig. 46)**. The neuron-like cells displayed a more depolarised V_{rest} when compared to those in control and Shh-expressing cultures, and 17.1% (12 cells out of 64) of these cells expressed a TTX-sensitive Na^+ current with a Na/C_m comparable to that recorded in controls. However, their K_{DR}/C_m was significantly higher when compared to the K_{DR}/C_m of controls and Shh-expressing cells. Pharmacological analysis revealed that the K_{DR} current was more sensitive to the application o 5 mM 4-AP than that recorded in controls. The subsequent application of 10 mM TEA did not lead to a further decrease in the amplitudes of the outwardly rectifying K^+ currents **(Table 8)**. The application of 100 μM GABA evoked a bicuculline-sensitive inward current in 5 cells out of 21 **(Table 8)**.

Taken together, these data show that the incidence of cells with a neuron-like current pattern is markedly increased in Wnt-7a-expressing cell cultures, while in Shh-expressing cell cultures the incidence is rather suppressed. Moreover, neuron-like cells in Wnt-7a-expressing cell cultures display increased K_{DR} current densities.

Fig. 50 Membrane properties of neuron-like cells in neonatal NS/PC cultures, 8 days after the onset of *in vitro* differentiation

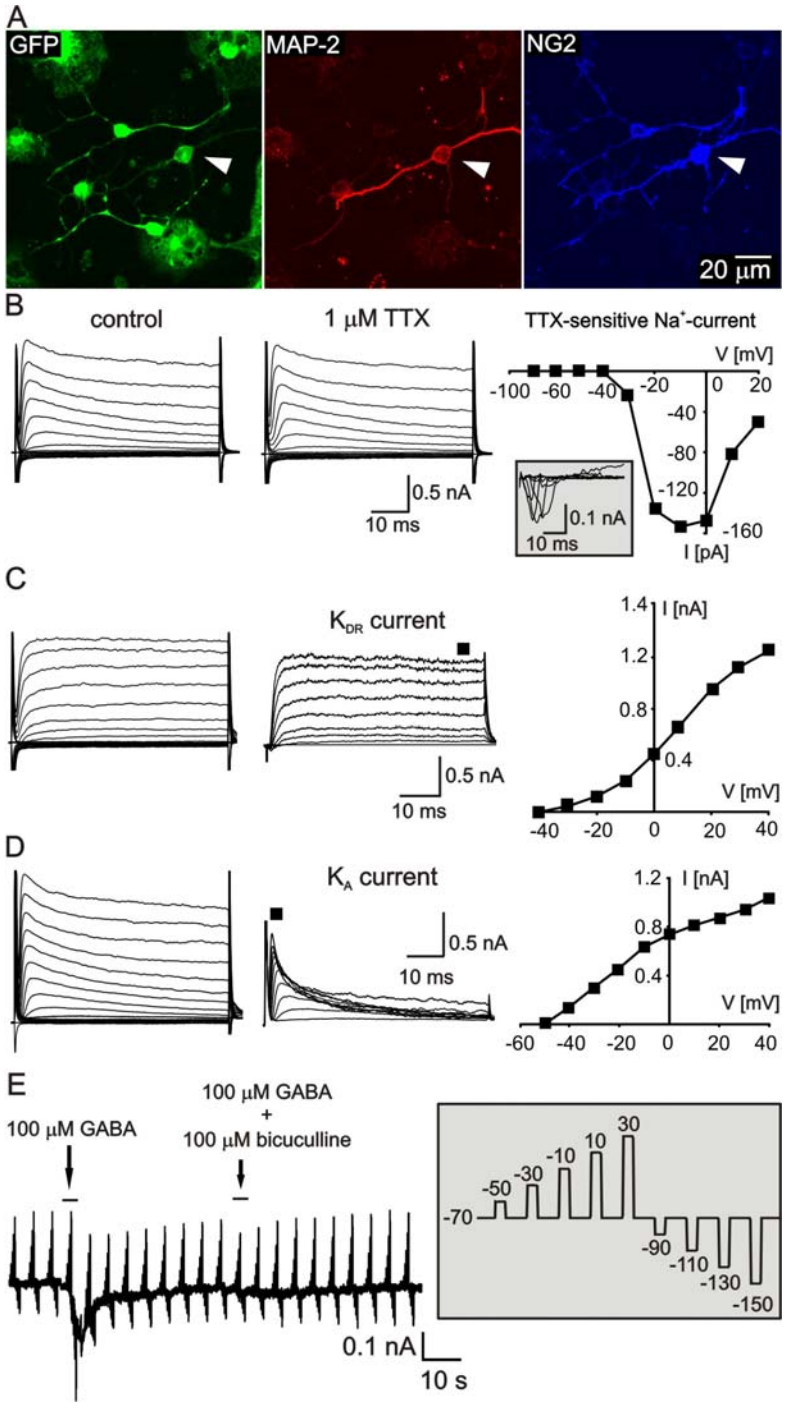

(A) Immunocytochemical identification of a recorded cell (indicated by arrowhead, **left)**, showing positive staining for MAP-2 **(middle)** and NG2 **(right)**. **(B)** Typical membrane current pattern of a neuron-like cell prior to **(left)** and after **(middle)** the application of 1 µM TTX, obtained by hyper- and depolarising the cell membrane from a holding potential of -70 mV to potentials ranging from -160 mV to +20 mV. The resulting I/V relationship for the TTX-sensitive current **(inset)** is shown in the right. **(C)** Current patterns obtained by hyper- and depolarising the cell membrane from a holding potential of -50 mV to potentials ranging from -140 mV to +40 mV **(left)** and the isolated K_{DR} current, obtained by passive-current subtraction **(middle)** and its I/V relationship **(right)**. **(D)** Current patterns obtained by hyper- and depolarising the cell membrane from a holding potential of -50 mV to potentials ranging from -140 mV to +40 mV, after a hyperpolarising prepulse to -110 mV **(left)**, and the isolated K_A current **(middle)** obtained by subtracting the currents shown in (C, left) from those shown in (D, left) and its I/V relationship **(right)**. **(E)** A typical inward current evoked by the application of 100 µM GABA and blocked by 100 µM bicuculline. The currents were obtained by clamping the cell membrane potential to different values, by rectangular voltage steps, from a holding potential of -70 mV to potentials ranging from -150 mV to +30 mV (see the inset).

Table 8 Membrane properties of neuron-like cells 8 days after the onset of *in vitro* differentiation

neuron-like		control	Shh	Wnt-7a
V_{rest}	[mV]	-78.8 ± 3.6	-76.4 ± 3.2	-58.3 ± 2.0***/###
C_m	[pF]	7.3 ± 0.6	7.3 ± 0.5	6.4 ± 0.4
IR	[MΩ]	1205.0 ± 149.1	1356.3 ± 284.0	1964.4 ± 210.3
K_A/C_m	[pA/pF]	83.5 ± 13.6	55.4 ± 7.2	105.2 ± 9.6 #
K_{DR}/C_m	[pA/pF]	60.5 ± 9.2	54.9 ± 8.6	122.2 ± 11.6**/##
n		19	20	64
Na^+/C_m	[pA/pF]	25.2 ± 6.9	(17.3; 10.1)[a]	33.8 ± 5.8
n		5	2	12
K_A + 4-AP	[%]	26.6 ± 9.2	47.5 ± 10.4	54.1 ± 12.3
K_A + 4-AP + TEA	[%]	34.3 ± 8.9	51.5 ± 10.7	72.8 ± 11.0
K_{DR} + 4-AP	[%]	42.1 ± 6.8	68.8 ± 4.3*	65.9 ± 7.2*
K_{DR} + 4-AP + TEA	[%]	53.0 ± 6.8	78.4 ± 3.0*	76.0 ± 6.1*
n		6	9	9
GABA/C_m	[pA/pF]	---	29.5 ± 7.5	21.4 ± 5.6
n		---	5	5

V_{rest}: resting membrane potential; **C_m:** membrane capacitance; **IR:** input resistance; **K_A/C_m, K_{DR}/C_m, Na/C_m, GABA/C_m:** K_A, K_{DR}, Na^+ and GABA current densities; **n:** number of cells; **K_A + 4-AP, K_A + 4AP + TEA, K_{DR} + 4-AP, K_{DR} + 4-AP + TEA:** relative amplitude decrease after the application of 4-AP (4-aminopyridine) or 4-AP in combination with TEA (tetraethylamonium chloride). Asterisks indicate significant differences between Shh- or Wnt-7a-expressing neuron-like cells and control neuron-like cells; crosshatches indicate significant differences between Shh- and Wnt-7a-expresssing neuron-like cells; */# $p< 0.05$; **/## $p< 0.01$, ***/### $p< 0.001$. [a] values of individual cells.

6. DISCUSSION

In the presented work we have characterised different types of NS/PCs during their *in vitro* proliferation and differentiation, as well as after transplantation into the damaged adult rat cortex. We have described and compared their immunohistochemical and membrane properties.

6.1 Characterisation of undifferentiated NS/PCs *in vitro*

The identification and characterisation of NS/PCs is an essential prerequisite of every *in vitro* as well as *in vivo* experiment. The GFP/NE-4C immortalised cell line was well described previously. It was shown that undifferentiated GFP/NE-4C cells express nestin (Schlett and Madarasz, 1997) and other early markers of undifferentiated cells, such as SSEA-1 and Otx2 (Varga et al., 2008), while lacking later markers of radial glia cells, such as RC2 (Jelitai et al., 2007). Together, the expression of these markers confirms the early neuroepithelial origin of GFP/NE-4C cells. Since this cell line is clonally-derived, the expression of cell specific markers is uniform through the entire cell population.

Primary cultures of NS/PCs, on the other hand, are more heterogeneous, especially when cultured in the form of neurospheres (Piao et al., 2006). In our experiments NS/PCs derived from D6-GFP embryonic as well as neonatal mouse brains expressed markers of undifferentiated neural stem cells as well as committed progenitors. The expression of cell specific markers in embryonic neurospheres corresponded to the expression observed in acutely isolated tissue from D6-GFP E12 mouse embryos, and the expression in neonatal neurospheres was similar to that described by others. Besides nestin, a common marker of all neural stem cells, the isolated embryonic tissue as well as D6-GFP-derived neurospheres expressed markers of radial glia cells, which are the prevailing neural stem/progenitor cell type in the E12 telencephalon (Hartfuss et al., 2001). They are still present in the neonatal brain, where they gradually transform into astrocytes and SVZ neural stem cells (Alves et al., 2002, Peretto et al., 2005). Accordingly, we have detected radial glia/adult neural stem cell markers in neonatal neurospheres. Besides these markers, the expression of neuronal markers, such as DCX and βIII tubulin, was detected in neurospheres. In agreement with our data, the expression of βIII tubulin has been detected in the E12 mouse cortex

(Qian et al., 2000) and, moreover, in the actively proliferating cells of the embryonic VZ (Menezes and Luskin, 1994). Its expression was also described in neurospheres (Kallur et al., 2006, Piao et al., 2006), and the appearance of βIII tubulin staining is in agreement with that observed in D6-GFP-positive neurospheres. Therefore, these cells might represent progenitors committed to a neuronal fate that are still proliferating or cells that have just left the cell cycle and started to differentiate. Similarly, DCX, a marker of migrating neurons (Bai et al., 2003, Tanaka et al., 2004, Friocourt et al., 2007), was detected by Western blotting as early as E12 (Vreugdenhil et al., 2007). A corresponding band was found in neurospheres of D6-GFP NS/PCs, and immunocytochemistry revealed a few positive cells in neonatal neurospheres, further supporting the presence of neuronally committed cells.

In neonatal NS/PCs immunocytochemical analysis revealed that neurospheres were heterogeneous with respect to the expression of NG2 and GFAP. This is consistent with previous findings showing NG2- and GFAP-positive cells in neurospheres derived from young adult mice (Brazel et al., 2005). While Shh had no apparent effect on the cellular composition of neurospheres, both immunocytochemistry and Western blotting showed that GFAP-positive cells were markedly suppressed in Wnt-7a-expressing neurospheres. Since both morphogenes increased the size of neurospheres, suggesting that they both promote the proliferation of NS/PCs within a single neurosphere, we can hypothesise that Wnt-7a might selectively maintain the proliferation of a subset of NS/PCs, as suggested in an *in vitro* study describing a subpopulation of neonatal NS/PCs responsive to Wnt-3a, which also operates through the Wnt/β-catenin signalling pathway (Hirsch et al., 2007). The proliferation of neonatal NS/PCs was also affected during the course of *in vitro* differentiation. Shh-expressing cell cultures showed increased proliferation 3 and 8 days after the onset of *in vitro* differentiation, suggesting that besides its role in neuronal differentiation, Shh maintains its mitogenic activity during the entire course of differentiation (3 and 8 days). The extensive proliferation induced by Wnt-7a was observed only after 3 days, suggesting that Wnt-7a sustains a mitogenic effect early in differentiation, while at later stages it rather acts as a differentiating factor. A similar effect was described for Wnt-3a during embryogenesis (Hirabayashi et al., 2004).

Additionally, NG2-positive cells, which were detected in the neonatal neurospheres, were not present in the D6-GFP embryonic brain-derived neurospheres.

This is not surprising, since NG2-positive cells that are able to form neurospheres were detected in the early postnatal brain (Belachew et al., 2003), while in the embryonic brain, NG2 was detected as late as E13; however, its expression was confined to the marginal zone of the developing spinal cord, and the expression did not overlap with radial glia markers (Diers-Fenger et al., 2001). Moreover, D6-GFP NS/PCs are confined to the germinal zone of the dorsal telencephalon, which does not give rise to cells of the oligodendrocyte lineage *in vivo* (Machon et al., 2005).

Interestingly, Western blot analysis provided more details about the expression of GFAP in both embryonic D6-GFP-derived as well as neonatal neurospheres. Several bands immunoreactive for GFAP were detected that might correspond to the existence of various GFAP isoforms (Roelofs et al., 2005), multiple GFAP splice variants (Hol et al., 2003, Quinlan et al., 2007) or posttranslational modifications (Kommers et al., 2002) in the population of GFAP-positive cells. Surprisingly, the ~35 kDa band, which was detected in the E12 embryonic tissue, was undetectable in the D6-GFP-derived neurospheres, while it was present in the lysates obtained from control neonatal neurospheres. This band might correspond to either an unknown GFAP isoform or a degradation product of GFAP. All the additional bands were, nevertheless, reduced or absent in Shh- and Wnt-7a-expressing neurospheres, indicating that the downstream targets of Shh or Wnt-7a signalling pathways might interfere with GFAP transcription. Additional bands of DCX were also detected in the embryonic tissue as well as derived neurospheres, and they might be related to the existence of various phosphorylated/dephosphorylated DCX proteins in the developing cortex (Shmueli et al., 2006), since it has been shown that DCX is phosphorylated by different kinases (Graham et al., 2004, Tanaka et al., 2004).

Taken together, the NS/PCs used in our work are antigenically identical to their counterparts present in the brain at the corresponding developmental stage. While GFP/NE-4C cells represent a uniform neural stem cell population, D6-GFP NS/PCs represent a mixed population of neural stem cells and committed progenitors, predominantly expressing markers of radial glia cells. In the neonatal NS/PCs, two separate populations exist based on GFAP and NG2 immunocytochemistry, and the GFAP-positive cells are suppressed by the expression of Wnt-7a.

6.2 Differentiation potential of embryonic and neonatal NS/PCs during their *in vitro* differentiation

The *in vitro* differentiation of NS/PCs is usually performed as a preliminary experiment to subsequent transplantation studies; however, it can also serve as a suitable tool for studying the differentiation mechanisms of NS/PCs.

The embryonic neuroectodermal GFP/NE-4C cell line was previously shown to be a suitable model for studying neurogenesis *in vitro* (Schlett et al., 1997, Schlett and Madarasz, 1997, Demeter et al., 2004, Jelitai et al., 2004, Jelitai et al., 2007). In our work however, the aim of the *in vitro* differentiation experiments was to verify the differentiation potential of these cells prior to transplantation into the adult rat brain. After RA induction, GFP/NE-4C cells started to form processes and developed a neuronal phenotype, as reported previously (Schlett and Madarasz, 1997, Schlett et al., 2000). From day 3 onwards, neuronal cells could be identified by the expression of the neuron-specific marker βIII tubulin, and they were found on top of non-differentiated cells, similarly as described (Schlett and Madarasz, 1997, Demeter et al., 2004). Interestingly, a recent study showed that after the induction of differentiation by RA, NE-4C cells differentiate into neuronal cells via RC2-positive cells (Jelitai et al., 2007), demonstrating that these cells copy the *in vivo* pattern observed during embryogenesis. Also ESCs were shown to recapitulate the transformation from NE-cells to radial glia cells and neurons under specific conditions (involving RA treatment) *in vitro* (Bibel et al., 2004, Bibel et al., 2007). Another study showed that during the course of *in vitro* differentiation of NE-4C cells, different sets of region-specific genes turn on. At the time when RC2-positive radial glia appear in the NE-4C cell culture, region-specific genes, including gastrulation brain homeobox 2 (gbx2), homeobox b2 and pax6 become active along with pro-neural genes (such as neurogenin 2). The expression of another set of "positional" genes, including emx2, dlx2 and nkx2.2, was detected only after the activation of the neuron-specific meprin-associated Traf homology gene (math2), which is expressed in postmitotic neurons (Varga et al., 2008). Although NE-4C cells were described as capable of developing into astrocytes and oligodendrocyte following RA treatment *in vitro* (Schlett et al., 1997, Varga et al., 2008), we did not identify any GFAP-, S100β-, or MOSP-positive cells during 10 days of *in vitro* differentiation. Other studies using RT-PCR and immunocytochemistry showed that GFAP is activated 10

days after the onset of *in vitro* differentiation and is more pronounced at day 14 (Varga et al., 2008, Hadinger et al., 2009). Recently it was discovered that RA treatment in the early days of *in vitro* differentiation is essential for inducing the formation of astrocytes in cultures of NE-4C cells. At the same time, it is the intrinsic RA produced by the cells that renders, but does not prevent, the production of astrocytes. The effect is mediated by nuclear RA receptor, and using a pan-RA receptor blocker immediately increased the formation of GFAP-positive astrocytes during the *in vitro* differentiation of NE-4C cells (Hadinger et al., 2009).

In the cultures of embryonic D6-GFP and neonatal NS/PCs, a broader spectrum of cell-specific markers was observed. Both were exposed to similar culture conditions, with the exception of RA induction, which was not included in the culture medium of embryonic D6-GFP NS/PCs, since they followed naturally their developmental pattern observed *in vivo* and produced predominantly neuronal cells. They expressed early neuronal markers, such as DCX and βIII tubulin, but also more mature markers, such as MAP-2 and NeuN. Compared to the D6-GFP cell cultures, the proportion of neuronal cells was lower in the cultures of neonatal NS/PCs; however, the over-expression of both Shh and Wnt-7a increased their numbers. Quantitative immunocytochemical analysis revealed that both morphogenes increased the number of newly derived and maturing neurons, which is in agreement with previous data showing that Wnts and Shh promote differentiation towards neurons *in vitro* (Muroyama et al., 2004, Yu et al., 2006, Wang et al., 2007a). We also detected increased Mash1 expression caused by these morphogenes, demonstrating their neurogenic potential. While Mash1 is a known down-stream target of Shh signalling, β-catenin was suggested to act by interfering with Notch signalling in neonatal NS/PCs (Hirsch et al., 2007). Although the number of Mash1-positive cells was shown to be increased by Wnt/β-catenin signalling in the adult SVZ (Adachi et al., 2007), the downstream components leading from β-catenin to Mash1 are not yet known. Strikingly, further quantitative analysis demonstrated that only neuronal cells in Wnt-7a-expressing cell cultures displayed longer and more developed cell processes, when compared to the same cells in Shh-expressing cell cultures and controls. We can thus hypothesise that Shh and Wnt-7a promote the generation of new neurons/neuroblasts, while only Wnt-7a affects their further growth and development.

GFAP-positive cells were detected in both embryonic D6-GFP as well as neonatal cell cultures. Interestingly, the expression of Wnt-7a markedly reduced the incidence of GFAP-positive cells (revealed by Western blot and further electrophysiological analysis) within the differentiated cell cultures, which is in agreement with previously published data showing that Wnt-7a suppresses gliogenesis *in vitro* (Kunke et al., 2009).

No cells immunostained for MOSP or O4 (markers of oligodendrocytes or their progenitors) were detected in either of the cell cultures, while both contained Olig2-positive cells, one week after the onset of *in vitro* differentiation. In the culture of D6-GFP cells Olig2-positive cells did not generally express GFP, although we have identified one Olig2-positive cell that was also weakly GFP-positive (see **Fig. 25)**. Since bFGF has been shown to promote a ventral fate in NS/PCs from the dorsal telencephalon (Abematsu et al., 2006), it is possible that the presence of bFGF in the culture medium during *in vitro* differentiation altered the cell's fate. Besides the fact that Olig2 might appear in the neurospheres due to the presence of growth factors, Olig2 is the earliest ventral marker of oligodendrocyte progenitors in the developing telencephalon (Parras et al., 2007), but also of GABA-ergic neurons (Ono et al., 2008). Therefore, the Olig2-positive cell that was almost GFP-negative might be an example of a cell losing its unique character (together with GFP) due to the *in vitro* conditions used in our experiments.

In the neonatal cell cultures, the most abundant cell population comprised NG2-positive cells, including also cells co-expressing a neuronal marker. In agreement with our findings, NG2-positive cells were detected previously in neurospheres, and during differentiation they were shown to give rise to neurons co-expressing NG2 and neuronal markers (Dromard et al., 2007). We suggest that cells that are solely NG2-positive represent uncommitted progenitors and that upon differentiation they produce predominantly neuronal cells **(see Fig. 51)**.

Fig. 51 The effect of Shh and Wnt-7a on neural stem cell proliferation and differentiation

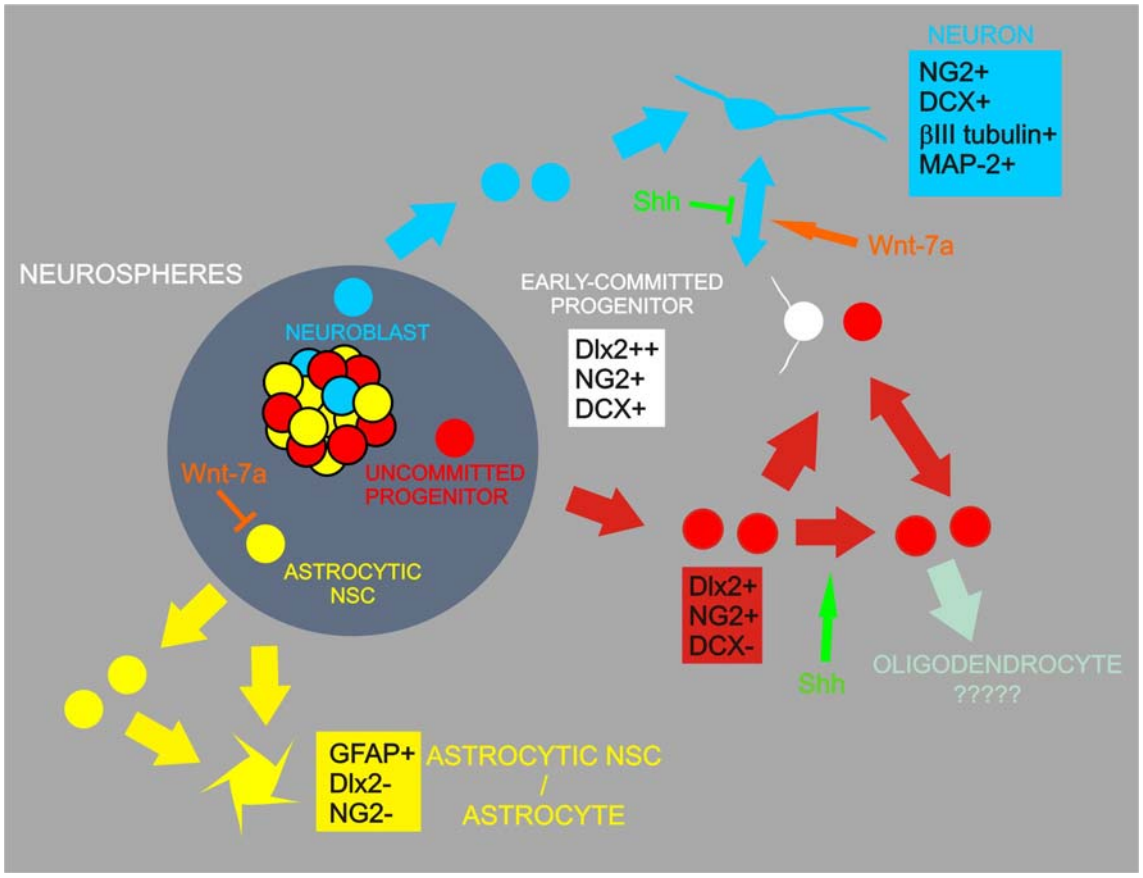

According to our proposed model both Shh and Wnt-7a increase the neurosphere size; however, Wnt-7a selectively maintains a subpopulation of NS/PCs. During the course of *in vitro* differentiation, Shh promotes proliferation, presumably of uncommitted progenitors, and hinders the transition form early committed progenitors towards neurons. Wnt-7a, on the other hand, suppresses the population of GFAP-positive cells and promotes a neuron-like phenotype in the differentiated cells.

6.3 Membrane properties of *in vitro* differentiated cells

Electrophysiological analysis revealed three distinct current patterns in the cultures of *in vitro* differentiated NS/PCs. While cells displaying passive and neuron-like currents were present in embryonic as well as neonatal cell cultures, cells displaying a complex current pattern were detected only in the neonatal cell cultures.

6.3.1 A passive current pattern in embryonic and neonatal cell cultures

Cells displaying a passive current pattern were detected in the cultures of D6-GFP NS/PCs as well as in the cultures of neonatal NS/PCs. A recent study using NE-4C cells also described undifferentiated nestin-positive cells with passive currents carried

predominantly by K^+ ions. A subset of these cells also displayed K_{DR} currents sensitive to 4-AP (Jelitai et al., 2007). These cells responded to GABA by an inward current (Jelitai et al., 2004).

We observed similar characteristics in the D6-GFP-derived passive cells, which additionally displayed Cs^+-sensitive K_{IR} currents, which have been described in cortical and hippocampal astrocytes (Anderova et al., 2004, Andreasen et al., 2007), but also in NSCs derived from the umbilical cord (Sun et al., 2005). Another *in vitro* study described embryonic NS/PCs from the E15 SVZ that expressed rather neuron-like characteristics, such as a depolarised V_{rest} and voltage-gated K_A and K_{DR} ion channels (Smith et al., 2008). The GABA-current densities in D6-GFP-derived passive cells were lower than those described in primary cultures of astrocytes (Tateishi et al., 2006, Zhou et al., 2006), but comparable to those described in cultures of non-differentiated NE-4C cells (Jelitai et al., 2004). D6-GFP/GFAP passive cells thus display membrane characteristics of neural stem cells as well as those of astrocytes.

The membrane properties of adult neural stem cells were described in detail *in situ* (Liu et al., 2006) as well as *in vitro* (Yasuda et al., 2008), and it was shown that many features are shared with those observed in astrocytes (Liu et al., 2006). Both control and Shh-expressing passive cells displayed similar characteristics as described in these cells, including high permeability of the cell membrane for K^+, a Cs^+ sensitive K_{IR} current, Ba^{2+} sensitive K^+ currents and cell membrane depolarisation following Ba^{2+} application. GFAP-positive cells in Wnt-7a-expressing cell cultures were morphologically and immunocytochemically similar to those observed in controls and Shh-expressing cell cultures, while they displayed significantly different membrane properties. They displayed increased IR and K_{DR} current densities, which mark the transition from stem cells to neuronally committed progenitors during the early phases of the neuronal differentiation of GFP/NE-4C cells *in vitro* (Jelitai et al., 2007). During the application of elevated K^+ in Wnt-7a-expressing passive cells, the values of V_{rev} did not reach the theoretical values calculated from the Nernst equation, suggesting that in these cells passive currents are conducted only partly by K^+ ions and that other ions, presumably Cl^- ions, might contribute to the depolarised V_{rest}. This was further confirmed by the moderate sensitivity of the passive currents to 10 mM $BaCl_2$, a commonly used blocker of time- and voltage-independent K^+ currents in glial cells (Liu et al., 2006). Additionally, in the Wnt-7a-expressing cell cultures these passive cells

displayed a decreased incidence of CsCl-sensitive K_{IR} currents, and their current densities were lower than those observed in passive cells of control and Shh-expressing cell cultures. Since it was shown that Kir4.1 channels contribute to the negative V_{rest} in glial cells (Butt and Kalsi, 2006, Tang et al., 2009), it is possible that the down-regulation of Kir4.1 channels (shown by Western blotting) is also partly responsible for the depolarised V_{rest} in passive cells of the Wnt-7a-expressing cell cultures. Thus, Wnt-7a passive cells exhibit electrophysiological characteristics similar to those of undifferentiated neural stem cells, or they might represent a transient stage between neural stem cells and neuronally committed progenitors.

6.3.2 A neuron-like current pattern in embryonic and neonatal cell cultures

Electrophysiological analysis revealed that all types of NS/PCs were able to produce immature neurons within a week of *in vitro* differentiation. They displayed outwardly rectifying K^+ currents (namely K_A and K_{DR} currents) as well as low Na^+ current densities without the ability to fire repetitive APs, as described by others (Jelitai et al., 2007, Goffredo et al., 2008, Leng et al., 2009). A similar current pattern was also recorded *in situ*, in neuroblasts of young murine SVZ and RMS however, these cells displayed only K_{DR}, but not K_A currents (Wang et al., 2003a, Bolteus and Bordey, 2004), while they displayed a low Na^+ current density and were also unable to fire action potentials (Wang et al., 2003a). Fully differentiated neurons, on the other hand, were shown to display higher Na^+ current densities and were able to generate repetitive APs (Westerlund et al., 2003, Pagani et al., 2006). In our *in vitro* experiments, only D6-GFP-derived neuronal cells were able to fire one AP, at the onset of current injection, suggesting that among the NS/PCs used, these are able to process their development closest to the stage of a fully functional neuron, presumably because they are endogenously programmed to neurogenesis. A number of *in vitro* studies have described immature neurons with small Na^+ current amplitudes, often lacking the ability to fire repetitive APs, even after three weeks of *in vitro* differentiation (Balasubramaniyan et al., 2004, Cai et al., 2004, Mo et al., 2007). A low Na^+ channel density or an immature form of the Na^+ channel might be the reason why GFP/NE-4C- and neonatal brain-derived neuronal cells failed to induce AP firing when exposed to elevated levels of external K^+ or after current injection. Interestingly, the electrophysiological analysis of the neonatal NS/PC cultures further confirmed the

disparity between the neurogenic effects of Shh and Wnt-7a. It clearly showed that Wnt-7a-expression promotes a neuron-like current pattern in differentiating cells.

We also tested the sensitivity of the outwardly rectifying currents to the ion channel blockers 4-AP and TEA. It was shown that in differentiated firing neurons *in vitro*, only K_A is highly sensitive to 5 mM 4-AP, while the sustained K_{DR} current is abolished by the application of 5 or 12 mM mM TEA (Westerlund et al., 2003, Johnson et al., 2007). Here we showed that in all neuronal cells, both K_A and K_{DR} currents are only partly sensitive to 4-AP, while the addition of TEA did not further increase the blockage significantly. An *in vitro* study using the GFP/NE-4C cell line showed that neuronal progenitors display a K_{DR} current highly sensitive to 5 mM 4-AP (~77% of K_{DR} current blocked), while differentiating neurons show variable sensitivity to 4-AP (20-70% of K_{DR} current blocked) and are increasingly sensitive to TEA (~60% of K_{DR} current blocked). These early neuronal cells, however, lacked the transient K_A current component and did not fire APs (Jelitai et al., 2007). It is therefore possible that the outwardly rectifying K^+ currents in our neuronal cells are also immature.

Interestingly, when we compared the current densities and ion channel blocker sensitivity of neuron-like cells in the cultures of neonatal NS/PCs, we found that Wnt-7a-expressing neuronal cells displayed higher K_{DR} current densities when compared to neuronal cells in controls and Shh-expressing cell cultures. Additionally, K_{DR} currents in the neuron-like cells of Shh- and Wnt-7a-expressing cell cultures displayed significantly higher sensitivity to 4-AP than those recorded in controls. Although the underlying mechanisms are not clear, one possible explanation is that the activation of Shh- and Wnt-7a-signalling pathways promote different stages of cell differentiation within a cell subpopulation. This can subsequently result in various maturation stages of the K^+ ion channels, marked by their altered composition, K^+ current densities and K^+ channel sensitivity to ion channel blockers. However, it remains to be elucidated what is the molecular basis of these processes, exactly how are they regulated and what is their role in the process of cell differentiation.

6.3.3 A complex current pattern in embryonic and neonatal cell cultures

An additional current pattern was detected in the cultures of neonatal NS/PCs, and it was associated with NG2-positive cells. We hypothesise that cells expressing solely NG2, low levels of Dlx2 and a complex current pattern represent uncommitted

progenitors, since it was shown that NG2-positive cells isolated from the early postnatal brain behave as neural progenitors *in vitro,* and they also have the ability to form neurospheres (Belachew et al., 2003), while the same cell population isolated from the adult brain is unable to form neurospheres *in vitro* (Buffo et al., 2008). Since a similar complex current pattern was described in NG2 glia of the juvenile hippocampus (Karram et al., 2008), it is possible that the functional characteristics of uncommitted/early committed progenitors are partly similar to NG2 glia. On the other hand, cells co-expressing NG2 and a neuronal marker are clearly defined as committed to a neuronal fate. Based on immunocytochemical and electrophysiological data they might, however, represent different stages of neuronal differentiation. NG2-positive cells with a neuronal marker expression limited to the cell soma and a complex current pattern might thus represent the early stages of neuronal commitment, while cells with a neuron-like current pattern that express NG2 and a neuronal marker simultaneously in the cell soma as well as in the cell processes might rather reflect a population of neuroblasts or neurons at the onset of differentiation (Jelitai et al., 2007). This hypothesis is further supported by our finding that cells with a neuronal morphology were highly Dlx2-positive. Dlx2 is a transcription factor known to be expressed in transit amplifying cells as well as their descendants – neuroblasts and differentiating neurons – and is known to promote neuroblast migration and differentiation (Brill et al., 2008, Colak et al., 2008). Furthermore, continuous Dlx2 expression marks the commitment of transit-amplifying progenitors to a neuronal fate in the adult SVZ *in vivo* (Doetsch et al., 2002). The most striking finding was that the incidence of NG2 cells displaying a complex current pattern was markedly reduced by Wnt-7a and enhanced by Shh. Therefore, we suggest that Wnt-7a accelerates the transition of early committed progenitors towards neuroblasts/differentiating neurons, while Shh maintains the population of uncommitted/early committed progenitors **(Fig. 51)**. We also showed that cells with a complex current pattern in the Wnt-7a-expressing cell cultures displayed a lower K_{IR} current density and a depolarised V_{rest} when compared to such cells in control and Shh-expressing cell cultures. Since it was described previously that the Kir4.1 channel is expressed by NPCs in the adult SVZ and is not expressed by migrating neuroblasts of the RMS (Yasuda et al., 2008), it is possible that Kir4.1 channel down-regulation partly correlates with the neurogenic and differentiation effect of Wnt-7a.

In conclusion, NS/PCs are able to produce neuronal cells with characteristics of neurons at early stages of differentiation. Among all the NS/PCs used, D6-GFP NS/PCs are most progressive in their development towards differentiated neurons, presumably because radial glia cells are direct predecessors of neurons *in vivo*, while GFP-NE-4C cells differentiate into neuronal cells via radial glia cells. Similarly, neonatal NS/PCs give rise to neurons via uncommitted and early committed progenitors, resulting in a prolonged period necessary for full differentiation. Moreover, the transition processes are affected by the expression of the morphogenes Shh and Wnt-7a and, in addition, the expression of Wnt-7a clearly shows that these morphogenes might directly affect the membrane properties of differentiated cells.

6.4 Differentiation potential of NS/PCs after their transplantation into the adult brain

The differentiation potential of transplanted NS/PCs was first studied using immunohistochemistry. While GFP/NE-4C immortalised cells generated neuronal cells, astrocytes and oligodendrocytes upon transplantation into the non-injured/injured rat brain, D6/GFP NS/PCs differentiated primarily into neuronal cells.

Previous studies demonstrated that immortalised NSC lines differentiate predominantly into astrocytes, while a smaller fraction of cells differentiate into neurons (Chu et al., 2004, Lee et al., 2007). Also, previous transplantation experiments with the GFP/NE-4C line showed that after transplantation into the lateral ventricle or striatum of adult mice, these cells have a slow proliferation rate, only a few of them migrate and less than 0.1% are able to differentiate into GFAP- or NF-positive cells. The same fate was observed in cells transplanted into the neonatal mouse or rat brain; however, in these animals, GFP/NE-4C cells expanded, suggesting that the neonatal environment supported their proliferation, while no sign of tissue disruption or tumour formation was observed (Demeter et al., 2004). Since we pre-treated the cells with RA prior to transplantation, it is possible that the pre-treatment might be a crucial signal for the differentiation of GFP/NE-4C cells, especially towards neuronal cells. Interestingly, the environment of the photochemical lesion had no apparent effect on morphology and immunohistchemical profiles of differentiated cells.

While GFP/NE-4C cell line differentiated into all major elements of the nervous system, D6/GFP primary NS/PCs derived from the E12 telencephalon differentiated

primarily into neuronal cells after transplantation into the adult rat brain. Moreover, they were able to express cortex-specific mDach1/GFP, suggesting that these cells are able to retain their endogenous program, which directs their fate towards neurons. Although it was demonstrated previously that the site of transplantation (performed either embryonically or postnatally) can influence NS/PCs towards a region-specific fate (Gaillard et al., 2003, Carletti et al., 2004, Klein et al., 2005, Kim et al., 2006, Vorasubin et al., 2007), the adult rat cortex, where neurogenesis has ceased, might provide only limited cues for region-specific differentiation. Furthermore, it has been suggested that the injury site might provide some cues that direct the differentiation of transplanted cells towards the neuronal rather than the glial lineage (Darsalia et al., 2007). However, D6-GFP NS/PCs differentiated into neuronal cells in both injured and non-injured cortex, suggesting that the phenotype obtained after one week of differentiation *in vivo* might be the result of the original program encoded in the cells rather than the cues provided by the injury (environment) itself. It is not clear whether the GFAP-positive cells detected in the intact brain one week after transplantation represent progenitor/stem cells, immature astrocytes (Chan-Ling et al., 2009) or reactive astrocytes. Further immunohistochemical analysis could help to determine the phenotype of these cells.

Interestingly, immunohistochemical analysis of a photochemical lesion transplanted with GFP/NE-4C or D6-GFP NS/PCs also revealed the presence of NeuN-positive- and DCX-positive/GFP-negative cells. These cells probably do not represent surviving endogenous neurons, as there was no positive staining for NeuN or DCX in photochemical lesions without transplanted cells (at both time points examined). These cells might thus represent cells that lost the GFP signal during the course of differentiation, as reported previously (Eriksson et al., 2003), or endogenous stem/progenitor cells that migrated into the lesion and differentiated into neurons. Although it was shown that injury promotes proliferation of GFAP-positive astrocytes in the cortex, these cells do not produce neurons or oligodendrocytes. However, they are able to proliferate *in vitro*, when exposed to mitogens, and to produce neurons, astrocytes and oligodendrocytes upon differentiation (Buffo et al., 2008). Since transplanted neural stem/progenitor cells can produce growth factors and mitogens and therefore act in a paracrine manner, it is likely that endogenous cells could be attracted by factors released by the implanted cells.

It was shown that in the early postnatal rodent brain, NG2-positive cells in the cortical grey matter remain mitotically active and are able to form neurospheres *in vitro*. Upon differentiation they give rise to neurons, as well as astrocytes and oligodendrocytes (Belachew et al., 2003). Moreover, NG2-positive cells were found to be the major proliferating cell population in the intact cerebral cortex of adult rats *in vivo* (Dawson et al., 2003). A subset of these proliferating cells co-express the neuronal marker DCX, and these cells produce new neurons (Dayer et al., 2005, Tamura et al., 2007). Acute brain injury, such as a cortical stab wound, leads to astrogliosis, in which GFAP-positive astrocytes increase their GFAP expression, while NG2-positive progenitors respond to the injury with cell proliferation (Alonso, 2005, Burns et al., 2009). An increased proliferation of NG2 glia was also observed after spreading depression (Tamura et al., 2004). Thus, endogenous cells with stem/progenitor properties could be attracted by factors released by transplanted neuroectodermal cells and respond to the presented cues by the generation of new neurons.

Our preliminary experiments with neonatal NS/PCs (data not included into this thesis) show that the fate of the NS/PCs is also influenced by the expressed morphogenes. While control cells showed poor survival and expressed solely NG2 one week after transplantation into the non-injured adult rat brain, Shh-expressing cells were NG2- and GFAP-positive and survived in great numbers. They also had the ability to migrate upon reaching the corpus callosum. However, only Wnt-7a-expressing cells were able to transform into DCX-positive cells. We can only speculate that Shh promotes the survival of transplanted cells, while Wnt-7a clearly promotes neuronal differentiation. It will be very interesting to evaluate the membrane properties of the transplanted cells and compare the data with those acquired *in vitro*.

In conclusion, NSCs derived from early neuroepithelium are tripotent upon transplantation into non-injured/injure adult rat brain, while E12-derived radial glia cells produce primarily neuronal cells. Additionally, radial glia cells are able to retain their region-specific features upon transplantation.

6.5 Membrane properties of transplanted cells

After transplantation into the intact or injured rat brain, a neuronal current pattern was identified in grafts of both GFP/NE-4C and D6-GFP NS/PCs. Cells displaying a passive current were detected only in the grafts of GFP/NE-4C cells.

6.5.1 Membrane properties of neuronal cells derived from transplanted NS/PCs

Both GFP/NE-4C- and D6-GFP-derived neuronal cells displayed the electrophysiological characteristics of maturing neurons. Their passive membrane properties, such as high IR and depolarised V_{rest}, were comparable with those observed in endogenous maturing neurons of the cortex (Kang et al., 2000; Yamada et al., 2004). While in neuronal cells differentiated *in vitro*, low Na^+ current densities were insufficient for firing repetitive APs, *in vivo* D6-GFP-derived neuronal cells (with Na^+/C_m values 3-4 times greater), were able to fire repetitively. However, the Na^+/C_m values did not reach those observed in transplanted, fully differentiated neurons (Englund et al., 2002, Wang et al., 2008). On the contrary, they corresponded with those previously reported in maturing endogenous neurons (Zhou and Hablitz, 1996, Picken Bahrey and Moody, 2003).

Surprisingly, when we compared the AP parameters of D6-GFP-neuronal cells derived *in vitro* and after transplantation into the adult brain, we found that the AP half-width duration was significantly lower in cells differentiated *in vitro* than in cells differentiated *in vivo*. It was reported that during neuronal maturation in the mouse cerebral cortex, neurons initially express low levels of Na^+/C_m, which increase with neuronal development, as well as the ability to fire spontaneous and repetitive APs (Picken Bahrey and Moody, 2003). With neuronal maturation the AP amplitude increases, while the duration of the AP decreases, as shown for cells differentiated *in vitro* (Johnson et al., 2007), *in vivo* and after transplantation into the lesioned brain (Zhou and Hablitz, 1996, Buhnemann et al., 2006). Compared to D6-GFP-derived neuronal cells *in vitro*, the K_{DR}/C_m and K_A/C_m were significantly lower in those derived *in vivo*. Since both K_A and K_{DR} currents participate in cell re-polarisation during the AP, the disparity between the Na^+/C_m and K^+ current densities might be responsible for the prolonged duration of the APs. Additionally, the outwardly rectifying K^+ currents of

neuronal cells differentiated *in vivo* displayed higher sensitivity to 4-AP than those recorded in neuronal cells *in vitro*, suggesting different stages of maturation of these channels.

The appearance of synaptophysin inside the lesions transplanted with GFP/NE-4C or D6-GFP NS/PCs suggests the presence of presynaptic terminals adjacent to the membranes of the transplanted cells and roughly corresponds to the morphological development of synapses in the brain (Hutcheon et al., 2004), suggesting that both types of NS/PCs have the potential to form synapses.

6.5.2 Membrane properties of passive cells derived from transplanted GFP/NE-4C cells

In the intact and lesioned cortex transplanted with GFP/NE-4C cells, GFP/GFAP-positive cells displayed two different current patterns, although the passive membrane properties of these cells were not significantly different. They might thus represent astrocytes at different stages of differentiation (Zhou et al., 2006) or represent two subpopulations of reactive astrocytes as described previously (Anderova et al., 2004). *In vivo* derived GFP-positive astrocytes showed significantly smaller K_{DR}, K_A, and K_{IR} current densities and higher IR values compared to mature endogenous astrocytes in the cortex. However, the C_m of GFP/GFAP-positive astrocytes was not significantly different from the C_m of mature cortical astrocytes (Bordey et al., 2001, Anderova et al., 2004).

In conclusion, both GFP/NE-4C and D6-GFP NS/PCs are able to give rise to neuronal cells after transplantation into the site of a cortical lesion. While GFP/NE-4C cells needed 3-4 weeks for neuronal production, D6-GFP NS/PCs produced firing neurons within one week after transplantation.

6.6 The role of GABA in neuronal differentiation

During embryonic development, as well as in the adult brain, neurotransmitters such as GABA or glutamate act as regulators of neurogenesis (Nakamichi et al., 2009). It was reported that during embryogenesis GABA decreases DNA synthesis and the effect is mediated by cell membrane depolarisation and the subsequent activation of Ca^{2+} voltage-gated ion channels, resulting in the inhibition of proliferation (LoTurco et al.,

1995). GABA was also shown to regulate neuronal migration and maturation (Cancedda et al., 2007, Heck et al., 2007) and the formation of synapses (Ge et al., 2006, Friocourt et al., 2007, Wang and Kriegstein, 2008). The underlying mechanism of GABA action has also been elucidated. Cl^- homeostasis in neurons/progenitors is maintained by the functional expression of Cl^- transporters and Cl^- channels. The Na^+-K^+-$2Cl^-$ co-transporter (NKCC1), which is responsible for the accumulation of Cl^- inside the neuron, is up-regulated during development, while the K^+-Cl^- co-transporter (KCC2), which extrudes Cl^- from the cells and is considered to be involved in the hyperpolarising effect of GABA in mature neurons, is down-regulated during development. This results in high intracellular concentrations of Cl^- ions (Yamada et al., 2004). The premature over-expression of KCC2 was shown to impair the morphological development of cortical neurons, and it was suggested that it is the cell depolarisation that is important for the effect of GABA, as the over-expression of inwardly rectifying K^+ channels had the same effect (Cancedda et al., 2007). Fast excitatory synaptic transmission in the pyramidal neurons of the neocortex is mediated by AMPA ionotropic glutamate receptors. These are heteromultimeric structures comprised of GluR1-4 (Swanson et al., 1997). However, newborn neurons of the cortex express $GABA_A$ receptors and receive depolarising GABA-ergic inputs from interneurons before they form glutamatergic synapses with each other (Owens et al., 1999, Hennou et al., 2002). It was suggested that depolarising GABA-ergic inputs cooperate with NMDA receptor activation, and subsequent Ca^{2+} influx activates signalling cascades leading to the expression of AMPA receptors at the synaptic site (Wang and Kriegstein, 2008). The sequential formation of GABA-ergic and glutamatergic synapses was also confirmed by an *in vitro* study showing that acutely isolated neurons from the E14 embryonic brain express high levels of functional $GABA_A$ receptors and are able to reform GABA-ergic synapses in a co-culture with GABA-ergic interneurons, while having low levels of functional glutamate receptors that are responsible for the lack of functional glutamatergic synapses (Deng et al., 2007). GABA-evoked currents and cell membrane depolarisation were also reported *in vitro*, in undifferentiated embryonic NSCs and newly derived neurons (Jelitai et al., 2004, Pagani et al., 2006). *In viv*o experiments showed that in the adult brain migrating neuroblasts synthesise and release GABA and both neuroblasts and SVZ type-B cells express $GABA_A$ receptors (Wang et al., 2003b, Bolteus and Bordey, 2004). Type-B cells also express the high-affinity

GABA transporter 4 (GAT-4) on processes ensheathing migrating precursors, and this transporter is responsible for GABA uptake. It was further shown that the extracellular levels of GABA control the speed of neuroblast migration via $GABA_A$ receptors on the neuroblasts and an intracellular mechanism involving Ca^{2+} release from internal stores. High levels of GABA reduce the migration speed, while GABA uptake into astrocytes (via GAT-4) enhances the speed of neuronal migration by clearing GABA released into the extracellular space (Bolteus and Bordey, 2004, Bolteus et al., 2005). GABA released from neuroblasts also affects the proliferation of type-A cells *in situ*. Blockage of the GAT-4 transporter reduced the number of proliferating type-B cells, while blocking the $GABA_A$ receptors with bicuculline increased the number of proliferating cells (Liu et al., 2005b).

It was shown that both proliferating and differentiating NE-4C cells contain GABA and respond to the application of GABA by an inward current, followed by a small Ca^{2+} influx. Furthermore, the presence of GABA at a certain phase of *in vitro* differentiation might be essential for neuronal production. The number of neurons was significantly lower when NE-4C cells were grown in the presence of bicuculline, either during the entire period of *in vitro* differentiation (day 1-7) or between days 4 and 7. In contrast, there were no changes in neuronal differentiation when the cells were treated with bicuculline during the first 3 days of *in vitro* differentiation (Jelitai et al., 2004), which is the period of proliferation and initial neuronal cell fate decision (Varga et al., 2008). Therefore, the response of GFP/NE-4C-derived neuronal cells to GABA might also be restricted to a certain phase of development, and we can not exclude the possibility that later on, these cells might also develop functional glutamatergic receptors.

In the D6-GFP NS/PC *in vitro* cultures, some of the cells contained GABA and GAD65/67, suggesting that some of the neuronal cells might differentiate into GABA-ergic interneurons. However, only one GABA-positive cell was detected *in vivo* and no GFP/GAD65/67 double stained cells were detected in the grafts. These findings suggest that the fate of D6-GFP cells is different during *in vitro* differentiation and upon transplantation into the adult rat brain, presumably due to the presence of bFGF in the culture medium (Abematsu et al., 2006). When we explored GAD65/67 expression in the transgenic D6-GFP mouse, we found that GAD65/67 did not co-localise with the GFP signal, demonstrating that the mDach1 gene is not active in interneurons, as was

shown by Machon *et al*., who showed that D6-GFP derived neurons do not express calretinin and calbindin (Machon et al., 2005). Another study indicated that glutamatergic neurons, including all projection neurons, are generated in the neocortical VZ of the dorsal telencephalon, while GABA-ergic interneurons are born in the ganglionic eminences of the ventral telencephalon (Parnavelas, 2002).

Interestingly, we did not detect any GABA-mediated response in the control neuronal cells derived from NS/PCs of the neonatal brain. However, it was shown that during the *in vitro* differentiation of adult neural stem cells, functional $GABA_A$ receptors are expressed in neurons from day 11 after the onset of *in vitro* differentiation, and a functional glutamate response was detected even later, 15 days after the onset of *in vitro* differentiation (Goffredo et al., 2008). It is thus possible that neonatal NS/PC-derived neurons need a longer period to express functional $GABA_A$ receptors. On the other hand, the functional expression of $GABA_A$ receptors in Shh- and Wnt-7a-expressing cell cultures (regardless of the current pattern) suggests that these morphogenes are potential regulators of GABA signalling in neonatal neural stem/progenitor cells during *in vitro* differentiation or that their effect might be partly mediated by GABA signalling.

Taken together, GABA seems to play an essential role in the differentiation and maturation of cells derived from both the embryonic as well as the neonatal brain.

6.7 The lack of a glutamate response in differentiated NS/PCs

Glutamate, another candidate neurotransmitter that affects neurogenesis, acts via NMDA or non-NMDA receptors. However, we did not detect any response to the application of glutamate in neuronal cells differentiated *in vitro* or *in vivo* after transplantation into the adult rat brain. NMDA receptors are heteromeric complexes, containing at least one NR1 and one or more NR2 subunits (Ikeda et al., 1992), and they were shown to affect embryonic NSC proliferation and neuronal differentiation *in vitro* (Mochizuki et al., 2007, Yoneyama et al., 2008). A previous study on GFP/NE-4C-derived neurons *in vitro* showed that NR1 subunit protein was detected in both non-differentiated and differentiated NE-4C cells, while NR2B subunit protein, essential for receptor activity, appeared 6 days after the induction of differentiation by RA; after 9 days the majority of the protein was localised in the membrane. Using

microspectrofluorimetry, it was shown that the application of NMDA increased the intracellular levels of Ca^{2+}, and this response was blocked by the addition of AP-5 (Jelitai et al., 2002). Because the NR2B subunit protein has been proposed to be a limiting factor in the co-assembly and cell surface targeting of the receptor (McIlhinney et al., 1998), the lack of the mature form of NR2B protein might explain the lack of response to glutamate. Furthermore, the NMDA receptors already present in the cell membrane can be affected by glycosylation and phosphorylation (Clark et al., 1998). NR1 and NR2B subunits were also detected in proliferating cells within neurospheres isolated from later stages of embryonic development. Blocking the receptors by MK801 affected the neurosphere growth, suggesting the role of these receptors in neural stem cell proliferation (Mochizuki et al., 2007).

Although we detected GluR subunits 1-4 by Western blotting in D6-GFP cell cultures, one week after the onset of *in vitro* differentiation, we did not detect any response to the application of glutamate in cells differentiated *in vitro* or in cells differentiated *in vivo*, after transplantation into the intact/injured rat brain, suggesting that these cell do not posses functional ionotropic glutamate receptors.

In the adult brain neuroblasts express Ca^{2+}-permeable GLUK5-containing kainate receptors, which are also involved in the regulation of migration speed, as blocking these channels with a specific antagonist decreased the rate of migration in the adult SVZ (Platel et al., 2008). However, we did not detect any glutamate-specific responses in any of the neonatal NS/PC types, leading to the conclusion that these cells also do not express functional ionotropic glutamate receptors.

In conclusion, our data show that NS/PCs derived from various developmental stages are able to differentiate into immature neurons *in vitro* as well as *in vivo,* upon transplantation into the adult injured rat brain. While the GFP/NE-4C cell line is tripotent upon transplantation, D6/GFP NS/PCs are primarily neurogenic. Moreover, D6-GFP cells are able to preserve their cortical identity, marked by the sustained expression of mDach1/GFP. Our *in vitro* study shows that the expression of Wnt-7a promotes the outgrowth of cell processes and a neuron-like current pattern in neuronal cells, while Shh enhances the less differentiated phenotype of neonatal NS/PCs.

6.8 Future prospects

Although the use of NS/PCs in clinical trials is rather limited to date, neural stem cell research provides important data for developing/optimizing new strategies for regenerative medicine that would eventually lead to successful cell replacement therapies.

Immortalized stem cell lines provide an unlimited source of identical cells with well-defined properties and known behaviour. Our data show that clonally-derived immortalized neural stem cell lines represent a suitable tool for studying the mechanisms of neurogenesis/gliogenesis both *in vitro* and *in vivo* after transplantation into the injured rat brain. While there is no definite answer about the ideal cell types for transplantation, region-specific NS/PCs are pre-programmed to produce distinct populations of cells within the developing nervous system and might thus represent a potent tool to specifically replace one or several cell populations in the damaged brain. Our data show that NS/PCs isolated from the embryonic dorsal telencephalon are able to retain the expression of a region-specific gene and display comparable membrane properties upon transplantation into the non-injured brain, and, more importantly, into the site of a cortical lesion. Neural stem cells with a less restricted fate, on the other hand, might provide more extensive possibilities for modifying their fate and thus a broader spectrum for their use. Genetic manipulations of NS/PCs can modify cell fate and differentiation, enhance cell survival, and promote transplanted cells to establish functional connections with the host tissue. Our *in vitro* study shows that the expression of Wnt-7a promotes the outgrowth of cell processes and a neuron-like current pattern in differentiating cells, while Shh enhances the less differentiated phenotype of neonatal NS/PCs. Viral transduction might thus provide one suitable tool for manipulating NSCs for the generation of new neurons and such a method may help develop new strategies for the treatment of neurodegenerative diseases and for regenerating damaged tissue after injury. However, deeper insight into the molecular processes of morphogene action is necessary to fully understand their role in NS/PC proliferation and differentiation. Finally, only a thorough functional analysis of terminally differentiated cells *in vitro* and the examination of transplants on a cellular level can reveal the actual outcome of our attempts to find a suitable source of transplantable cells.

7. CONCLUSIONS

The major findings of this study are summarised below:

1. Embryonic as well as neonatal NS/PCs differentiate into neuronal cells *in vitro*.
2. After transplantation into the adult non-injured/injured rat brain, GFP/NE-4C cells survive and differentiate into neuronal cells, astrocytes and oligodendrocytes, while D6-GFP NS/PCs differentiate primarily into neurons.
3. D6-GFP *in vivo* derived neurons are able to fire action potentials.
4. Shh and Wnt-7a promote proliferation in single neurospheres and at the onset of differentiation, while subsequently, only Shh promotes proliferation. Additionally, Wnt-7a expression suppresses the number of GFAP-positive cells in neurospheres derived from neonatal NS/PCs.
5. Shh and Wnt-7a increase the number of neuronal cells during *in vitro* differentiation, while only Wnt-7a promotes the outgrowth of neuronal processes.
6. Shh promotes the current pattern of uncommitted/early committed progenitors in differentiated cells, while Wnt-7a clearly promotes the neuronal current pattern in differentiated cells.

8. LIST OF PUBLICATIONS

8.1 Publications related to the thesis and contributions of individual co-authors:

1. Anderova M., Kubinova S., Jelitai M., Neprasova H., Glogarova K., **Prajerova I.**, Urdzikova L., Chvatal A., Sykova E. (2006). Transplantation of embryonic neuroectodermal progenitor cells into the site of a photochemical lesion: immunohistochemical and electrophysiological analysis. *J Neurobiol*. 66(10):1084-100. **(IF 3.239)**

CONTROBUTIONS:
Photochemical lesions, cell transplantation into lesions: Kubinova S., Urdzikova L, Prajerova I.
Cell transplantation into the intact cortex: Prajerova I.
Cell culture: Jelitai M., Glogarova K., Prajerova I.
In vitro differentiation and patch-clamp recordings: Prajerova I., Anderova M, Neprasova H.
In situ recordings, immunohistochemical analysis, electrophysiological data analysis: Prajerova I., Anderova M.

2. Prajerova I., Honsa P., Chvatal A. and Anderova M. (2010). Neural Stem/Progenitor Cells Derived from the Embryonic Dorsal Telencephalon of D6/GFP Mice Differentiate Primarily into Neurons After Transplantation into a Cortical Lesion. *Cell Mol Neurobiol.* 30(2):199-218. **(IF 2.55)**

CONTROBUTIONS:
Cell isolation and *in vitro* differentiation: Prajerova I.
Patch-clamp recording *in vitro*: Prajerova I, Honsa P.
Photochemical lesions and cell transplantations: Prajerova I.
Patch-clamp recording *in situ*: Prajerova I.
Immunohistochemical analysis: Prajerova I., Anderova M.

3. Prajerova I., Honsa P., Chvatal A. and Anderova M. Diverse effects of Shh and Wnt-7a on the electrophysiological properties of neonatal NS/PCs *in vitro.*
Submitted to Neuroscience

CONTROBUTIONS:
Cell culture and *in vitro* differentiation: Prajerova I.
Immunocytochemical analysis: Prajerova I.
Quantitative immunocytochemistry: Prajerova I., Anderova M., Honsa P.
Western blot analysis: Honsa P.
Patch-clamp recording *in vitro*: Prajerova I., Honsa P.

8.2 Other publications

4. Benesova J, Hock M, Butenko O, **Prajerova I**, Anderova M, Chvatal A. (2009). Quantification of astrocyte volume changes during ischemia in situ reveals two populations of astrocytes in the cortex of GFAP/EGFP mice. *J Neurosci Res* 87(1):96-111.
(IF 3.38)

5. Chvatal A, Anderova M, Neprasova H, **Prajerova I**, Benesova J, Butenko O, Verkhratsky A. (2008). Pathological potential of astroglia (Review). *Physiol Res 57 Suppl* 3:S101-10.
(IF 1.75)

6. Chvatal A., Anderova M., Hock M., **Prajerova I**., Neprasova H., Chvatal V., Kirchhoff F., Sykova E. (2007). Three-dimensional confocal morphometry reveals structural changes in astrocyte morphology in situ. *J Neurosci Res.* 85(2):260-271.
(IF 4.17)

9. REFERENCES

Abematsu M, Kagawa T, Fukuda S, Inoue T, Takebayashi H, Komiya S, Taga T (Basic fibroblast growth factor endows dorsal telencephalic neural progenitors with the ability to differentiate into oligodendrocytes but not gamma-aminobutyric acidergic neurons. J Neurosci Res 83:731-743.2006).

Adachi K, Mirzadeh Z, Sakaguchi M, Yamashita T, Nikolcheva T, Gotoh Y, Peltz G, Gong L, Kawase T, Alvarez-Buylla A, Okano H, Sawamoto K (Beta-catenin signaling promotes proliferation of progenitor cells in the adult mouse subventricular zone. Stem Cells 25:2827-2836.2007).

Aguirre AA, Chittajallu R, Belachew S, Gallo V (NG2-expressing cells in the subventricular zone are type C-like cells and contribute to interneuron generation in the postnatal hippocampus. J Cell Biol 165:575-589.2004).

Ahlenius H, Visan V, Kokaia M, Lindvall O, Kokaia Z (Neural stem and progenitor cells retain their potential for proliferation and differentiation into functional neurons despite lower number in aged brain. J Neurosci 29:4408-4419.2009).

Ahn S, Joyner AL (In vivo analysis of quiescent adult neural stem cells responding to Sonic hedgehog. Nature 437:894-897.2005).

Akesson E, Piao JH, Samuelsson EB, Holmberg L, Kjaeldgaard A, Falci S, Sundstrom E, Seiger A (Long-term culture and neuronal survival after intraspinal transplantation of human spinal cord-derived neurospheres. Physiol Behav 92:60-66.2007).

Akimoto J, Itoh H, Miwa T, Ikeda K (Immunohistochemical study of glutamine synthetase expression in early glial development. Brain Res Dev Brain Res 72:9-14.1993).

Alonso G (NG2 proteoglycan-expressing cells of the adult rat brain: possible involvement in the formation of glial scar astrocytes following stab wound. Glia 49:318-338.2005).

Alonso M, Ortega-Perez I, Grubb MS, Bourgeois JP, Charneau P, Lledo PM (Turning astrocytes from the rostral migratory stream into neurons: a role for the olfactory sensory organ. J Neurosci 28:11089-11102.2008).

Alves JA, Barone P, Engelender S, Froes MM, Menezes JR (Initial stages of radial glia astrocytic transformation in the early postnatal anterior subventricular zone. J Neurobiol 52:251-265.2002).

Amankulor NM, Hambardzumyan D, Pyonteck SM, Becher OJ, Joyce JA, Holland EC (Sonic hedgehog pathway activation is induced by acute brain injury and regulated by injury-related inflammation. J Neurosci 29:10299-10308.2009).

Anderova M, Antonova T, Petrik D, Neprasova H, Chvatal A, Sykova E (Voltage-dependent potassium currents in hypertrophied rat astrocytes after a cortical stab wound. Glia 48:311-326.2004).

Andreasen M, Skov J, Nedergaard S (Inwardly rectifying K(+) (Kir) channels antagonize ictal-like epileptiform activity in area CA1 of the rat hippocampus. Hippocampus 17:1037-1048.2007).

Anthony TE, Klein C, Fishell G, Heintz N (Radial glia serve as neuronal progenitors in all regions of the central nervous system. Neuron 41:881-890.2004).

Anthony TE, Mason HA, Gridley T, Fishell G, Heintz N (Brain lipid-binding protein is a direct target of Notch signaling in radial glial cells. Genes Dev 19:1028-1033.2005).

Babu H, Cheung G, Kettenmann H, Palmer TD, Kempermann G (Enriched monolayer precursor cell cultures from micro-dissected adult mouse dentate gyrus yield functional granule cell-like neurons. PLoS One 2:e388.2007).

Bafico A, Liu G, Yaniv A, Gazit A, Aaronson SA (Novel mechanism of Wnt signalling inhibition mediated by Dickkopf-1 interaction with LRP6/Arrow. Nat Cell Biol 3:683-686.2001).

Bai J, Ramos RL, Ackman JB, Thomas AM, Lee RV, LoTurco JJ (RNAi reveals doublecortin is required for radial migration in rat neocortex. Nat Neurosci 6:1277-1283.2003).

Bakshi A, Shimizu S, Keck CA, Cho S, LeBold DG, Morales D, Arenas E, Snyder EY, Watson DJ, McIntosh TK (Neural progenitor cells engineered to secrete GDNF show enhanced survival, neuronal differentiation and improve cognitive function following traumatic brain injury. Eur J Neurosci 23:2119-2134.2006).

Balasubramaniyan V, de Haas AH, Bakels R, Koper A, Boddeke HW, Copray JC (Functionally deficient neuronal differentiation of mouse embryonic neural stem cells in vitro. Neurosci Res 49:261-265.2004).

Balordi F, Fishell G (Hedgehog signaling in the subventricular zone is required for both the maintenance of stem cells and the migration of newborn neurons. J Neurosci 27:5936-5947.2007a).

Balordi F, Fishell G (Mosaic removal of hedgehog signaling in the adult SVZ reveals that the residual wild-type stem cells have a limited capacity for self-renewal. J Neurosci 27:14248-14259.2007b).

Banerjee SB, Rajendran R, Dias BG, Ladiwala U, Tole S, Vaidya VA (Recruitment of the Sonic hedgehog signalling cascade in electroconvulsive seizure-mediated regulation of adult rat hippocampal neurogenesis. Eur J Neurosci 22:1570-1580.2005).

Barry PH (JPCalc, a software package for calculating liquid junction potential corrections in patch-clamp, intracellular, epithelial and bilayer measurements and for correcting junction potential measurements. J Neurosci Methods 51:107-116.1994).

Basak O, Taylor V (Identification of self-replicating multipotent progenitors in the embryonic nervous system by high Notch activity and Hes5 expression. Eur J Neurosci 25:1006-1022.2007).

Bauer S, Patterson PH (The cell cycle-apoptosis connection revisited in the adult brain. J Cell Biol 171:641-650.2005).

Belachew S, Chittajallu R, Aguirre AA, Yuan X, Kirby M, Anderson S, Gallo V (Postnatal NG2 proteoglycan-expressing progenitor cells are intrinsically multipotent and generate functional neurons. J Cell Biol 161:169-186.2003).

Benninger F, Beck H, Wernig M, Tucker KL, Brustle O, Scheffler B (Functional integration of embryonic stem cell-derived neurons in hippocampal slice cultures. J Neurosci 23:7075-7083.2003).

Bhat RA, Stauffer B, Komm BS, Bodine PV (Structure-function analysis of secreted frizzled-related protein-1 for its Wnt antagonist function. J Cell Biochem 102:1519-1528.2007).

Bibel M, Richter J, Lacroix E, Barde YA (Generation of a defined and uniform population of CNS progenitors and neurons from mouse embryonic stem cells. Nat Protoc 2:1034-1043.2007).

Bibel M, Richter J, Schrenk K, Tucker KL, Staiger V, Korte M, Goetz M, Barde YA (Differentiation of mouse embryonic stem cells into a defined neuronal lineage. Nat Neurosci 7:1003-1009.2004).

Bittman K, Owens DF, Kriegstein AR, LoTurco JJ (Cell coupling and uncoupling in the ventricular zone of developing neocortex. J Neurosci 17:7037-7044.1997).

Bolteus AJ, Bordey A (GABA release and uptake regulate neuronal precursor migration in the postnatal subventricular zone. J Neurosci 24:7623-7631.2004).

Bolteus AJ, Garganta C, Bordey A (Assays for measuring extracellular GABA levels and cell migration rate in acute slices. Brain Res Brain Res Protoc 14:126-134.2005).

Bonaguidi MA, Peng CY, McGuire T, Falciglia G, Gobeske KT, Czeisler C, Kessler JA (Noggin expands neural stem cells in the adult hippocampus. J Neurosci 28:9194-9204.2008).

Bordey A, Lyons SA, Hablitz JJ, Sontheimer H (Electrophysiological characteristics of reactive astrocytes in experimental cortical dysplasia. J Neurophysiol 85:1719-1731.2001).

Brantjes H, Roose J, van De Wetering M, Clevers H (All Tcf HMG box transcription factors interact with Groucho-related co-repressors. Nucleic Acids Res 29:1410-1419.2001).

Brazel CY, Limke TL, Osborne JK, Miura T, Cai J, Pevny L, Rao MS (Sox2 expression defines a heterogeneous population of neurosphere-forming cells in the adult murine brain. Aging Cell 4:197-207.2005).

Brenner M, Kisseberth WC, Su Y, Besnard F, Messing A (GFAP promoter directs astrocyte-specific expression in transgenic mice. J Neurosci 14:1030-1037.1994).

Breunig JJ, Silbereis J, Vaccarino FM, Sestan N, Rakic P (Notch regulates cell fate and dendrite morphology of newborn neurons in the postnatal dentate gyrus. Proc Natl Acad Sci U S A 104:20558-20563.2007).

Brill MS, Snapyan M, Wohlfrom H, Ninkovic J, Jawerka M, Mastick GS, Ashery-Padan R, Saghatelyan A, Berninger B, Gotz M (A dlx2- and pax6-dependent transcriptional code for periglomerular neuron specification in the adult olfactory bulb. J Neurosci 28:6439-6452.2008).

Buffo A, Rite I, Tripathi P, Lepier A, Colak D, Horn AP, Mori T, Gotz M (Origin and progeny of reactive gliosis: A source of multipotent cells in the injured brain. Proc Natl Acad Sci U S A 105:3581-3586.2008).

Buglino JA, Resh MD (Hhat is a palmitoylacyltransferase with specificity for N-palmitoylation of Sonic Hedgehog. J Biol Chem 283:22076-22088.2008).

Buhnemann C, Scholz A, Bernreuther C, Malik CY, Braun H, Schachner M, Reymann KG, Dihne M (Neuronal differentiation of transplanted embryonic stem cell-derived precursors in stroke lesions of adult rats. Brain 129:3238-3248.2006).

Burns KA, Murphy B, Danzer SC, Kuan CY (Developmental and post-injury cortical gliogenesis: a genetic fate-mapping study with Nestin-CreER mice. Glia 57:1115-1129.2009).

Butt AM, Kalsi A (Inwardly rectifying potassium channels (Kir) in central nervous system glia: a special role for Kir4.1 in glial functions. J Cell Mol Med 10:33-44.2006).

Cacci E, Villa A, Parmar M, Cavallaro M, Mandahl N, Lindvall O, Martinez-Serrano A, Kokaia Z (Generation of human cortical neurons from a new immortal fetal neural stem cell line. Exp Cell Res 313:588-601.2007).

Cai J, Cheng A, Luo Y, Lu C, Mattson MP, Rao MS, Furukawa K (Membrane properties of rat embryonic multipotent neural stem cells. J Neurochem 88:212-226.2004).

Cai J, Wu Y, Mirua T, Pierce JL, Lucero MT, Albertine KH, Spangrude GJ, Rao MS (Properties of a fetal multipotent neural stem cell (NEP cell). Dev Biol 251:221-240.2002).

Cancedda L, Fiumelli H, Chen K, Poo MM (Excitatory GABA action is essential for morphological maturation of cortical neurons in vivo. J Neurosci 27:5224-5235.2007).

Capela A, Temple S (LeX/ssea-1 is expressed by adult mouse CNS stem cells, identifying them as nonependymal. Neuron 35:865-875.2002).

Capela A, Temple S (LeX is expressed by principle progenitor cells in the embryonic nervous system, is secreted into their environment and binds Wnt-1. Dev Biol 291:300-313.2006).

Cappuccio I, Calderone A, Busceti CL, Biagioni F, Pontarelli F, Bruno V, Storto M, Terstappen GT, Gaviraghi G, Fornai F, Battaglia G, Melchiorri D, Zukin RS, Nicoletti F, Caricasole A (Induction of Dickkopf-1, a negative modulator of the Wnt pathway, is required for the development of ischemic neuronal death. J Neurosci 25:2647-2657.2005).

Carlen M, Meletis K, Goritz C, Darsalia V, Evergren E, Tanigaki K, Amendola M, Barnabe-Heider F, Yeung MS, Naldini L, Honjo T, Kokaia Z, Shupliakov O, Cassidy RM, Lindvall O, Frisen J (Forebrain ependymal cells are Notch-dependent and generate neuroblasts and astrocytes after stroke. Nat Neurosci 12:259-267.2009).

Carletti B, Grimaldi P, Magrassi L, Rossi F (Engraftment and differentiation of neocortical progenitor cells transplanted to the embryonic brain in utero. J Neurocytol 33:309-319.2004).

Carpenter D, Stone DM, Brush J, Ryan A, Armanini M, Frantz G, Rosenthal A, de Sauvage FJ (Characterization of two patched receptors for the vertebrate hedgehog protein family. Proc Natl Acad Sci U S A 95:13630-13634.1998).

Caspary T, Garcia-Garcia MJ, Huangfu D, Eggenschwiler JT, Wyler MR, Rakeman AS, Alcorn HL, Anderson KV (Mouse Dispatched homolog1 is required for long-range, but not juxtacrine, Hh signaling. Curr Biol 12:1628-1632.2002).

Cesetti T, Obernier K, Bengtson CP, Fila T, Mandl C, Holzl-Wenig G, Worner K, Eckstein V, Ciccolini F (Analysis of stem cell lineage progression in the neonatal subventricular zone identifies EGFR+/NG2- cells as transit-amplifying precursors. Stem Cells 27:1443-1454.2009).

Chan-Ling T, Chu Y, Baxter L, Weible Ii M, Hughes S (In vivo characterization of astrocyte precursor cells (APCs) and astrocytes in developing rat retinae: differentiation, proliferation, and apoptosis. Glia 57:39-53.2009).

Chen JK, Taipale J, Cooper MK, Beachy PA (Inhibition of Hedgehog signaling by direct binding of cyclopamine to Smoothened. Genes Dev 16:2743-2748.2002).

Chen MH, Li YJ, Kawakami T, Xu SM, Chuang PT (Palmitoylation is required for the production of a soluble multimeric Hedgehog protein complex and long-range signaling in vertebrates. Genes Dev 18:641-659.2004).

Cheung HO, Zhang X, Ribeiro A, Mo R, Makino S, Puviindran V, Law KK, Briscoe J, Hui CC (The kinesin protein Kif7 is a critical regulator of Gli transcription factors in mammalian hedgehog signaling. Sci Signal 2:ra29.2009).

Chiasson BJ, Tropepe V, Morshead CM, van der Kooy D (Adult mammalian forebrain ependymal and subependymal cells demonstrate proliferative potential, but only subependymal cells have neural stem cell characteristics. J Neurosci 19:4462-4471.1999).

Chu K, Kim M, Chae SH, Jeong SW, Kang KS, Jung KH, Kim J, Kim YJ, Kang L, Kim SU, Yoon BW (Distribution and in situ proliferation patterns of intravenously injected immortalized human neural stem-like cells in rats with focal cerebral ischemia. Neurosci Res 50:459-465.2004).

Chuang PT, McMahon AP (Vertebrate Hedgehog signalling modulated by induction of a Hedgehog-binding protein. Nature 397:617-621.1999).

Chvatal A, Anderova M, Kirchhoff F (Three-dimensional confocal morphometry - a new approach for studying dynamic changes in cell morphology in brain slices. J Anat 210:671-683.2007).

Clark RA, Gurd JW, Bissoon N, Tricaud N, Molnar E, Zamze SE, Dwek RA, McIlhinney RA, Wing DR (Identification of lectin-purified neural glycoproteins, GPs 180, 116, and 110, with NMDA and AMPA receptor subunits: conservation of glycosylation at the synapse. J Neurochem 70:2594-2605.1998).

Clevers H (Wnt/beta-catenin signaling in development and disease. Cell 127:469-480.2006).

Colak D, Mori T, Brill MS, Pfeifer A, Falk S, Deng C, Monteiro R, Mummery C, Sommer L, Gotz M (Adult neurogenesis requires Smad4-mediated bone morphogenic protein signaling in stem cells. J Neurosci 28:434-446.2008).

Comelli MC, Guidolin D, Seren MS, Zanoni R, Canella R, Rubini R, Manev H (Time course, localization and pharmacological modulation of immediate early inducible genes, brain-derived neurotrophic factor and trkB messenger RNAs in the rat brain following photochemical stroke. Neuroscience 55:473-490.1993).

Corbit KC, Aanstad P, Singla V, Norman AR, Stainier DY, Reiter JF (Vertebrate Smoothened functions at the primary cilium. Nature 437:1018-1021.2005).

Coskun V, Wu H, Blanchi B, Tsao S, Kim K, Zhao J, Biancotti JC, Hutnick L, Krueger RC, Jr., Fan G, de Vellis J, Sun YE (CD133+ neural stem cells in the ependyma of mammalian postnatal forebrain. Proc Natl Acad Sci U S A 105:1026-1031.2008).

Dahmane N, Sanchez P, Gitton Y, Palma V, Sun T, Beyna M, Weiner H, Ruiz i Altaba A (The Sonic Hedgehog-Gli pathway regulates dorsal brain growth and tumorigenesis. Development 128:5201-5212.2001).

Dai P, Akimaru H, Tanaka Y, Maekawa T, Nakafuku M, Ishii S (Sonic Hedgehog-induced activation of the Gli1 promoter is mediated by GLI3. J Biol Chem 274:8143-8152.1999).

Daniels DL, Weis WI (Beta-catenin directly displaces Groucho/TLE repressors from Tcf/Lef in Wnt-mediated transcription activation. Nat Struct Mol Biol 12:364-371.2005).

Danilov AI, Gomes-Leal W, Ahlenius H, Kokaia Z, Carlemalm E, Lindvall O (Ultrastructural and antigenic properties of neural stem cells and their progeny in adult rat subventricular zone. Glia 57:136-152.2009).

Dann CE, Hsieh JC, Rattner A, Sharma D, Nathans J, Leahy DJ (Insights into Wnt binding and signalling from the structures of two Frizzled cysteine-rich domains. Nature 412:86-90.2001).

Darsalia V, Kallur T, Kokaia Z (Survival, migration and neuronal differentiation of human fetal striatal and cortical neural stem cells grafted in stroke-damaged rat striatum. Eur J Neurosci 26:605-614.2007).

Dawson MR, Polito A, Levine JM, Reynolds R (NG2-expressing glial progenitor cells: an abundant and widespread population of cycling cells in the adult rat CNS. Mol Cell Neurosci 24:476-488.2003).

Dayer AG, Cleaver KM, Abouantoun T, Cameron HA (New GABAergic interneurons in the adult neocortex and striatum are generated from different precursors. J Cell Biol 168:415-427.2005).

Dayer AG, Ford AA, Cleaver KM, Yassaee M, Cameron HA (Short-term and long-term survival of new neurons in the rat dentate gyrus. J Comp Neurol 460:563-572.2003).

De Ferrari GV, Moon RT (The ups and downs of Wnt signaling in prevalent neurological disorders. Oncogene 25:7545-7553.2006).

De Filippis L, Ferrari D, Rota Nodari L, Amati B, Snyder E, Vescovi AL (Immortalization of human neural stem cells with the c-myc mutant T58A. PLoS One 3:e3310.2008).

Demeter K, Herberth B, Duda E, Domonkos A, Jaffredo T, Herman JP, Madarasz E (Fate of cloned embryonic neuroectodermal cells implanted into the adult, newborn and embryonic forebrain. Exp Neurol 188:254-267.2004).

Deng L, Yao J, Fang C, Dong N, Luscher B, Chen G (Sequential postsynaptic maturation governs the temporal order of GABAergic and glutamatergic synaptogenesis in rat embryonic cultures. J Neurosci 27:10860-10869.2007).

Diers-Fenger M, Kirchhoff F, Kettenmann H, Levine JM, Trotter J (AN2/NG2 protein-expressing glial progenitor cells in the murine CNS: isolation, differentiation, and association with radial glia. Glia 34:213-228.2001).

Doetsch F, Caille I, Lim DA, Garcia-Verdugo JM, Alvarez-Buylla A (Subventricular zone astrocytes are neural stem cells in the adult mammalian brain. Cell 97:703-716.1999a).

Doetsch F, Garcia-Verdugo JM, Alvarez-Buylla A (Cellular composition and three-dimensional organization of the subventricular germinal zone in the adult mammalian brain. J Neurosci 17:5046-5061.1997).

Doetsch F, Garcia-Verdugo JM, Alvarez-Buylla A (Regeneration of a germinal layer in the adult mammalian brain. Proc Natl Acad Sci U S A 96:11619-11624.1999b).

Doetsch F, Petreanu L, Caille I, Garcia-Verdugo JM, Alvarez-Buylla A (EGF converts transit-amplifying neurogenic precursors in the adult brain into multipotent stem cells. Neuron 36:1021-1034.2002).

Dromard C, Bartolami S, Deleyrolle L, Takebayashi H, Ripoll C, Simonneau L, Prome S, Puech S, Tran VB, Duperray C, Valmier J, Privat A, Hugnot JP (NG2 and Olig2 expression provides evidence for phenotypic deregulation of cultured central nervous system and peripheral nervous system neural precursor cells. Stem Cells 25:340-353.2007).

Elias LA, Wang DD, Kriegstein AR (Gap junction adhesion is necessary for radial migration in the neocortex. Nature 448:901-907.2007).

Englund U, Bjorklund A, Wictorin K, Lindvall O, Kokaia M (Grafted neural stem cells develop into functional pyramidal neurons and integrate into host cortical circuitry. Proc Natl Acad Sci U S A 99:17089-17094.2002).

Eriksson C, Bjorklund A, Wictorin K (Neuronal differentiation following transplantation of expanded mouse neurosphere cultures derived from different embryonic forebrain regions. Exp Neurol 184:615-635.2003).

Fan G, Martinowich K, Chin MH, He F, Fouse SD, Hutnick L, Hattori D, Ge W, Shen Y, Wu H, ten Hoeve J, Shuai K, Sun YE (DNA methylation controls the timing of astrogliogenesis through regulation of JAK-STAT signaling. Development 132:3345-3356.2005).

Favaro R, Valotta M, Ferri AL, Latorre E, Mariani J, Giachino C, Lancini C, Tosetti V, Ottolenghi S, Taylor V, Nicolis SK (Hippocampal development and neural stem cell maintenance require Sox2-dependent regulation of Shh. Nat Neurosci 12:1248-1256.2009).

Filippov V, Kronenberg G, Pivneva T, Reuter K, Steiner B, Wang LP, Yamaguchi M, Kettenmann H, Kempermann G (Subpopulation of nestin-expressing progenitor cells in the adult murine hippocampus shows electrophysiological and morphological characteristics of astrocytes. Mol Cell Neurosci 23:373-382.2003).

Fogarty M, Grist M, Gelman D, Marin O, Pachnis V, Kessaris N (Spatial genetic patterning of the embryonic neuroepithelium generates GABAergic interneuron diversity in the adult cortex. J Neurosci 27:10935-10946.2007).

Friocourt G, Liu JS, Antypa M, Rakic S, Walsh CA, Parnavelas JG (Both doublecortin and doublecortin-like kinase play a role in cortical interneuron migration. J Neurosci 27:3875-3883.2007).

Fuccillo M, Joyner AL, Fishell G (Morphogen to mitogen: the multiple roles of hedgehog signalling in vertebrate neural development. Nat Rev Neurosci 7:772-783.2006).

Fujiwara Y, Tanaka N, Ishida O, Fujimoto Y, Murakami T, Kajihara H, Yasunaga Y, Ochi M (Intravenously injected neural progenitor cells of transgenic rats can migrate to the injured spinal cord and differentiate into neurons, astrocytes and oligodendrocytes. Neurosci Lett 366:287-291.2004).

Fukuda S, Kato F, Tozuka Y, Yamaguchi M, Miyamoto Y, Hisatsune T (Two distinct subpopulations of nestin-positive cells in adult mouse dentate gyrus. J Neurosci 23:9357-9366.2003).

Gaiano N, Nye JS, Fishell G (Radial glial identity is promoted by Notch1 signaling in the murine forebrain. Neuron 26:395-404.2000).

Gaillard A, Nasarre C, Roger M (Early (E12) cortical progenitors can change their fate upon heterotopic transplantation. Eur J Neurosci 17:1375-1383.2003).

Gao Z, Ure K, Ables JL, Lagace DC, Nave KA, Goebbels S, Eisch AJ, Hsieh J (Neurod1 is essential for the survival and maturation of adult-born neurons. Nat Neurosci 12:1090-1092.2009).

Ge S, Goh EL, Sailor KA, Kitabatake Y, Ming GL, Song H (GABA regulates synaptic integration of newly generated neurons in the adult brain. Nature 439:589-593.2006).

Gleason D, Fallon JH, Guerra M, Liu JC, Bryant PJ (Ependymal stem cells divide asymmetrically and transfer progeny into the subventricular zone when activated by injury. Neuroscience 156:81-88.2008).

Goetz JA, Singh S, Suber LM, Kull FJ, Robbins DJ (A highly conserved amino-terminal region of sonic hedgehog is required for the formation of its freely diffusible multimeric form. J Biol Chem 281:4087-4093.2006).

Goffredo D, Conti L, Di Febo F, Biella G, Tosoni A, Vago G, Biunno I, Moiana A, Bolognini D, Toselli M, Cattaneo E (Setting the conditions for efficient, robust and reproducible generation of functionally active neurons from adult subventricular zone-derived neural stem cells. Cell Death Differ 15:1847-1856.2008).

Gorski JA, Talley T, Qiu M, Puelles L, Rubenstein JL, Jones KR (Cortical excitatory neurons and glia, but not GABAergic neurons, are produced in the Emx1-expressing lineage. J Neurosci 22:6309-6314.2002).

Graham ME, Ruma-Haynes P, Capes-Davis AG, Dunn JM, Tan TC, Valova VA, Robinson PJ, Jeffrey PL (Multisite phosphorylation of doublecortin by cyclin-dependent kinase 5. Biochem J 381:471-481.2004).

Gritti A, Bonfanti L, Doetsch F, Caille I, Alvarez-Buylla A, Lim DA, Galli R, Verdugo JM, Herrera DG, Vescovi AL (Multipotent neural stem cells reside into the rostral extension and olfactory bulb of adult rodents. J Neurosci 22:437-445.2002).

Haas SJ, Beckmann S, Petrov S, Andressen C, Wree A, Schmitt O (Transplantation of immortalized mesencephalic progenitors (CSM14.1 cells) into the neonatal parkinsonian rat caudate putamen. J Neurosci Res 85:778-786.2007).

Haas SJ, Petrov S, Kronenberg G, Schmitt O, Wree A (Orthotopic transplantation of immortalized mesencephalic progenitors (CSM14.1 cells) into the substantia nigra of

hemiparkinsonian rats induces neuronal differentiation and motoric improvement. J Anat 212:19-30.2008).

Hack MA, Saghatelyan A, de Chevigny A, Pfeifer A, Ashery-Padan R, Lledo PM, Gotz M (Neuronal fate determinants of adult olfactory bulb neurogenesis. Nat Neurosci 8:865-872.2005).

Hack MA, Sugimori M, Lundberg C, Nakafuku M, Gotz M (Regionalization and fate specification in neurospheres: the role of Olig2 and Pax6. Mol Cell Neurosci 25:664-678.2004).

Hadinger N, Varga BV, Berzsenyi S, Kornyei Z, Madarasz E, Herberth B (Astroglia genesis in vitro: distinct effects of retinoic acid in different phases of neural stem cell differentiation. Int J Dev Neurosci 27:365-375.2009).

Hamill OP, Marty A, Neher E, Sakmann B, Sigworth FJ (Improved patch-clamp techniques for high-resolution current recording from cells and cell-free membrane patches. Pflugers Arch 391:85-100.1981).

Han YG, Spassky N, Romaguera-Ros M, Garcia-Verdugo JM, Aguilar A, Schneider-Maunoury S, Alvarez-Buylla A (Hedgehog signaling and primary cilia are required for the formation of adult neural stem cells. Nat Neurosci 11:277-284.2008).

Hartfuss E, Galli R, Heins N, Gotz M (Characterization of CNS precursor subtypes and radial glia. Dev Biol 229:15-30.2001).

Haskell GT, LaMantia AS (Retinoic acid signaling identifies a distinct precursor population in the developing and adult forebrain. J Neurosci 25:7636-7647.2005).

Hatada I, Namihira M, Morita S, Kimura M, Horii T, Nakashima K (Astrocyte-specific genes are generally demethylated in neural precursor cells prior to astrocytic differentiation. PLoS ONE 3:e3189.2008).

Hatakeyama J, Bessho Y, Katoh K, Ookawara S, Fujioka M, Guillemot F, Kageyama R (Hes genes regulate size, shape and histogenesis of the nervous system by control of the timing of neural stem cell differentiation. Development 131:5539-5550.2004).

Hattiangady B, Rao MS, Shetty AK (Plasticity of hippocampal stem/progenitor cells to enhance neurogenesis in response to kainate-induced injury is lost by middle age. Aging Cell 7:207-224.2008).

Haubensak W, Attardo A, Denk W, Huttner WB (Neurons arise in the basal neuroepithelium of the early mammalian telencephalon: a major site of neurogenesis. Proc Natl Acad Sci U S A 101:3196-3201.2004).

Haycraft CJ, Banizs B, Aydin-Son Y, Zhang Q, Michaud EJ, Yoder BK (Gli2 and Gli3 localize to cilia and require the intraflagellar transport protein polaris for processing and function. PLoS Genet 1:e53.2005).

Heck N, Kilb W, Reiprich P, Kubota H, Furukawa T, Fukuda A, Luhmann HJ (GABA-A receptors regulate neocortical neuronal migration in vitro and in vivo. Cereb Cortex 17:138-148.2007).

Hennou S, Khalilov I, Diabira D, Ben-Ari Y, Gozlan H (Early sequential formation of functional GABA(A) and glutamatergic synapses on CA1 interneurons of the rat foetal hippocampus. Eur J Neurosci 16:197-208.2002).

Hinoi T, Yamamoto H, Kishida M, Takada S, Kishida S, Kikuchi A (Complex formation of adenomatous polyposis coli gene product and axin facilitates glycogen synthase kinase-3 beta-dependent phosphorylation of beta-catenin and down-regulates beta-catenin. J Biol Chem 275:34399-34406.2000).

Hirabayashi Y, Itoh Y, Tabata H, Nakajima K, Akiyama T, Masuyama N, Gotoh Y (The Wnt/beta-catenin pathway directs neuronal differentiation of cortical neural precursor cells. Development 131:2791-2801.2004).

Hirsch C, Campano LM, Wohrle S, Hecht A (Canonical Wnt signaling transiently stimulates proliferation and enhances neurogenesis in neonatal neural progenitor cultures. Exp Cell Res 313:572-587.2007).

Hitoshi S, Seaberg RM, Koscik C, Alexson T, Kusunoki S, Kanazawa I, Tsuji S, van der Kooy D (Primitive neural stem cells from the mammalian epiblast differentiate to definitive neural stem cells under the control of Notch signaling. Genes Dev 18:1806-1811.2004).

Hol EM, Roelofs RF, Moraal E, Sonnemans MA, Sluijs JA, Proper EA, de Graan PN, Fischer DF, van Leeuwen FW (Neuronal expression of GFAP in patients with Alzheimer pathology and identification of novel GFAP splice forms. Mol Psychiatry 8:786-796.2003).

Huangfu D, Anderson KV (Cilia and Hedgehog responsiveness in the mouse. Proc Natl Acad Sci U S A 102:11325-11330.2005).

Huangfu D, Liu A, Rakeman AS, Murcia NS, Niswander L, Anderson KV (Hedgehog signalling in the mouse requires intraflagellar transport proteins. Nature 426:83-87.2003).

Hutcheon B, Fritschy JM, Poulter MO (Organization of GABA receptor alpha-subunit clustering in the developing rat neocortex and hippocampus. Eur J Neurosci 19:2475-2487.2004).

Ide Y, Fujiyama F, Okamoto-Furuta K, Tamamaki N, Kaneko T, Hisatsune T (Rapid integration of young newborn dentate gyrus granule cells in the adult hippocampal circuitry. Eur J Neurosci 28:2381-2392.2008).

Ikeda K, Nagasawa M, Mori H, Araki K, Sakimura K, Watanabe M, Inoue Y, Mishina M (Cloning and expression of the epsilon 4 subunit of the NMDA receptor channel. FEBS Lett 313:34-38.1992).

Imayoshi I, Sakamoto M, Ohtsuka T, Takao K, Miyakawa T, Yamaguchi M, Mori K, Ikeda T, Itohara S, Kageyama R (Roles of continuous neurogenesis in the structural and functional integrity of the adult forebrain. Nat Neurosci 11:1153-1161.2008).

Jelitai M, Anderova M, Chvatal A, Madarasz E (Electrophysiological characterization of neural stem/progenitor cells during in vitro differentiation: study with an immortalized neuroectodermal cell line. J Neurosci Res 85:1606-1617.2007).

Jelitai M, Anderova M, Marko K, Kekesi K, Koncz P, Sykova E, Madarasz E (Role of gamma-aminobutyric acid in early neuronal development: studies with an embryonic neuroectodermal stem cell clone. J Neurosci Res 76:801-811.2004).

Jelitai M, Schlett K, Varju P, Eisel U, Madarasz E (Regulated appearance of NMDA receptor subunits and channel functions during in vitro neuronal differentiation. J Neurobiol 51:54-65.2002).

Jia J, Kolterud A, Zeng H, Hoover A, Teglund S, Toftgard R, Liu A (Suppressor of Fused inhibits mammalian Hedgehog signaling in the absence of cilia. Dev Biol 330:452-460.2009).

Jiao J, Chen DF (Induction of neurogenesis in nonconventional neurogenic regions of the adult central nervous system by niche astrocyte-produced signals. Stem Cells 26:1221-1230.2008).

Jin K, Xie L, Childs J, Sun Y, Mao XO, Logvinova A, Greenberg DA (Cerebral neurogenesis is induced by intranasal administration of growth factors. Ann Neurol 53:405-409.2003).

Johansson CB, Momma S, Clarke DL, Risling M, Lendahl U, Frisen J (Identification of a neural stem cell in the adult mammalian central nervous system. Cell 96:25-34.1999).

Johnson MA, Weick JP, Pearce RA, Zhang SC (Functional neural development from human embryonic stem cells: accelerated synaptic activity via astrocyte coculture. J Neurosci 27:3069-3077.2007).

Kallur T, Darsalia V, Lindvall O, Kokaia Z (Human fetal cortical and striatal neural stem cells generate region-specific neurons in vitro and differentiate extensively to neurons after intrastriatal transplantation in neonatal rats. J Neurosci Res 84:1630-1644.2006).

Kam M, Curtis MA, McGlashan SR, Connor B, Nannmark U, Faull RL (The cellular composition and morphological organization of the rostral migratory stream in the adult human brain. J Chem Neuroanat 37:196-205.2009).

Kaneko N, Sawamoto K (Adult neurogenesis and its alteration under pathological conditions. Neurosci Res 63:155-164.2009).

Kee N, Teixeira CM, Wang AH, Frankland PW (Preferential incorporation of adult-generated granule cells into spatial memory networks in the dentate gyrus. Nat Neurosci 10:355-362.2007).

Kim HT, Kim IS, Lee IS, Lee JP, Snyder EY, Park KI (Human neurospheres derived from the fetal central nervous system are regionally and temporally specified but are not committed. Exp Neurol 199:222-235.2006).

Kim SU, de Vellis J (Stem cell-based cell therapy in neurological diseases: a review. J Neurosci Res 87:2183-2200.2009).

Klein C, Butt SJ, Machold RP, Johnson JE, Fishell G (Cerebellum- and forebrain-derived stem cells possess intrinsic regional character. Development 132:4497-4508.2005).

Komada M, Saitsu H, Kinboshi M, Miura T, Shiota K, Ishibashi M (Hedgehog signaling is involved in development of the neocortex. Development 135:2717-2727.2008).

Komekado H, Yamamoto H, Chiba T, Kikuchi A (Glycosylation and palmitoylation of Wnt-3a are coupled to produce an active form of Wnt-3a. Genes Cells 12:521-534.2007).

Komitova M, Zhu X, Serwanski DR, Nishiyama A (NG2 cells are distinct from neurogenic cells in the postnatal mouse subventricular zone. J Comp Neurol 512:702-716.2009).

Kommers T, Rodnight R, Boeck C, Vendite D, Oliveira D, Horn J, Oppelt D, Wofchuk S (Phosphorylation of glial fibrillary acidic protein is stimulated by glutamate via NMDA receptors in cortical microslices and in mixed neuronal/glial cell cultures prepared from the cerebellum. Brain Res Dev Brain Res 137:139-148.2002).

Kosodo Y, Roper K, Haubensak W, Marzesco AM, Corbeil D, Huttner WB (Asymmetric distribution of the apical plasma membrane during neurogenic divisions of mammalian neuroepithelial cells. Embo J 23:2314-2324.2004).

Kozubenko N, Turnovcova K, Kapcalova M, Butenko O, Anderova M, Rusnakova V, Kubista M, Hampl A, Jendelova P, Sykova E (Analysis of in vitro and in vivo characteristics of human embryonic stem cell-derived neural precursors. Cell Transplant.2009).

Kronenberg G, Reuter K, Steiner B, Brandt MD, Jessberger S, Yamaguchi M, Kempermann G (Subpopulations of proliferating cells of the adult hippocampus respond differently to physiologic neurogenic stimuli. J Comp Neurol 467:455-463.2003).

Kuan CY, Schloemer AJ, Lu A, Burns KA, Weng WL, Williams MT, Strauss KI, Vorhees CV, Flavell RA, Davis RJ, Sharp FR, Rakic P (Hypoxia-ischemia induces DNA synthesis without cell proliferation in dying neurons in adult rodent brain. J Neurosci 24:10763-10772.2004).

Kunke D, Bryja V, Mygland L, Arenas E, Krauss S (Inhibition of canonical Wnt signaling promotes gliogenesis in P0-NSCs. Biochem Biophys Res Commun 386:628-633.2009).

Kuwabara T, Hsieh J, Muotri A, Yeo G, Warashina M, Lie DC, Moore L, Nakashima K, Asashima M, Gage FH (Wnt-mediated activation of NeuroD1 and retro-elements during adult neurogenesis. Nat Neurosci 12:1097-1105.2009).

Lai K, Kaspar BK, Gage FH, Schaffer DV (Sonic hedgehog regulates adult neural progenitor proliferation in vitro and in vivo. Nat Neurosci 6:21-27.2003).

Lee HJ, Kim KS, Kim EJ, Choi HB, Lee KH, Park IH, Ko Y, Jeong SW, Kim SU (Brain transplantation of immortalized human neural stem cells promotes functional recovery in mouse intracerebral hemorrhage stroke model. Stem Cells 25:1204-1212.2007).

Lee SI, Kim BG, Hwang DH, Kim HM, Kim SU (Overexpression of Bcl-XL in human neural stem cells promotes graft survival and functional recovery following transplantation in spinal cord injury. J Neurosci Res 87:3186-3197.2009).

Lee ST, Park JE, Lee K, Kang L, Chu K, Kim SU, Kim M, Roh JK (Noninvasive method of immortalized neural stem-like cell transplantation in an experimental model of Huntington's disease. J Neurosci Methods 152:250-254.2006).

Lei ZN, Zhang LM, Sun FY (Beta-catenin siRNA inhibits ischemia-induced striatal neurogenesis in adult rat brain following a transient middle cerebral artery occlusion. Neurosci Lett 435:108-112.2008).

Leng J, Jiang L, Chen H, Zhang X (Brain-derived neurotrophic factor and electrophysiological properties of voltage-gated ion channels during neuronal stem cell development. Brain Res 1272:14-24.2009).

Lewis PM, Dunn MP, McMahon JA, Logan M, Martin JF, St-Jacques B, McMahon AP (Cholesterol modification of sonic hedgehog is required for long-range signaling activity and effective modulation of signaling by Ptc1. Cell 105:599-612.2001).

Lie DC, Colamarino SA, Song HJ, Desire L, Mira H, Consiglio A, Lein ES, Jessberger S, Lansford H, Dearie AR, Gage FH (Wnt signalling regulates adult hippocampal neurogenesis. Nature 437:1370-1375.2005).

Lindvall O, Kokaia Z (Stem cells for the treatment of neurological disorders. Nature 441:1094-1096.2006).

Liu A, Wang B, Niswander LA (Mouse intraflagellar transport proteins regulate both the activator and repressor functions of Gli transcription factors. Development 132:3103-3111.2005a).

Liu C, Li Y, Semenov M, Han C, Baeg GH, Tan Y, Zhang Z, Lin X, He X (Control of beta-catenin phosphorylation/degradation by a dual-kinase mechanism. Cell 108:837-847.2002).

Liu X, Bolteus AJ, Balkin DM, Henschel O, Bordey A (GFAP-expressing cells in the postnatal subventricular zone display a unique glial phenotype intermediate between radial glia and astrocytes. Glia 54:394-410.2006).

Liu X, Wang Q, Haydar TF, Bordey A (Nonsynaptic GABA signaling in postnatal subventricular zone controls proliferation of GFAP-expressing progenitors. Nat Neurosci 8:1179-1187.2005b).

LoTurco JJ, Owens DF, Heath MJ, Davis MB, Kriegstein AR (GABA and glutamate depolarize cortical progenitor cells and inhibit DNA synthesis. Neuron 15:1287-1298.1995).

Lundberg AS, Randell SH, Stewart SA, Elenbaas B, Hartwell KA, Brooks MW, Fleming MD, Olsen JC, Miller SW, Weinberg RA, Hahn WC (Immortalization and transformation of primary human airway epithelial cells by gene transfer. Oncogene 21:4577-4586.2002).

Machold R, Hayashi S, Rutlin M, Muzumdar MD, Nery S, Corbin JG, Gritli-Linde A, Dellovade T, Porter JA, Rubin LL, Dudek H, McMahon AP, Fishell G (Sonic hedgehog is required for progenitor cell maintenance in telencephalic stem cell niches. Neuron 39:937-950.2003).

Machon O, Backman M, Krauss S, Kozmik Z (The cellular fate of cortical progenitors is not maintained in neurosphere cultures. Mol Cell Neurosci 30:388-397.2005).

Machon O, van den Bout CJ, Backman M, Rosok O, Caubit X, Fromm SH, Geronimo B, Krauss S (Forebrain-specific promoter/enhancer D6 derived from the mouse Dach1 gene controls expression in neural stem cells. Neuroscience 112:951-966.2002).

Malatesta P, Appolloni I, Calzolari F (Radial glia and neural stem cells. Cell Tissue Res 331:165-178.2008).

Malatesta P, Hack MA, Hartfuss E, Kettenmann H, Klinkert W, Kirchhoff F, Gotz M (Neuronal or glial progeny: regional differences in radial glia fate. Neuron 37:751-764.2003).

Malatesta P, Hartfuss E, Gotz M (Isolation of radial glial cells by fluorescent-activated cell sorting reveals a neuronal lineage. Development 127:5253-5263.2000).

Marti E, Bovolenta P (Sonic hedgehog in CNS development: one signal, multiple outputs. Trends Neurosci 25:89-96.2002).

McCarthy M, Turnbull DH, Walsh CA, Fishell G (Telencephalic neural progenitors appear to be restricted to regional and glial fates before the onset of neurogenesis. J Neurosci 21:6772-6781.2001).

McIlhinney RA, Le Bourdelles B, Molnar E, Tricaud N, Streit P, Whiting PJ (Assembly intracellular targeting and cell surface expression of the human N-methyl-D-aspartate receptor subunits NR1a and NR2A in transfected cells. Neuropharmacology 37:1355-1367.1998).

Menezes JR, Luskin MB (Expression of neuron-specific tubulin defines a novel population in the proliferative layers of the developing telencephalon. J Neurosci 14:5399-5416.1994).

Menn B, Garcia-Verdugo JM, Yaschine C, Gonzalez-Perez O, Rowitch D, Alvarez-Buylla A (Origin of oligodendrocytes in the subventricular zone of the adult brain. J Neurosci 26:7907-7918.2006).

Merkle FT, Mirzadeh Z, Alvarez-Buylla A (Mosaic organization of neural stem cells in the adult brain. Science 317:381-384.2007).

Merkle FT, Tramontin AD, Garcia-Verdugo JM, Alvarez-Buylla A (Radial glia give rise to adult neural stem cells in the subventricular zone. Proc Natl Acad Sci U S A 101:17528-17532.2004).

Mignone JL, Kukekov V, Chiang AS, Steindler D, Enikolopov G (Neural stem and progenitor cells in nestin-GFP transgenic mice. J Comp Neurol 469:311-324.2004).

Mii Y, Taira M (Secreted Frizzled-related proteins enhance the diffusion of Wnt ligands and expand their signalling range. Development 136:4083-4088.2009).

Miles GB, Yohn DC, Wichterle H, Jessell TM, Rafuse VF, Brownstone RM (Functional properties of motoneurons derived from mouse embryonic stem cells. J Neurosci 24:7848-7858.2004).

Miller JR (The Wnts. Genome Biol 3:REVIEWS3001.2002).

Mirzadeh Z, Merkle FT, Soriano-Navarro M, Garcia-Verdugo JM, Alvarez-Buylla A (Neural stem cells confer unique pinwheel architecture to the ventricular surface in neurogenic regions of the adult brain. Cell Stem Cell 3:265-278.2008).

Miyata T, Kawaguchi A, Okano H, Ogawa M (Asymmetric inheritance of radial glial fibers by cortical neurons. Neuron 31:727-741.2001).

Miyata T, Kawaguchi A, Saito K, Kawano M, Muto T, Ogawa M (Asymmetric production of surface-dividing and non-surface-dividing cortical progenitor cells. Development 131:3133-3145.2004).

Mo Z, Moore AR, Filipovic R, Ogawa Y, Kazuhiro I, Antic SD, Zecevic N (Human cortical neurons originate from radial glia and neuron-restricted progenitors. J Neurosci 27:4132-4145.2007).

Mochizuki N, Takagi N, Kurokawa K, Kawai T, Besshoh S, Tanonaka K, Takeo S (Effect of NMDA receptor antagonist on proliferation of neurospheres from embryonic brain. Neurosci Lett 417:143-148.2007).

Modo M, Rezaie P, Heuschling P, Patel S, Male DK, Hodges H (Transplantation of neural stem cells in a rat model of stroke: assessment of short-term graft survival and acute host immunological response. Brain Res 958:70-82.2002).

Moreno MM, Linster C, Escanilla O, Sacquet J, Didier A, Mandairon N (Olfactory perceptual learning requires adult neurogenesis. Proc Natl Acad Sci U S A 106:17980-17985.2009).

Mothe AJ, Kulbatski I, Parr A, Mohareb M, Tator CH (Adult spinal cord stem/progenitor cells transplanted as neurospheres preferentially differentiate into oligodendrocytes in the adult rat spinal cord. Cell Transplant 17:735-751.2008).

Mujtaba T, Piper DR, Kalyani A, Groves AK, Lucero MT, Rao MS (Lineage-restricted neural precursors can be isolated from both the mouse neural tube and cultured ES cells. Dev Biol 214:113-127.1999).

Muroyama Y, Kondoh H, Takada S (Wnt proteins promote neuronal differentiation in neural stem cell culture. Biochem Biophys Res Commun 313:915-921.2004).

Nakahira E, Yuasa S (Neuronal generation, migration, and differentiation in the mouse hippocampal primoridium as revealed by enhanced green fluorescent protein gene transfer by means of in utero electroporation. J Comp Neurol 483:329-340.2005).

Nakamichi N, Takarada T, Yoneda Y (Neurogenesis mediated by gamma-aminobutyric acid and glutamate signaling. J Pharmacol Sci 110:133-149.2009).

Ninkovic J, Mori T, Gotz M (Distinct modes of neuron addition in adult mouse neurogenesis. J Neurosci 27:10906-10911.2007).

Noctor SC, Flint AC, Weissman TA, Dammerman RS, Kriegstein AR (Neurons derived from radial glial cells establish radial units in neocortex. Nature 409:714-720.2001).

Noctor SC, Flint AC, Weissman TA, Wong WS, Clinton BK, Kriegstein AR (Dividing precursor cells of the embryonic cortical ventricular zone have morphological and molecular characteristics of radial glia. J Neurosci 22:3161-3173.2002).

Noctor SC, Martinez-Cerdeno V, Ivic L, Kriegstein AR (Cortical neurons arise in symmetric and asymmetric division zones and migrate through specific phases. Nat Neurosci 7:136-144.2004).

Nusse R, Varmus HE (Many tumors induced by the mouse mammary tumor virus contain a provirus integrated in the same region of the host genome. Cell 31:99-109.1982).

Olsson M, Bjorklund A, Campbell K (Early specification of striatal projection neurons and interneuronal subtypes in the lateral and medial ganglionic eminence. Neuroscience 84:867-876.1998).

Ono K, Takebayashi H, Ikeda K, Furusho M, Nishizawa T, Watanabe K, Ikenaka K (Regional- and temporal-dependent changes in the differentiation of Olig2 progenitors in the forebrain, and the impact on astrocyte development in the dorsal pallium. Dev Biol 320:456-468.2008).

Owens DF, Liu X, Kriegstein AR (Changing properties of GABA(A) receptor-mediated signaling during early neocortical development. J Neurophysiol 82:570-583.1999).

Pagani F, Lauro C, Fucile S, Catalano M, Limatola C, Eusebi F, Grassi F (Functional properties of neurons derived from fetal mouse neurospheres are compatible with those of neuronal precursors in vivo. J Neurosci Res 83:1494-1501.2006).

Palma V, Lim DA, Dahmane N, Sanchez P, Brionne TC, Herzberg CD, Gitton Y, Carleton A, Alvarez-Buylla A, Ruiz i Altaba A (Sonic hedgehog controls stem cell behavior in the postnatal and adult brain. Development 132:335-344.2005).

Pan Y, Wang C, Wang B (Phosphorylation of Gli2 by protein kinase A is required for Gli2 processing and degradation and the Sonic Hedgehog-regulated mouse development. Dev Biol 326:177-189.2009).

Panagiotakos G, Alshamy G, Chan B, Abrams R, Greenberg E, Saxena A, Bradbury M, Edgar M, Gutin P, Tabar V (Long-term impact of radiation on the stem cell and oligodendrocyte precursors in the brain. PLoS One 2:e588.2007).

Parent JM, Vexler ZS, Gong C, Derugin N, Ferriero DM (Rat forebrain neurogenesis and striatal neuron replacement after focal stroke. Ann Neurol 52:802-813.2002).

Parmar M, Skogh C, Bjorklund A, Campbell K (Regional specification of neurosphere cultures derived from subregions of the embryonic telencephalon. Mol Cell Neurosci 21:645-656.2002).

Parnavelas JG (The origin of cortical neurons. Braz J Med Biol Res 35:1423-1429.2002).

Parras CM, Galli R, Britz O, Soares S, Galichet C, Battiste J, Johnson JE, Nakafuku M, Vescovi A, Guillemot F (Mash1 specifies neurons and oligodendrocytes in the postnatal brain. Embo J 23:4495-4505.2004).

Parras CM, Hunt C, Sugimori M, Nakafuku M, Rowitch D, Guillemot F (The proneural gene Mash1 specifies an early population of telencephalic oligodendrocytes. J Neurosci 27:4233-4242.2007).

Pastrana E, Cheng LC, Doetsch F (Simultaneous prospective purification of adult subventricular zone neural stem cells and their progeny. Proc Natl Acad Sci U S A 106:6387-6392.2009).

Peretto P, Giachino C, Aimar P, Fasolo A, Bonfanti L (Chain formation and glial tube assembly in the shift from neonatal to adult subventricular zone of the rodent forebrain. J Comp Neurol 487:407-427.2005).

Petryniak MA, Potter GB, Rowitch DH, Rubenstein JL (Dlx1 and Dlx2 control neuronal versus oligodendroglial cell fate acquisition in the developing forebrain. Neuron 55:417-433.2007).

Pforte C, Henrich-Noack P, Baldauf K, Reymann KG (Increase in proliferation and gliogenesis but decrease of early neurogenesis in the rat forebrain shortly after transient global ischemia. Neuroscience 136:1133-1146.2005).

Piao JH, Odeberg J, Samuelsson EB, Kjaeldgaard A, Falci S, Seiger A, Sundstrom E, Akesson E (Cellular composition of long-term human spinal cord- and forebrain-derived neurosphere cultures. J Neurosci Res 84:471-482.2006).

Picken Bahrey HL, Moody WJ (Early development of voltage-gated ion currents and firing properties in neurons of the mouse cerebral cortex. J Neurophysiol 89:1761-1773.2003).

Plaschke K, Staub J, Ernst E, Marti HH (VEGF overexpression improves mice cognitive abilities after unilateral common carotid artery occlusion. Exp Neurol 214:285-292.2008).

Platel JC, Gordon V, Heintz T, Bordey A (GFAP-GFP neural progenitors are antigenically homogeneous and anchored in their enclosed mosaic niche. Glia 57:66-78.2009).

Platel JC, Heintz T, Young S, Gordon V, Bordey A (Tonic activation of GLUK5 kainate receptors decreases neuroblast migration in whole-mounts of the subventricular zone. J Physiol 586:3783-3793.2008).

Pollard SM, Conti L, Sun Y, Goffredo D, Smith A (Adherent neural stem (NS) cells from fetal and adult forebrain. Cereb Cortex 16 Suppl 1:i112-120.2006).

Pons S, Marti E (Sonic hedgehog synergizes with the extracellular matrix protein vitronectin to induce spinal motor neuron differentiation. Development 127:333-342.2000).

Porter JA, Young KE, Beachy PA (Cholesterol modification of hedgehog signaling proteins in animal development. Science 274:255-259.1996).

Qian X, Shen Q, Goderie SK, He W, Capela A, Davis AA, Temple S (Timing of CNS cell generation: a programmed sequence of neuron and glial cell production from isolated murine cortical stem cells. Neuron 28:69-80.2000).

Quinlan RA, Brenner M, Goldman JE, Messing A (GFAP and its role in Alexander disease. Exp Cell Res 313:2077-2087.2007).

Quinones-Hinojosa A, Sanai N, Soriano-Navarro M, Gonzalez-Perez O, Mirzadeh Z, Gil-Perotin S, Romero-Rodriguez R, Berger MS, Garcia-Verdugo JM, Alvarez-Buylla A (Cellular composition and cytoarchitecture of the adult human subventricular zone: a niche of neural stem cells. J Comp Neurol 494:415-434.2006).

Rappa G, Kunke D, Holter J, Diep DB, Meyer J, Baum C, Fodstad O, Krauss S, Lorico A (Efficient expansion and gene transduction of mouse neural stem/progenitor cells on recombinant fibronectin. Neuroscience 124:823-830.2004).

Rijsewijk F, Schuermann M, Wagenaar E, Parren P, Weigel D, Nusse R (The Drosophila homolog of the mouse mammary oncogene int-1 is identical to the segment polarity gene wingless. Cell 50:649-657.1987).

Roelofs RF, Fischer DF, Houtman SH, Sluijs JA, Van Haren W, Van Leeuwen FW, Hol EM (Adult human subventricular, subgranular, and subpial zones contain astrocytes with a specialized intermediate filament cytoskeleton. Glia 52:289-300.2005).

Rohatgi R, Milenkovic L, Scott MP (Patched1 regulates hedgehog signaling at the primary cilium. Science 317:372-376.2007).

Ruiz i Altaba A, Sanchez P, Dahmane N (Gli and hedgehog in cancer: tumours, embryos and stem cells. Nat Rev Cancer 2:361-372.2002).

Sahara S, O'Leary DD (Fgf10 regulates transition period of cortical stem cell differentiation to radial glia controlling generation of neurons and basal progenitors. Neuron 63:48-62.2009).

Salic A, Lee E, Mayer L, Kirschner MW (Control of beta-catenin stability: reconstitution of the cytoplasmic steps of the wnt pathway in Xenopus egg extracts. Mol Cell 5:523-532.2000).

Sanberg PR, Willing AE, Garbuzova-Davis S, Saporta S, Liu G, Sanberg CD, Bickford PC, Klasko SK, El-Badri NS (Umbilical cord blood-derived stem cells and brain repair. Ann N Y Acad Sci 1049:67-83.2005).

Sasaki H, Nishizaki Y, Hui C, Nakafuku M, Kondoh H (Regulation of Gli2 and Gli3 activities by an amino-terminal repression domain: implication of Gli2 and Gli3 as primary mediators of Shh signaling. Development 126:3915-3924.1999).

Schabitz WR, Steigleder T, Cooper-Kuhn CM, Schwab S, Sommer C, Schneider A, Kuhn HG (Intravenous brain-derived neurotrophic factor enhances poststroke sensorimotor recovery and stimulates neurogenesis. Stroke 38:2165-2172.2007).

Schlett K, Czirok A, Tarnok K, Vicsek T, Madarasz E (Dynamics of cell aggregation during in vitro neurogenesis by immortalized neuroectodermal progenitors. J Neurosci Res 60:184-194.2000).

Schlett K, Herberth B, Madarasz E (In vitro pattern formation during neurogenesis in neuroectodermal progenitor cells immortalized by p53-deficiency. Int J Dev Neurosci 15:795-804.1997).

Schlett K, Madarasz E (Retinoic acid induced neural differentiation in a neuroectodermal cell line immortalized by p53 deficiency. J Neurosci Res 47:405-415.1997).

Seri B, Garcia-Verdugo JM, Collado-Morente L, McEwen BS, Alvarez-Buylla A (Cell types, lineage, and architecture of the germinal zone in the adult dentate gyrus. J Comp Neurol 478:359-378.2004).

Seri B, Garcia-Verdugo JM, McEwen BS, Alvarez-Buylla A (Astrocytes give rise to new neurons in the adult mammalian hippocampus. J Neurosci 21:7153-7160.2001).

Shen Q, Wang Y, Kokovay E, Lin G, Chuang SM, Goderie SK, Roysam B, Temple S (Adult SVZ stem cells lie in a vascular niche: a quantitative analysis of niche cell-cell interactions. Cell Stem Cell 3:289-300.2008).

Shetty AK (Progenitor cells from the CA3 region of the embryonic day 19 rat hippocampus generate region-specific neuronal phenotypes in vitro. Hippocampus 14:595-614.2004).

Shibata T, Yamada K, Watanabe M, Ikenaka K, Wada K, Tanaka K, Inoue Y (Glutamate transporter GLAST is expressed in the radial glia-astrocyte lineage of developing mouse spinal cord. J Neurosci 17:9212-9219.1997).

Shmueli A, Gdalyahu A, Sapoznik S, Sapir T, Tsukada M, Reiner O (Site-specific dephosphorylation of doublecortin (DCX) by protein phosphatase 1 (PP1). Mol Cell Neurosci 32:15-26.2006).

Smith DO, Rosenheimer JL, Kalil RE (Delayed rectifier and A-type potassium channels associated with Kv 2.1 and Kv 4.3 expression in embryonic rat neural progenitor cells. PLoS ONE 3:e1604.2008).

Spassky N, Merkle FT, Flames N, Tramontin AD, Garcia-Verdugo JM, Alvarez-Buylla A (Adult ependymal cells are postmitotic and are derived from radial glial cells during embryogenesis. J Neurosci 25:10-18.2005).

Su Y, Fu C, Ishikawa S, Stella A, Kojima M, Shitoh K, Schreiber EM, Day BW, Liu B (APC is essential for targeting phosphorylated beta-catenin to the SCFbeta-TrCP ubiquitin ligase. Mol Cell 32:652-661.2008).

Suh H, Consiglio A, Ray J, Sawai T, D'Amour KA, Gage FH (In vivo fate analysis reveals the multipotent and self-renewal capacities of Sox2+ neural stem cells in the adult hippocampus. Cell Stem Cell 1:515-528.2007).

Sun D, Bullock MR, McGinn MJ, Zhou Z, Altememi N, Hagood S, Hamm R, Colello RJ (Basic fibroblast growth factor-enhanced neurogenesis contributes to cognitive recovery in rats following traumatic brain injury. Exp Neurol 216:56-65.2009).

Sun J, Gao Q, Miller K, Wang X, Wang J, Liu W, Bao L, Zhang J, Zhang L, Poon WS, Gao Y (Dopaminergic differentiation of grafted GFP transgenic neuroepithelial stem cells in the brain of a rat model of Parkinson's disease. Neurosci Lett 420:23-28.2007).

Sun W, Buzanska L, Domanska-Janik K, Salvi RJ, Stachowiak MK (Voltage-sensitive and ligand-gated channels in differentiating neural stem-like cells derived from the nonhematopoietic fraction of human umbilical cord blood. Stem Cells 23:931-945.2005).

Suzuki SO, Goldman JE (Multiple cell populations in the early postnatal subventricular zone take distinct migratory pathways: a dynamic study of glial and neuronal progenitor migration. J Neurosci 23:4240-4250.2003).

Swanson GT, Kamboj SK, Cull-Candy SG (Single-channel properties of recombinant AMPA receptors depend on RNA editing, splice variation, and subunit composition. J Neurosci 17:58-69.1997).

Tago K, Nakamura T, Nishita M, Hyodo J, Nagai S, Murata Y, Adachi S, Ohwada S, Morishita Y, Shibuya H, Akiyama T (Inhibition of Wnt signaling by ICAT, a novel beta-catenin-interacting protein. Genes Dev 14:1741-1749.2000).

Tamamaki N, Nakamura K, Okamoto K, Kaneko T (Radial glia is a progenitor of neocortical neurons in the developing cerebral cortex. Neurosci Res 41:51-60.2001).

Tamura Y, Kataoka Y, Cui Y, Takamori Y, Watanabe Y, Yamada H (Multi-directional differentiation of doublecortin- and NG2-immunopositive progenitor cells in the adult rat neocortex in vivo. Eur J Neurosci 25:3489-3498.2007).

Tamura Y, Kataoka Y, Cui Y, Yamada H (Cellular proliferation in the cerebral cortex following neural excitation in rats. Neurosci Res 50:129-133.2004).

Tanaka DH, Maekawa K, Yanagawa Y, Obata K, Murakami F (Multidirectional and multizonal tangential migration of GABAergic interneurons in the developing cerebral cortex. Development 133:2167-2176.2006).

Tanaka T, Serneo FF, Tseng HC, Kulkarni AB, Tsai LH, Gleeson JG (Cdk5 phosphorylation of doublecortin ser297 regulates its effect on neuronal migration. Neuron 41:215-227.2004).

Tang X, Taniguchi K, Kofuji P (Heterogeneity of Kir4.1 channel expression in glia revealed by mouse transgenesis. Glia 57:1706-1715.2009).

Tateishi N, Shimoda T, Manako J, Katsumata S, Shinagawa R, Ohno H (Relevance of astrocytic activation to reductions of astrocytic GABAA receptors. Brain Res 1089:79-91.2006).

Tavazoie M, Van der Veken L, Silva-Vargas V, Louissaint M, Colonna L, Zaidi B, Garcia-Verdugo JM, Doetsch F (A specialized vascular niche for adult neural stem cells. Cell Stem Cell 3:279-288.2008).

Tempe D, Casas M, Karaz S, Blanchet-Tournier MF, Concordet JP (Multisite protein kinase A and glycogen synthase kinase 3beta phosphorylation leads to Gli3 ubiquitination by SCFbetaTrCP. Mol Cell Biol 26:4316-4326.2006).

Thored P, Heldmann U, Gomes-Leal W, Gisler R, Darsalia V, Taneera J, Nygren JM, Jacobsen SE, Ekdahl CT, Kokaia Z, Lindvall O (Long-term accumulation of microglia with proneurogenic phenotype concomitant with persistent neurogenesis in adult subventricular zone after stroke. Glia 57:835-849.2009).

Toledo EM, Colombres M, Inestrosa NC (Wnt signaling in neuroprotection and stem cell differentiation. Prog Neurobiol 86:281-296.2008).

Varga BV, Hadinger N, Gocza E, Dulberg V, Demeter K, Madarasz E, Herberth B (Generation of diverse neuronal subtypes in cloned populations of stem-like cells. BMC Dev Biol 8:89.2008).

Vazey EM, Chen K, Hughes SM, Connor B (Transplanted adult neural progenitor cells survive, differentiate and reduce motor function impairment in a rodent model of Huntington's disease. Exp Neurol 199:384-396.2006).

Villa A, Liste I, Courtois ET, Seiz EG, Ramos M, Meyer M, Juliusson B, Kusk P, Martinez-Serrano A (Generation and properties of a new human ventral mesencephalic neural stem cell line. Exp Cell Res 315:1860-1874.2009).

Vokes SA, Ji H, McCuine S, Tenzen T, Giles S, Zhong S, Longabaugh WJ, Davidson EH, Wong WH, McMahon AP (Genomic characterization of Gli-activator targets in sonic hedgehog-mediated neural patterning. Development 134:1977-1989.2007).

Vorasubin B, Weedin J, Saljooque F, Wilkes N, Eng M, U HS (Selective differentiation of central nervous system-derived stem cells in response to cues from specific regions of the developing brain. J Neurosurg 107:145-154.2007).

Vreugdenhil E, Kolk SM, Boekhoorn K, Fitzsimons CP, Schaaf M, Schouten T, Sarabdjitsingh A, Sibug R, Lucassen PJ (Doublecortin-like, a microtubule-associated protein expressed in radial glia, is crucial for neuronal precursor division and radial process stability. Eur J Neurosci 25:635-648.2007).

Wang C, Ruther U, Wang B (The Shh-independent activator function of the full-length Gli3 protein and its role in vertebrate limb digit patterning. Dev Biol 305:460-469.2007a).

Wang DD, Kriegstein AR (GABA regulates excitatory synapse formation in the neocortex via NMDA receptor activation. J Neurosci 28:5547-5558.2008).

Wang DD, Krueger DD, Bordey A (Biophysical properties and ionic signature of neuronal progenitors of the postnatal subventricular zone in situ. J Neurophysiol 90:2291-2302.2003a).

Wang DD, Krueger DD, Bordey A (GABA depolarizes neuronal progenitors of the postnatal subventricular zone via GABAA receptor activation. J Physiol 550:785-800.2003b).

Wang L, Chopp M, Zhang RL, Zhang L, Letourneau Y, Feng YF, Jiang A, Morris DC, Zhang ZG (The Notch pathway mediates expansion of a progenitor pool and neuronal differentiation in adult neural progenitor cells after stroke. Neuroscience 158:1356-1363.2009).

Wang L, Zhang ZG, Gregg SR, Zhang RL, Jiao Z, LeTourneau Y, Liu X, Feng Y, Gerwien J, Torup L, Leist M, Noguchi CT, Chen ZY, Chopp M (The Sonic hedgehog pathway mediates carbamylated erythropoietin-enhanced proliferation and differentiation of adult neural progenitor cells. J Biol Chem 282:32462-32470.2007b).

Wang W, Jin K, Mao XO, Close N, Greenberg DA, Xiong ZG (Electrophysiological properties of mouse cortical neuron progenitors differentiated in vitro and in vivo. Int J Clin Exp Med 1:145-153.2008).

Wei P, Liu J, Zhou HL, Han ZT, Wu QY, Pang JX, Liu S, Wang TH (Effects of engrafted neural stem cells derived from GFP transgenic mice in Parkinson's diseases rats. Neurosci Lett 419:49-54.2007).

Westerlund U, Moe MC, Varghese M, Berg-Johnsen J, Ohlsson M, Langmoen IA, Svensson M (Stem cells from the adult human brain develop into functional neurons in culture. Exp Cell Res 289:378-383.2003).

Wexler EM, Paucer A, Kornblum HI, Plamer TD, Geschwind DH (Endogenous Wnt signaling maintains neural progenitor cell potency. Stem Cells 27:1130-1141.2009).

Willert K, Brown JD, Danenberg E, Duncan AW, Weissman IL, Reya T, Yates JR, 3rd, Nusse R (Wnt proteins are lipid-modified and can act as stem cell growth factors. Nature 423:448-452.2003).

Wu SX, Goebbels S, Nakamura K, Kometani K, Minato N, Kaneko T, Nave KA, Tamamaki N (Pyramidal neurons of upper cortical layers generated by NEX-positive progenitor cells in the subventricular zone. Proc Natl Acad Sci U S A 102:17172-17177.2005).

Xu Q, Tam M, Anderson SA (Fate mapping Nkx2.1-lineage cells in the mouse telencephalon. J Comp Neurol 506:16-29.2008).

Xu Q, Wonders CP, Anderson SA (Sonic hedgehog maintains the identity of cortical interneuron progenitors in the ventral telencephalon. Development 132:4987-4998.2005).

Xuan AG, Luo M, Ji WD, Long DH (Effects of engrafted neural stem cells in Alzheimer's disease rats. Neurosci Lett 450:167-171.2009).

Yamada J, Okabe A, Toyoda H, Kilb W, Luhmann HJ, Fukuda A (Cl- uptake promoting depolarizing GABA actions in immature rat neocortical neurones is mediated by NKCC1. J Physiol 557:829-841.2004).

Yasuda T, Bartlett PF, Adams DJ (K(ir) and K(v) channels regulate electrical properties and proliferation of adult neural precursor cells. Mol Cell Neurosci 37:284-297.2008).

Yasuhara T, Matsukawa N, Hara K, Yu G, Xu L, Maki M, Kim SU, Borlongan CV (Transplantation of human neural stem cells exerts neuroprotection in a rat model of Parkinson's disease. J Neurosci 26:12497-12511.2006).

Yoneyama M, Nakamichi N, Fukui M, Kitayama T, Georgiev DD, Makanga JO, Nakamura N, Taniura H, Yoneda Y (Promotion of neuronal differentiation through activation of N-methyl-D-aspartate receptors transiently expressed by undifferentiated neural progenitor cells in fetal rat neocortex. J Neurosci Res 86:2392-2402.2008).

Young KM, Fogarty M, Kessaris N, Richardson WD (Subventricular zone stem cells are heterogeneous with respect to their embryonic origins and neurogenic fates in the adult olfactory bulb. J Neurosci 27:8286-8296.2007).

Yu JM, Kim JH, Song GS, Jung JS (Increase in proliferation and differentiation of neural progenitor cells isolated from postnatal and adult mice brain by Wnt-3a and Wnt-5a. Mol Cell Biochem 288:17-28.2006).

Yuasa S (Development of astrocytes in the mouse embryonic cerebrum tracked by tenascin-C gene expression. Arch Histol Cytol 64:119-126.2001).

Zeng X, Huang H, Tamai K, Zhang X, Harada Y, Yokota C, Almeida K, Wang J, Doble B, Woodgett J, Wynshaw-Boris A, Hsieh JC, He X (Initiation of Wnt signaling: control of Wnt coreceptor Lrp6 phosphorylation/activation via frizzled, dishevelled and axin functions. Development 135:367-375.2008).

Zeng X, Tamai K, Doble B, Li S, Huang H, Habas R, Okamura H, Woodgett J, He X (A dual-kinase mechanism for Wnt co-receptor phosphorylation and activation. Nature 438:873-877.2005).

Zhang H, Wang Y, Zhao Y, Yin Y, Xu Q (Immortalized human neural progenitor cells from the ventral telencephalon with the potential to differentiate into GABAergic neurons. J Neurosci Res 86:1217-1226.2008).

Zheng T, Marshall GP, 2nd, Laywell ED, Steindler DA (Neurogenic astrocytes transplanted into the adult mouse lateral ventricle contribute to olfactory neurogenesis, and reveal a novel intrinsic subependymal neuron. Neuroscience 142:175-185.2006).

Zhou FM, Hablitz JJ (Postnatal development of membrane properties of layer I neurons in rat neocortex. J Neurosci 16:1131-1139.1996).

Zhou M, Schools GP, Kimelberg HK (Development of GLAST(+) astrocytes and NG2(+) glia in rat hippocampus CA1: mature astrocytes are electrophysiologically passive. J Neurophysiol 95:134-143.2006).

Zhuo L, Sun B, Zhang CL, Fine A, Chiu SY, Messing A (Live astrocytes visualized by green fluorescent protein in transgenic mice. Dev Biol 187:36-42.1997).